

Supplementary Materials for

Rapid approach to complex boronic acids

Constantinos G. Neochoritis, Shabnam Shaabani, Maryam Ahmadianmoghaddam, Tryfon Zarganes-Tzitzikas, Li Gao, Michaela Novotná, Tatiana Mitriková, Atilio Reyes Romero, Marina Ika Irianti, Ruixue Xu, Joe Olechno, Richard Ellson, Victoria Helan, Michael Kossenjans, Matthew R. Groves, Alexander Dömling*

*Corresponding author. Email: a.s.s.domling@rug.nl

Published 5 July 2019, *Sci. Adv.* **5**, eaaw4607 (2019)

DOI: 10.1126/sciadv.aaw4607

This PDF file includes:

Supplementary Materials and Methods

Fig. S1. Isocyanide syntheses.

Fig. S2. Reactions in destination plate I.

Fig. S3. Reactions in destination plate II.

Fig. S4. Reactions in destination plate III.

Fig. S5. Reactions in destination plate IV.

Fig. S6. Labcyte Echo plate reformat software.

Fig. S7. Heat plots with product structures, green for major product formation, yellow for medium product formation, and blue for no product formation.

Fig. S8. Stabilization effect of **18a** as proof of interaction with MptpB as assessed by DSF.

Fig. S9. Binding curve of **18a** to the fluorescently labeled MptpB sample as assessed by MST.

Fig. S10. Three-dimensional structure of the target phosphatase.

Fig. S11. Proposed docking model for **18a** covalently bound to Cys¹⁶⁰ (PDB ID: 2OZ5).

Fig. S12. Proposed docking model for **18a** covalently bound to Ser⁵⁷ (PDB ID: 2OZ5).

Fig. S13. Proposed docking model for **18a** covalently bound to Thr²²³ (PDB ID: 2OZ5).

Fig. S14. ADE technology.

Table S1. Summary table of the docking scores for Covdock and Scorpion.

Scheme S1. Quality control results for destination plate I.

Scheme S2. Performance of formylphenyl boronic acids in destination plate I.

Scheme S3. Performance of isocyanides in GBB-3CR reaction in destination plate I.

Scheme S4. Performance of isocyanides in Ugi-based macrocycles in destination plate I.

Scheme S5. Performance of isocyanides in U-4CR in destination plate I.

Scheme S6. Performance of isocyanides in UT-4CR in destination plate I.

Scheme S7. Performance of carboxylic acids in U-4CR in destination plate I.

Scheme S8. Performance of amines in U-4CR in destination plate I.

Scheme S9. Performance of amines in UT-4CR in destination plate I.

Scheme S10. Performance of amidines in GBB-3CR reaction in destination plate I.

Scheme S11. Performance of α,ω -amino carboxylic acids in Ugi-based macrocycles in destination plate I.

Scheme S12. Quality control results for destination plate II.

Scheme S13. Performance of aminophenyl boronic acids in destination plate II.

Scheme S14. Performance of isocyanides in U-4CR in destination plate II.

Scheme S15. Performance of isocyanides in UT-4CR in destination plate II.

Scheme S16. Performance of oxo components in U-4CR in destination plate II.

Scheme S17. Performance of oxo components in UT-4CR in destination plate II.

Scheme S18. Performance of carboxylic acids in U-4CR in destination plate II.

Scheme S19. Quality control results for destination plate III.

Scheme S20. Performance of carboxyphenyl boronic acids in destination plate III.

Scheme S21. Performance of isocyanides in U-4CR in destination plate III.

Scheme S22. Performance of isocyanides in U-4CR with CH_2O in destination plate III.

Scheme S23. Performance of oxo component in U-4CR in destination plate III.

Scheme S24. Performance of amines in U-4CR in destination plate III.

Scheme S25. Performance of amines in U-4CR with CH_2O in destination plate III.

Scheme S26. Quality control results for destination plate IV.

Scheme S27. Performance of MCR boronic acid building blocks in destination plate IV.

Scheme S28. Performance of aryl halides in destination plate IV.

References (42–58)

Supplementary Materials and Methods

1. Isocyanide synthesis

All isocyanides were prepared in house by either performing the Ugi (42-45), Hoffman (46, 47) or our described Leuckart-Wallach reductive amination procedure (48) (fig. S1).

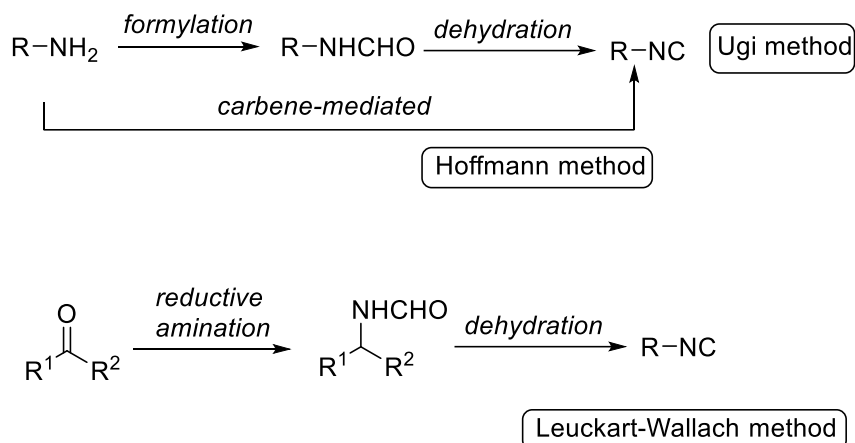


Fig. S1. Isocyanide syntheses.

2. Nanomole-scale chemical reactions

2.1. General materials

Stock solutions were prepared in glass flat bottom vials (Screening devices, Catalog#: 9920-812FBT, 2.0 mL (Topas) Plate) and they were kept at $-20\text{ }^\circ\text{C}$.

Nanomole-scale chemistry was performed using Echo qualified 384-well polypropylene microplate (Labcyte, Catalog#: PP-0200, clear, flat bottom) according to the producers' manual.

384-Well source and destination plates were sealed by a sealing tape (Thermo Scientific, Catalog#: 232701, polyolefin acrylate) and were kept at $-20\text{ }^\circ\text{C}$.

2.2. Nanomole-scale automated chemistry

2.2.1. Stock solution preparation

Stock solutions of formylphenyl boronic acids were prepared as 0.5 M, **A1** in ethylene glycol/2-methoxyethanol (2:3), **A2** in ethylene glycol/2-methoxyethanol (1:2), **A3** in 2-methoxyethanol.

Stock solutions of aminophenyl boronic acids were prepared as 0.5 M, **B1** and **B2** in 2-methoxyethanol, **B3** in ethylene glycol/2-methoxyethanol (1:1). $N(\text{Et})_3$ (1 eq) was added to **B3** stock solution in order to release the free amine from the corresponding HCl salt.

Stock solutions of carboxyphenyl boronic acids (**C1-C3**) were prepared as 0.5 M in 2-methoxyethanol.

Stock solutions of amidines (**D2, D4, D5, D7-D21, D23, D24, D26, D28, D30, D32, D34, D36, D38**) were prepared as 0.5 M in ethylene glycol. Due to the insolubility of some amidines in ethylene glycol, their stock solutions were instead prepared as 0.5 M: **D1** in ethylene glycol/2-methoxyethanol (1:2); **D22, D25, D27, D29, D31** in 2-methoxyethanol. Due to the insolubility of some of the amidines in 0.5 M 2-methoxyethanol, their stock solutions were diluted to 0.25 M (**D33, D35, D37**) and 0.16 M (**D3, D39, D6**), respectively.

Stock solutions of isocyanides (**E1, E3-E6, E8,E9, E13, E15, E16, E18-E21, E23-E25, E27, E29-E32, E34-E37, E39-E41, E43-E45, E47-E49, E52, E54, E56, E57, E59, E61, E63-E66**) were prepared as 0.5 M in ethylene glycol. Due to the insolubility of some isocyanides (**E2, E7, E10, E11, E12, E14, E17,**

E22, E26, E28, E33, E38, E42, E46, E50, E51, E53, E55, E58, E60, E62, E67, E68) in ethylene glycol, their stock solutions were instead prepared as 0.5 M in 2-methoxyethanol.

Stock solutions of carboxylic acids (**F1-F31, F33-F34, F36-F44, F46-F49, F51-F67, F69-F72**) were prepared as 0.5 M in 2-methoxyethanol. Due to insolubility of some carboxylic acids (**F32, F35, F45, F50, F68**) in 0.5 M 2-methoxyethanol, their stock solutions were diluted to 0.25 M.

Stock solutions of primary amines (**G3, G6, G9, G10, G17, G20, G22-G28, G30, G31, G33, G38**) were prepared as 0.5 M in ethylene glycol. Due to insolubility of some primary amines in ethylene glycol, their stock solutions were instead prepared as 0.5 M: **G13** in ethylene glycol/2-methoxyethanol (5:1); **G5, G14** in ethylene glycol/2-methoxyethanol (3:1); **G15, G32, G34, G39** in ethylene glycol/2-methoxyethanol (2:1); **G8, G11, G16, G18, G19** in ethylene glycol/2-methoxyethanol (1:1); **G1, G4, G7, G12, G21, G29, G35, G36, G37** in ethylene glycol/2-methoxyethanol (1:2); **G2** in 2-methoxyethanol.

Stock solutions of all secondary amines (**G40-G65, G67-G70**) were prepared as 0.5 M in ethylene glycol except **G66** which was prepared as 0.5 in 2-methoxyethanol.

Stock solutions of aldehydes and ketones (**H4-H6, H9, H14-H16, H20-H22, H24-H29, H32, H34-H35, H37, H38, H40-H43, H45, H46, H49, H51, H54, H55, H57, H59, H62, H63, H65, H69**) were prepared as 0.5 M in ethylene glycol. Due to insolubility of some aldehydes and ketones in ethylene glycol, their stock solutions were instead prepared as 0.5 M: **H70** in ethylene glycol/2-methoxyethanol (4:1); **H1, H3, H10, H11, H17, H31, H36, H48, H52, H58, H68** in ethylene glycol/2-methoxyethanol (2:1); **H2, H7, H8, H12, H13, H18, H19, H50, H61, H64, H67** in ethylene glycol/2-methoxyethanol (1:1); **H44, H56** in ethylene glycol/2-methoxyethanol (1:2); **H33** in ethylene glycol/2-methoxyethanol (2:3); **H23, H30, H39, H47, H53, H60, H66** in 2-methoxyethanol.

Stock solutions of α,ω -amino carboxylic acids (**I1, I3, I5-I21, I23-I33**) were prepared as 0.5 M in ethylene glycol. Due to insolubility of **I4** in ethylene glycol, its stock solutions was instead prepared as 0.5 M in ethylene glycol/2-methoxyethanol (4:1). Due to the insolubility of some of **I2** and **I22** in 0.5 M ethylene glycol, their stock solutions were diluted to 0.25 M.

Stock solutions of aryl halides were prepared as 0.25 M: **J4** in ethylene glycol; **J1, J3, J6, J9, J13, J16, J20, J22, J23, J27, J29** in ethylene glycol/2-methoxyethanol (2.5:1); **J2, J17** in ethylene glycol/2-methoxyethanol (2:1.5); **J24** in ethylene glycol/2-methoxyethanol (1:1); **J7** in ethylene glycol/2-methoxyethanol (1.5:2); **J5, J10, J11, J12, J14, J15, J18, J19, J25, J26, J28** in ethylene glycol/2-methoxyethanol (1:2.5); **J8, J21** in 2-methoxyethanol.

Stock solutions of MCR boronic acid building blocks were prepared as 0.25 M: **K5** in ethylene glycol; **K1** in ethylene glycol/2-methoxyethanol (2:1); **K2-K4, K6, K7** in 2-methoxyethanol.

Stock solutions of $\text{Pd}(\text{PPh}_3)_4$ and K_2CO_3 were prepared as 0.25 M in 2-methoxyethanol and water, respectively. Stock solutions of $\text{Sc}(\text{OTf})_3$ and TMSN_3 were prepared as 0.5 M in ethylene glycol.

2.2.2. Nano scale synthesis

The stock solutions were dispensed to a 384-well source plate using Eppendorf multi-channel pipettes. The Echo 555 was used to transfer the starting materials into the corresponding well in the destination plate.

Destination plate I

Formylphenyl boronic acids were used as oxo component in GBB-3CR reaction (wells A1-D24 in destination plate I), Ugi-based macrocyclisation using bifunctional α,ω -amino carboxylic acids (wells E1-H24 in destination plate I), U-4CR (wells I1-L24 in destination plate I) and UT-4CR (wells M1-P24 in destination plate I) as shown in fig. S2.

For GBB-3CR reaction, amidines (1 eq, 1000 nL), formylphenyl boronic acids (1 eq, 1000 nL), Sc(OTf)₃ (10 mol%, 100 nL) and isocyanides (1 eq, 1000 nL) were transferred into the corresponding well in the destination plate, respectively. In case of diluted amidines with 0.25 M and 0.16 M concentration, 2000 nL and 3000 nL were transferred, respectively.

For Ugi-based macrocyclisation, α,ω -amino carboxylic acids (1 eq, 1000 nL), formylphenyl boronic acids (1 eq, 1000 nL) and isocyanides (1 eq, 1000 nL) were transferred into the corresponding well in the destination plate, respectively. In case of diluted α,ω -amino carboxylic acids with 0.25 M concentration, 2000 nL was transferred.

For U-4CR, amines (1 eq, 750 nL), formylphenyl boronic acids (1 eq, 750 nL), carboxylic acids (1 eq, 750 nL) and isocyanides (1 eq, 750 nL) were transferred into the corresponding well in the destination plate, respectively. In case of diluted carboxylic acids with 0.25 M concentration, 1500 nL was transferred.

For UT-4CR, amines (1 eq, 750 nL), formylphenyl boronic acids (1 eq, 750 nL), isocyanides (1 eq, 750 nL) and TMSN₃ (1 eq, 750 nL) were transferred into the corresponding well in the destination plate, respectively.

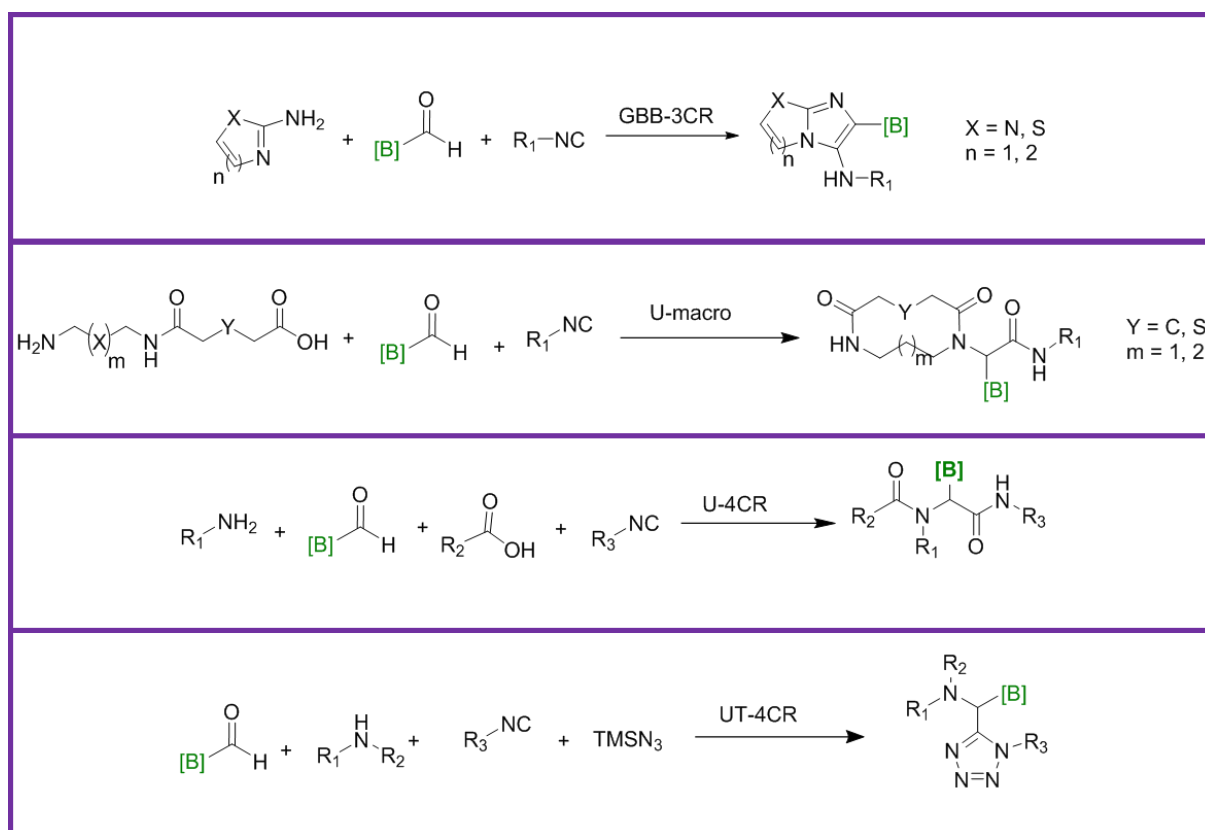


Fig. S2. Reactions in destination plate I.

Destination plate II

Aminophenyl boronic acids were used as amine component in U-4CR (wells A1-H24 in destination plate II) and UT-4CR (wells I1-P24 in destination plate II) as shown in fig. S3.

For U-4CR, oxo components (1 eq, 750 nL), aminophenyl boronic acids (1 eq, 750 nL), carboxylic acids (1 eq, 750 nL) and isocyanides (1 eq, 750 nL) were transferred into the corresponding well in the

destination plate, respectively. In case of diluted carboxylic acids with 0.25 M concentration, 1500 nL was transferred.

For UT-4CR, aminophenyl boronic acids (1 eq, 750 nL), oxo components (1 eq, 750 nL), isocyanides (1 eq, 750 nL) and TMSN₃ (1 eq, 750 nL) were transferred into the corresponding well in the destination plate, respectively.

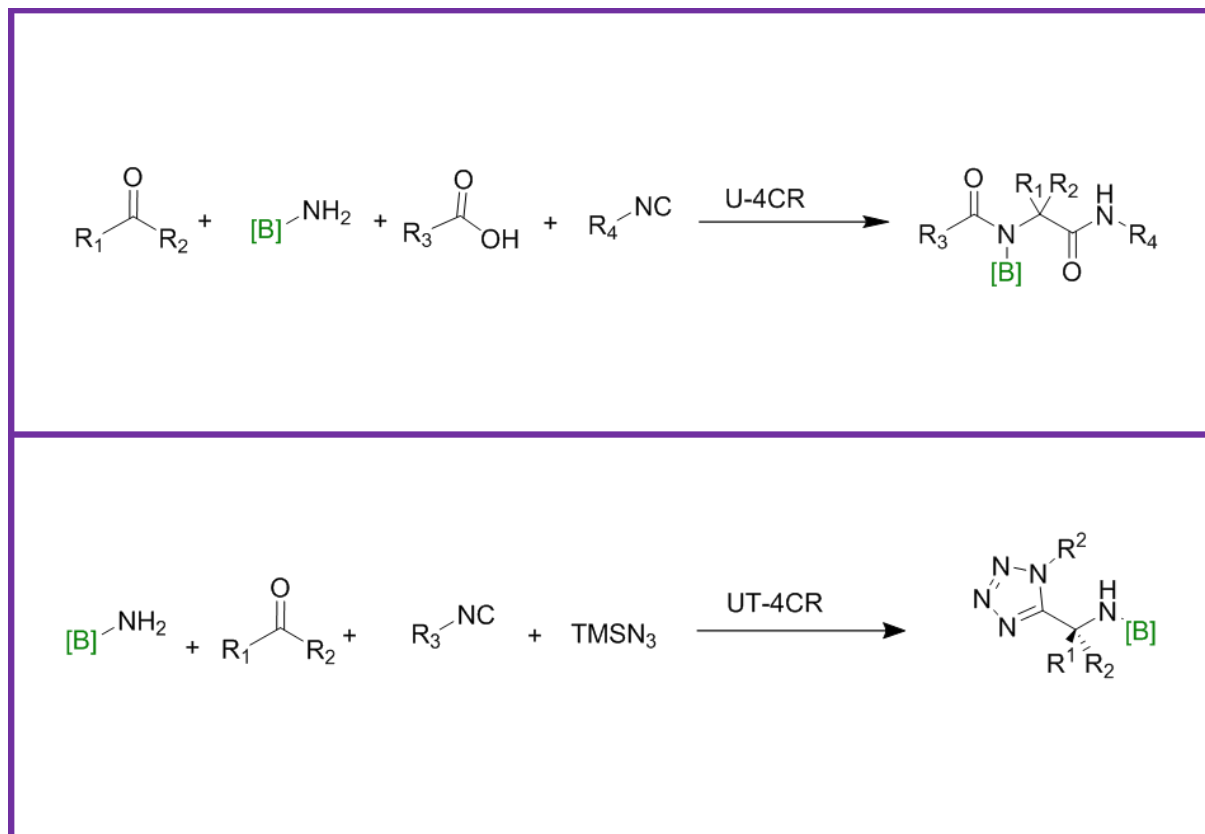


Fig. S3. Reactions in destination plate II.

Destination plate III

Carboxyphenyl boronic acids were used as acid component in U-4CR (wells A1-P24 in destination plate III) as shown in fig. S4. For U-4CR, amines (1 eq, 750 nL), oxo components (1 eq, 750 nL), carboxyphenyl boronic acids (1 eq, 750 nL) and isocyanides (1 eq, 750 nL) were transferred into the corresponding well in the destination plate, respectively. In wells I1-P24, formaldehyde was used as oxo component.

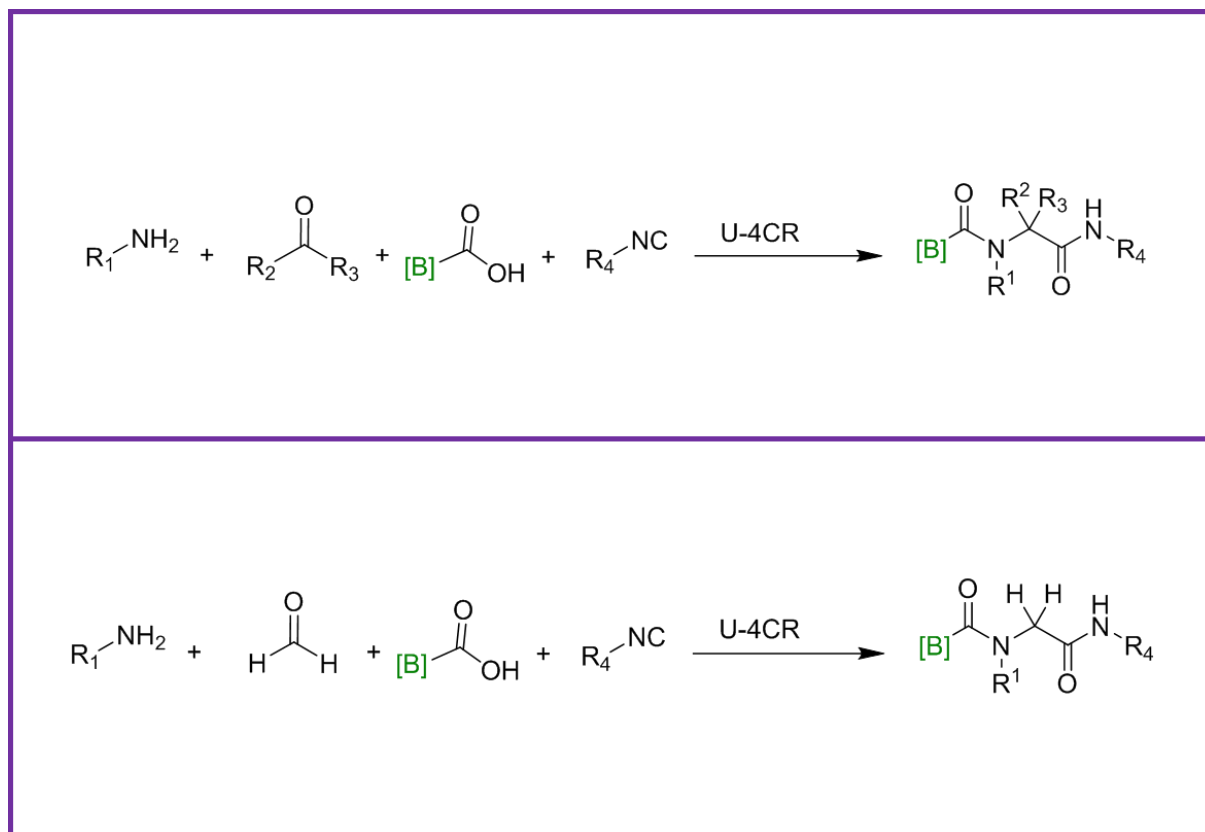


Fig. S4. Reactions in destination plate III.

Destination plate IV

MCR boronic acid building blocks were used in Suzuki coupling (wells A1-H24 in destination plate IV) as shown in fig. S5. For Suzuki coupling, MCR boronic acid building blocks (1 eq, 1000 nL), K_2CO_3 (1.1 eq, 1100 nL), $Pd(PPh_3)_4$ (20 mol%, 200 nL) and aryl halides (1 eq, 1000 nL) were transferred into the corresponding well in the destination plate, respectively.

Once the starting materials transfer of destination plates I, II and III was completed (~150 min for each plate), the destination plates were covered with the sealing film and was then placed for 12 h at 23 °C on an orbital shaker.

The starting materials transfer of destination plate IV took ~80 min. Afterwards destination plate IV was placed in an oven at 50 °C overnight.

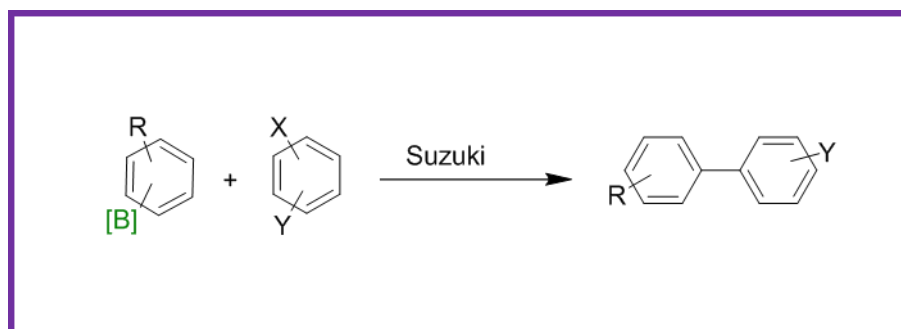


Fig. S5. Reactions in destination plate IV.

2.2.3. Pick list preparation

Labcyte Echo plate reformat software using custom mapping mode with the run protocol as defined by a pick list was used (fig. S6A).

In order to generate a random library of products (N=384 and N=192), a modified version of our previously reported program RandReactor was used (49). The smiles files of the starting materials with the corresponding location in the source plate and mrv file of reaction were the input of the RandReactor program. The smiles file of the randomly generated products with their corresponding locations in the source and destination plate were the output of the RandReactor program. The smiles file was converted to a csv file which was the required format for Labcyte Echo plate reformat software (fig. S6B). The structures of the products are shown in fig. S6.

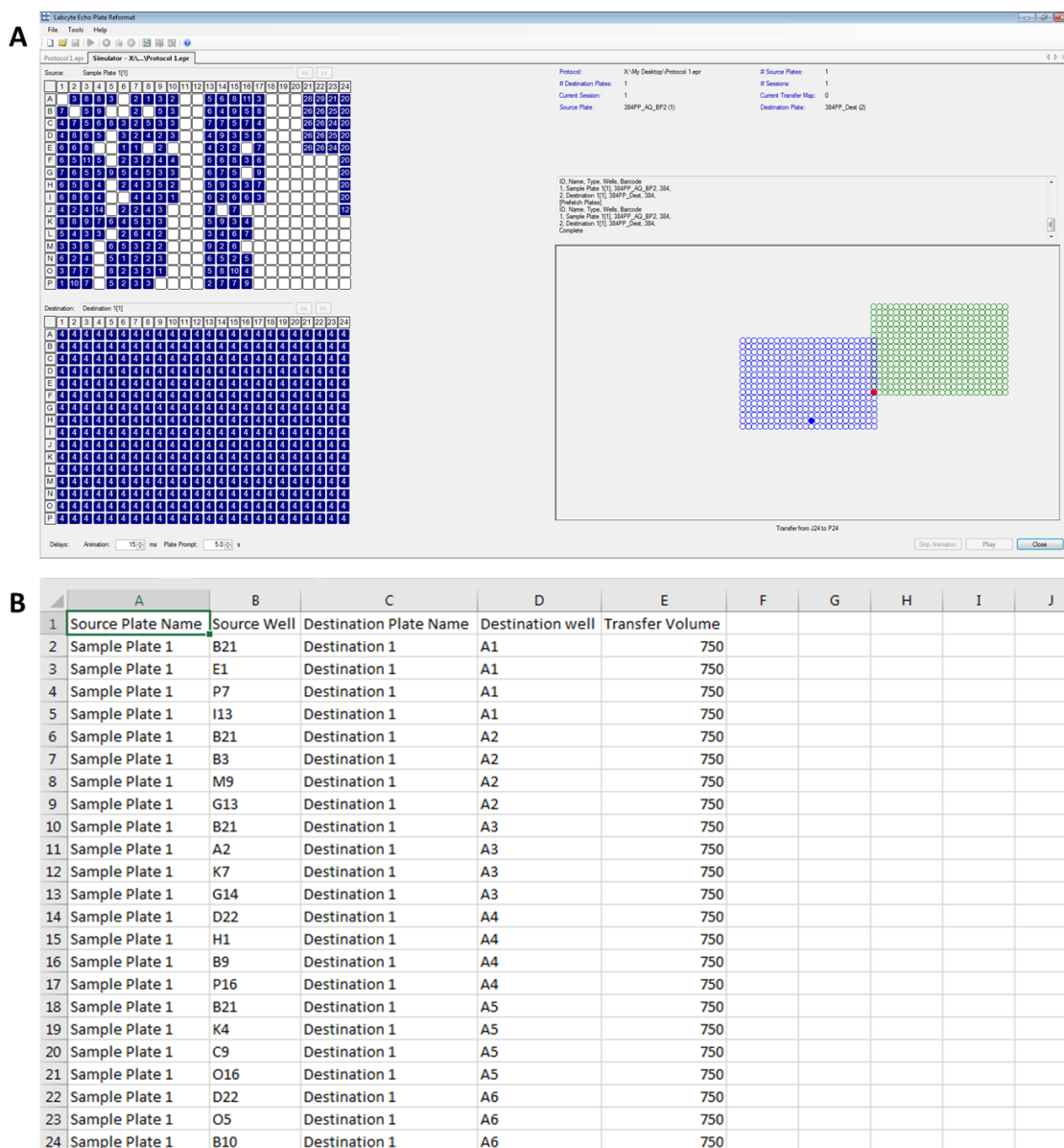


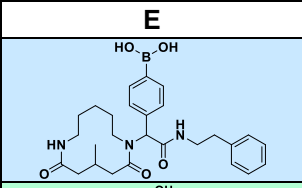
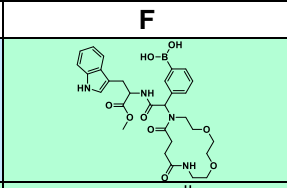
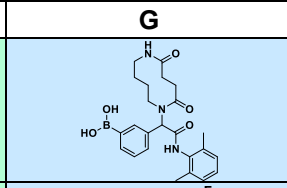
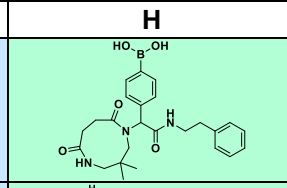
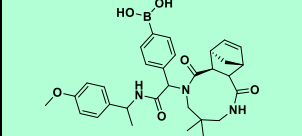
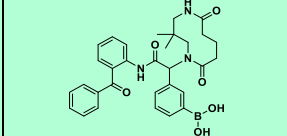
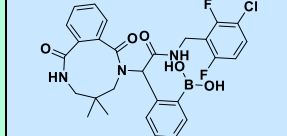
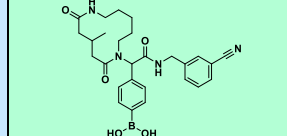
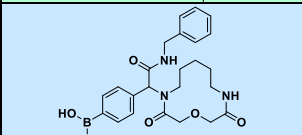
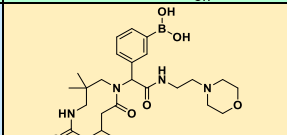
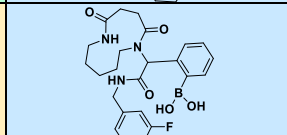
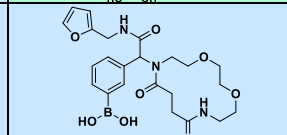
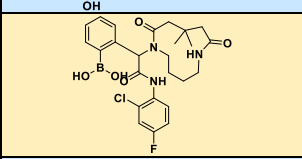
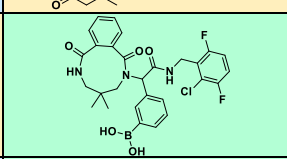
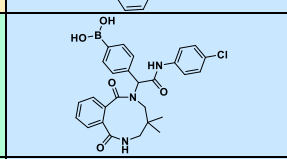
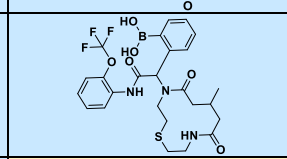
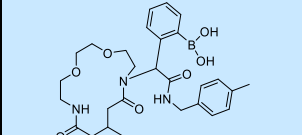
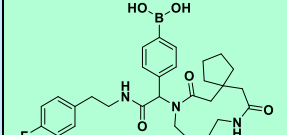
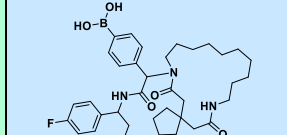
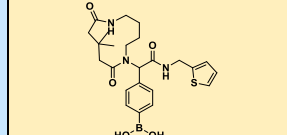
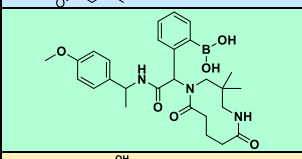
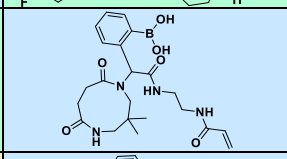
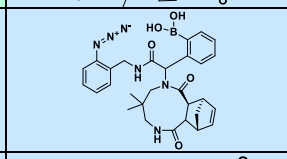
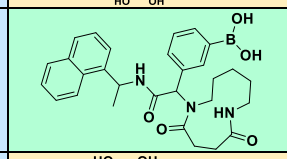
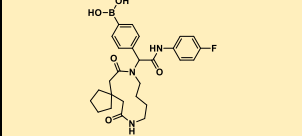
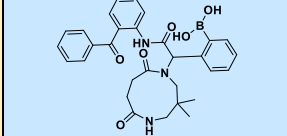
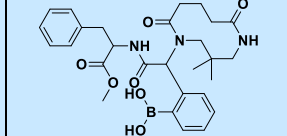
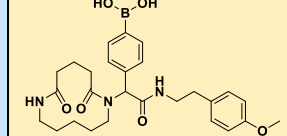
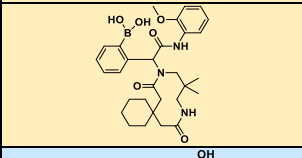
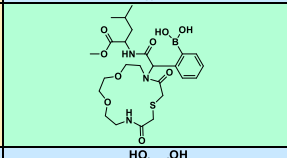
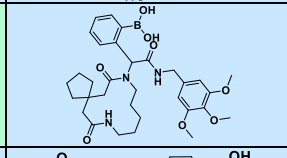
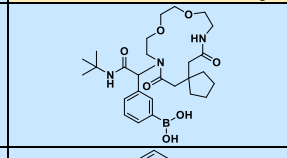
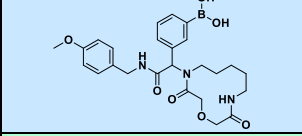
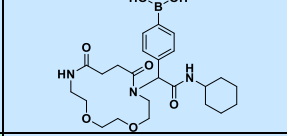
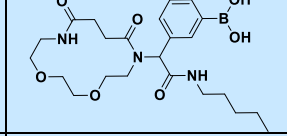
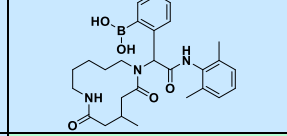
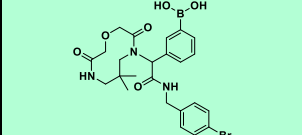
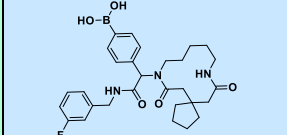
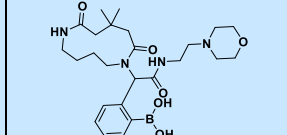
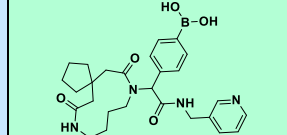
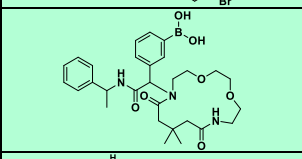
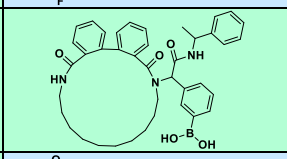
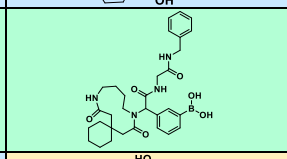
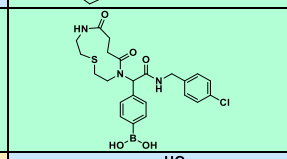
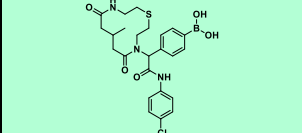
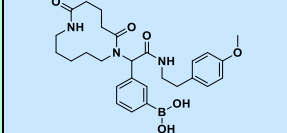
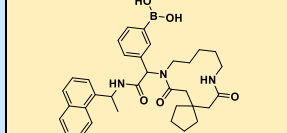
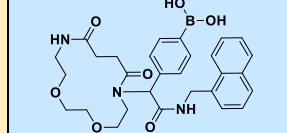
Fig. S6. Labcyte Echo plate reformat software. (A) Showing on top the source plate and below the destination plate II; **(B)** Picklist in csv format required for Labcyte Echo plate reformat software.

Destination plate I

	A	B	C	D
1				
2				
3				
4				
5				
6				
7				
8				
9				
10				
11				
12				

	A	B	C	D
13				
14				
15				
16				
17				
18				
19				
20				
21				
22				
23				
24				

	E	F	G	H
1				
2				
3				
4				
5				
6				
7				
8				
9				
10				
11				
12				

	E	F	G	H
13				
14				
15				
16				
17				
18				
19				
20				
21				
22				
23				
24				

	I	J	K	L
1				
2				
3				
4				
5				
6				
7				
8				
9				
10				
11				
12				

	I	J	K	L
13				
14				
15				
16				
17				
18				
19				
20				
21				
22				
23				
24				

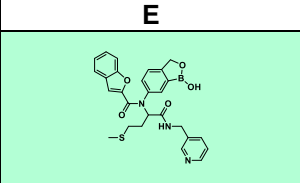
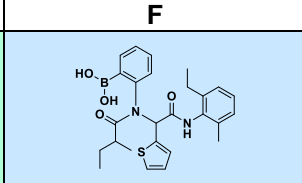
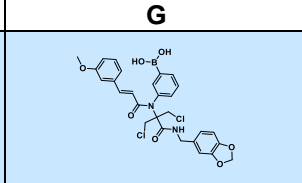
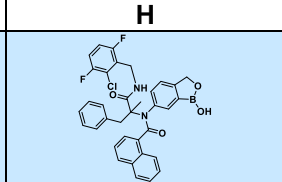
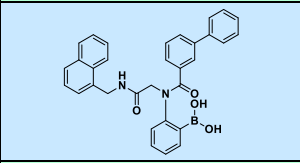
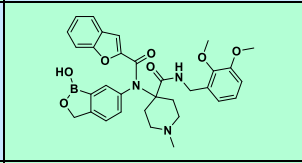
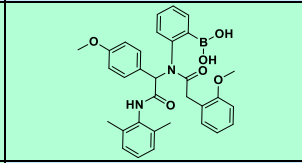
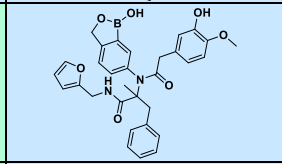
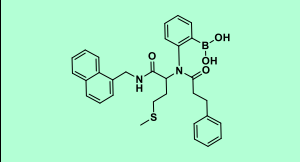
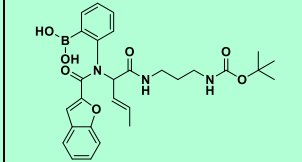
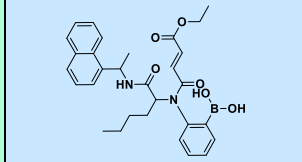
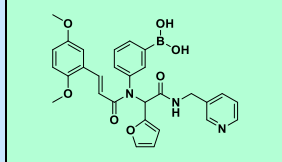
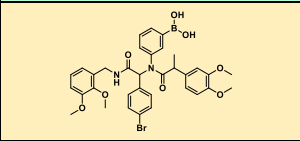
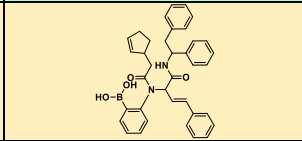
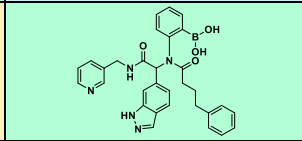
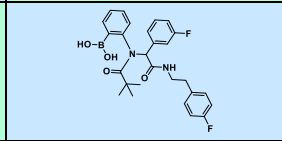
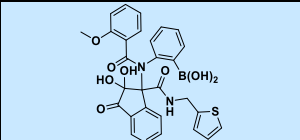
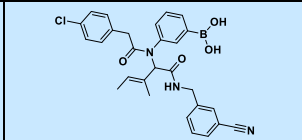
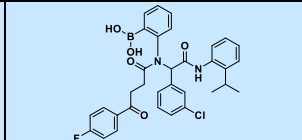
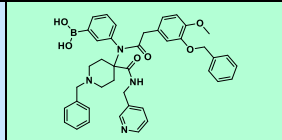
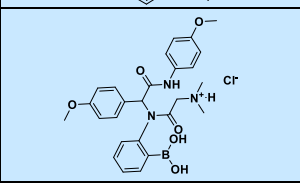
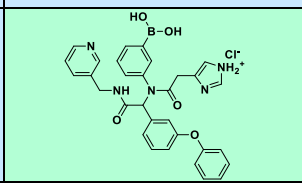
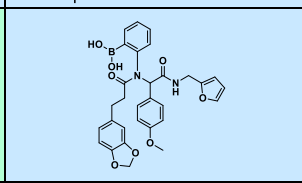
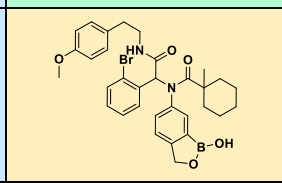
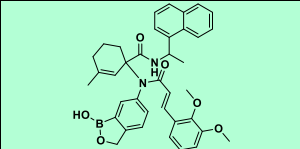
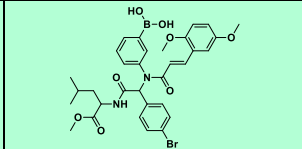
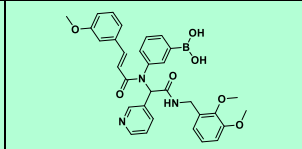
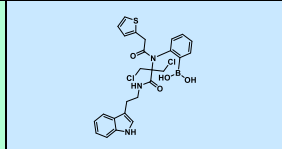
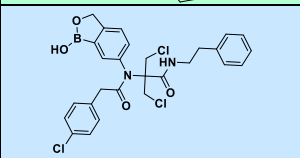
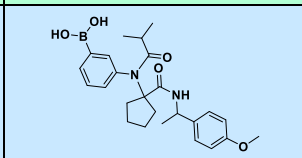
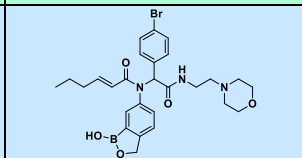
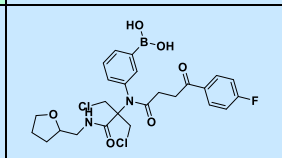
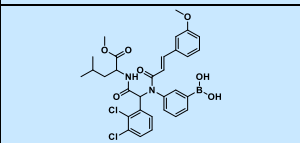
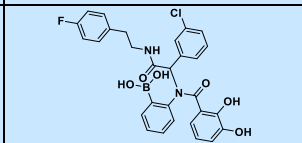
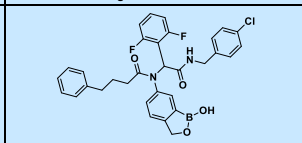
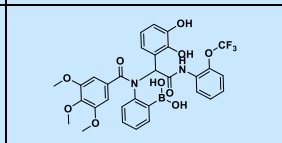
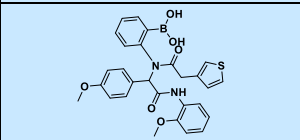
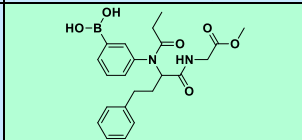
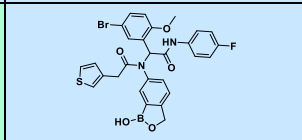
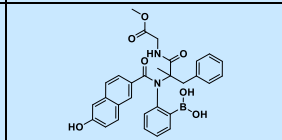
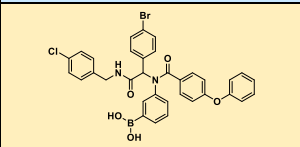
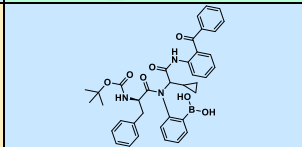
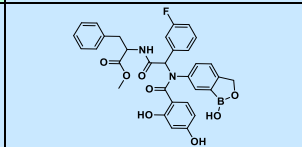
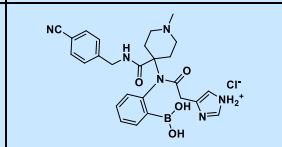
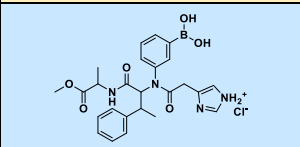
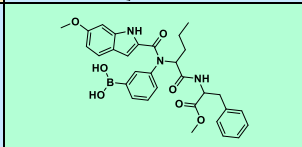
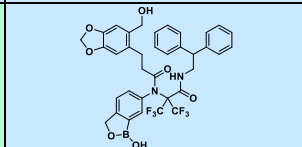
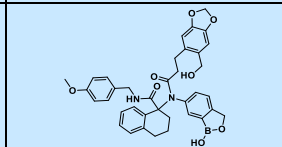
	M	N	O	P
1				
2				
3				
4				
5				
6				
7				
8				
9				
10				
11				
12				

	M	N	O	P
13				
14				
15				
16				
17				
18				
19				
20				
21				
22				
23				
24				

Destination plate II

	A	B	C	D
1				
2				
3				
4				
5				
6				
7				
8				
9				
10				
11				
12				

	A	B	C	D
13				
14				
15				
16				
17				
18				
19				
20				
21				
22				
23				
24				


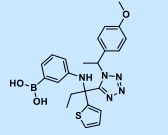
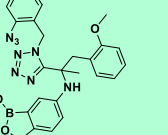
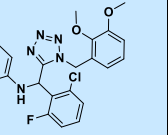

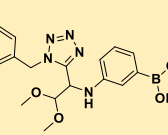
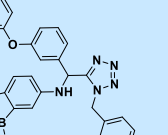
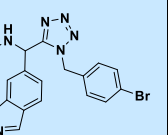
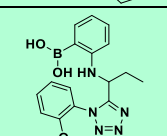
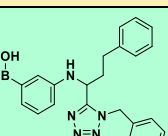
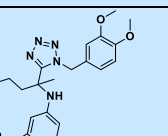
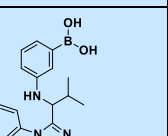
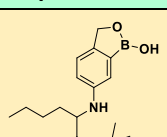
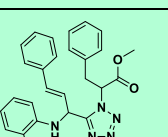
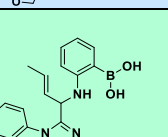
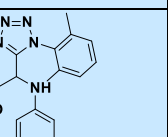
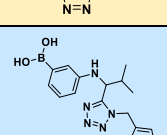
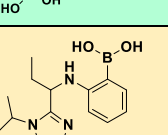
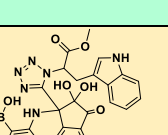
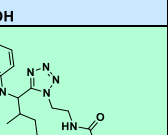
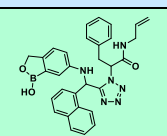
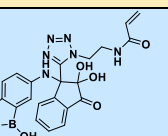
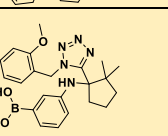
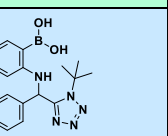
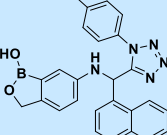
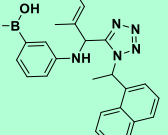
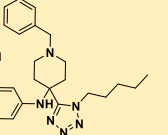
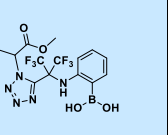
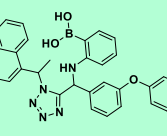
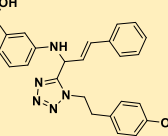
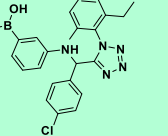
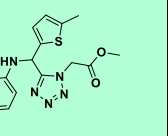
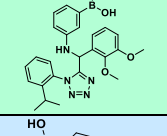
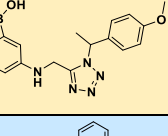
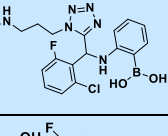
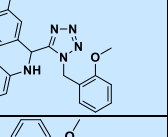
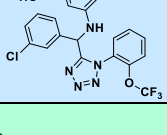
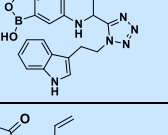
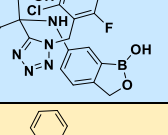
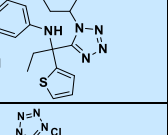
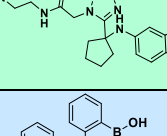
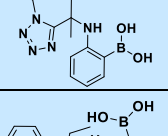
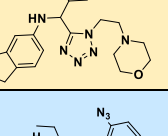
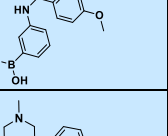
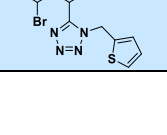
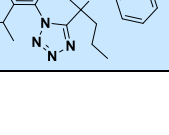
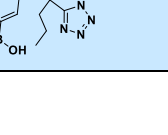
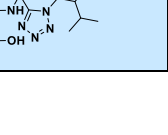
	E	F	G	H
1				
2				
3				
4				
5				
6				
7				
8				
9				
10				
11				
12				

	E	F	G	H
13				
14				
15				
16				
17				
18				
19				
20				
21				
22				
23				
24				

	I	J	K	L
1				
2				
3				
4				
5				
6				
7				
8				
9				
10				
11				
12				

	I	J	K	L
13				
14				
15				
16				
17				
18				
19				
20				
21				
22				
23				
24				

	M	N	O	P
1				
2				
3				
4				
5				
6				
7				
8				
9				
10				
11				
12				

	M	N	O	P
13				
14				
15				
16				
17				
18				
19				
20				
21				
22				
23				
24				

Destination plate III

	A	B	C	D
1				
2				
3				
4				
5				
6				
7				
8				
9				
10				
11				
12				

	A	B	C	D
13				
14				
15				
16				
17				
18				
19				
20				
21				
22				
23				
24				

	E	F	G	H
1				
2				
3				
4				
5				
6				
7				
8				
9				
10				
11				
12				

	E	F	G	H
13				
14				
15				
16				
17				
18				
19				
20				
21				
22				
23				
24				

	I	J	K	L
1				
2				
3				
4				
5				
6				
7				
8				
9				
10				
11				
12				

Destination plate IV

	A	B	C	D
1				
2				
3				
4				
5				
6				
7				
8				
9				
10				
11				
12				

	A	B	C	D
13				
14				
15				
16				
17				
18				
19				
20				
21				
22				
23				
24				

	E	F	G	H
1				
2				
3				
4				
5				
6				
7				
8				
9				
10				
11				

12				
	E	F	G	H
13				
14				
15				
16				
17				
18				
19				
20				
21				
22				
23				

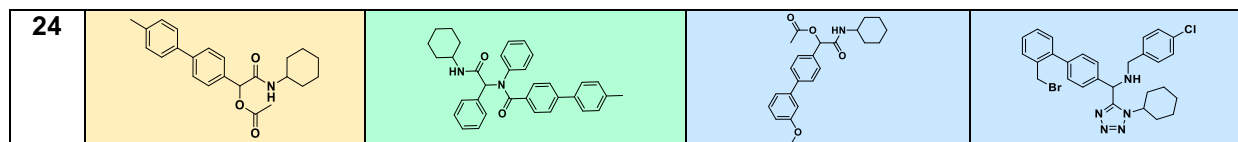


Fig. S7. Heat plots with product structures, green for major product formation, yellow for medium product formation, and blue for no product formation.

2.3. Quality control (QC)

The analytics of all wells were performed by SFC-UV-MS. Mass spectra were measured on a Waters Investigator Supercritical Fluid Chromatograph with a 3100 MS Detector (ESI⁺) via flow injection analysis (FIA) and MassLynx software.

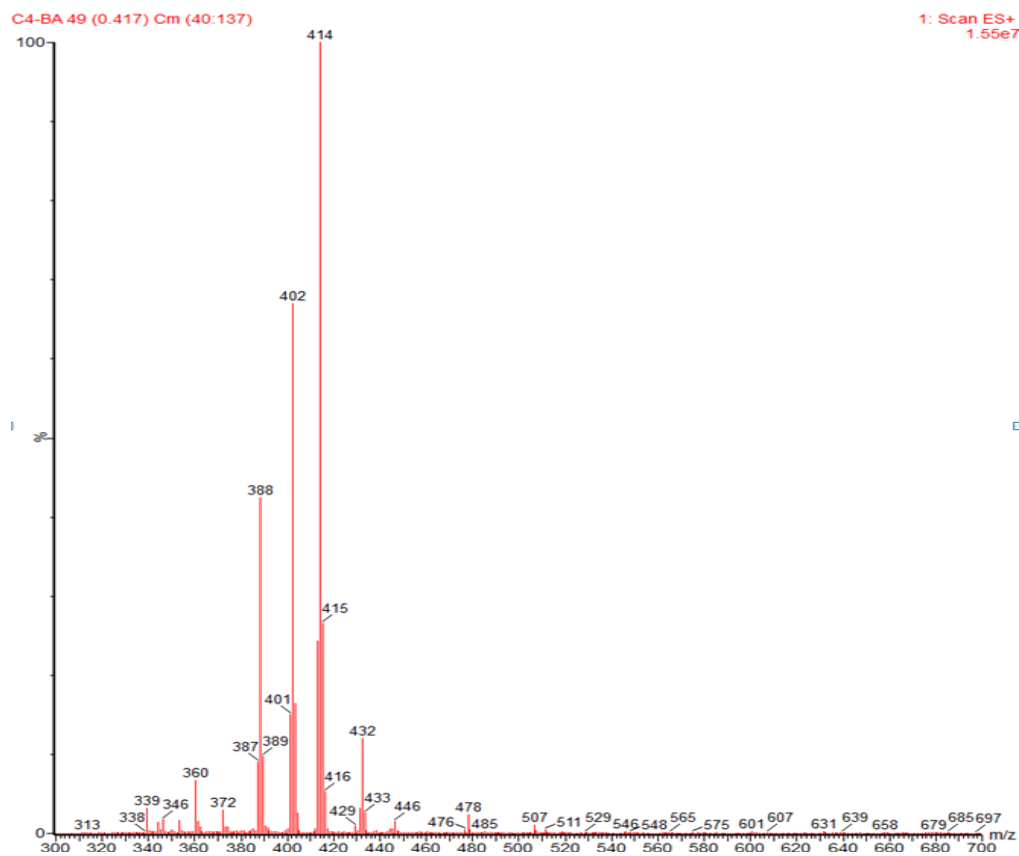
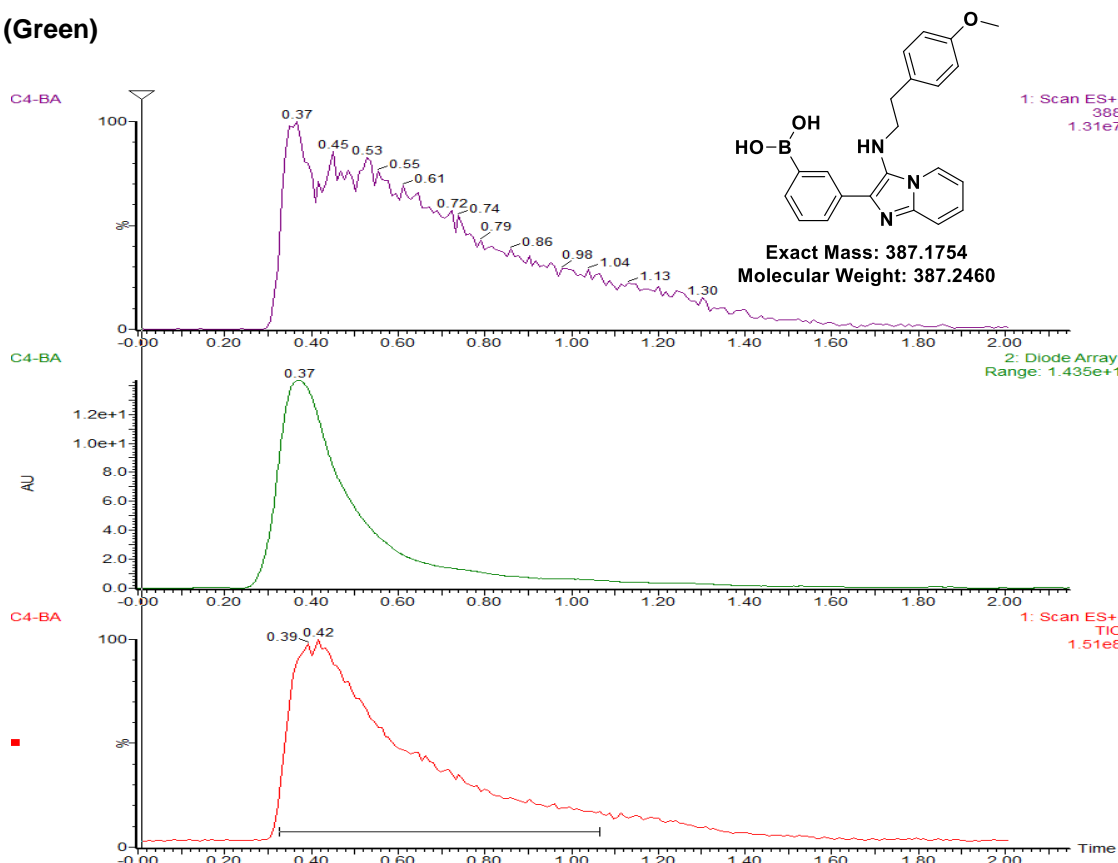
Conditions: eluent composition: MeOH, 2% H₂O, 0.1% formic acid; run time: 2 min; flow rate: 1 mL/min.

Each well of the destination plate was diluted with 100 μ L ethylene glycol and then the chromatographic analysis was done by MS using an autosampler. A right-click and drag operation of the total ion current (TIC) spectrum generated a mass chromatogram for the selected range. If the peak corresponding to M+1 or M+15 (methyl ester) or M+27 (cyclic ethylene glycol ester) or M+45 (ethylene glycol monoester) or M+Na or M+K was the major peak, the well received a green designation and otherwise yellow (50). If the peak of M+1 or M+15 or M+27 or M+45 or M+Na or M+K was absent, the well received a blue designation.

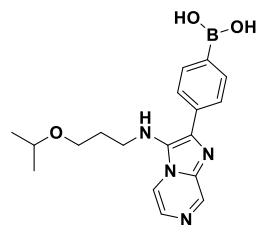
The SFC analytic of one well took ~2 min, resulting in an overall measuring time for the 1344 wells of around 45 h.

Examples of SFC-MS analytics directly out of the 384-well plate (Destination plate I)

C4 (Green)



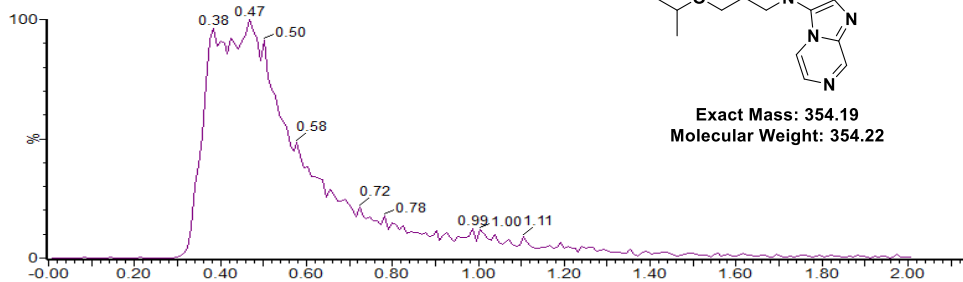
A2 (Green)



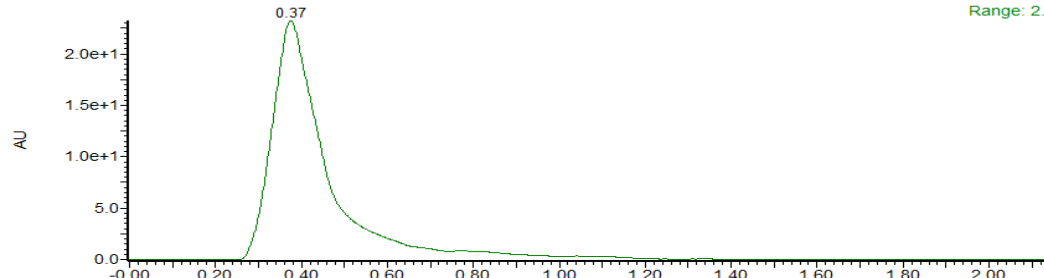
Exact Mass: 354.19
Molecular Weight: 354.22

1: Scan ES+
355
1.54e7

A2-BA

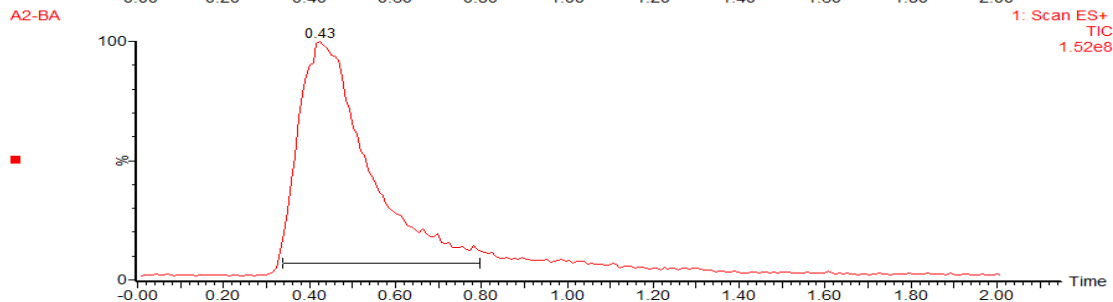


A2-BA



2: Diode Array
Range: 2.343e+1

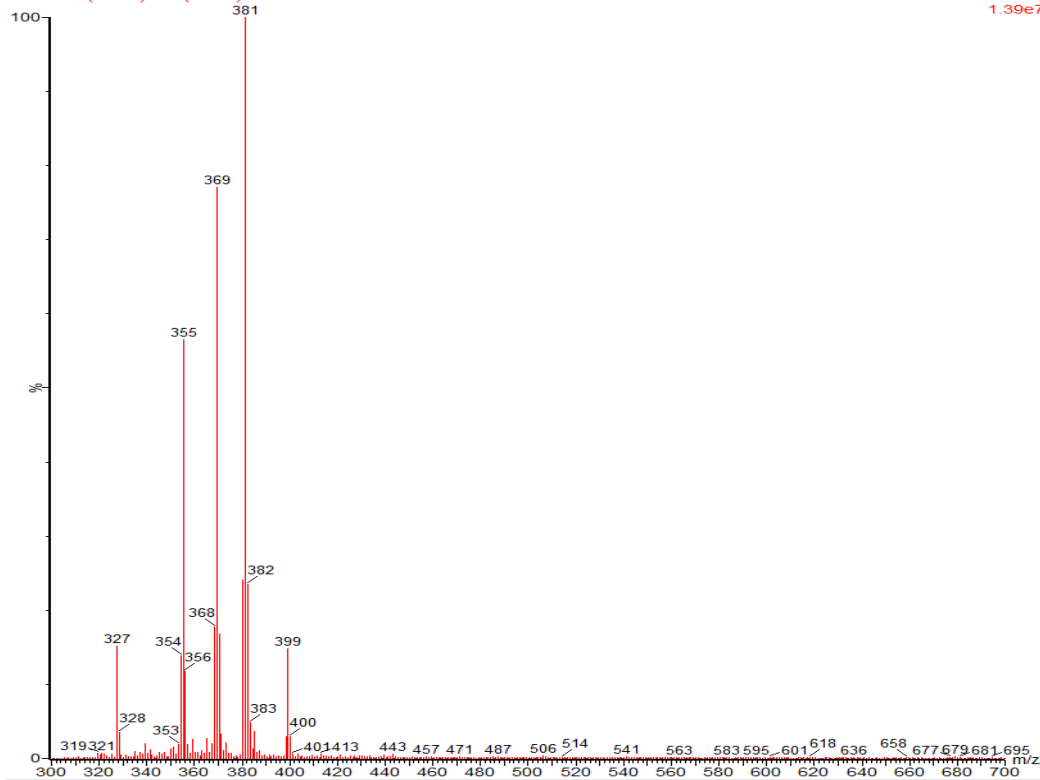
A2-BA



1: Scan ES+
TIC
1.52e8

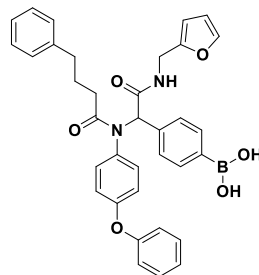
■

A2-BA 50 (0.425) Cm (40-94)



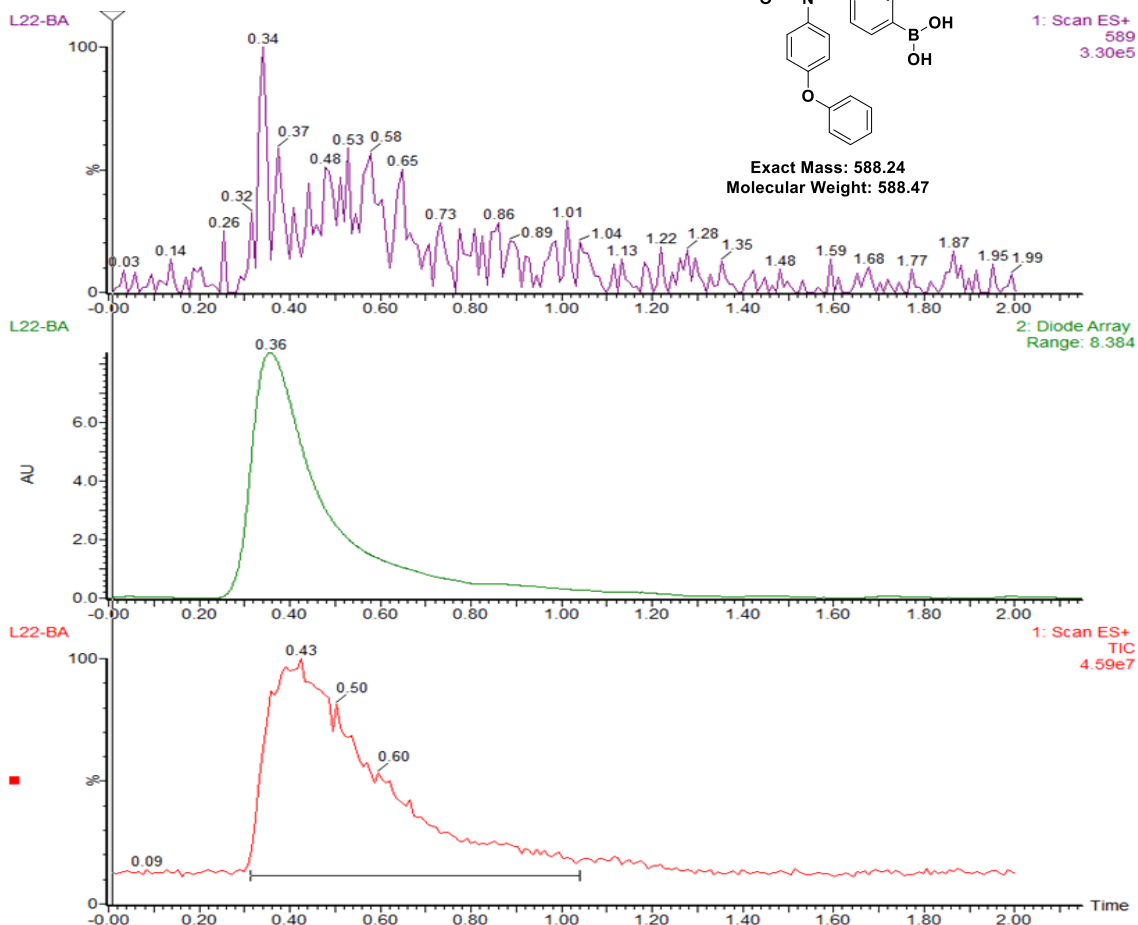
1: Scan ES+
1.39e7

L22 (Green)

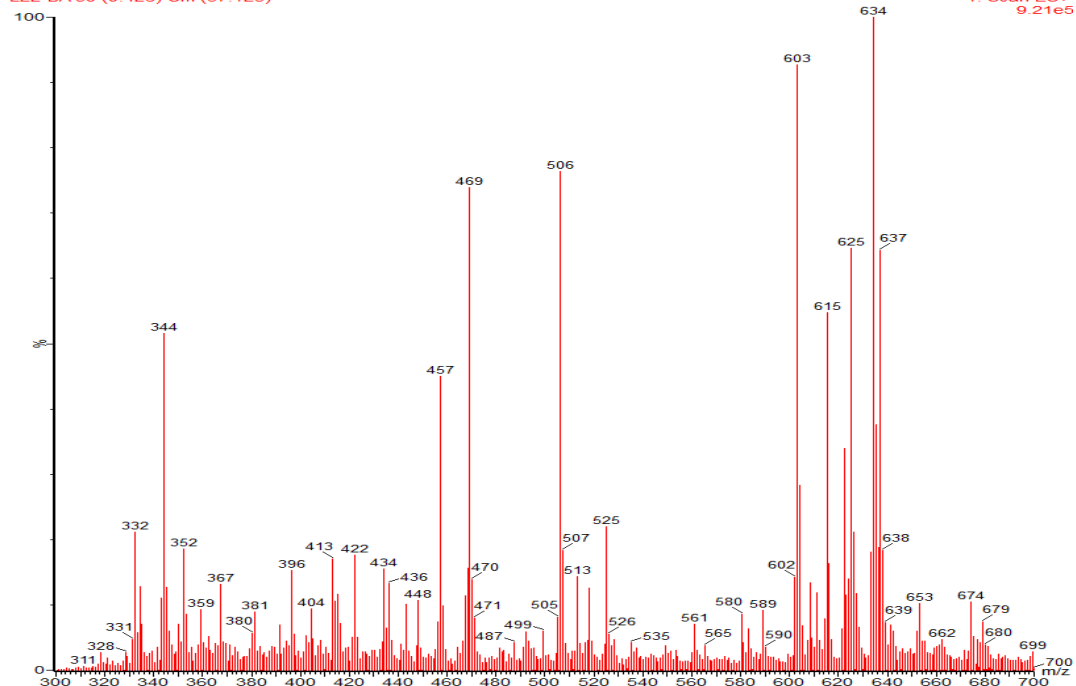


Exact Mass: 588.24
Molecular Weight: 588.47

1: Scan ES+
589
3.30e5

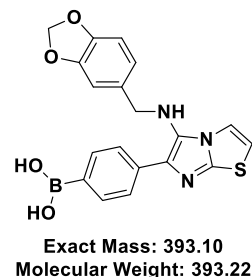


L22-BA 50 (0.426) Cm (37:125)

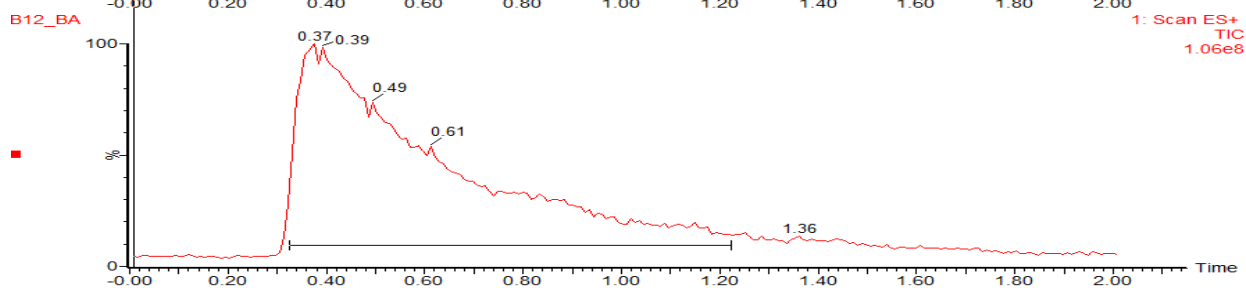
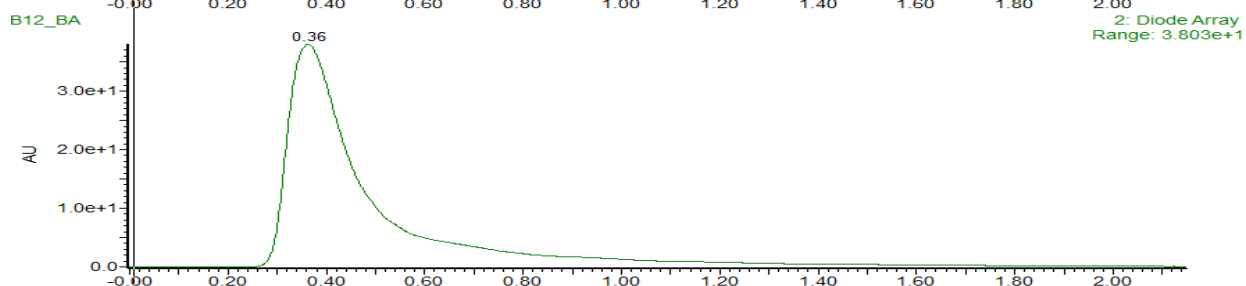
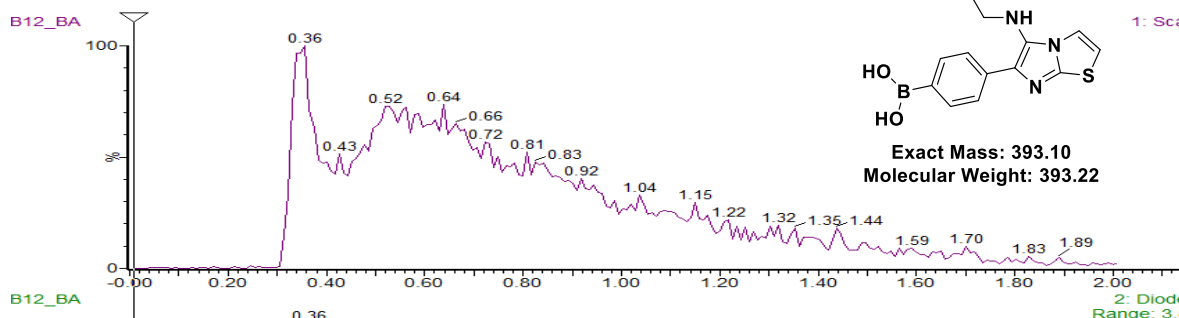


1: Scan ES+
9.21e5

B12 (Green)

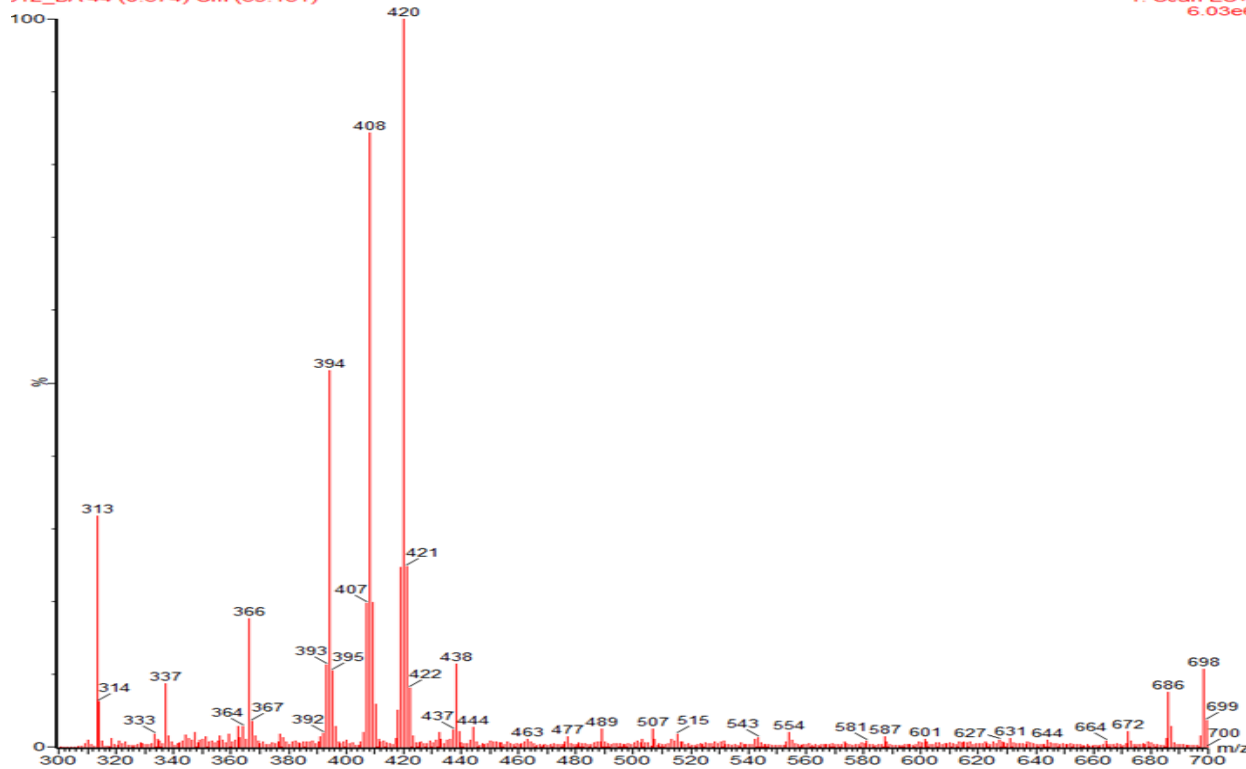


1: Scan ES+
394
7.10e6

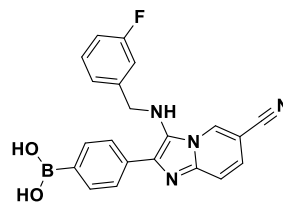


312_BA 44 (0.374) Cm (39:151)

1: Scan ES+
6.03e6

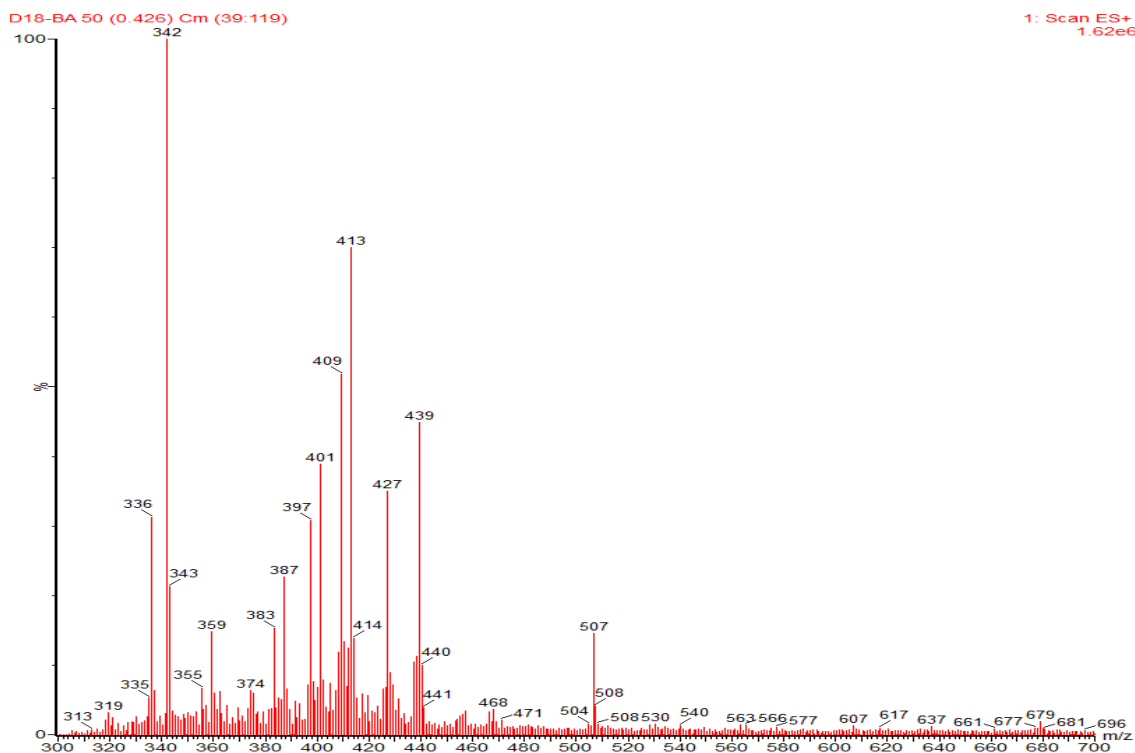
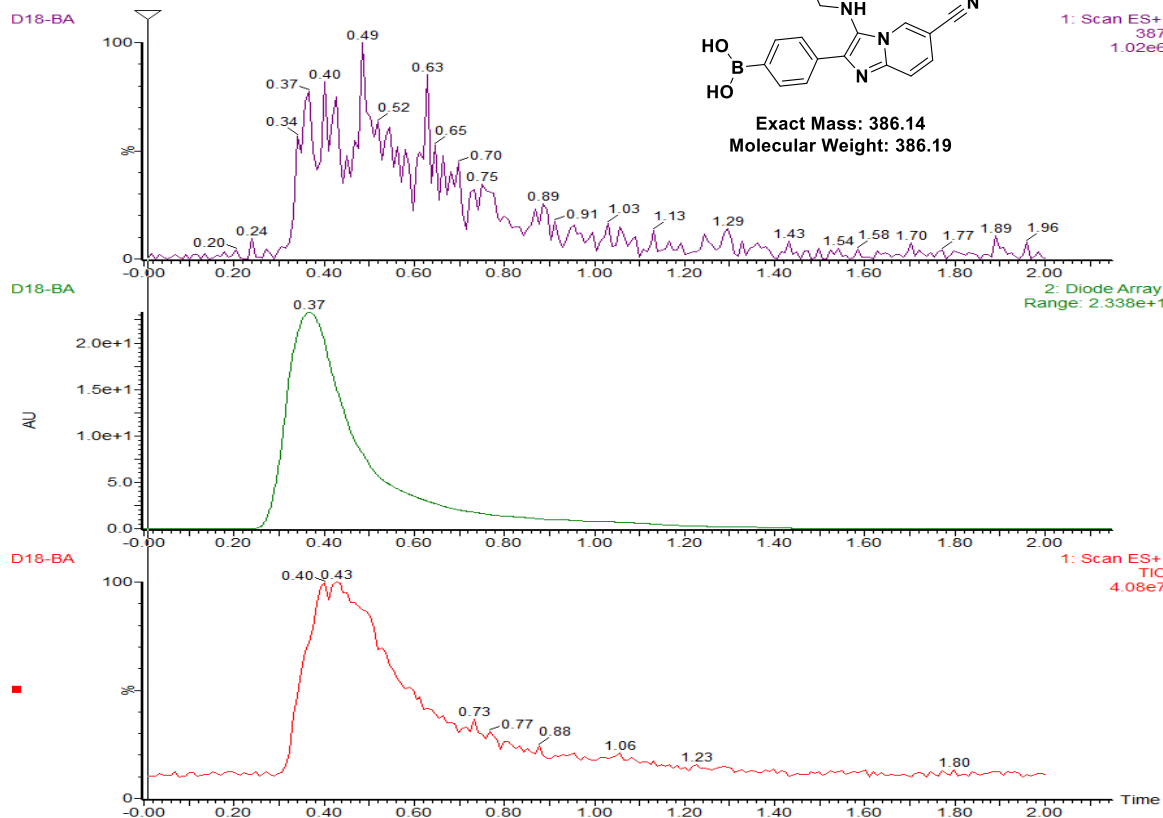


D18 (Green)

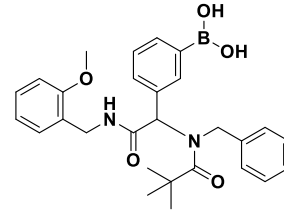


Exact Mass: 386.14
Molecular Weight: 386.19

1: Scan ES+
387
1.02e6

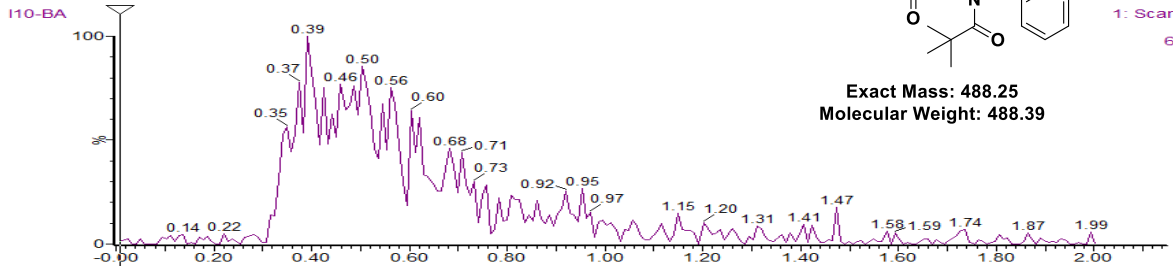


I10 (Green)

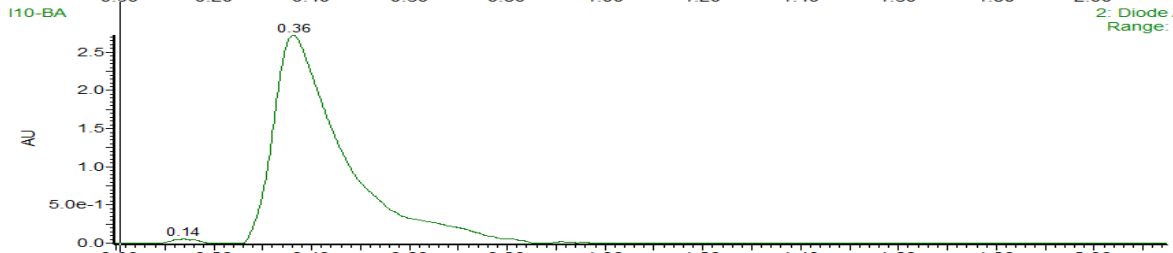


Exact Mass: 488.25
Molecular Weight: 488.39

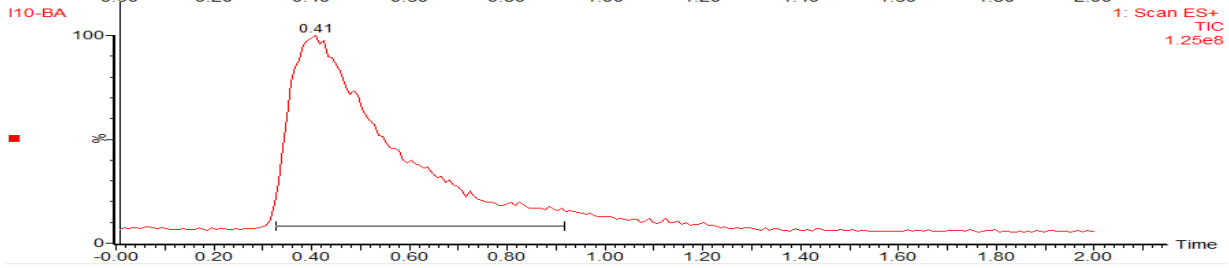
1: Scan ES+
489
6.50e5



2: Diode Array
Range: 2.968

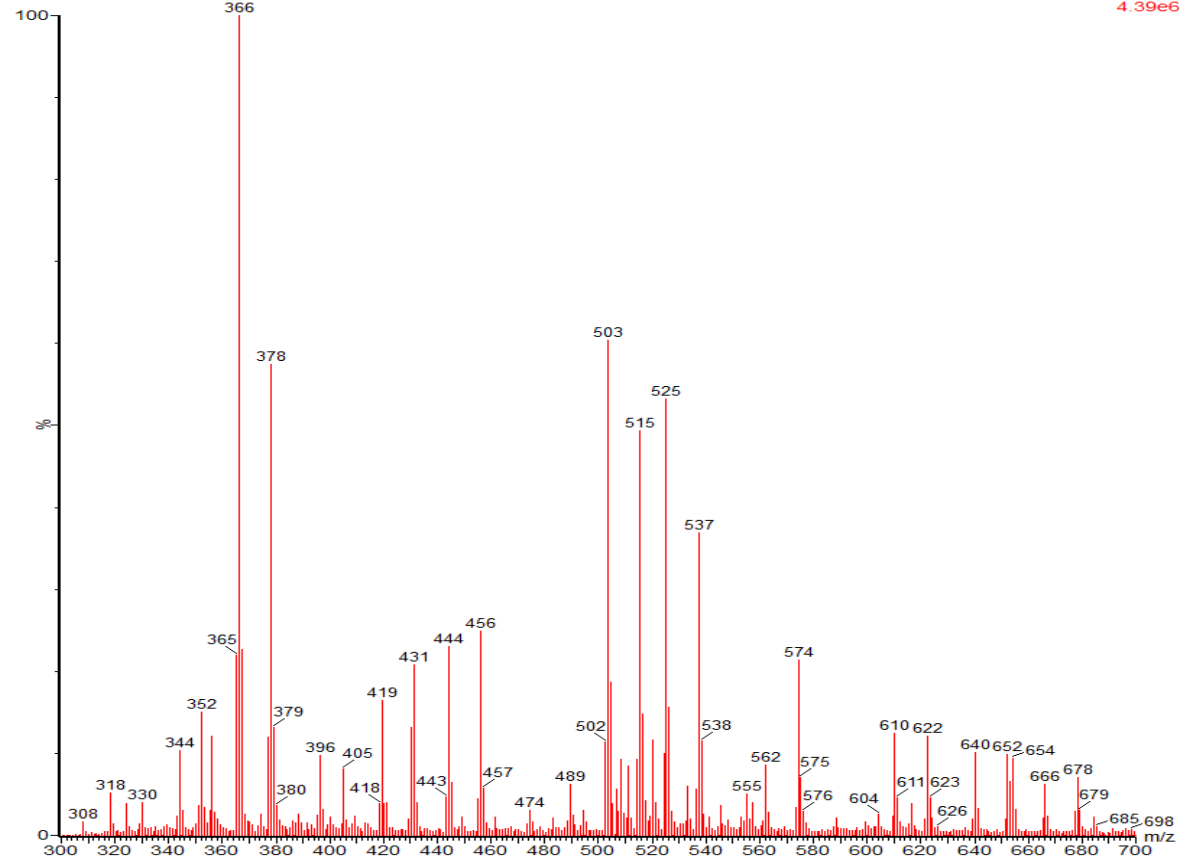


1: Scan ES+
TIC
1.25e8

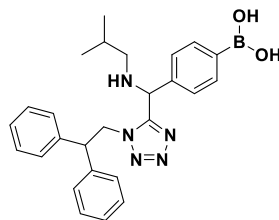


I10-BA 48 (0.409) Cm (40:107)

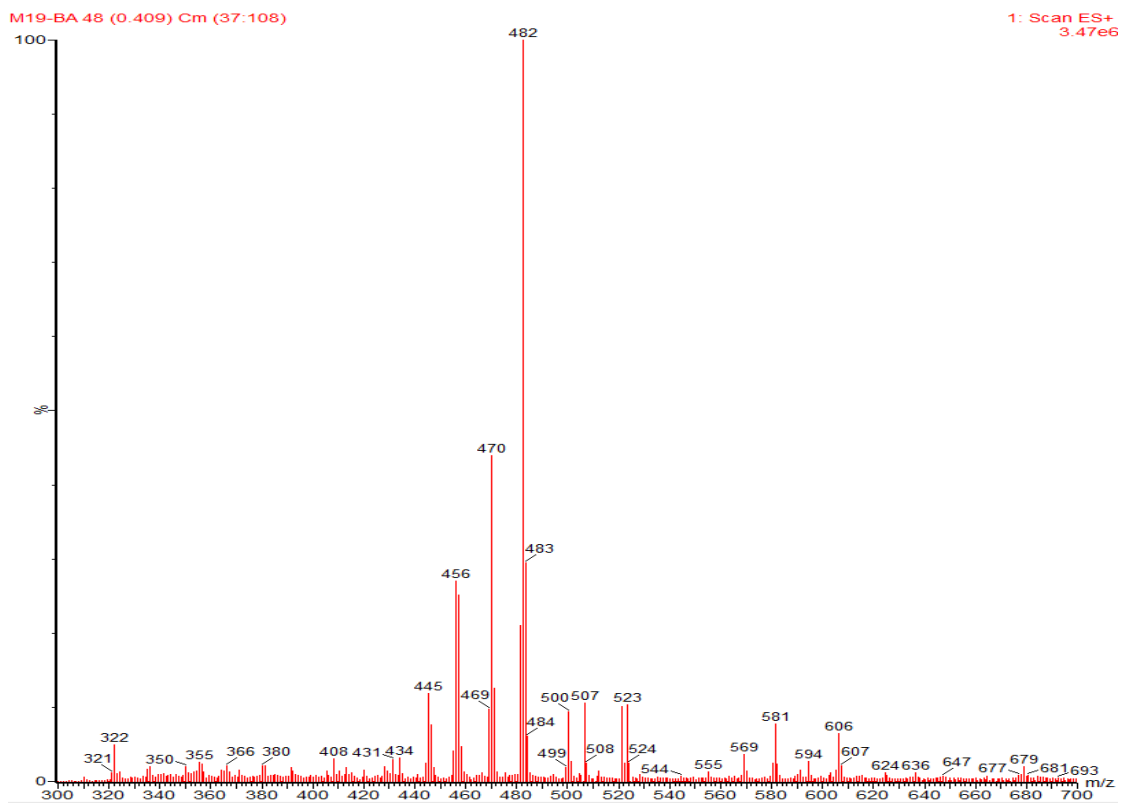
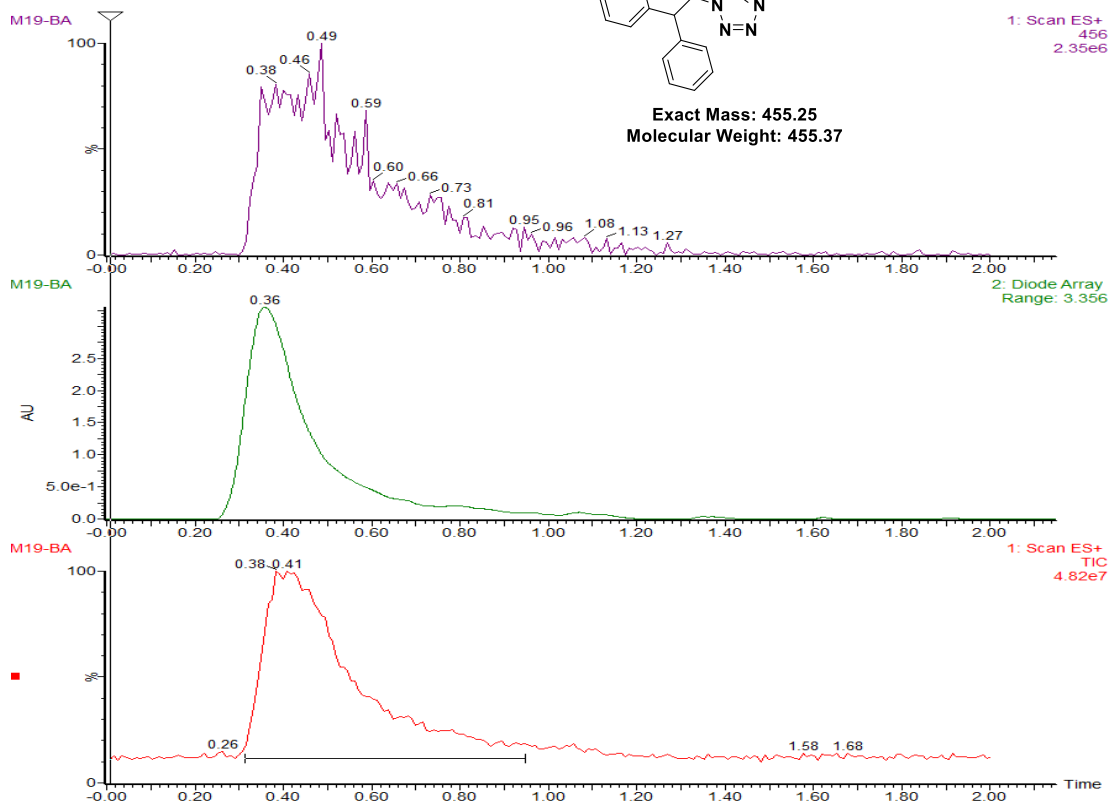
1: Scan ES+
4.39e6



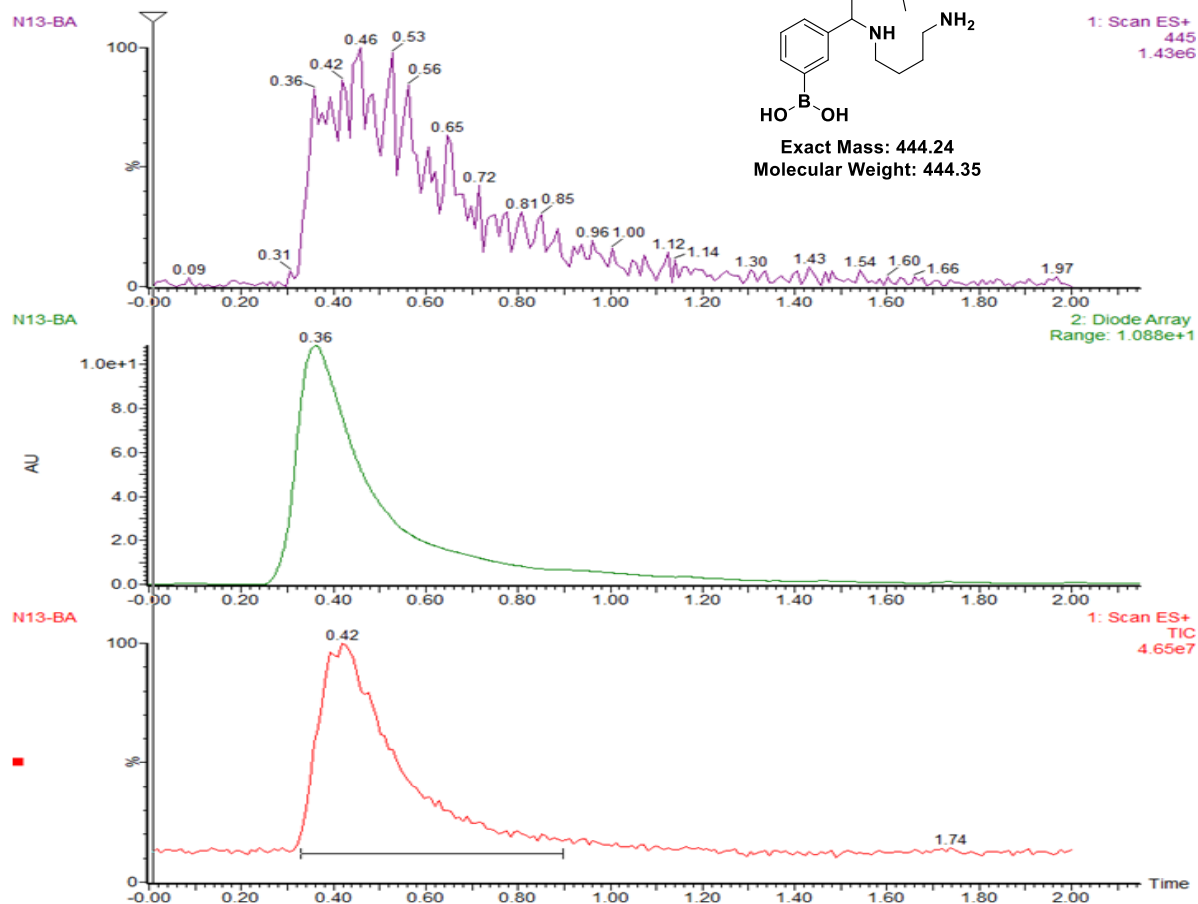
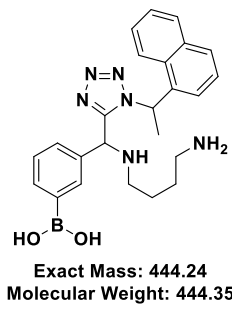
M19 (Green)



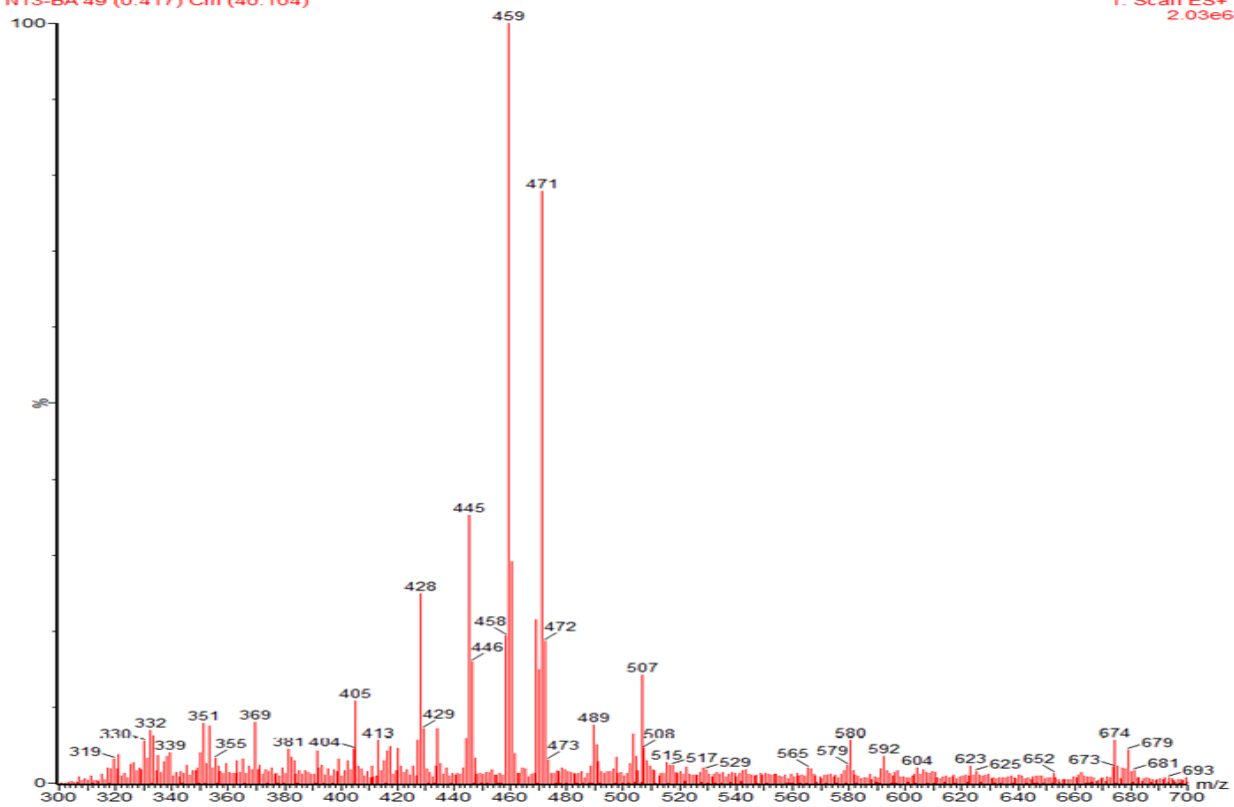
Exact Mass: 455.25
Molecular Weight: 455.37



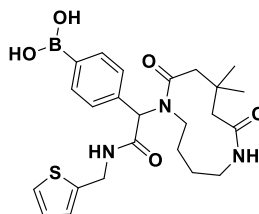
N13 (Green)



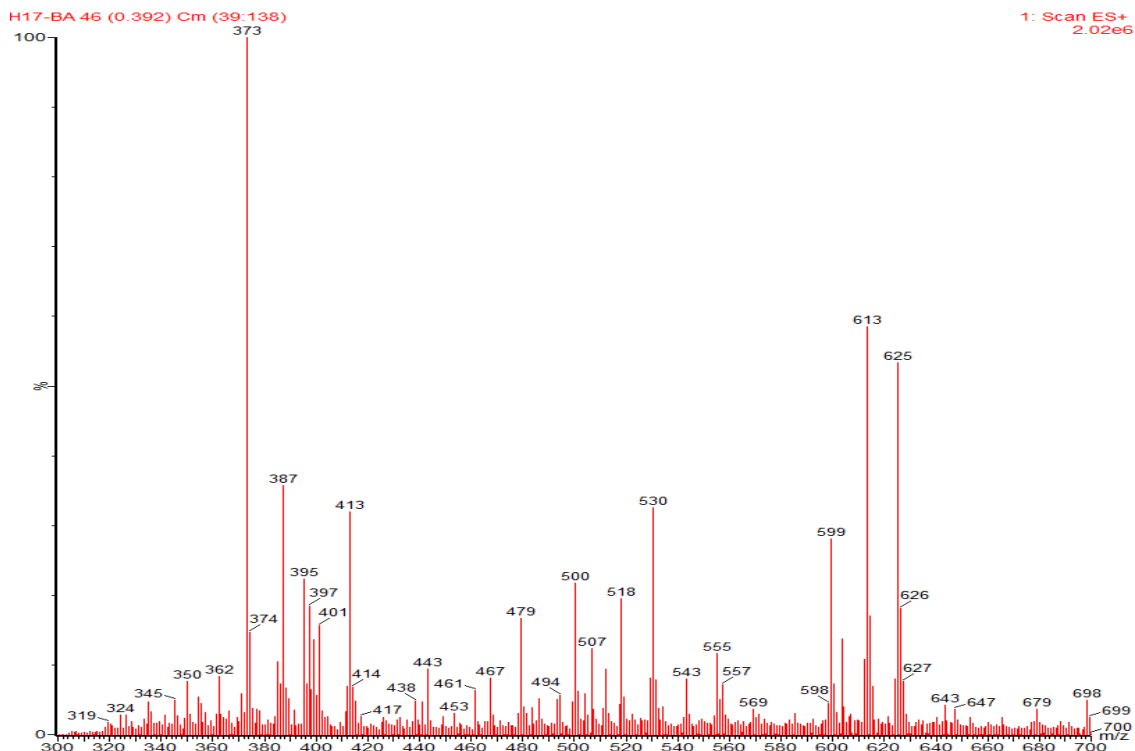
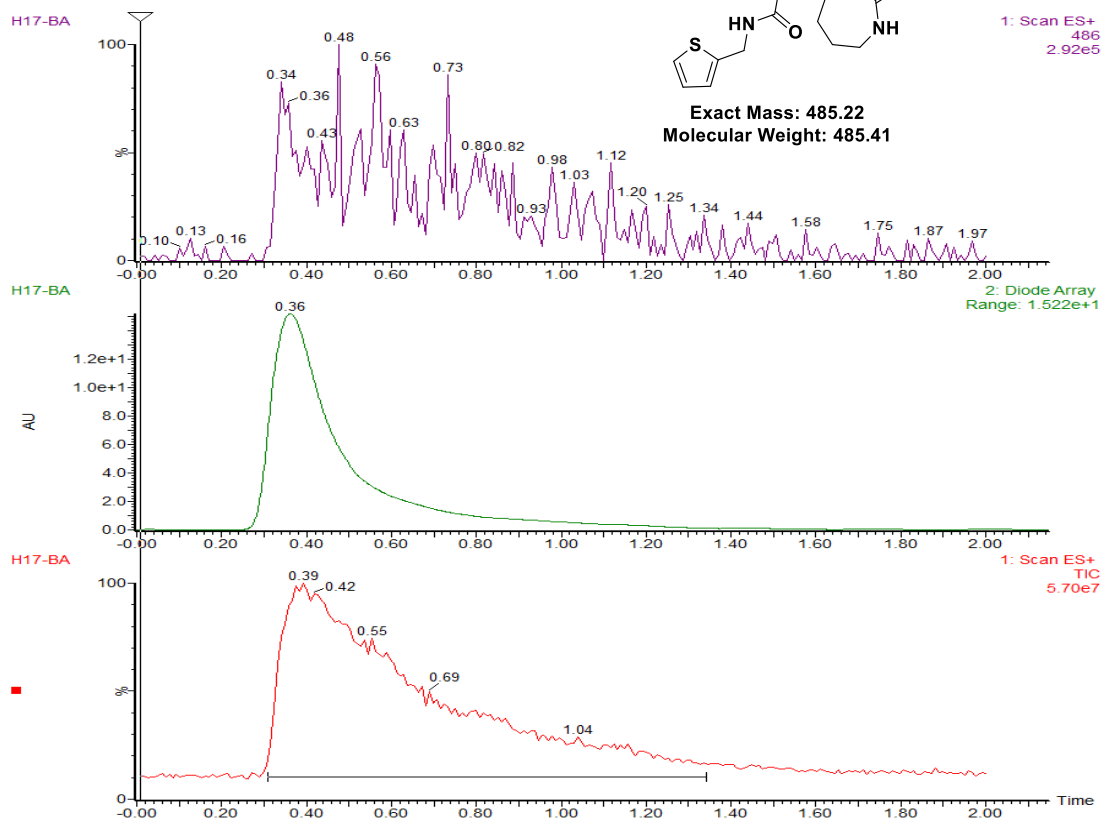
N13-BA 49 (0.417) Cm (40:104)



H17 (Yellow)

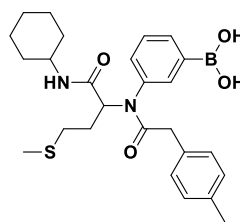


Exact Mass: 485.22
Molecular Weight: 485.41

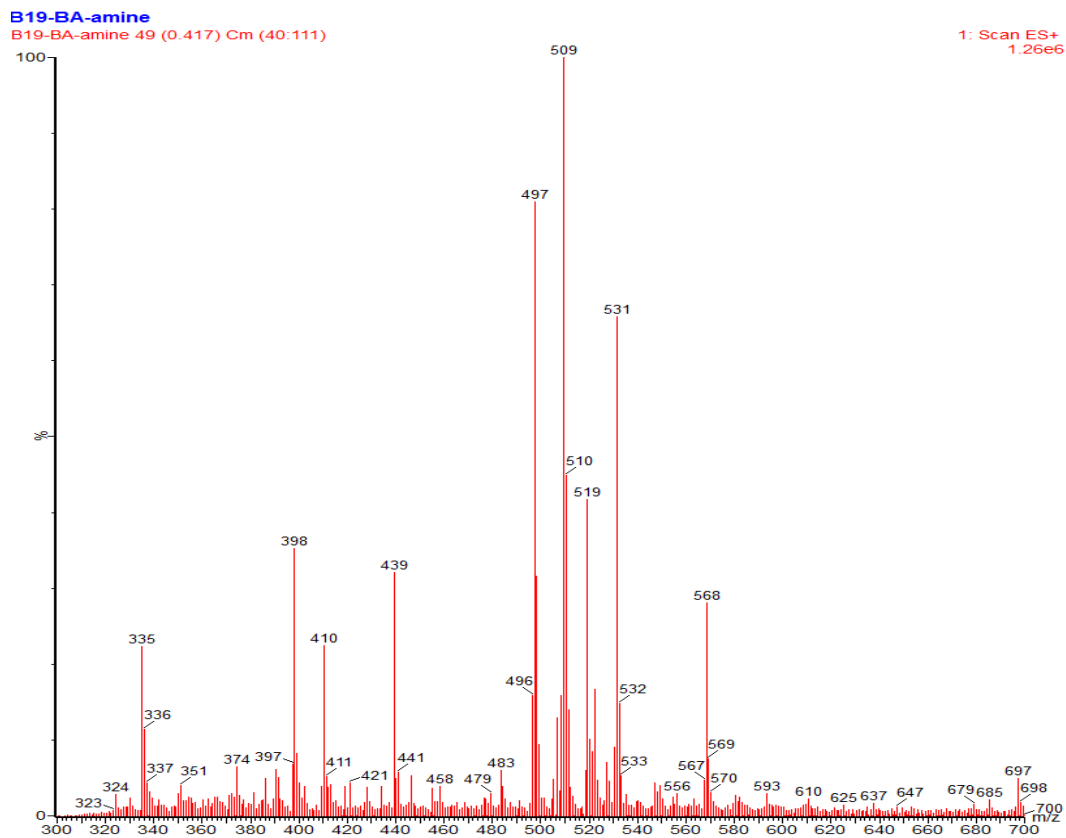
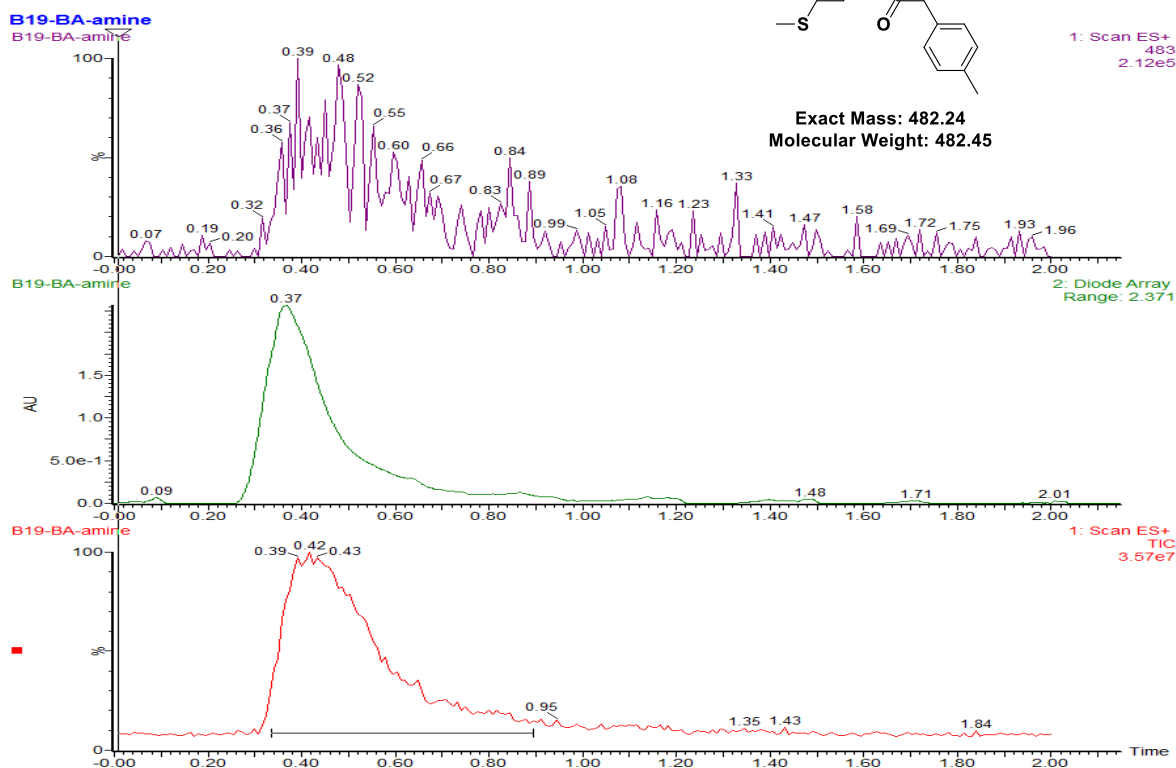


Examples of SFC-MS analytics directly out of the 384-well plate (Destination plate II)

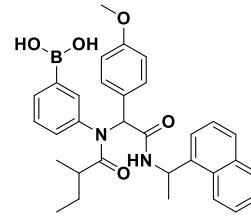
B19 (Green)



Exact Mass: 482.24
Molecular Weight: 482.45



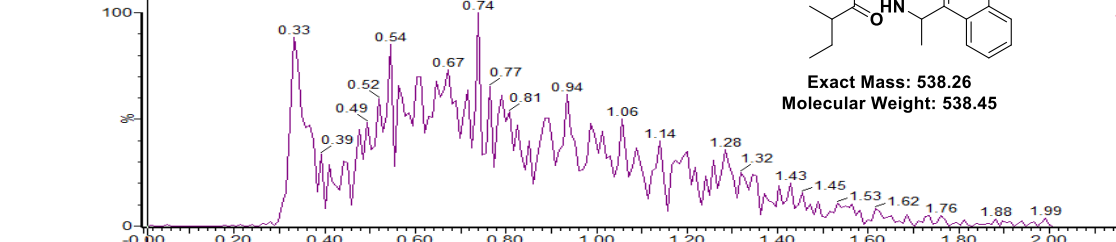
D17 (Green)



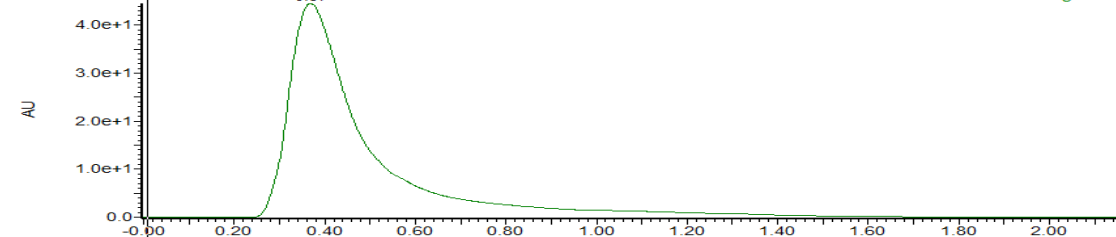
Exact Mass: 538.26
Molecular Weight: 538.45

1: Scan ES+
539
1.14e6

D17-BA-amine
D17-BA-amine

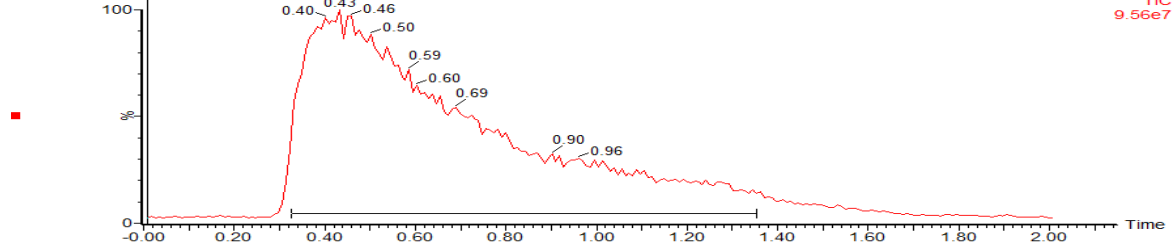


D17-BA-amine



2: Diode Array
Range: 4.451e+1

D17-BA-amine

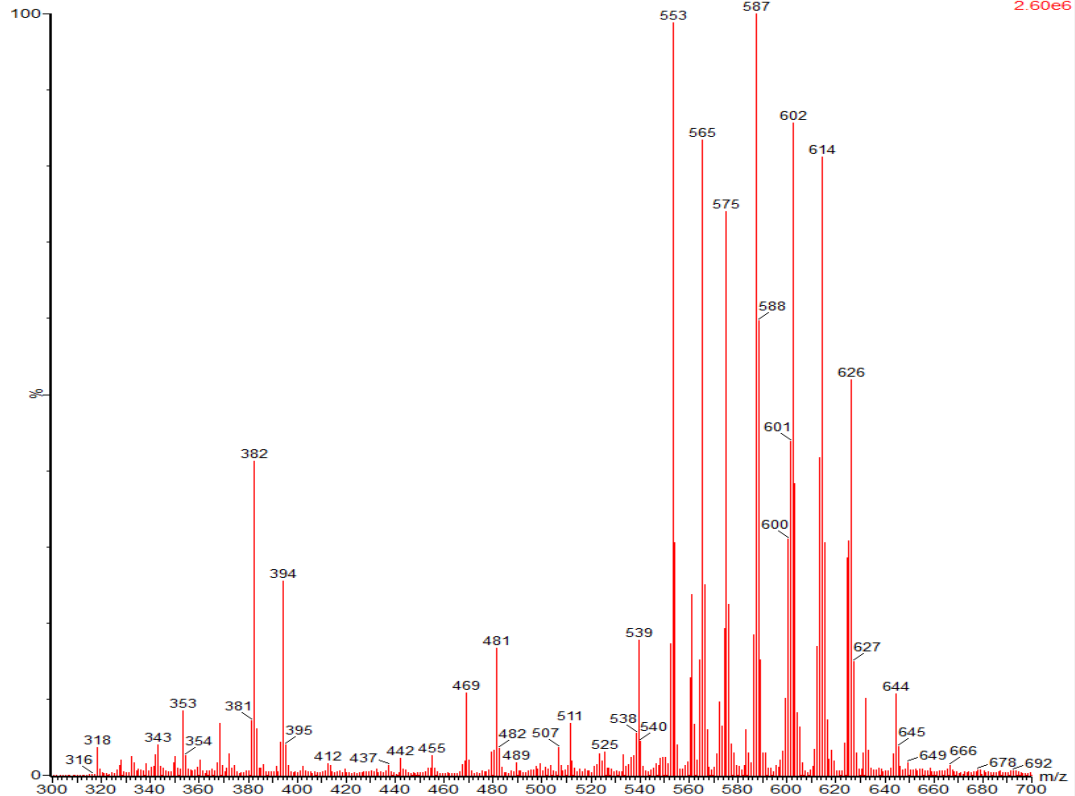


1: Scan ES+
TIC
9.56e7

D17-BA-amine

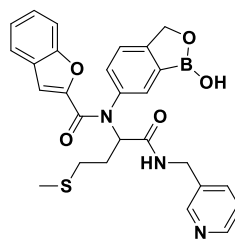
D17-BA-amine 51 (0.434) Cm (39:155)

1: Scan ES+
2.60e6

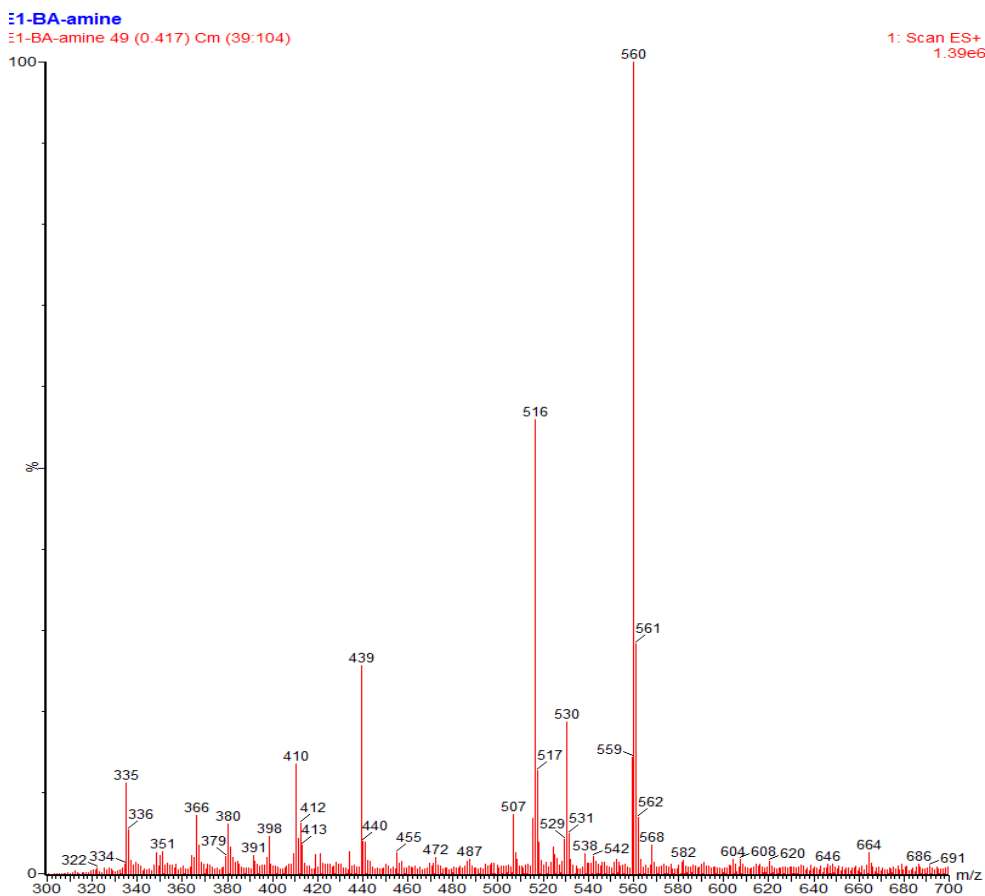
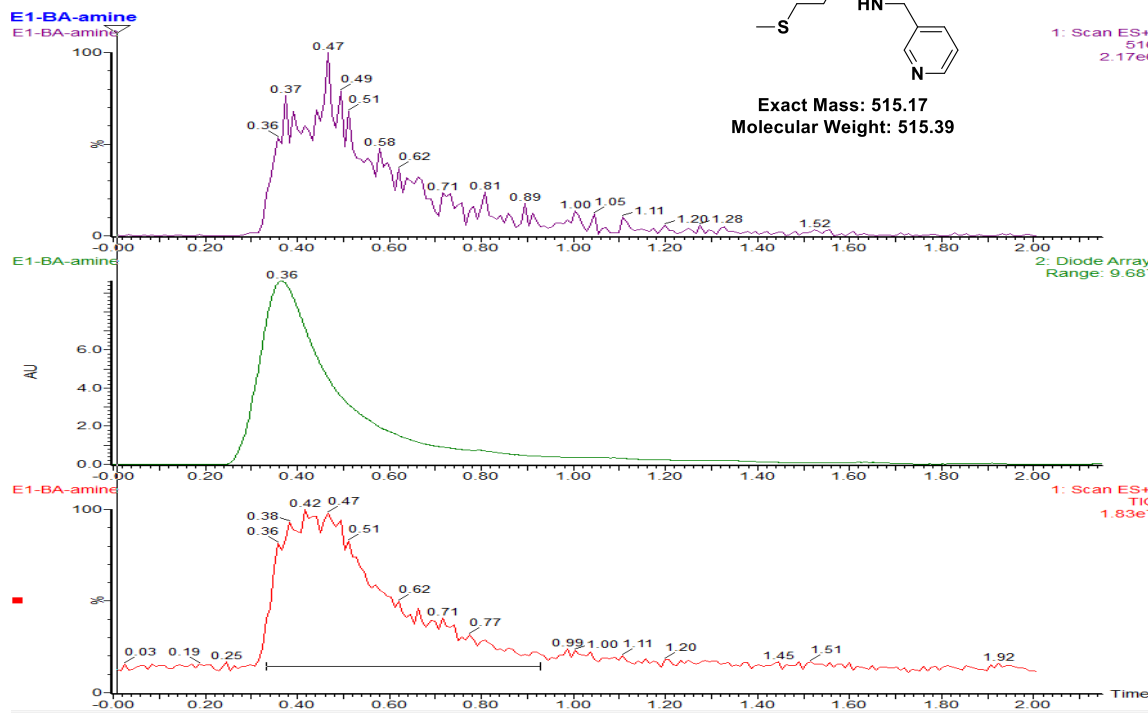


E1 (Green)

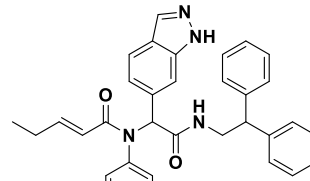
M + 45



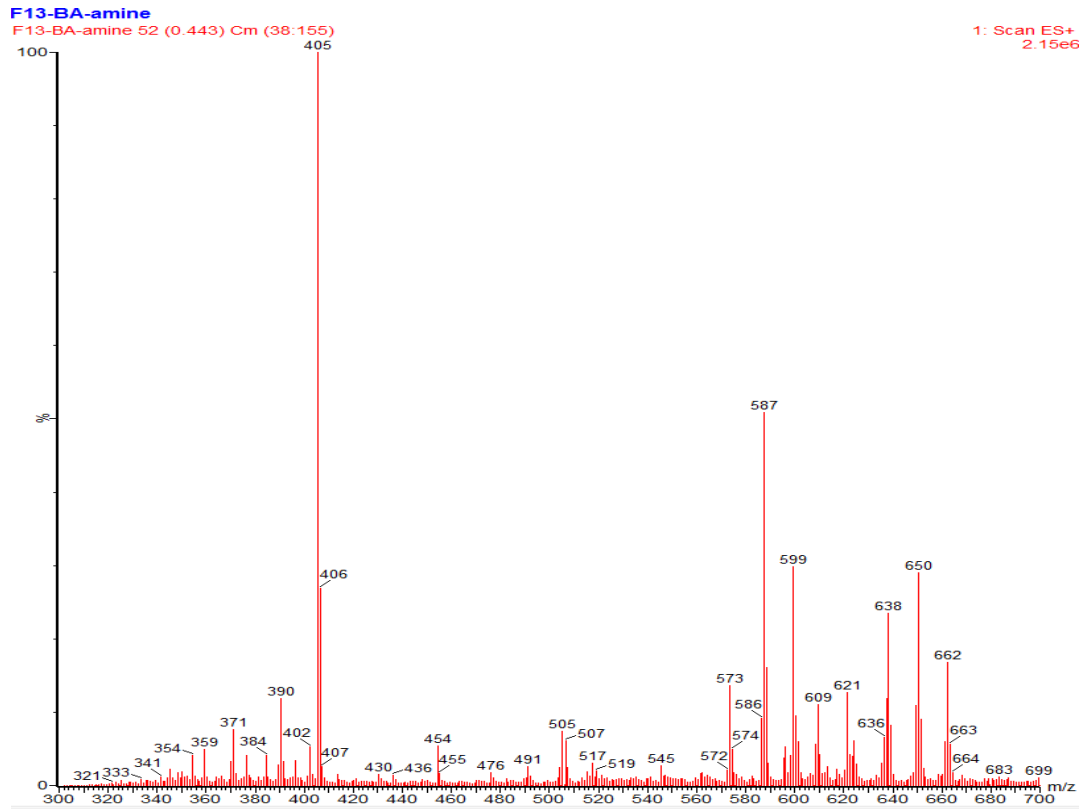
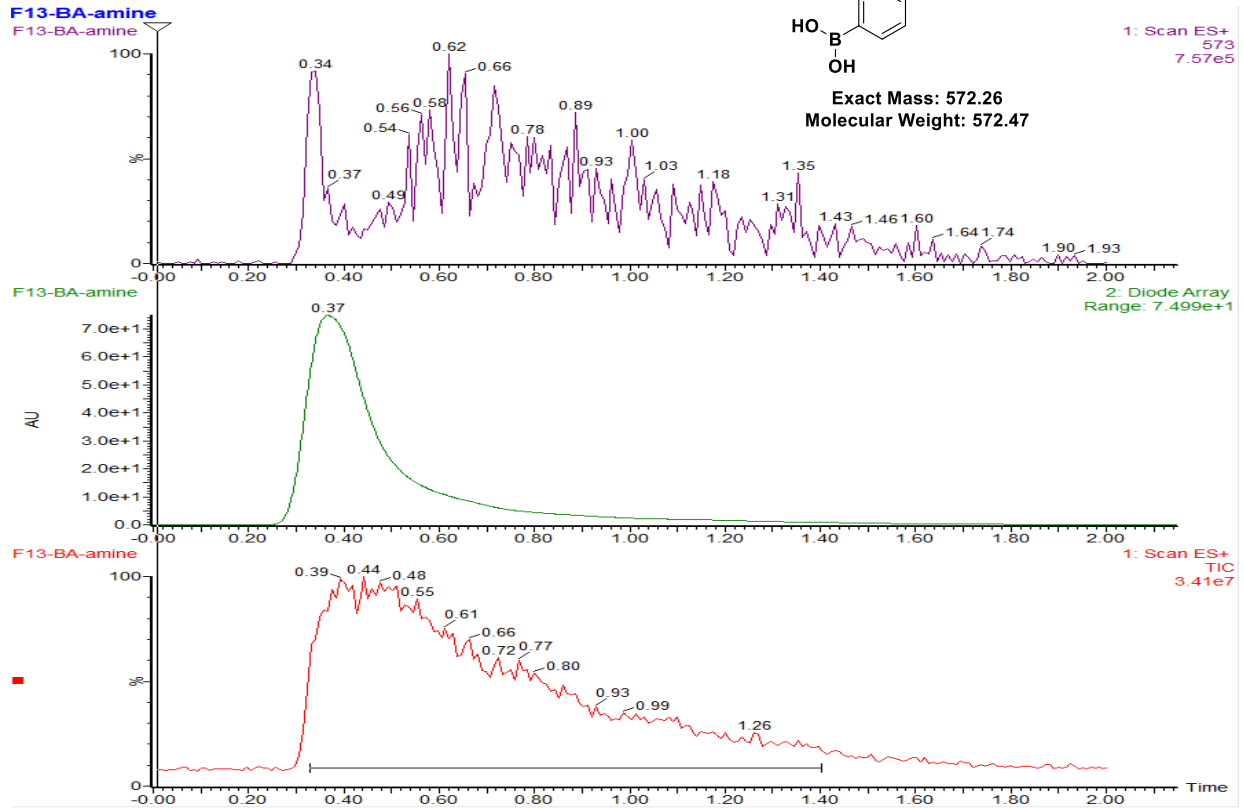
Exact Mass: 515.17
Molecular Weight: 515.39



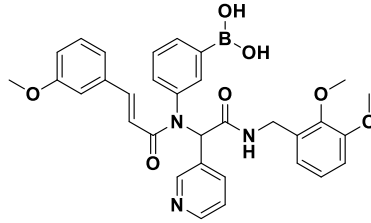
F13 (Green)



Exact Mass: 572.26
Molecular Weight: 572.47



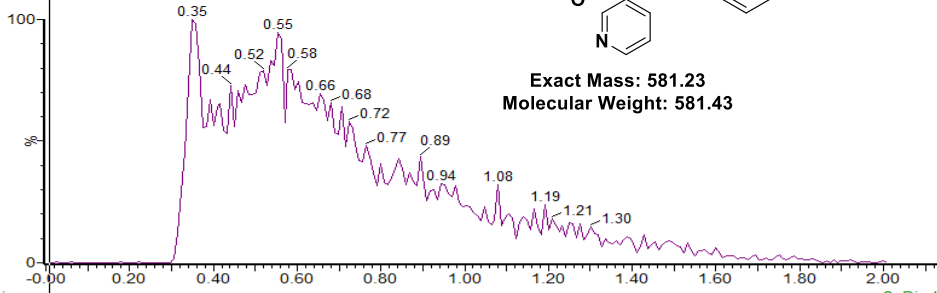
G7(Green)



Exact Mass: 581.23
Molecular Weight: 581.43

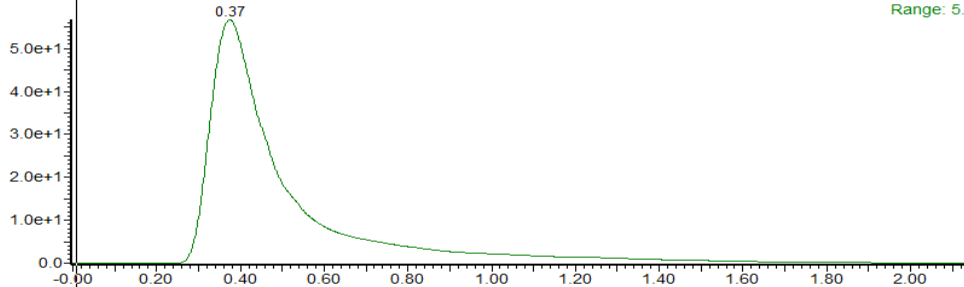
1: Scan ES+
582
7.00e6

G7-BA-amine
G7-BA-amine



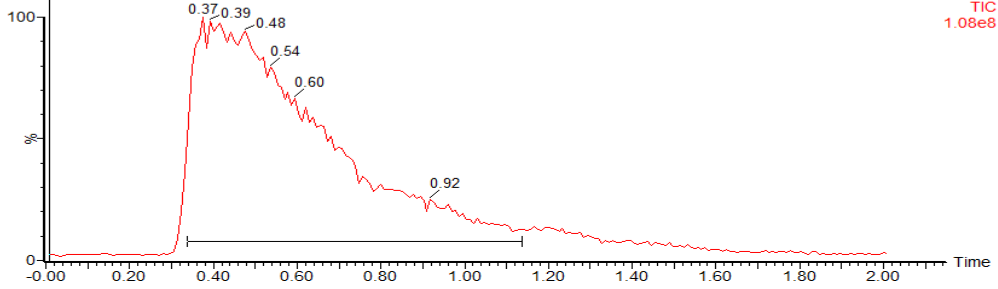
G7-BA-amine

AU



2: Diode Array
Range: 5.669e+1

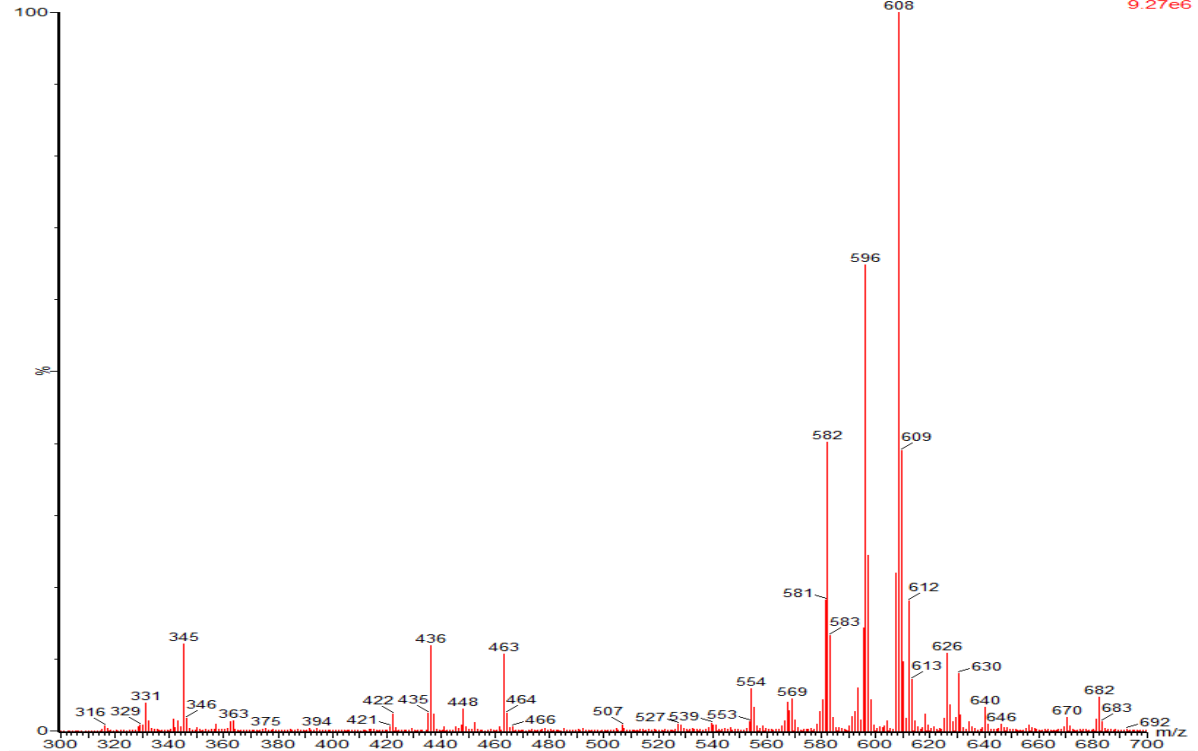
G7-BA-amine



1: Scan ES+
TIC
1.08e8

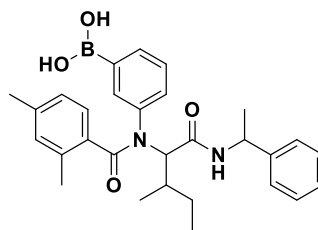
G7-BA-amine

G7-BA-amine 44 (0.374) Cm (40:121)



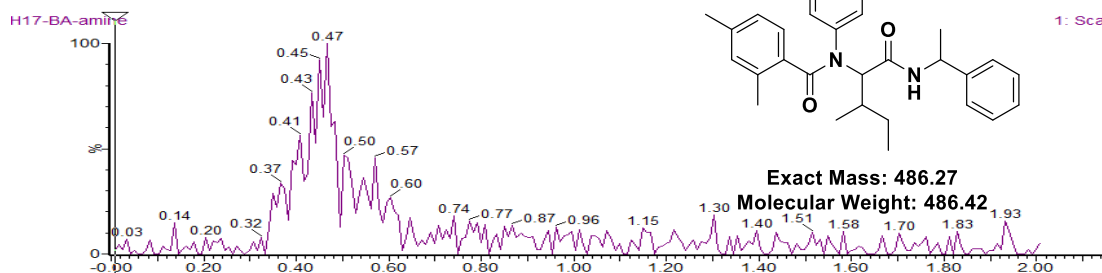
1: Scan ES+
9.27e6

H17 (Green)

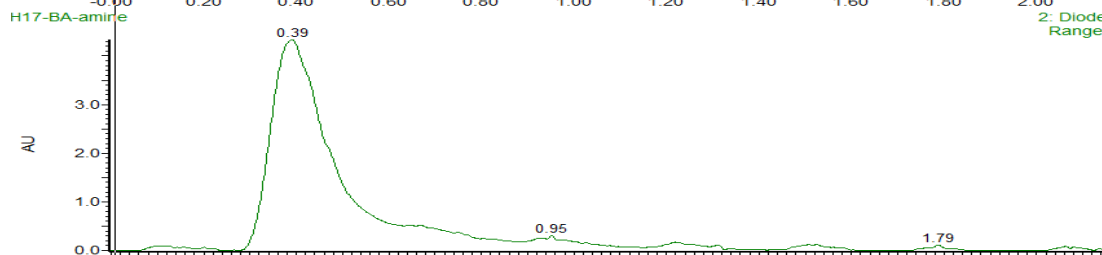


1: Scan ES+
487
3.96e5

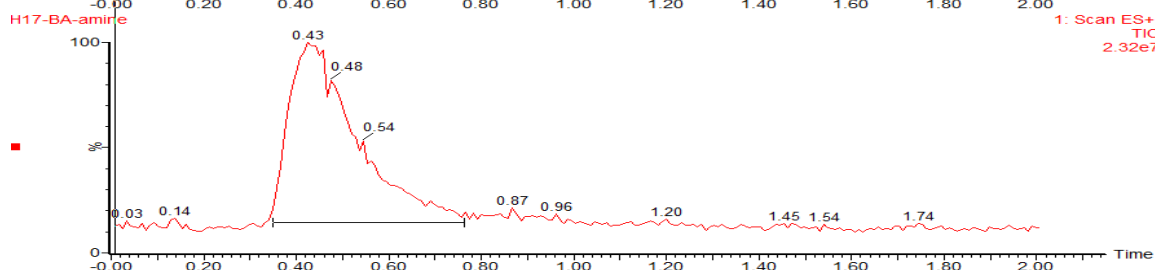
Exact Mass: 486.27
Molecular Weight: 486.42



2: Diode Array
Range: 4.372



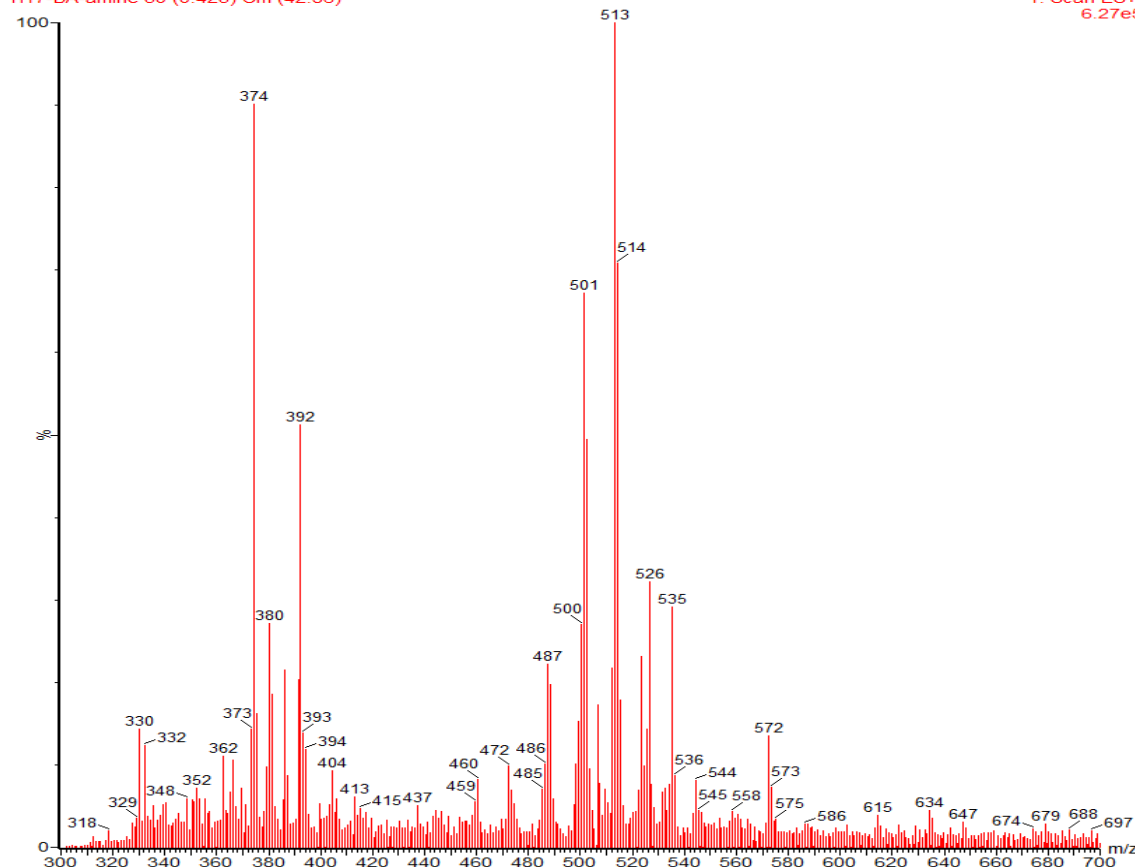
1: Scan ES+
TIC
2.32e7



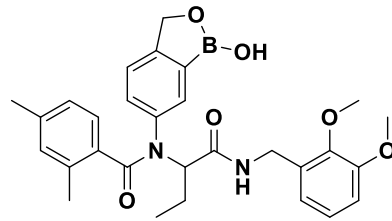
H17-BA-amine

H17-BA-amine 50 (0.425) Cm (42:86)

1: Scan ES+
6.27e5



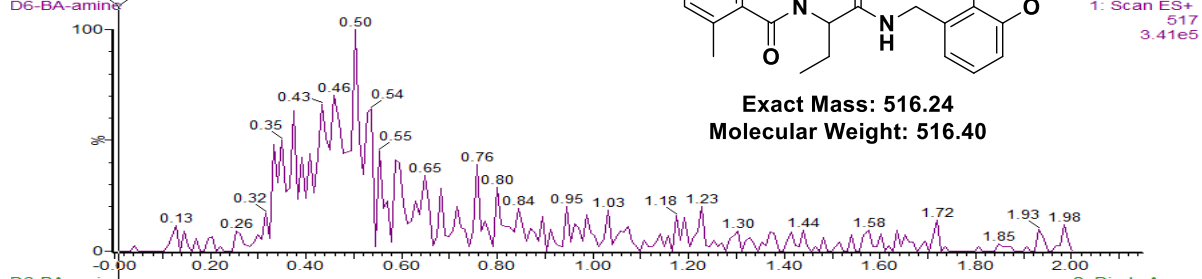
D6 (Green)



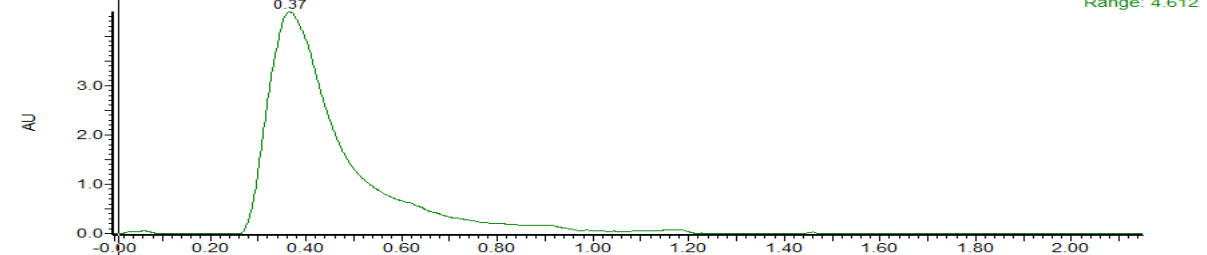
Exact Mass: 516.24
Molecular Weight: 516.40

1: Scan ES+
517
3.41e5

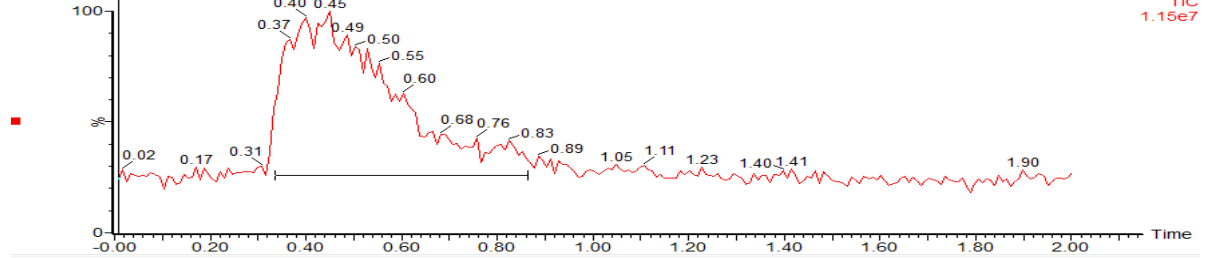
D6-BA-amine



D6-BA-amine



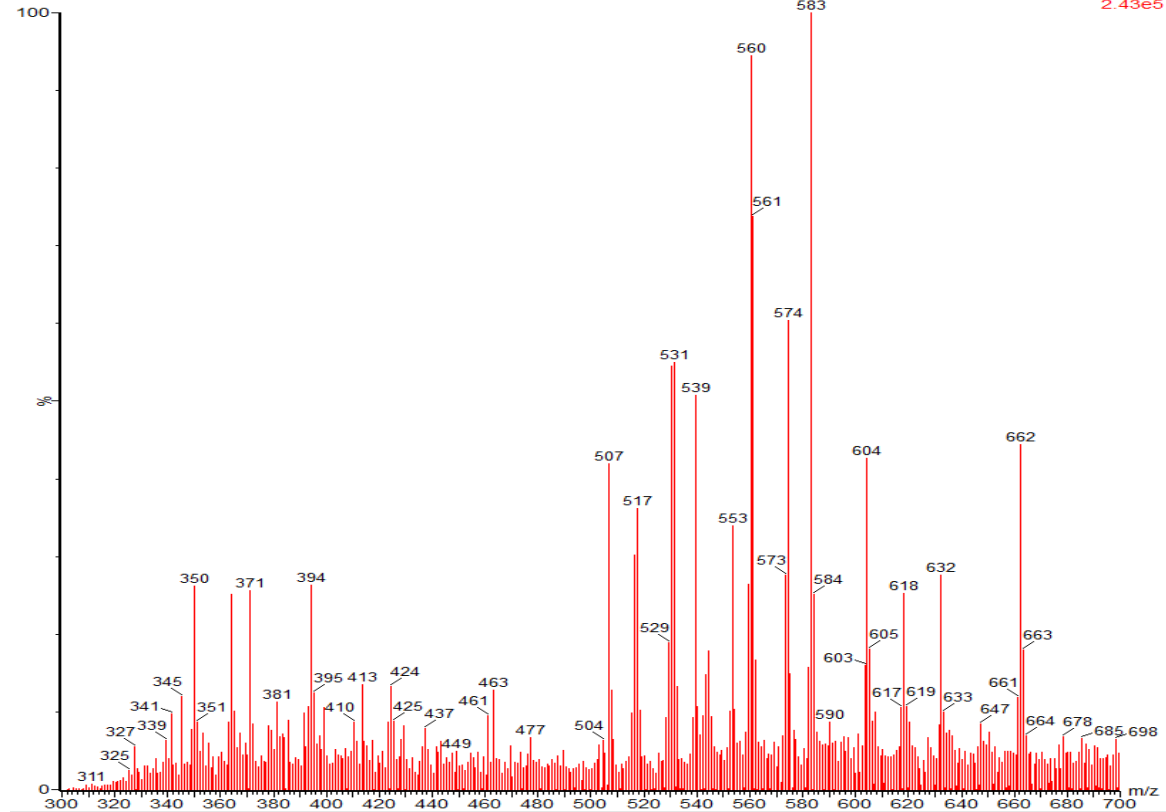
D6-BA-amine



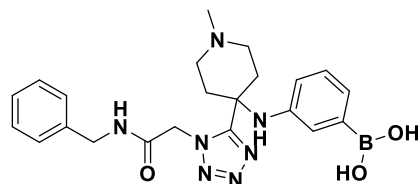
D6-BA-amine

D6-BA-amine 53 (0.451) Cm (41:103)

1: Scan ES+
2.43e5



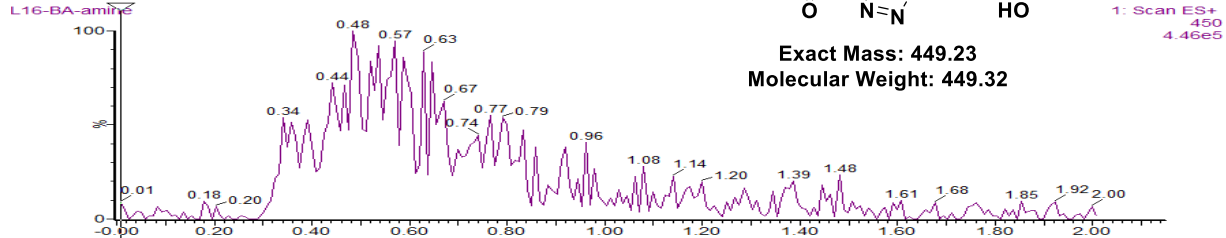
L16 (Green)



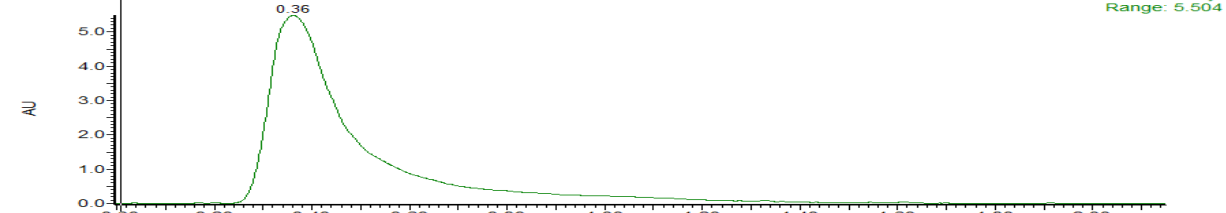
Exact Mass: 449.23
Molecular Weight: 449.32

1: Scan ES+
450
4.46e5

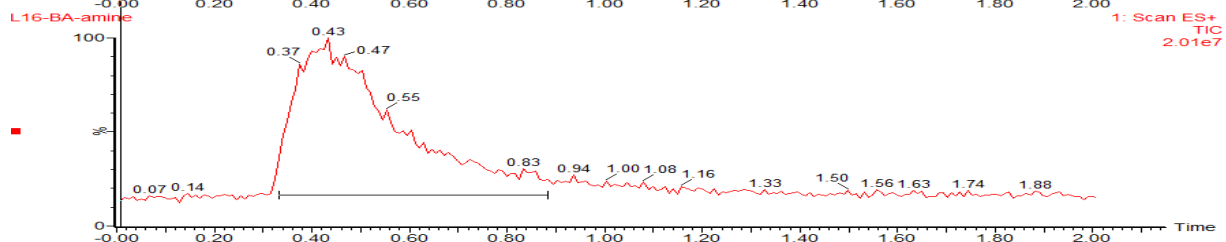
L16-BA-amine



L16-BA-amine



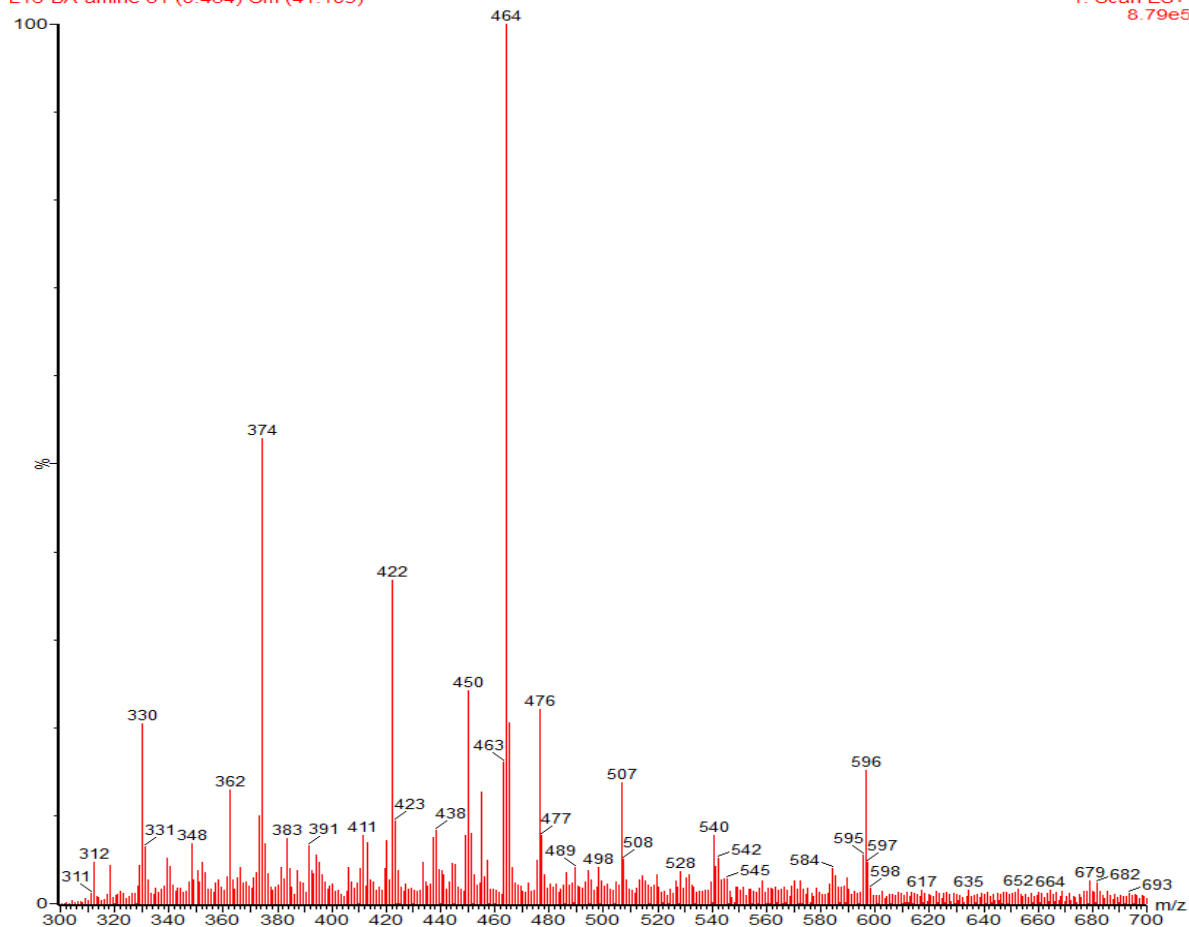
L16-BA-amine



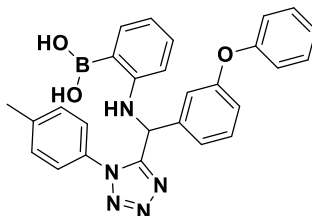
L16-BA-amine

L16-BA-amine 51 (0.434) Cm (41:109)

1: Scan ES+
8.79e5

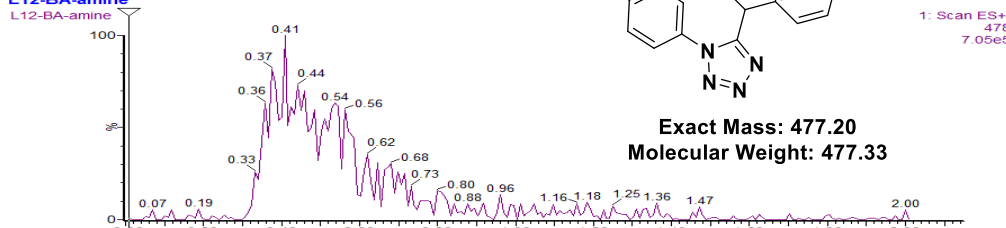


L12 (Yellow)

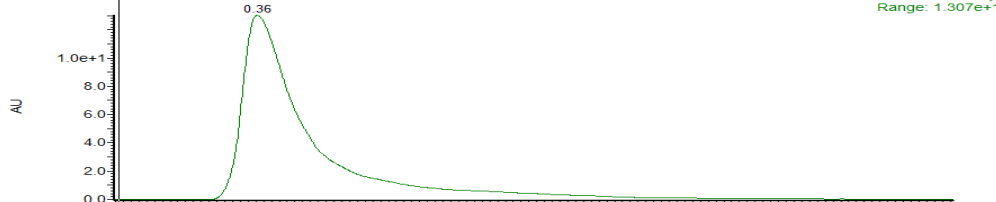


Exact Mass: 477.20
Molecular Weight: 477.33

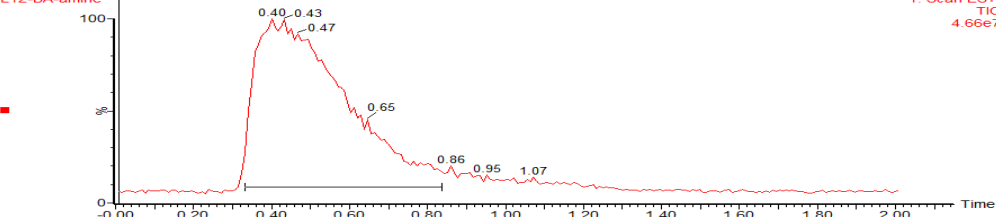
L12-BA-amine



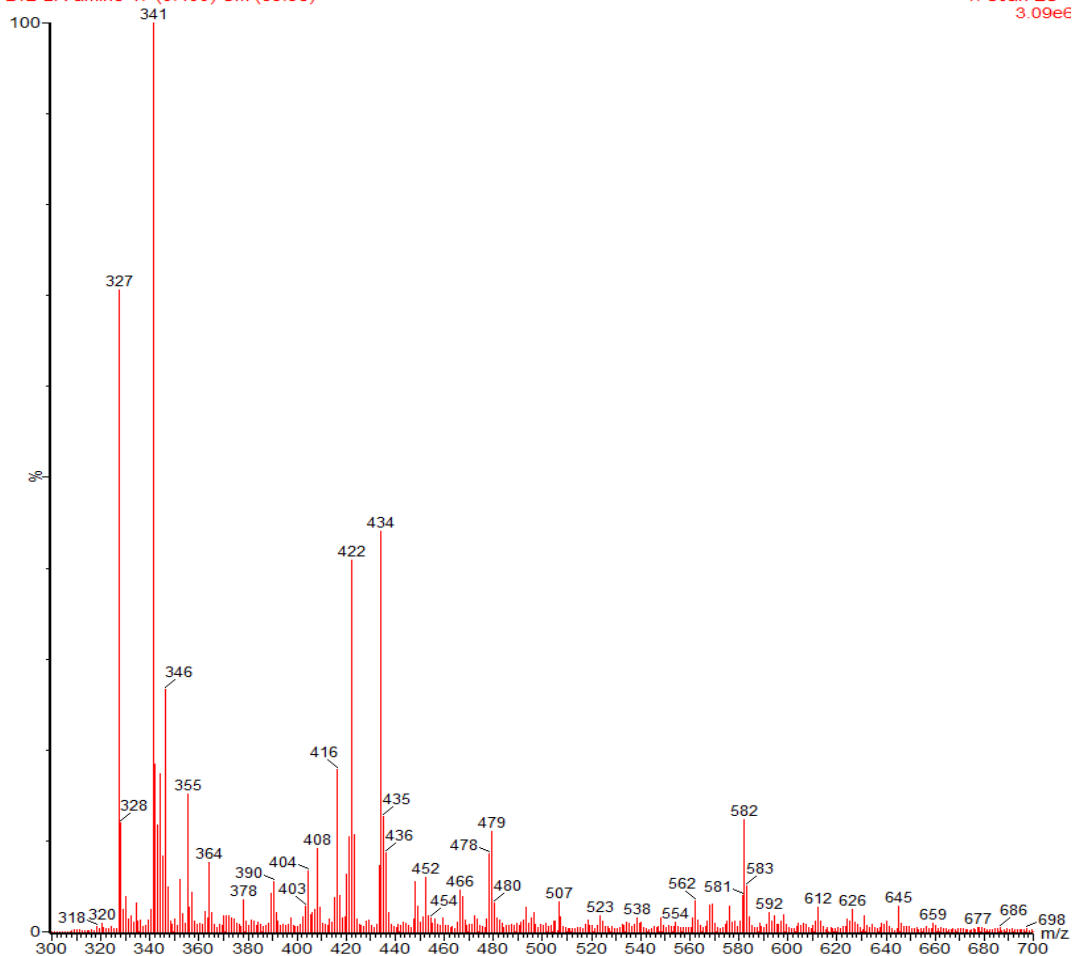
L12-BA-amine



L12-BA-amine



L12-BA-amine 47 (0.400) Cm (39.96)

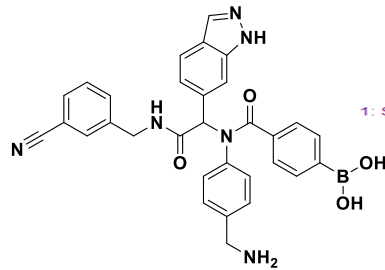
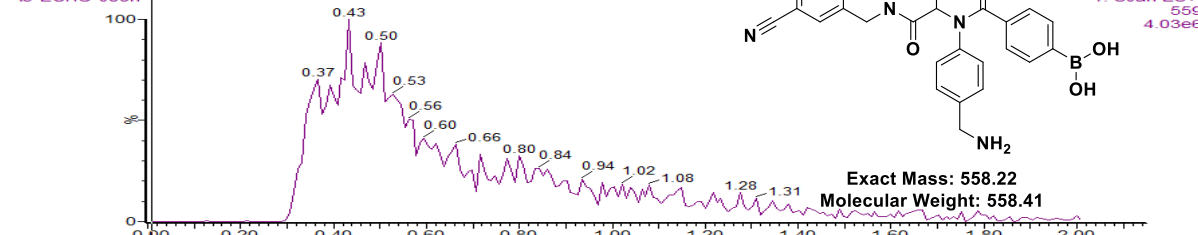


Examples of SFC-MS analytics directly out of the 384-well plate (Destination plate III)

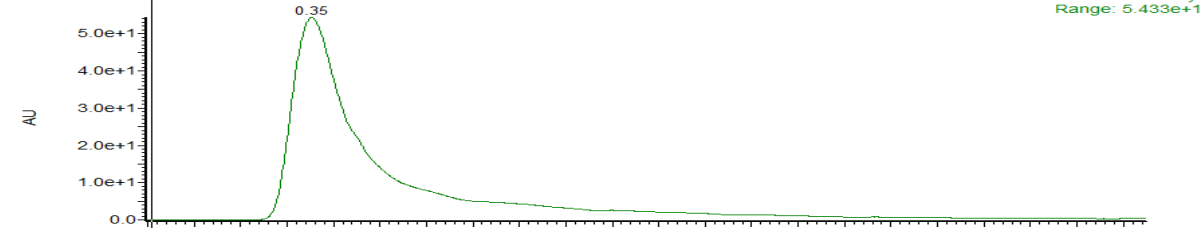
A9 (Green)

A9-ECHO-cooh

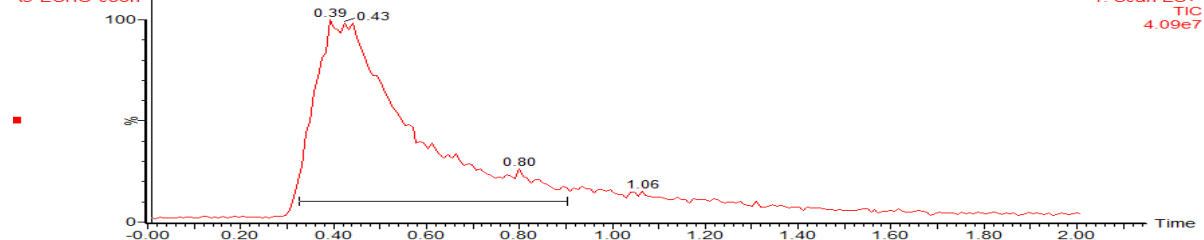
A9-ECHO-cooh



A9-ECHO-cooh

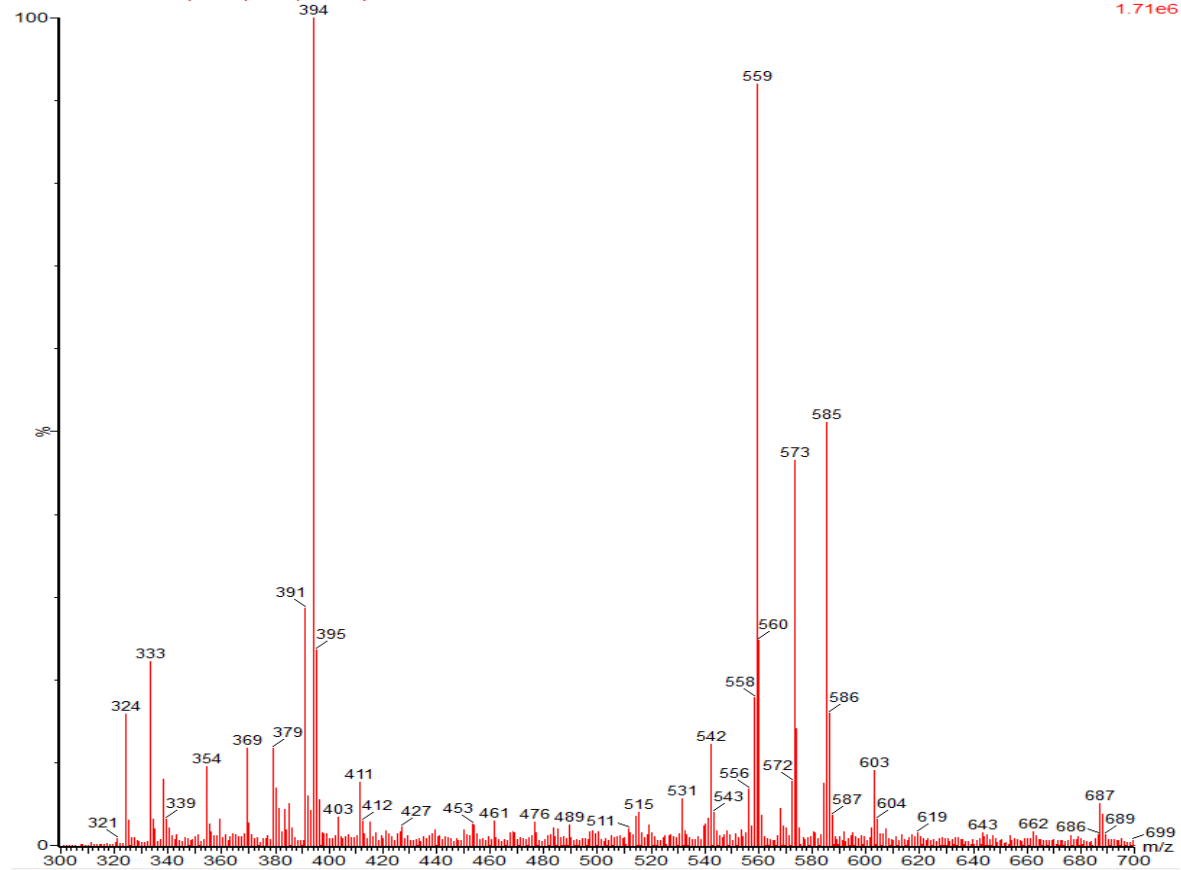


A9-ECHO-cooh

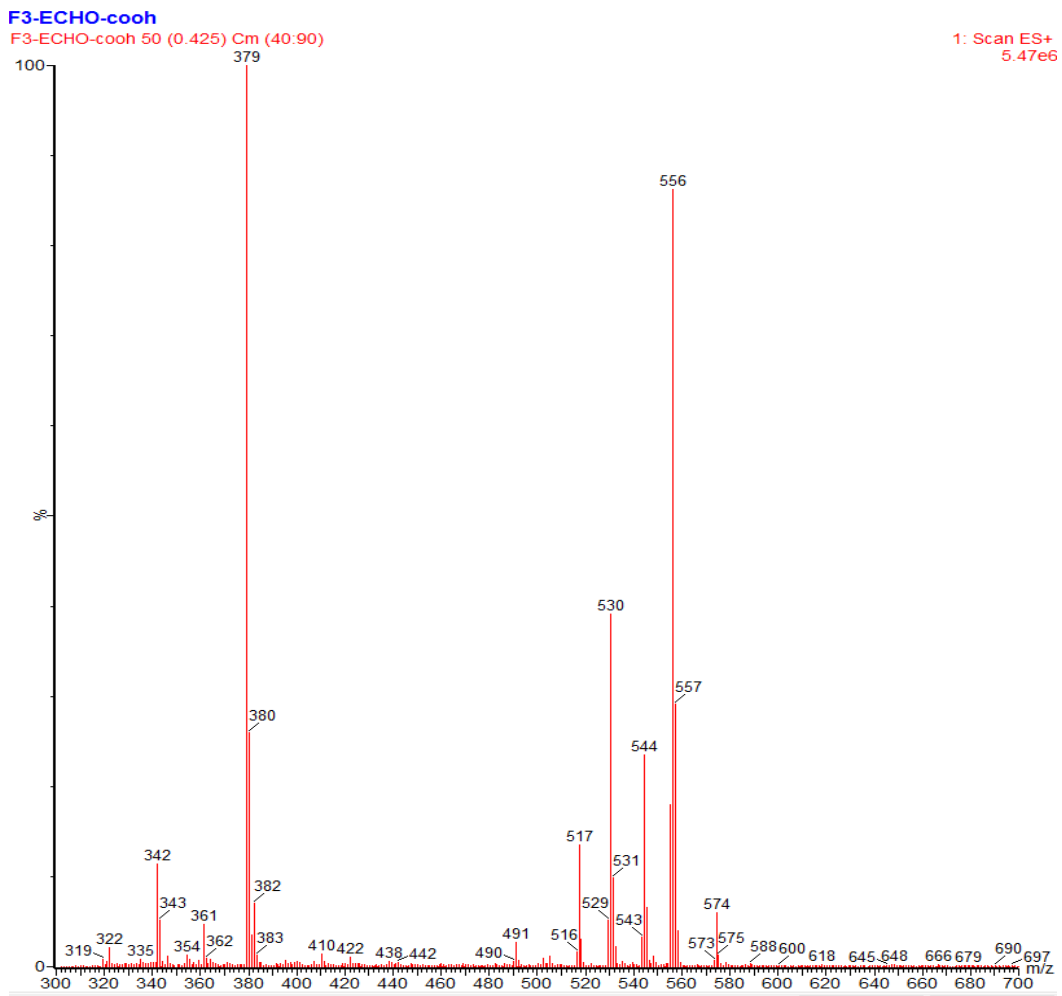
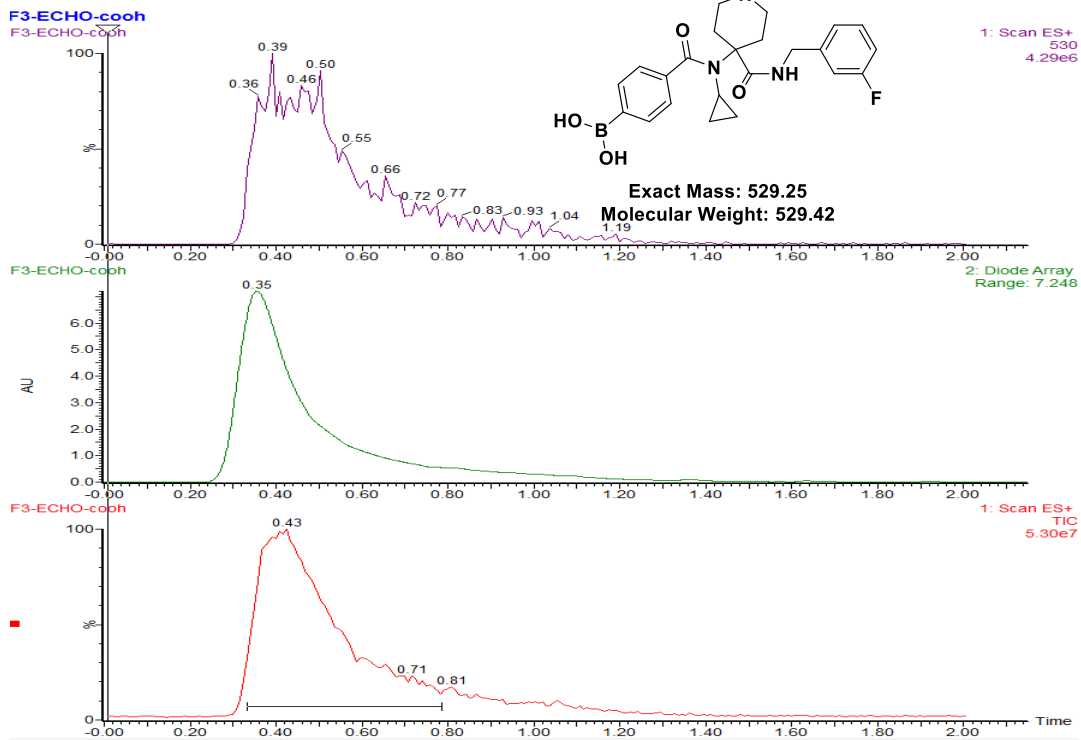


A9-ECHO-cooh

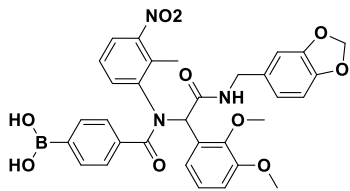
A9-ECHO-cooh 46 (0.391) Cm (39:116)



F3 (Green)



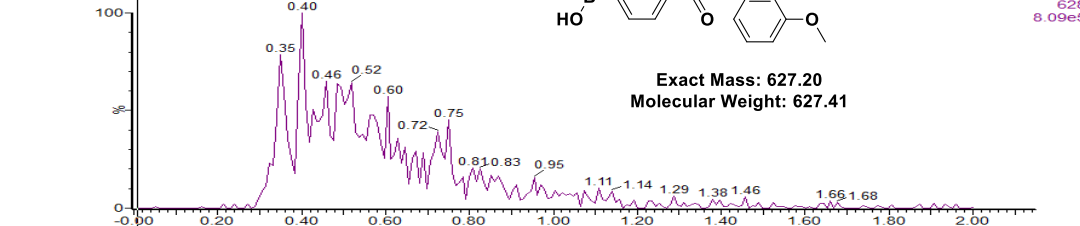
H5 (Green)



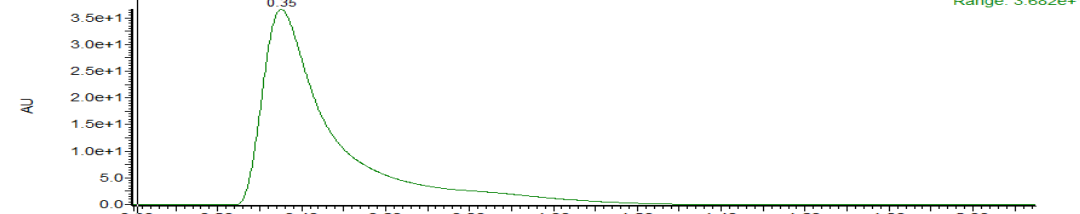
Exact Mass: 627.20
Molecular Weight: 627.41

1: Scan ES+
628
8.09e5

H5-ECHO-cooh

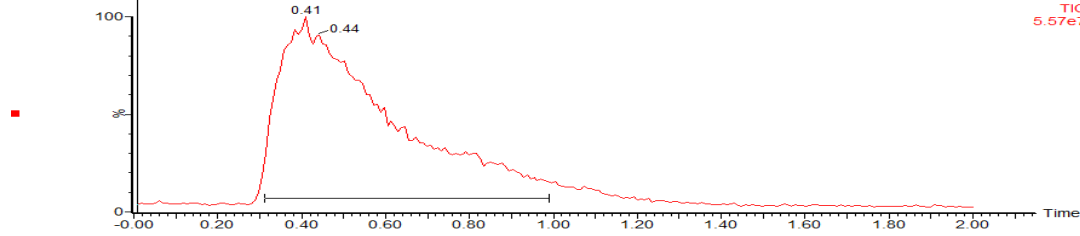


H5-ECHO-cooh



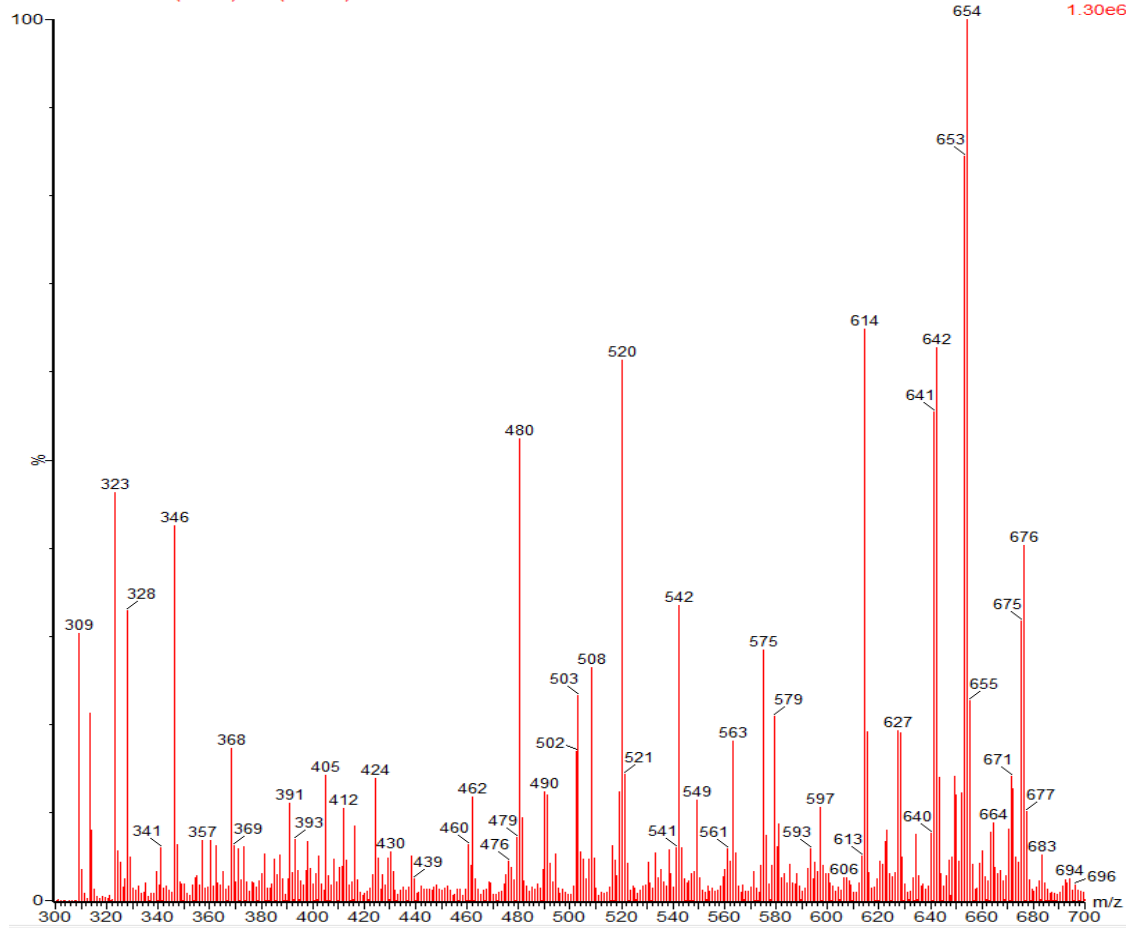
2: Diode Array
Range: 3.682e+1

H5-ECHO-cooh



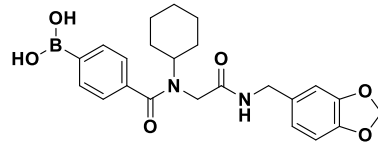
1: Scan ES+
TIC
5.57e7

H5-ECHO-cooh 48 (0.409) Cm (38:113)



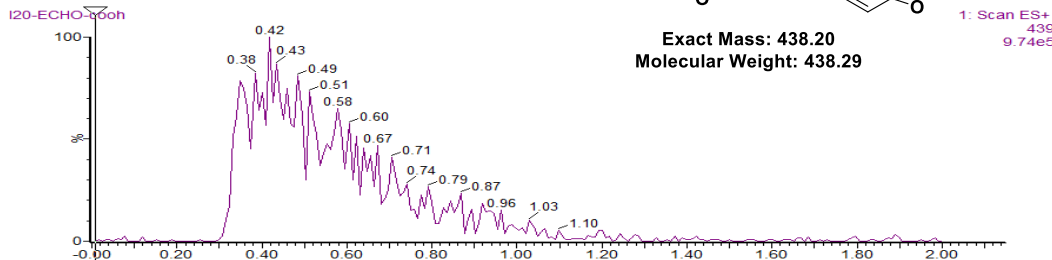
1: Scan ES+
1.30e6

I20 (Green)

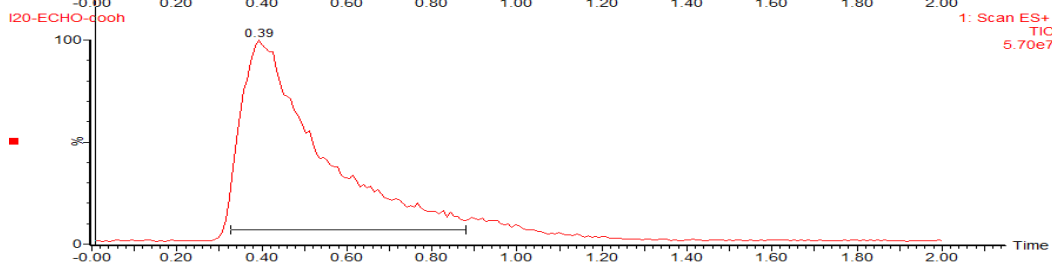
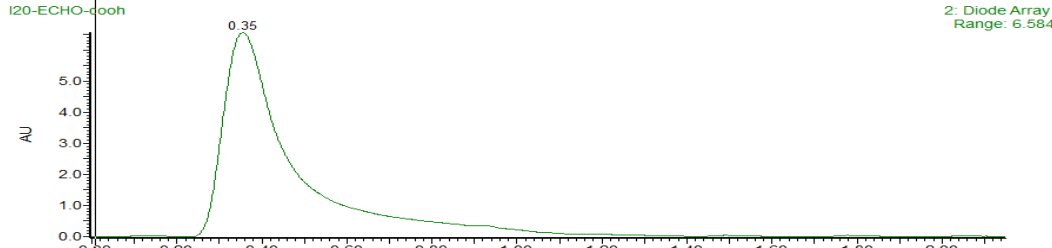


Exact Mass: 438.20
Molecular Weight: 438.29

1: Scan ES+
439
9.74e5



2: Diode Array
Range: 6.584

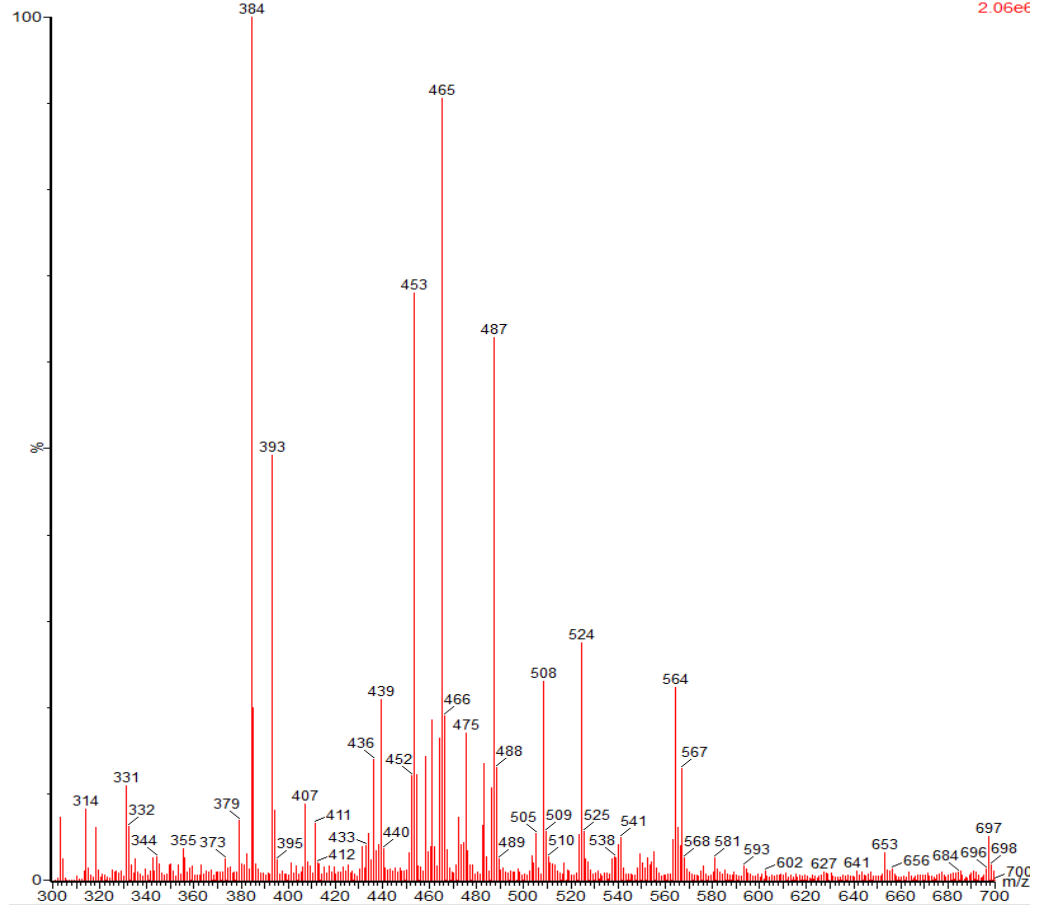


1: Scan ES+
TIC
5.70e7

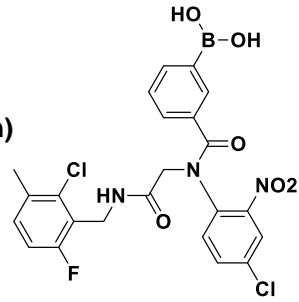
I20-ECHO-cooh

I20-ECHO-cooh 46 (0.392) Cm (39:101)

1: Scan ES+
2.06e6

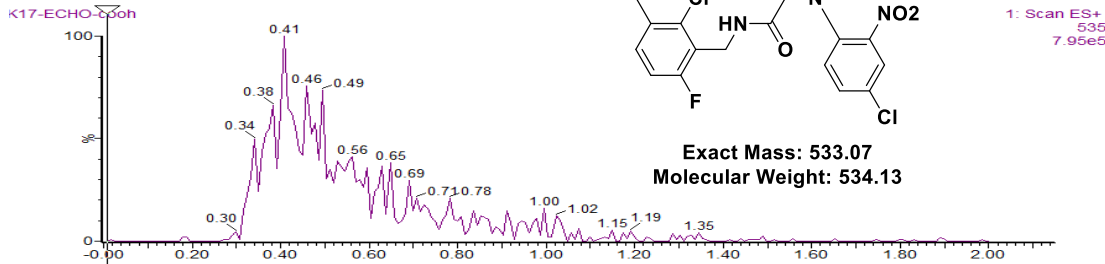


K17 (Green)

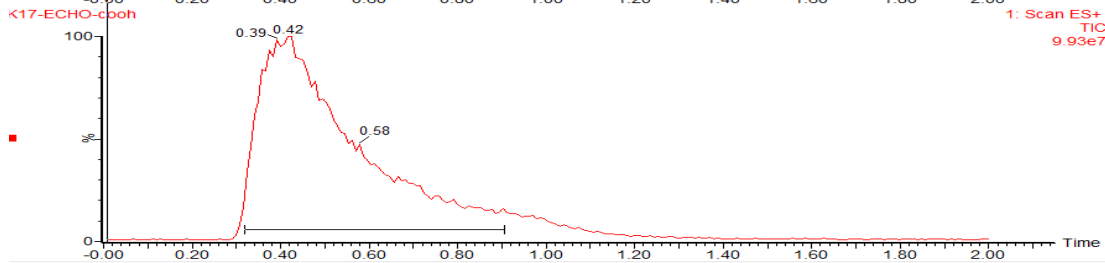
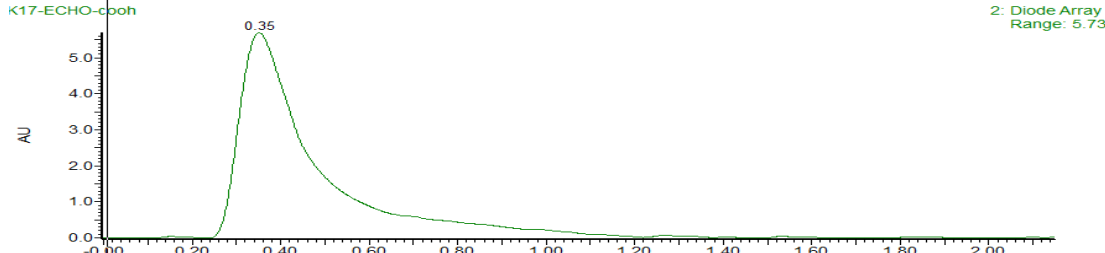


Exact Mass: 533.07
Molecular Weight: 534.13

1: Scan ES+
535
7.95e5



2: Diode Array
Range: 5.73

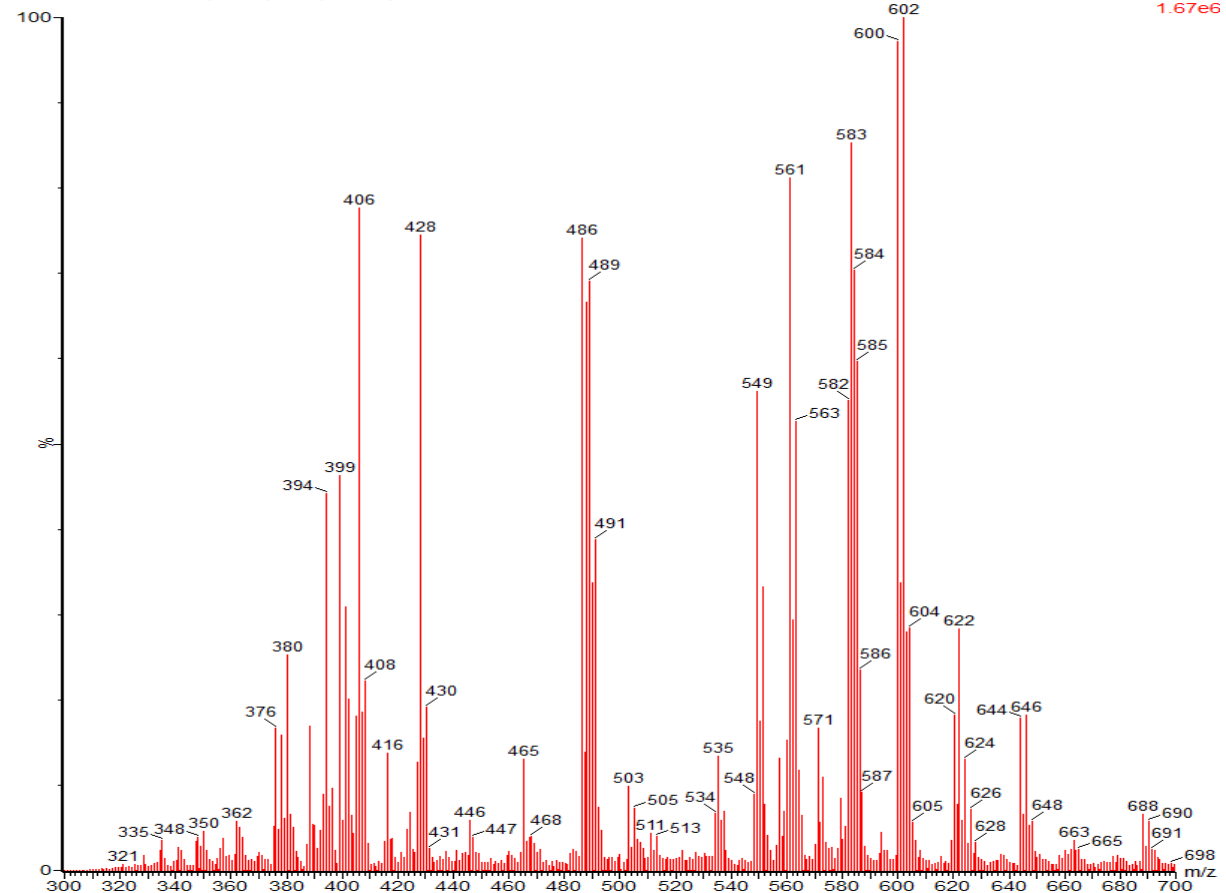


1: Scan ES+
TIC
9.93e7

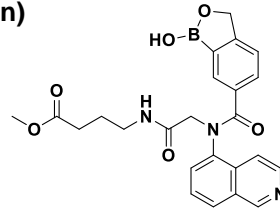
K17-ECHO-cooh

K17-ECHO-cooh 49 (0.417) Cm (39:112)

1: Scan ES+
1.67e6



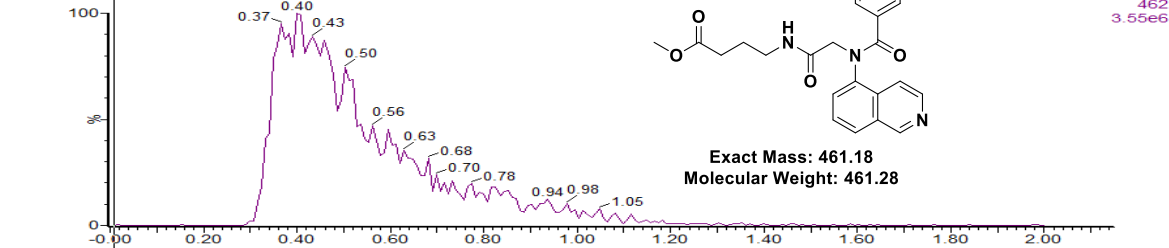
K20 (Green)



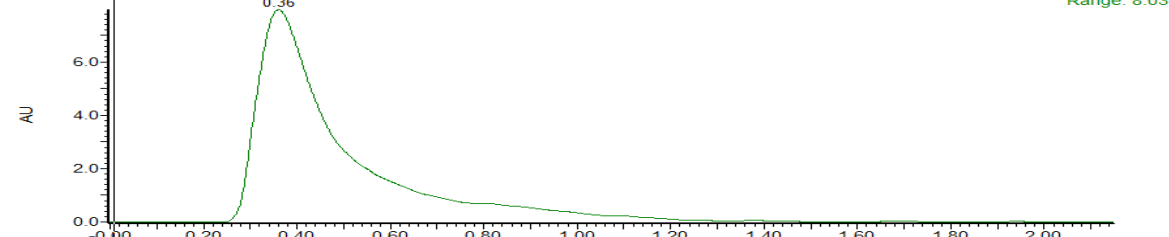
Exact Mass: 461.18
Molecular Weight: 461.28

1: Scan ES+
462
3.55e6

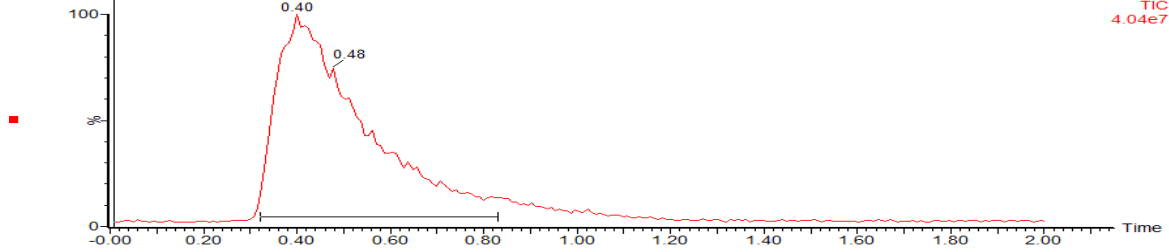
K20-ECHO-cooh



K20-ECHO-cooh



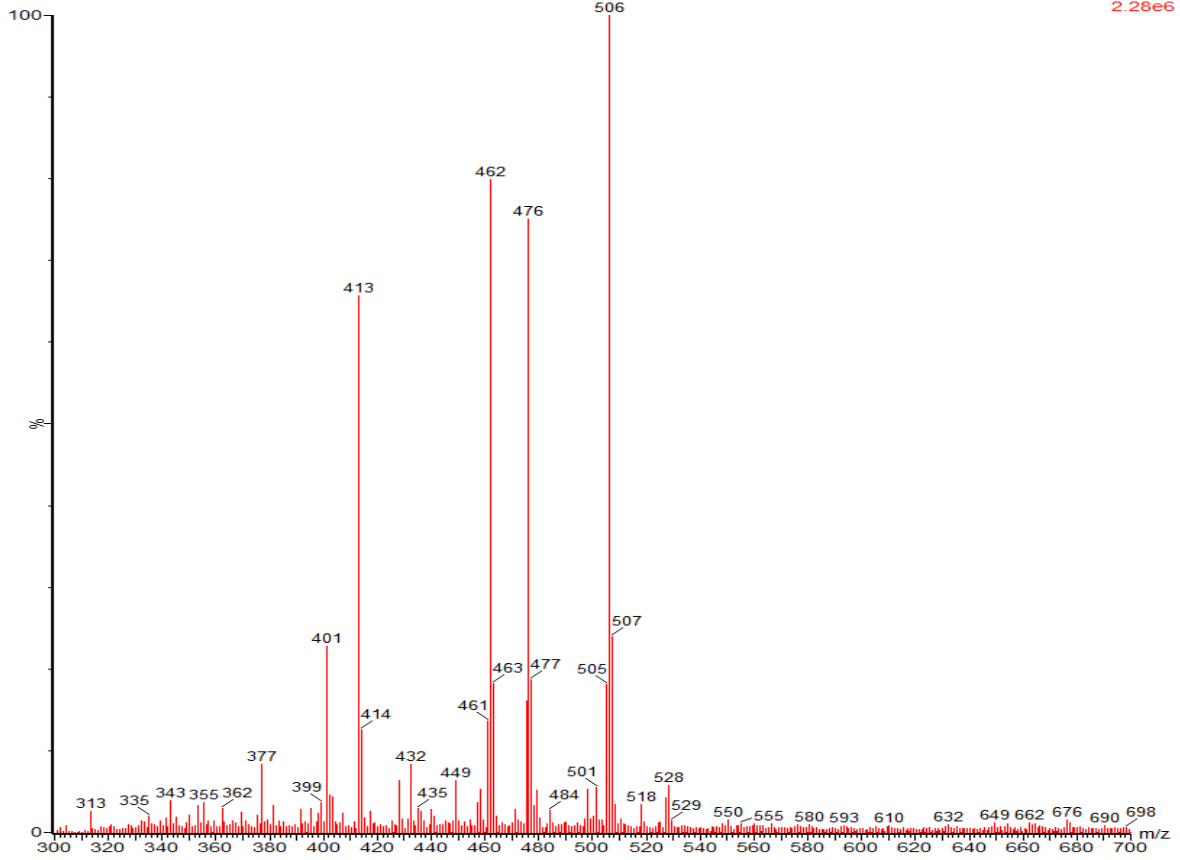
K20-ECHO-cooh



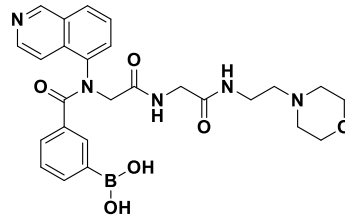
K20-ECHO-cooh

K20-ECHO-cooh 47 (0.400) Cm (40:90)

1: Scan ES+
2.28e6



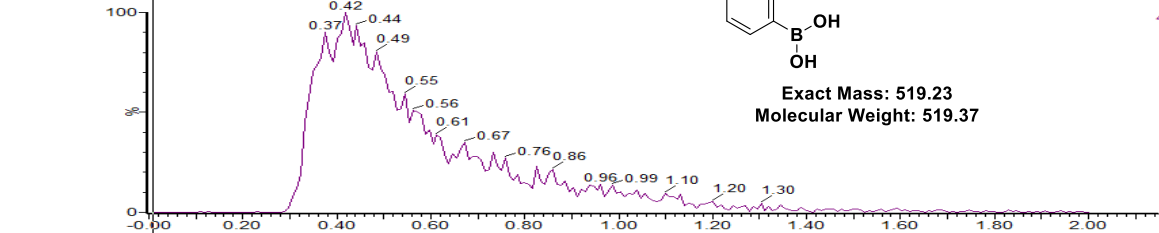
L7 (Green)



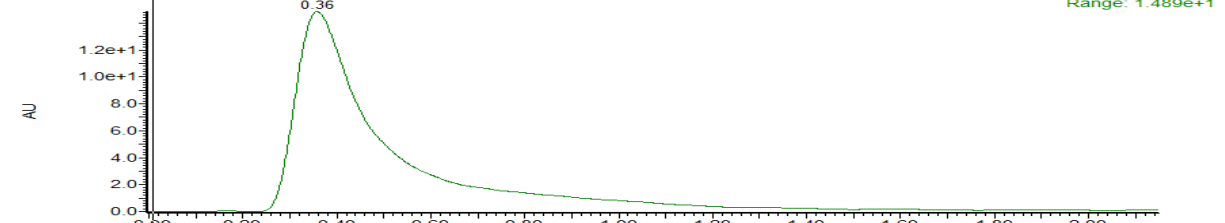
Exact Mass: 519.23
Molecular Weight: 519.37

1: Scan ES+
S20
4.95e6

L7-ECHO-cooh
L7-ECHO-cooh

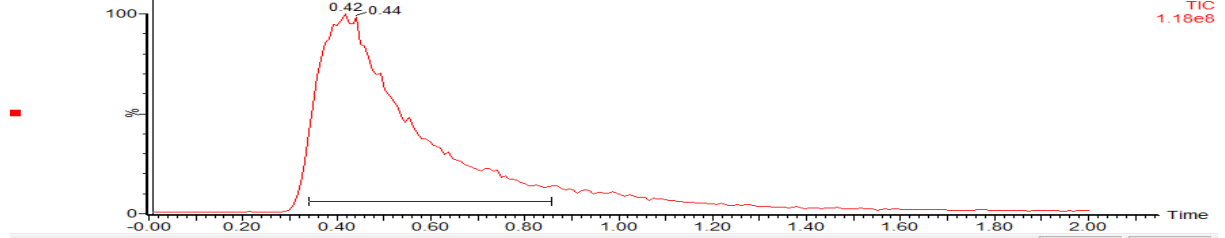


L7-ECHO-cooh



2: Diode Array
Range: 1.489e+1

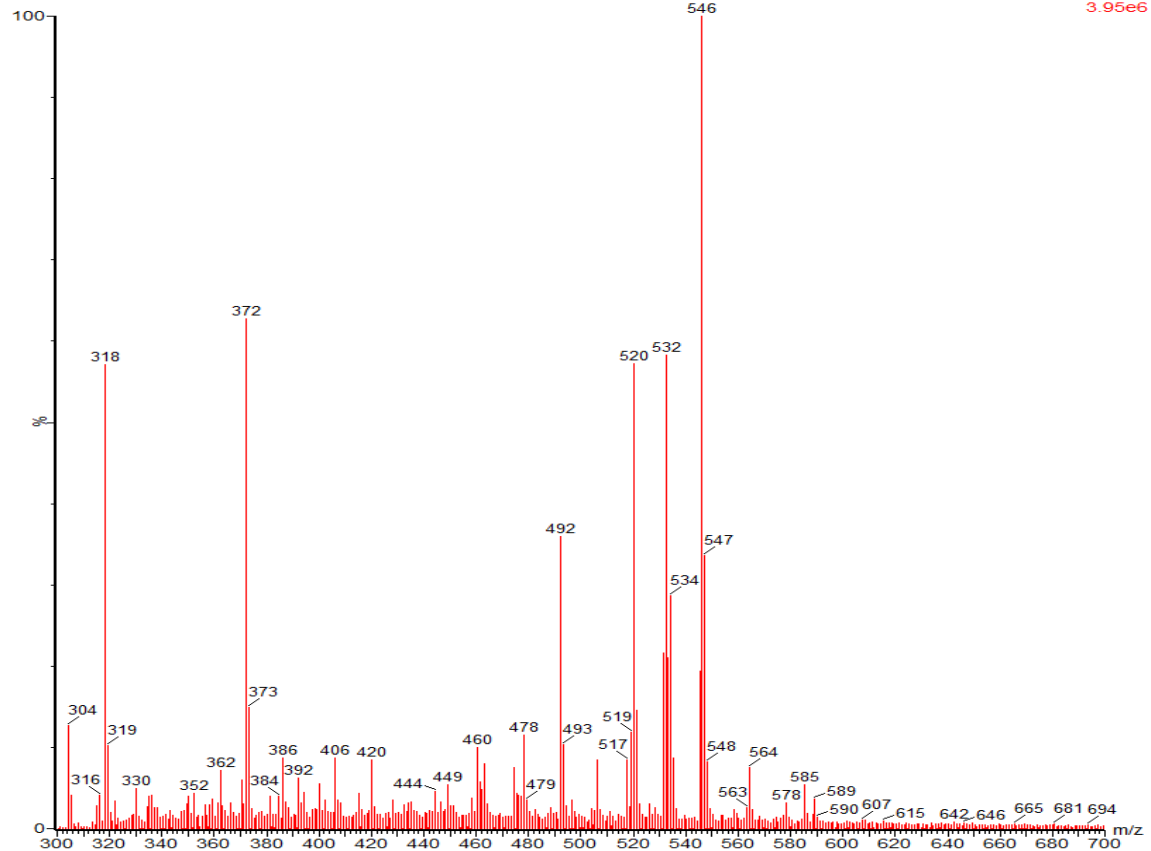
L7-ECHO-cooh



1: Scan ES+
TIC
1.16e8

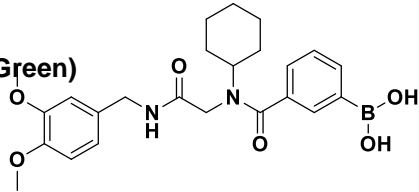
L7-ECHO-cooh

L7-ECHO-cooh 49 (0.417) Cm (38:104)



1: Scan ES+
3.95e6

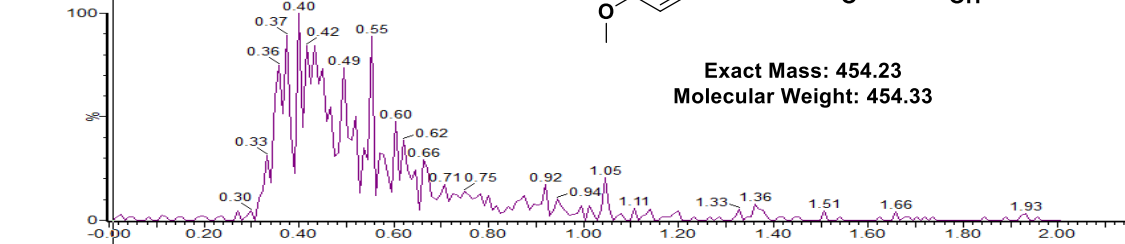
M7 (Green)



Exact Mass: 454.23
Molecular Weight: 454.33

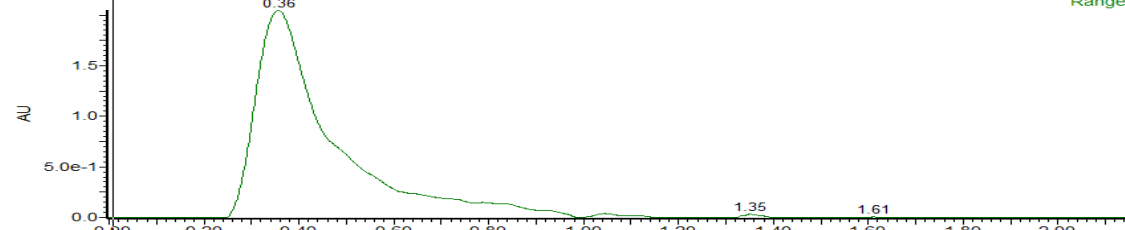
1: Scan ES+
455
4.27e5

M7-ECHO-cooh
M7-ECHO-cooh



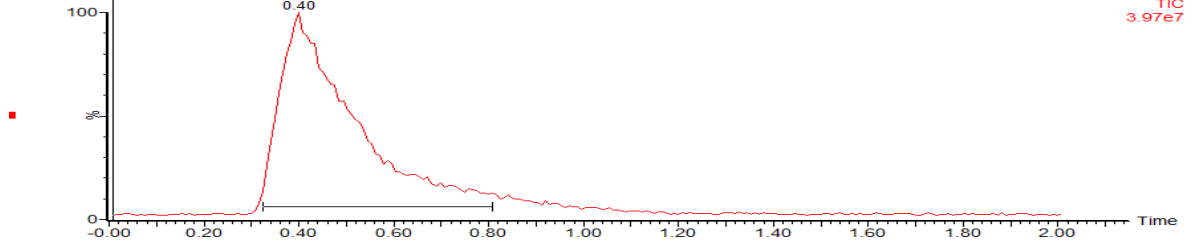
M7-ECHO-cooh

2: Diode Array
Range: 2.127



M7-ECHO-cooh

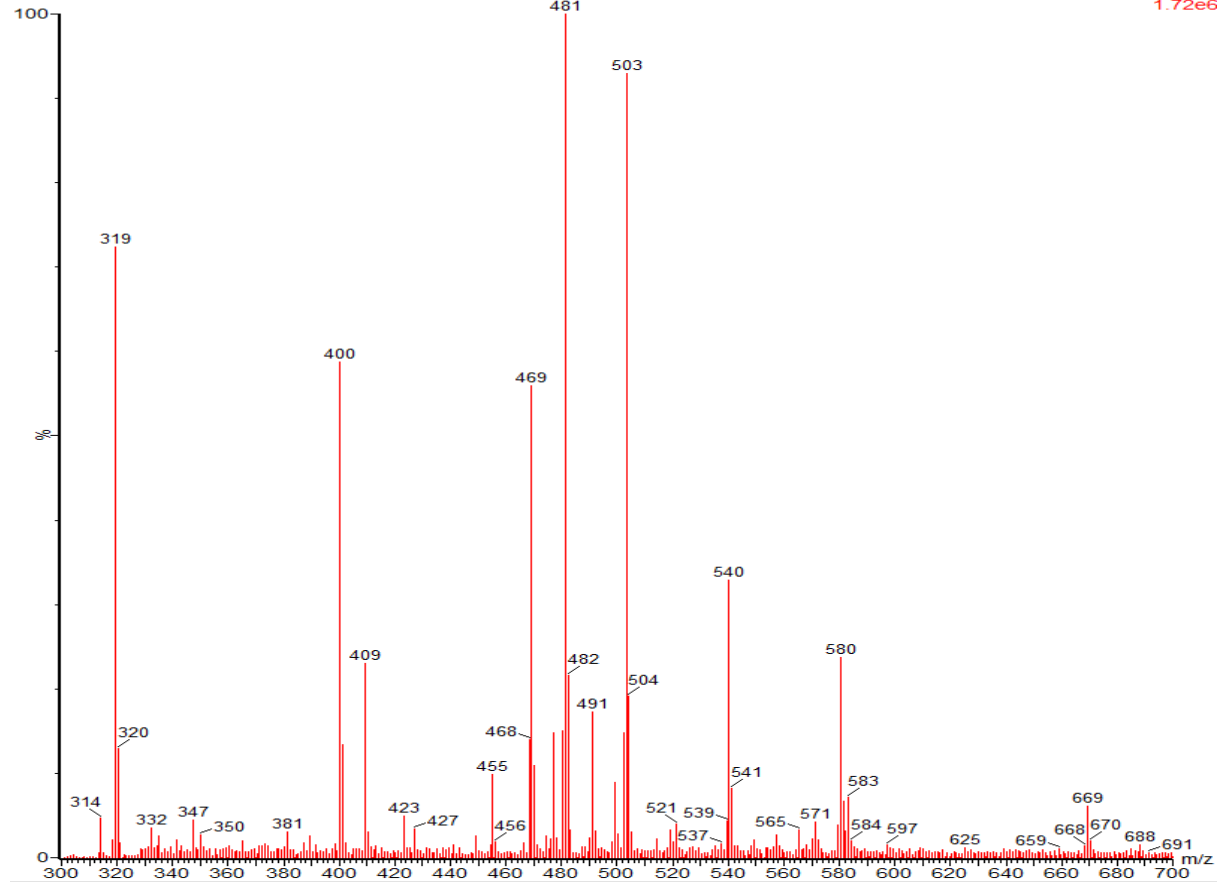
1: Scan ES+
TIC
3.97e7



M7-ECHO-cooh

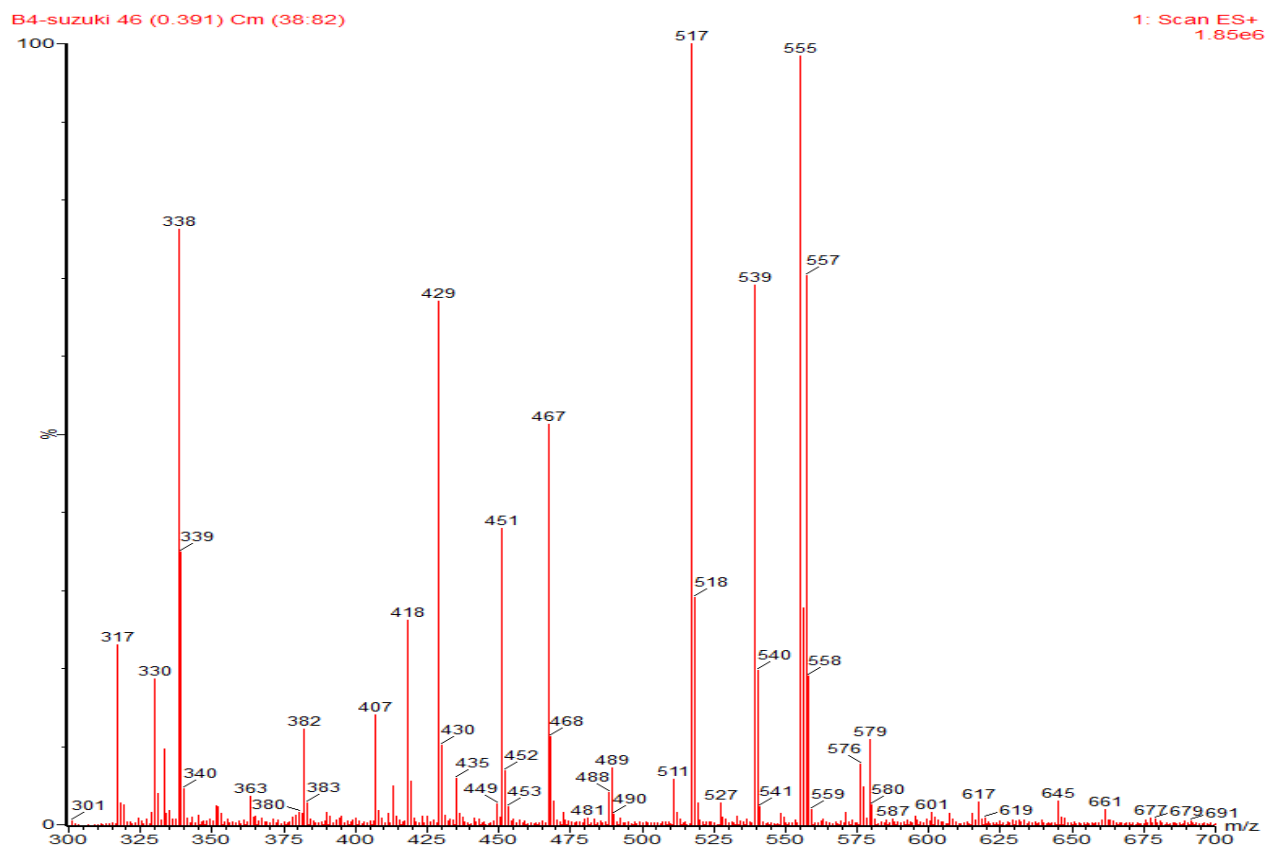
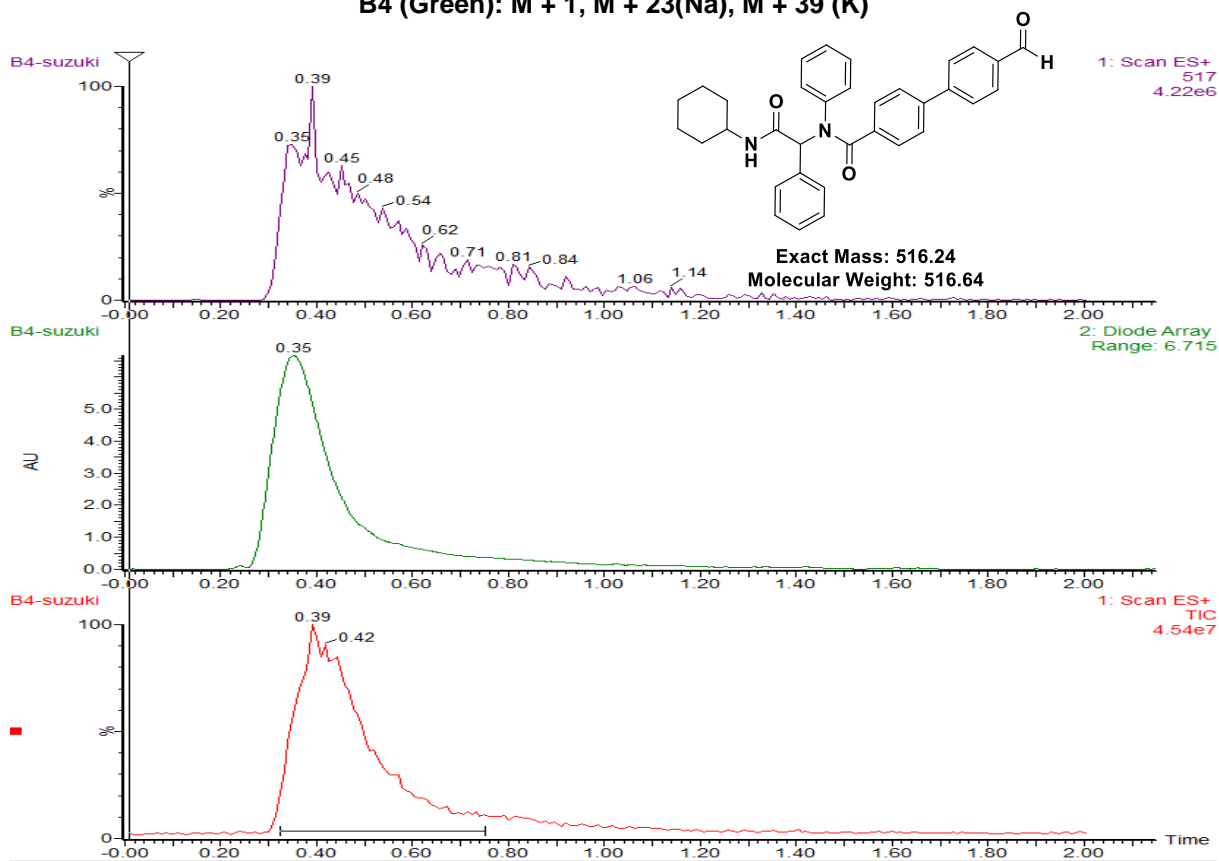
M7-ECHO-cooh 47 (0.400) Cm (40:87)

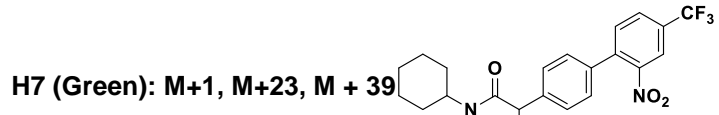
1: Scan ES+
1.72e6



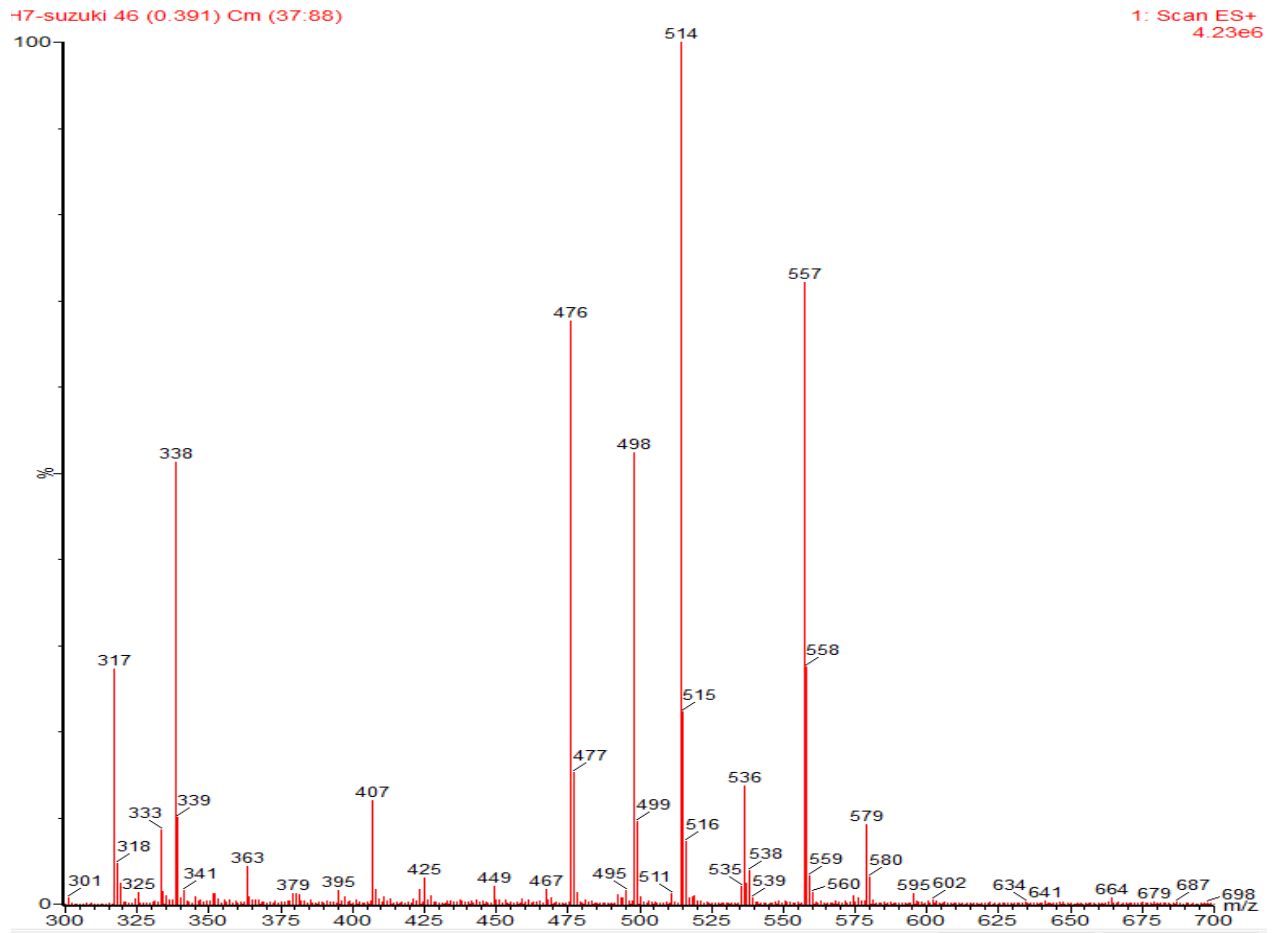
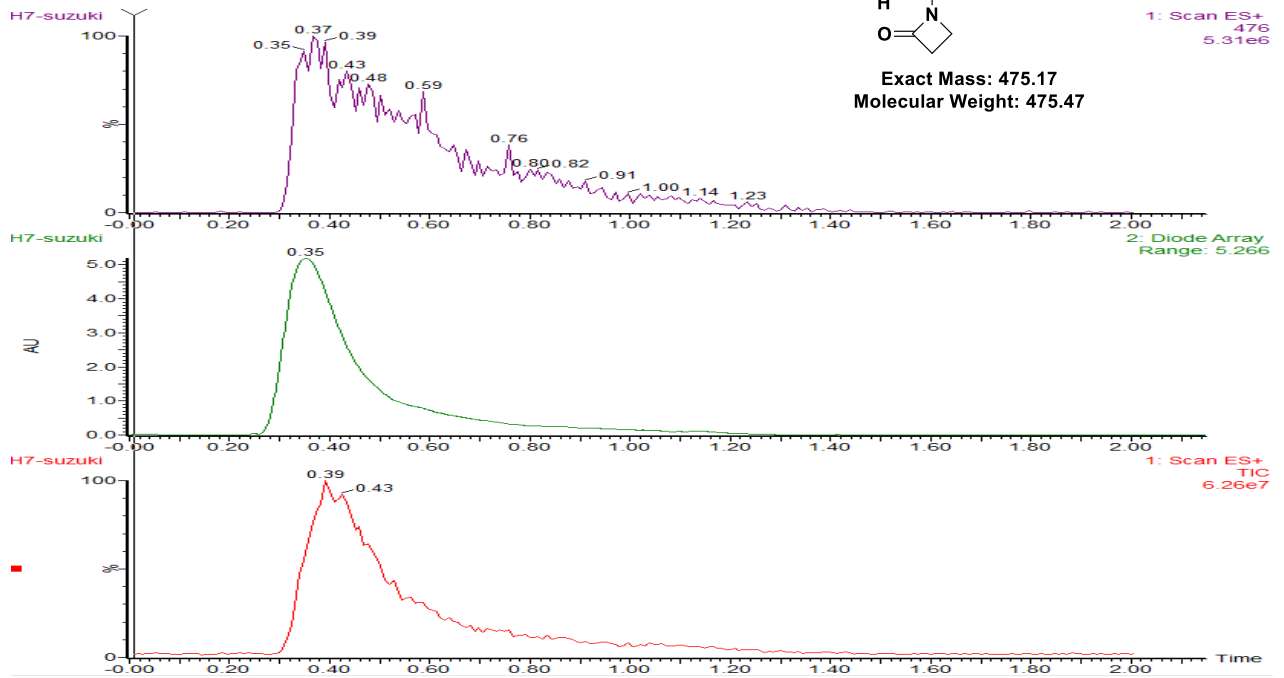
Examples of SFC-MS analytics directly out of the 384-well plate (Destination plate IV)

B4 (Green): M + 1, M + 23(Na), M + 39 (K)

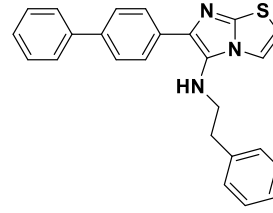




Exact Mass: 475.17
Molecular Weight: 475.47



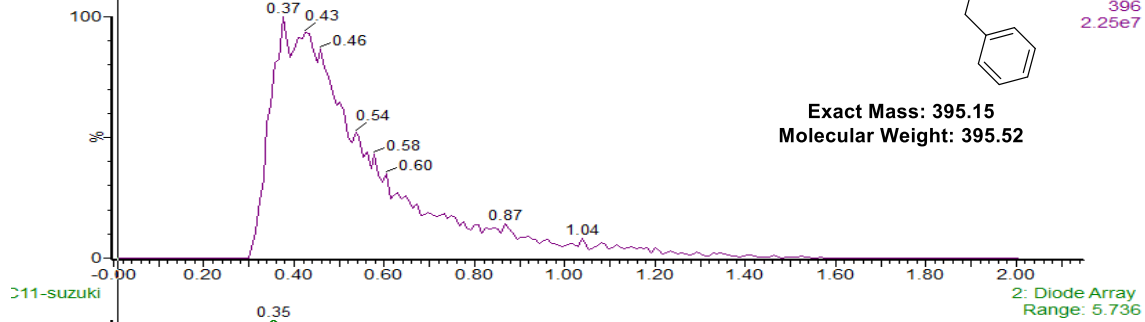
C11 (Green)



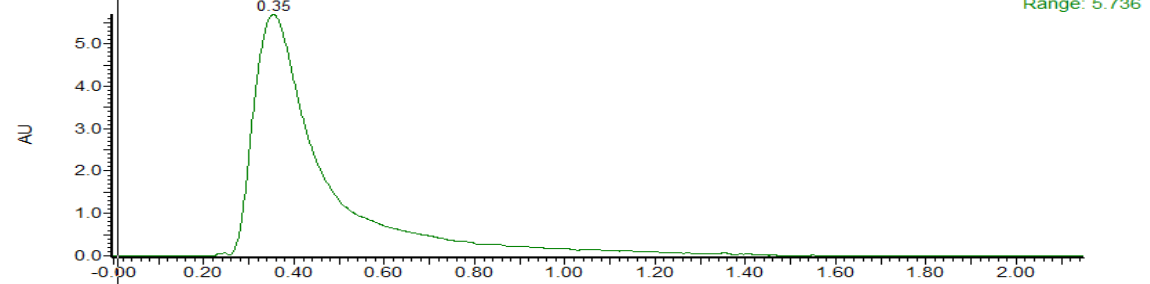
Exact Mass: 395.15
Molecular Weight: 395.52

C11-suzuki

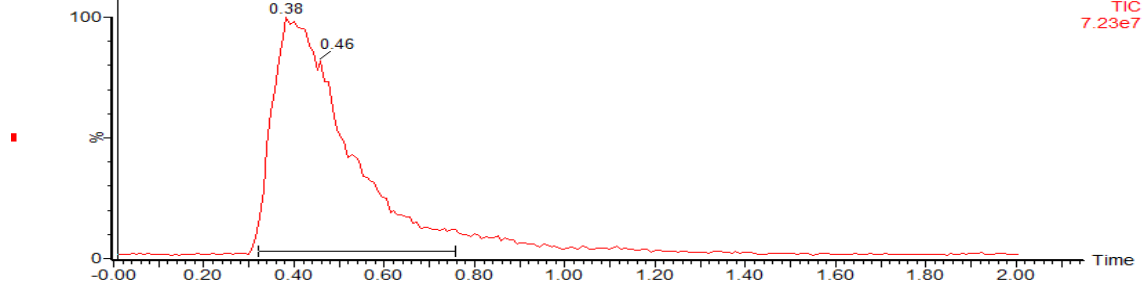
C11-suzuki



C11-suzuki

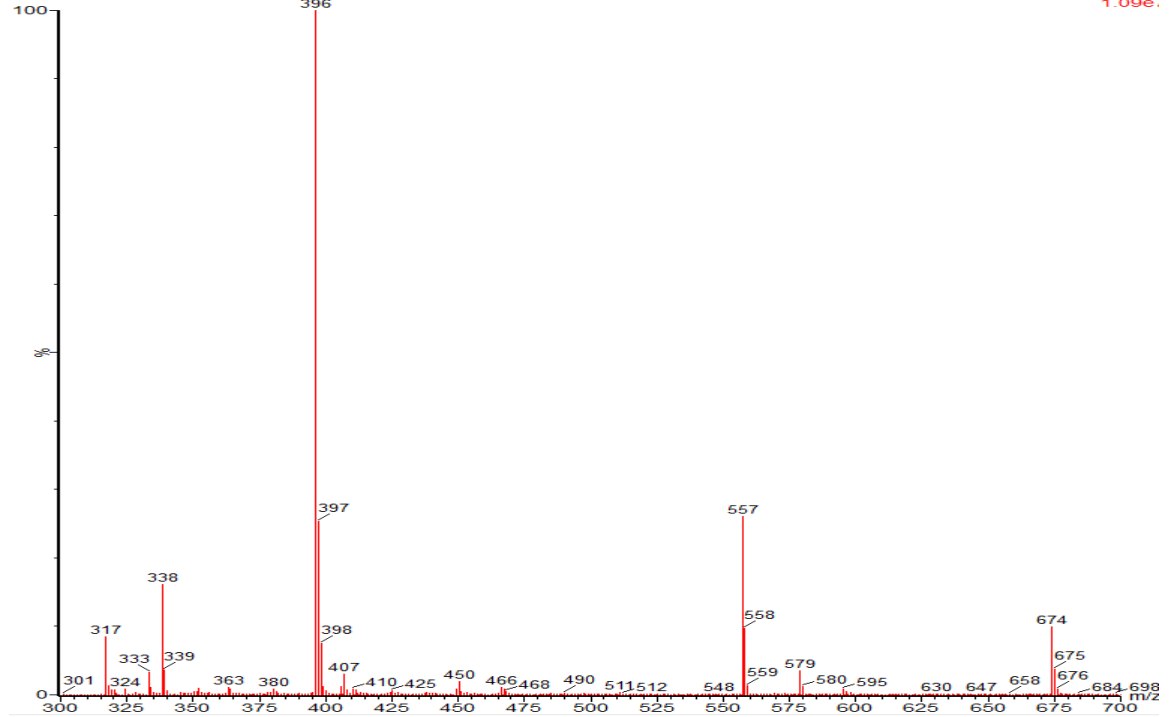


C11-suzuki

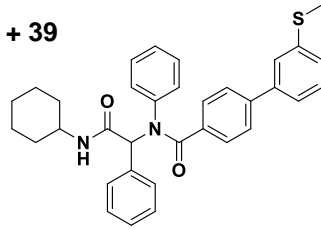


C11-suzuki

C11-suzuki 45 (0.383) Cm (37:90)



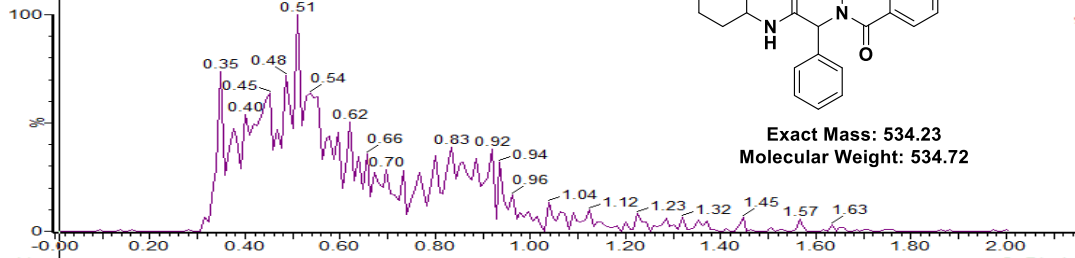
D8 (Green): M + 1, M + 23, M + 39



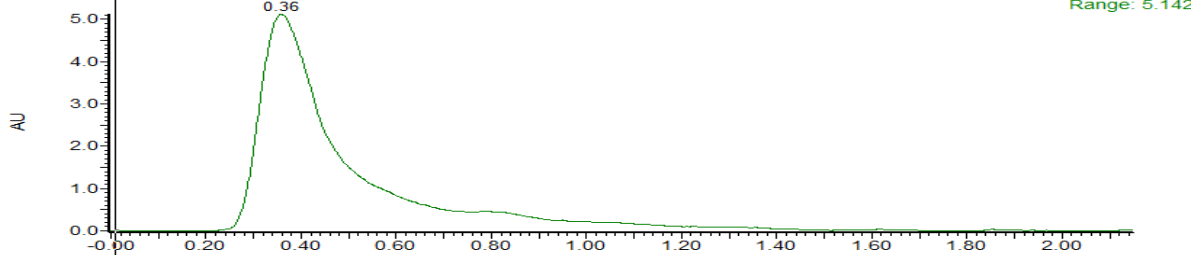
Exact Mass: 534.23
Molecular Weight: 534.72

1: Scan ES+
535
9.99e6

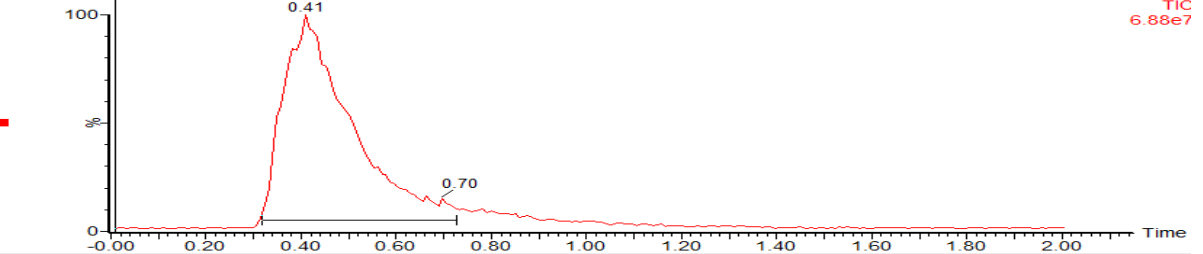
D8-suzuki
D8-suzuki



D8-suzuki



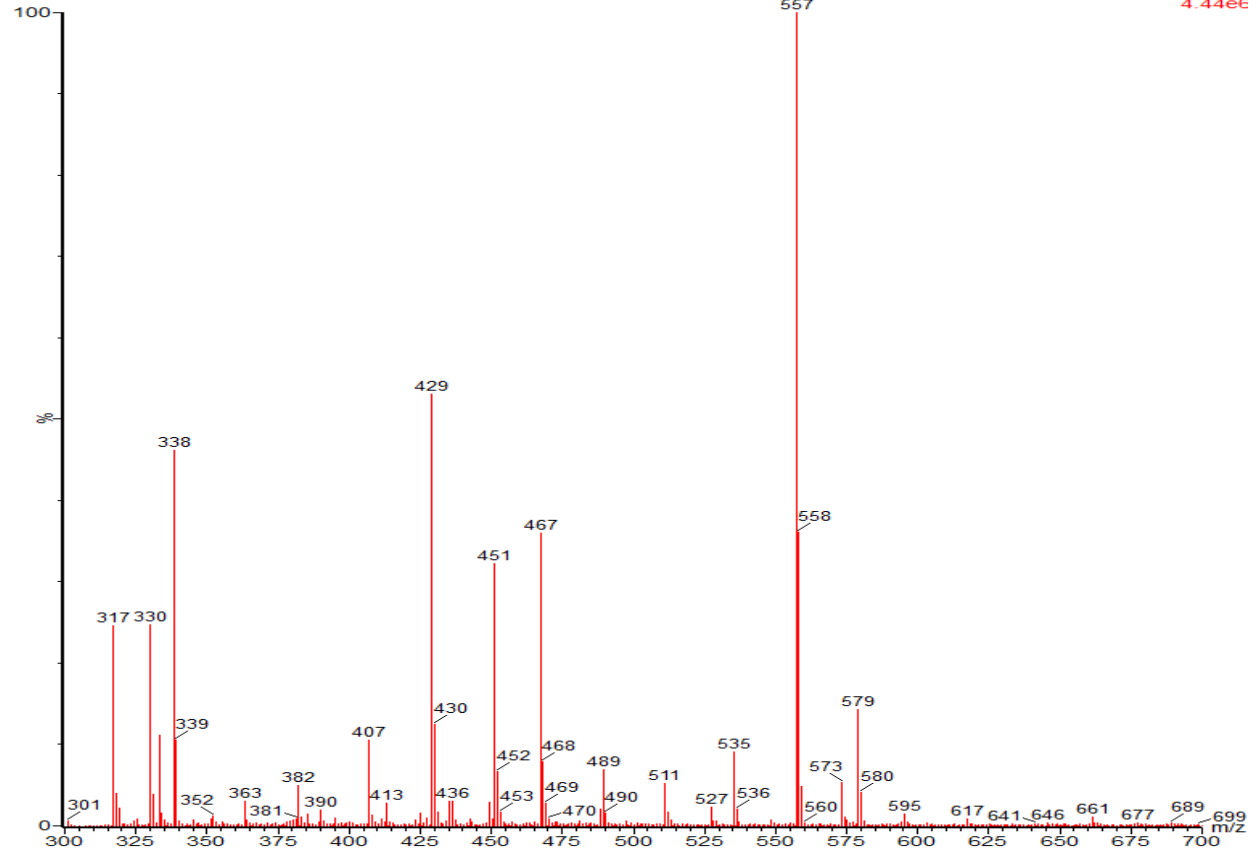
D8-suzuki



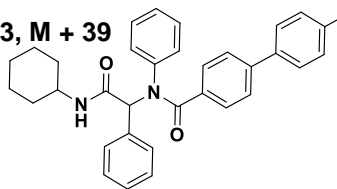
D8-suzuki

D8-suzuki 48 (0.408) Cm (38-91)

1: Scan ES+
4.44e6

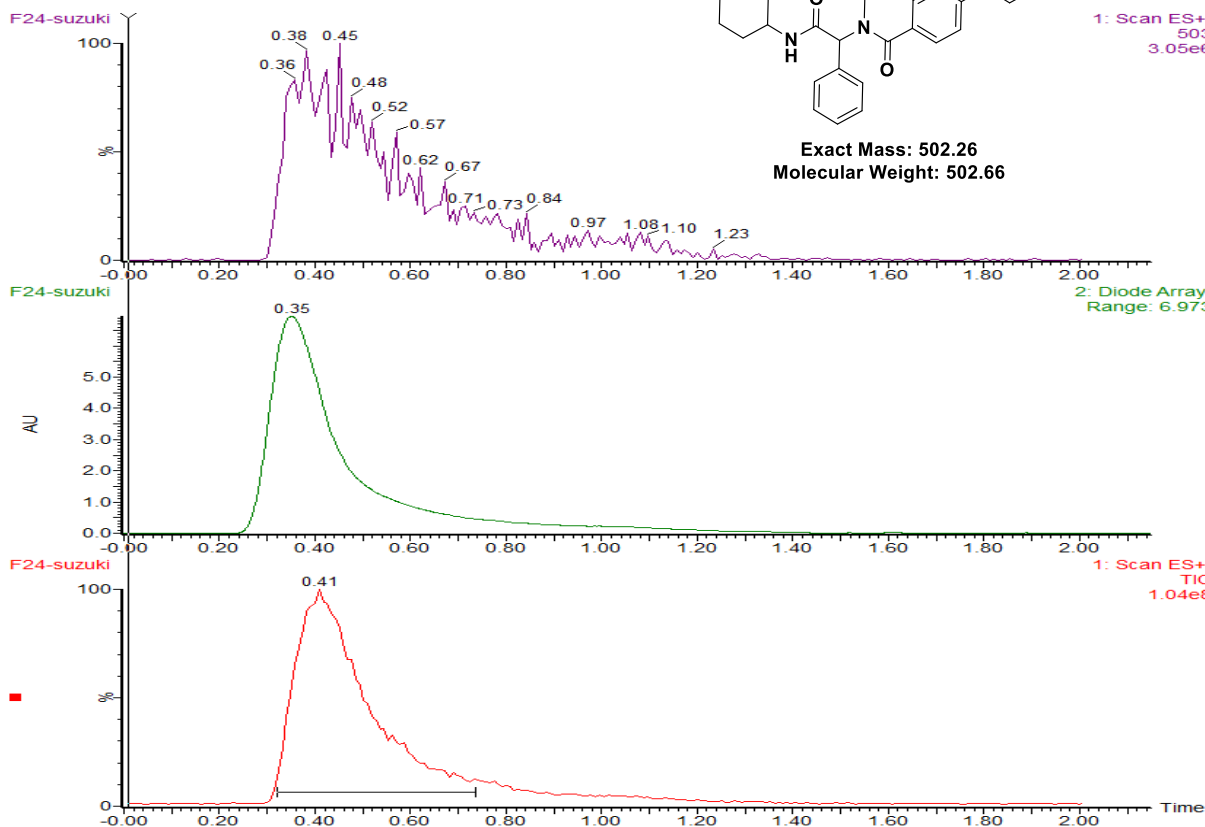


F24 (Green): M + 1, M + 23, M + 39



Exact Mass: 502.26
Molecular Weight: 502.66

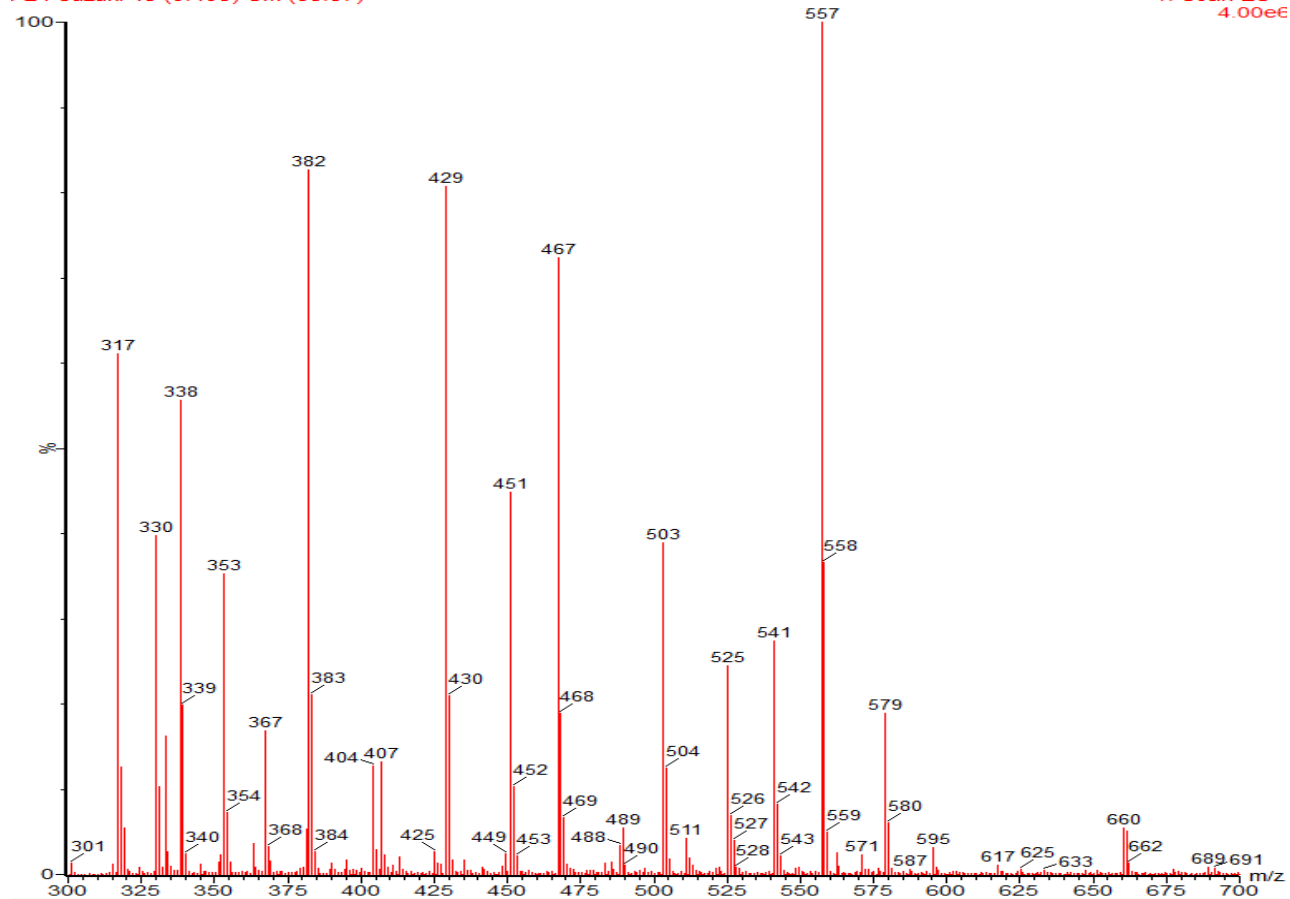
1: Scan ES+
503
3.05e6



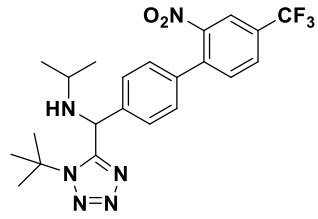
F24-suzuki

F24-suzuki 48 (0.408) Cm (38:87)

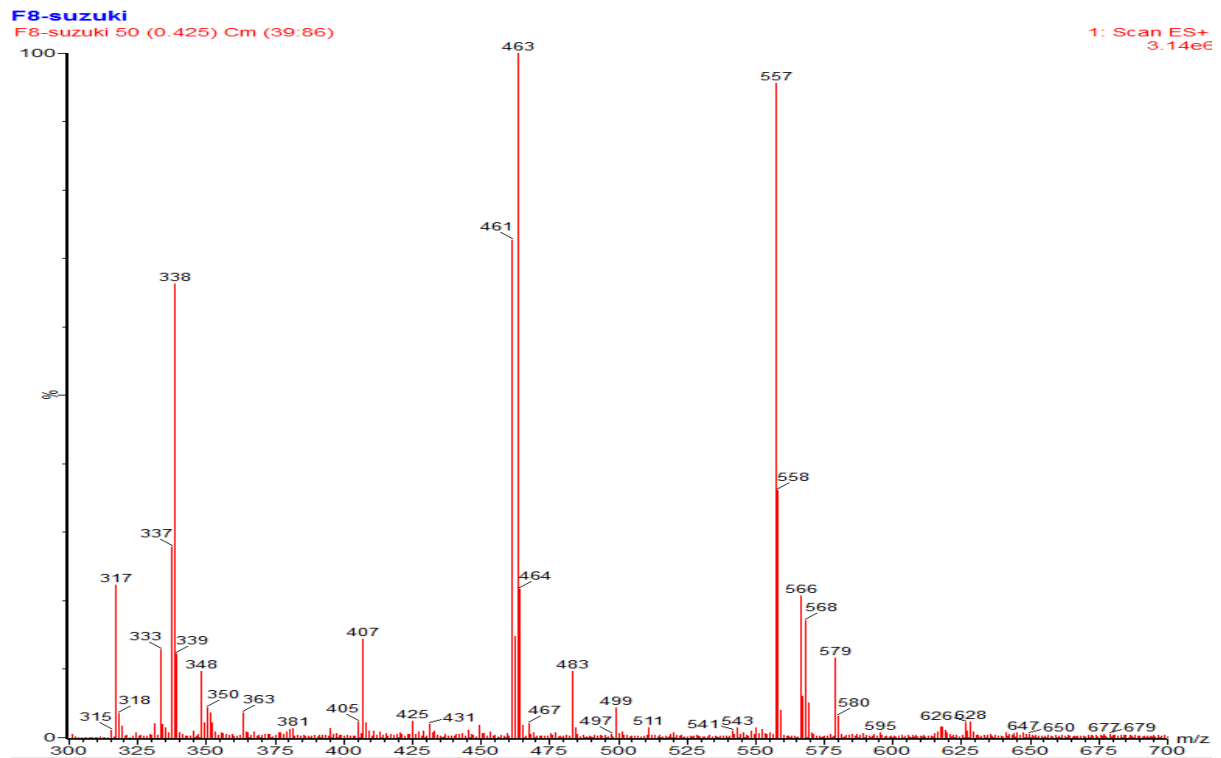
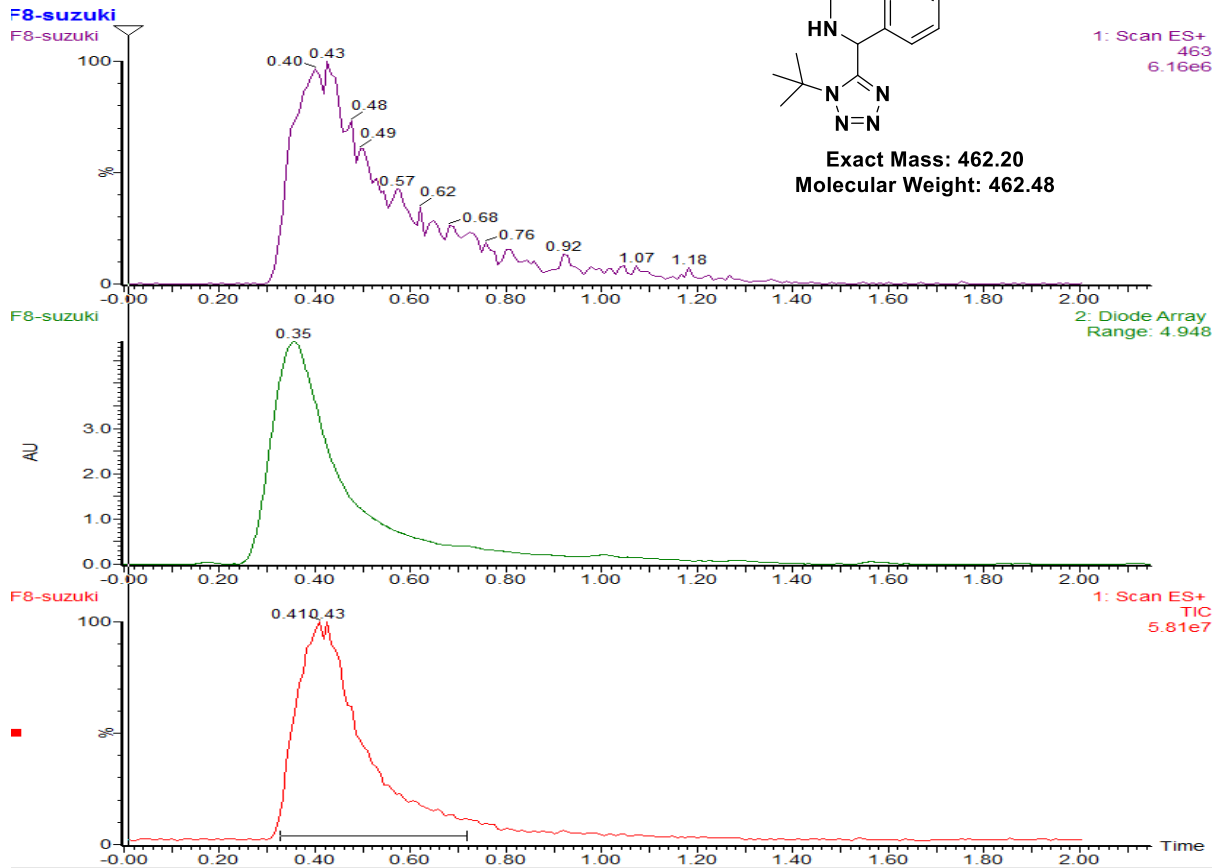
1: Scan ES+
4.00e6



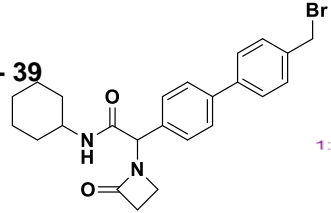
F8 (Green)



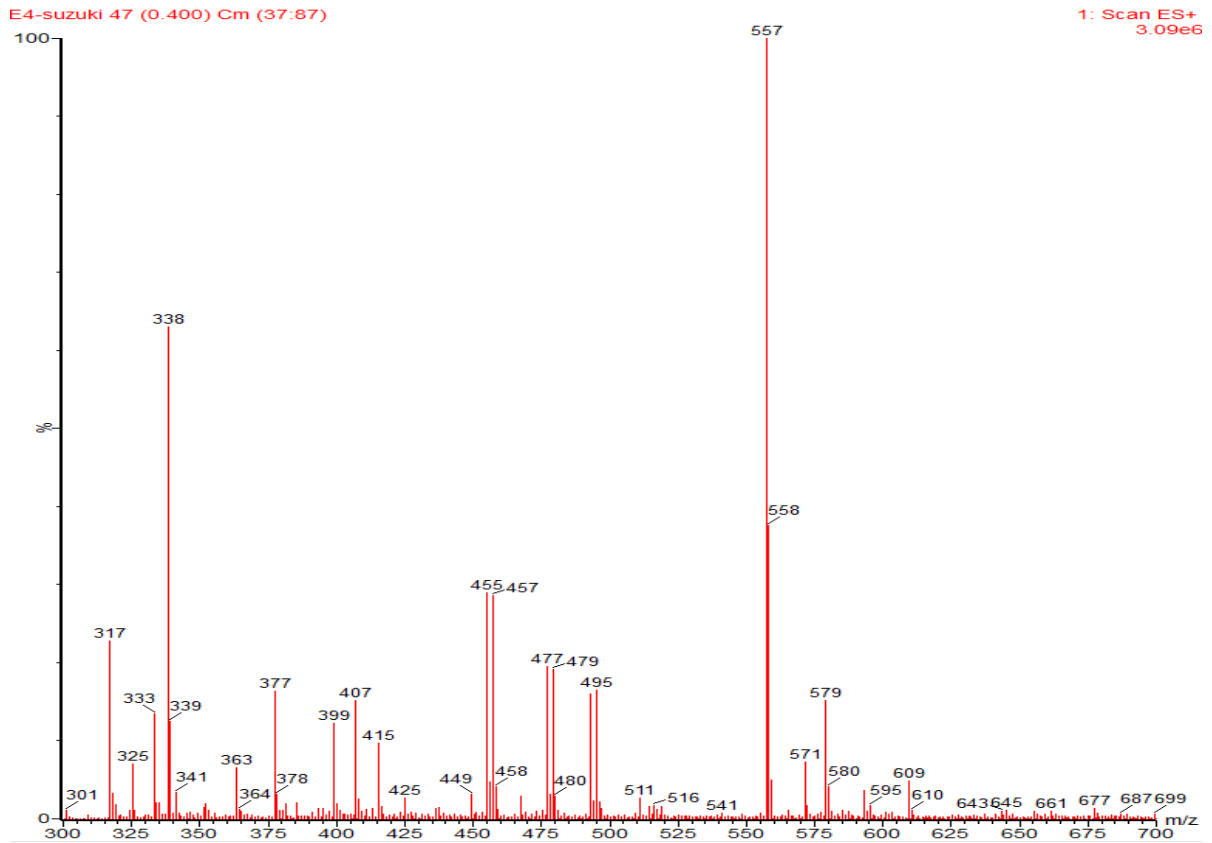
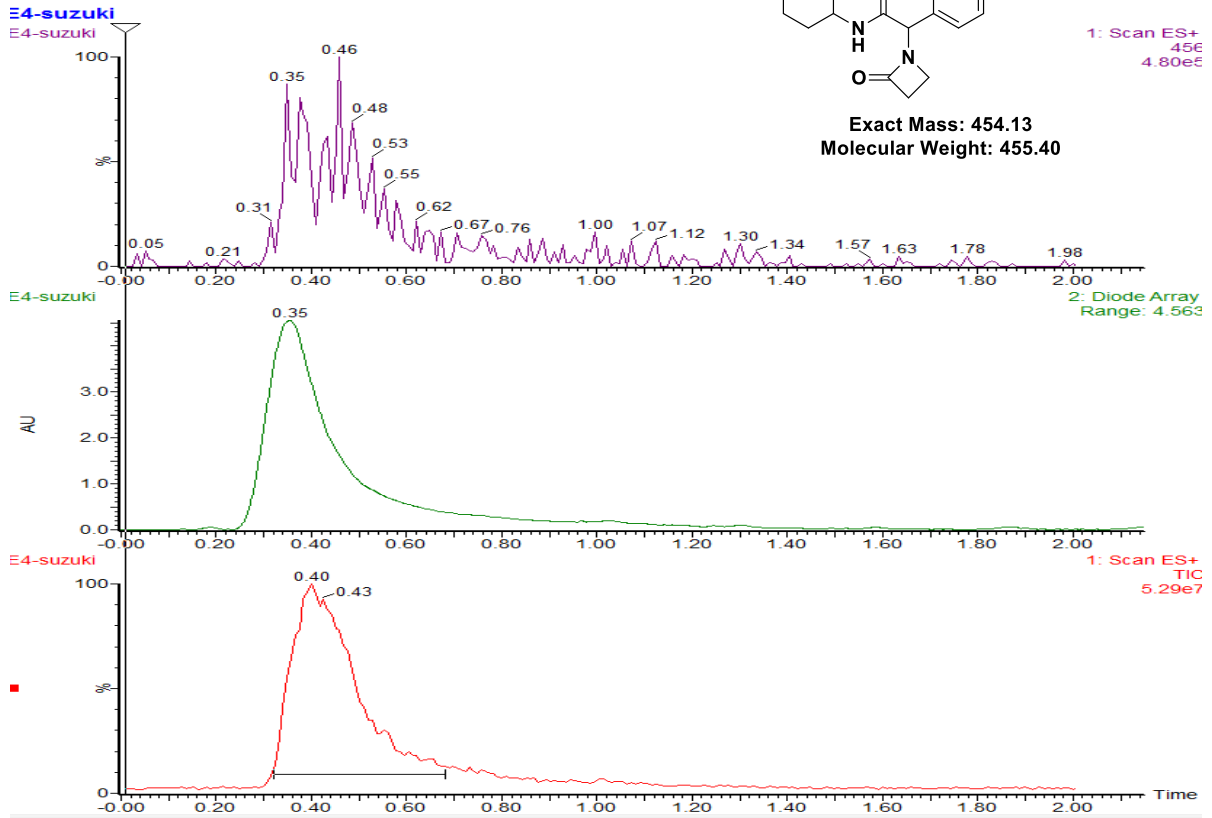
Exact Mass: 462.20
Molecular Weight: 462.48



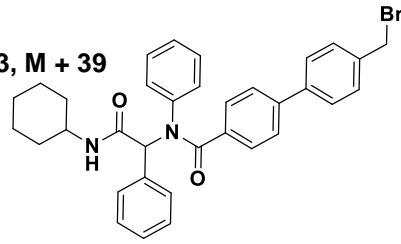
E4 (Green): M + 1, M + 23, M + 39



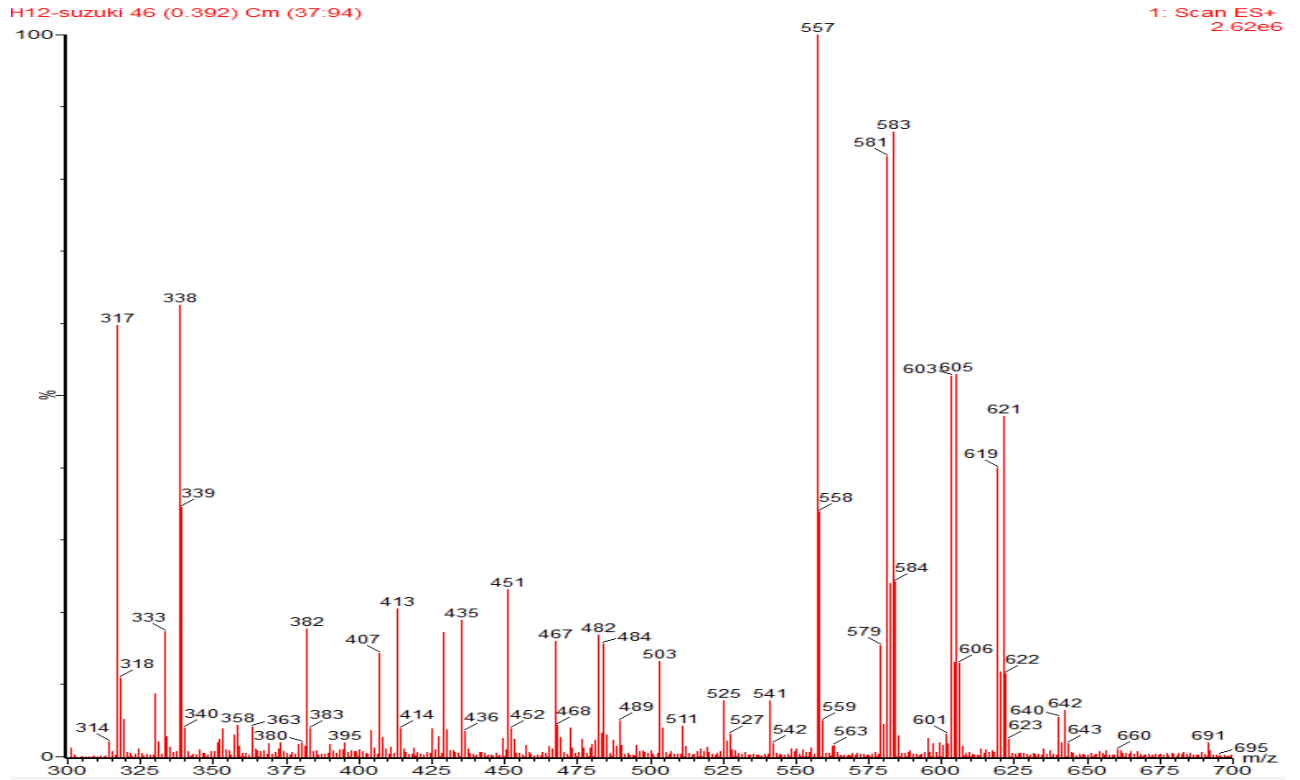
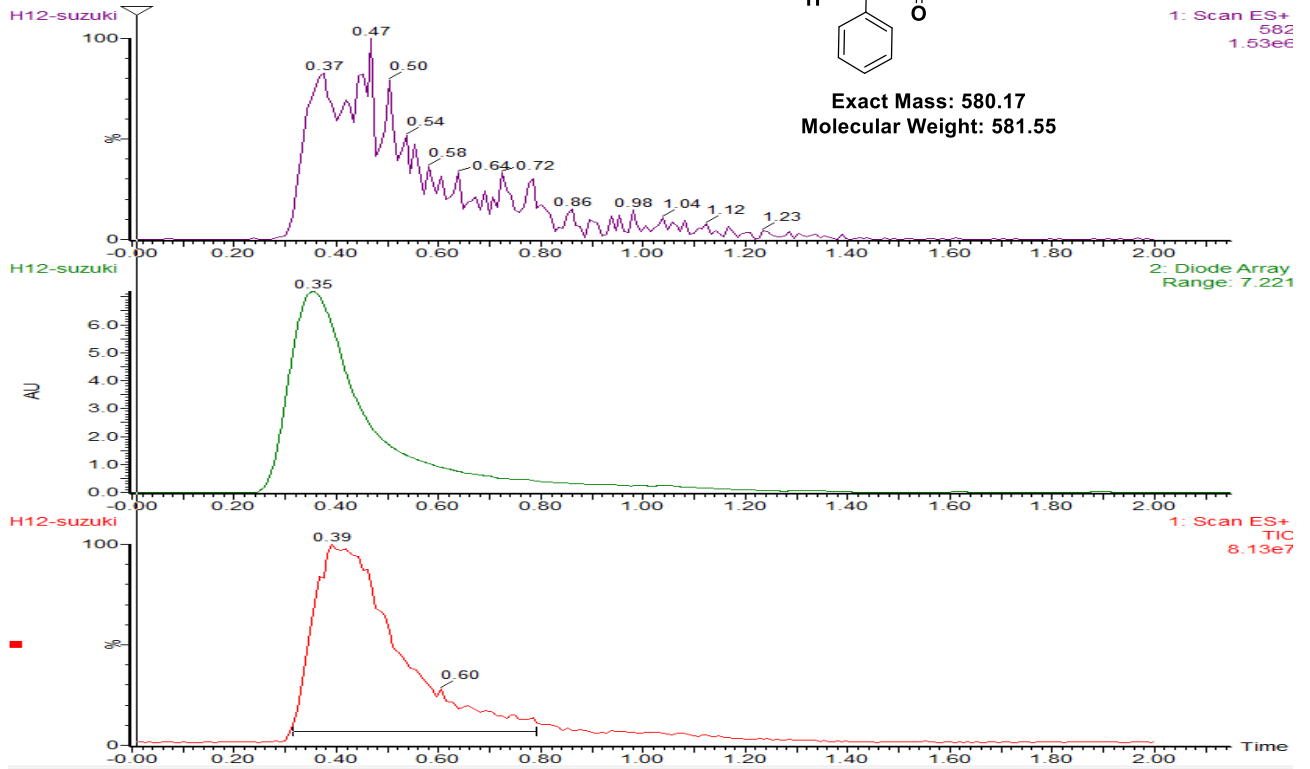
Exact Mass: 454.13
Molecular Weight: 455.40



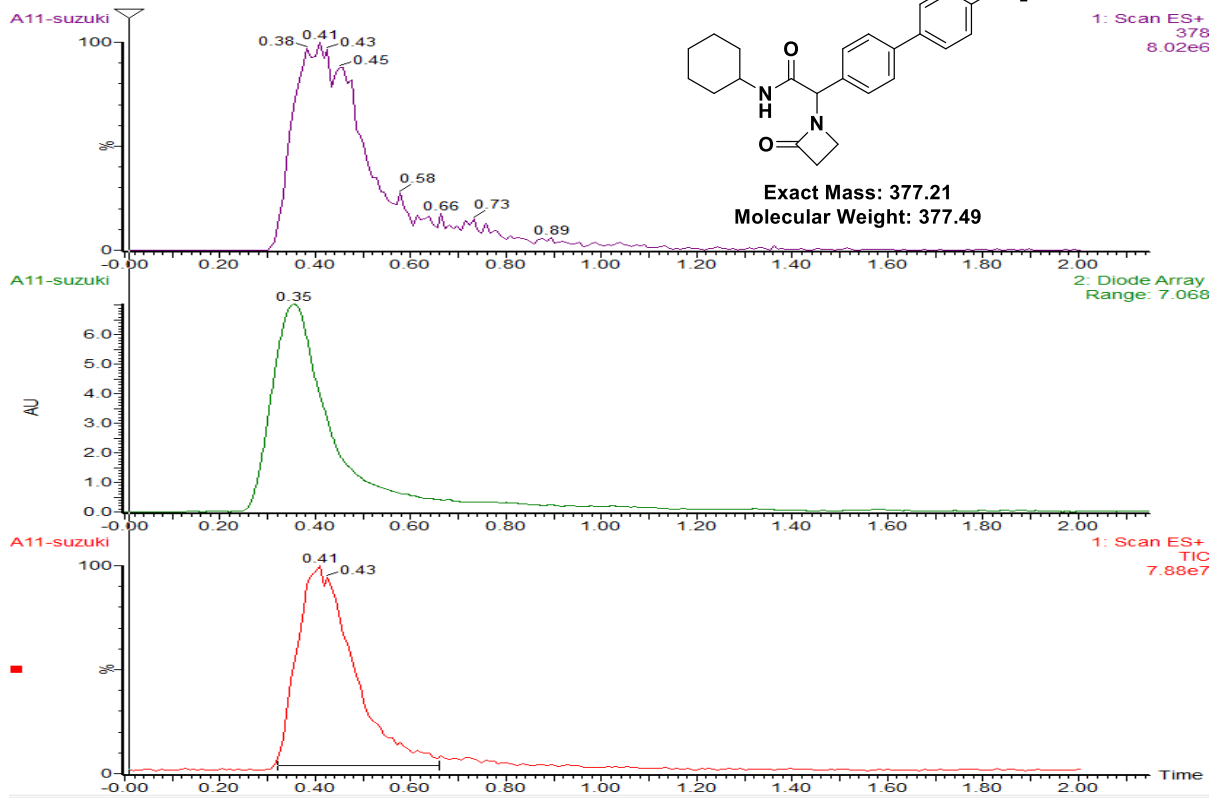
H12 (Green): M + 1, M + 23, M + 39



Exact Mass: 580.17
Molecular Weight: 581.55

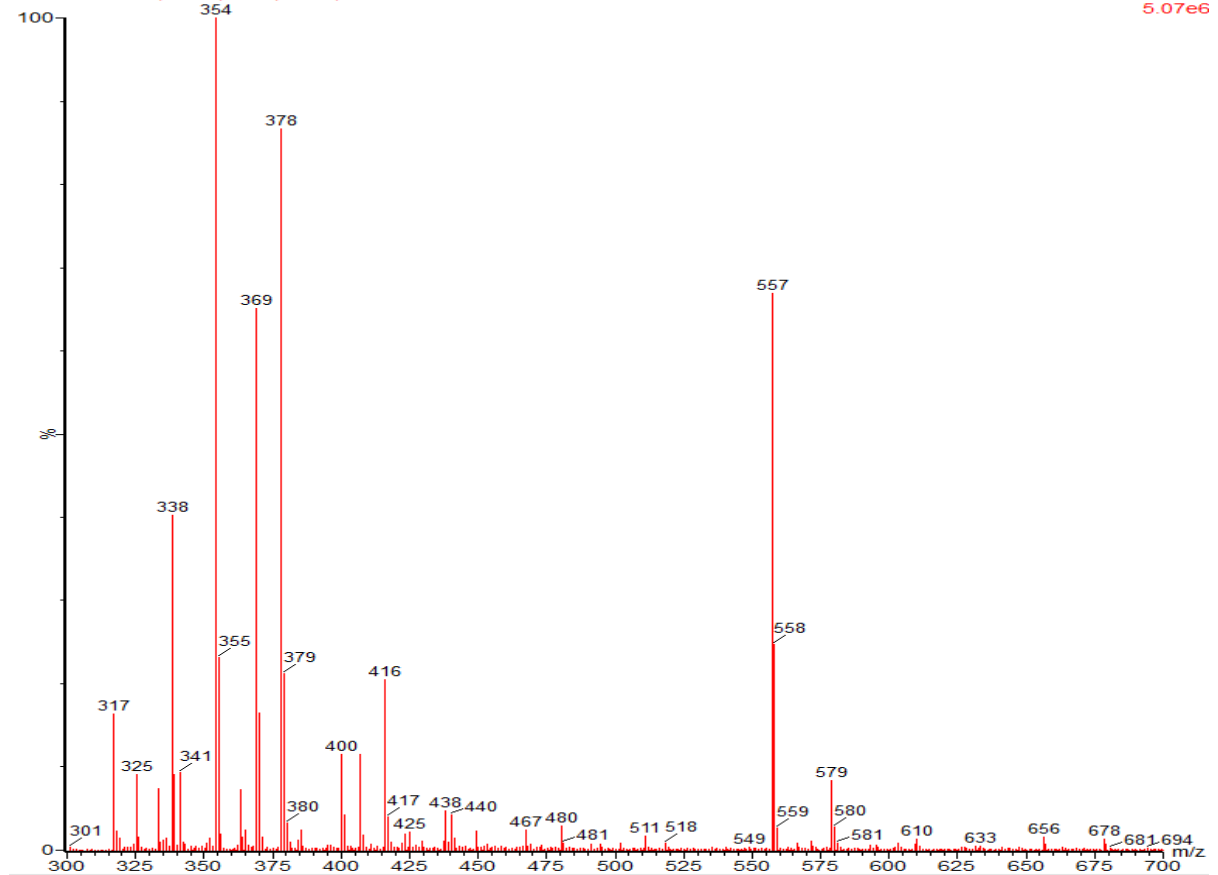


A11 (Green): M + 1, M + 23, M + 39

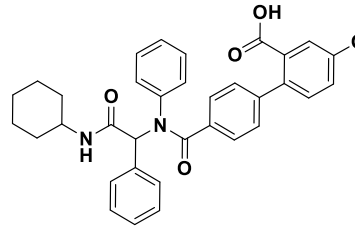


A11-suzuki

A11-suzuki 48 (0.408) Cm (39:74)

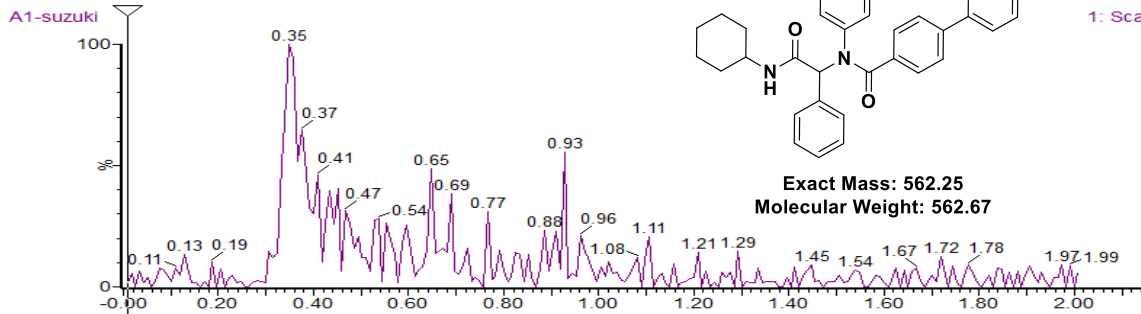


A1 (Yellow)

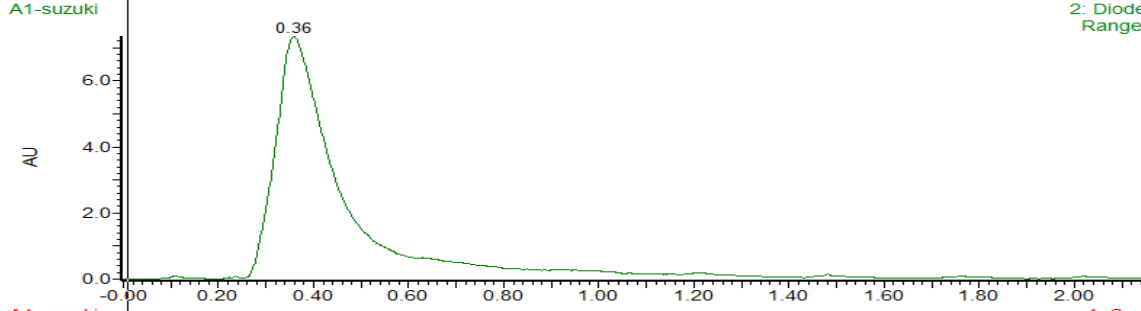


Exact Mass: 562.25
Molecular Weight: 562.67

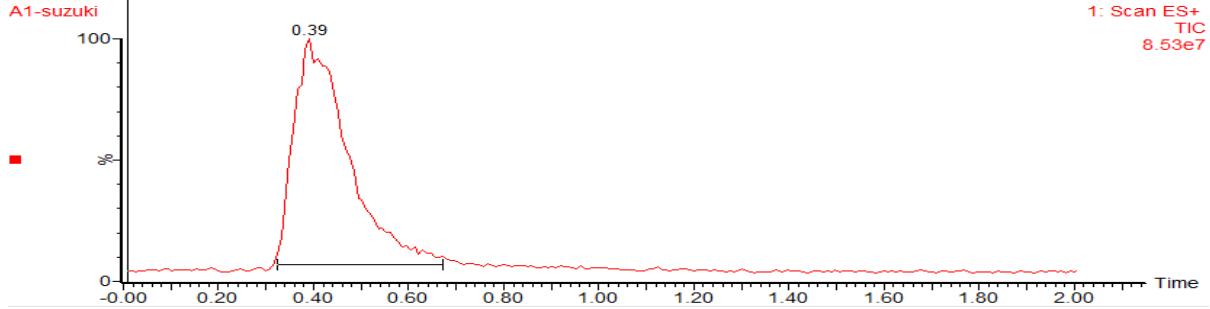
1: Scan ES+
563
3.56e5



A1-suzuki
2: Diode Array
Range: 7.361

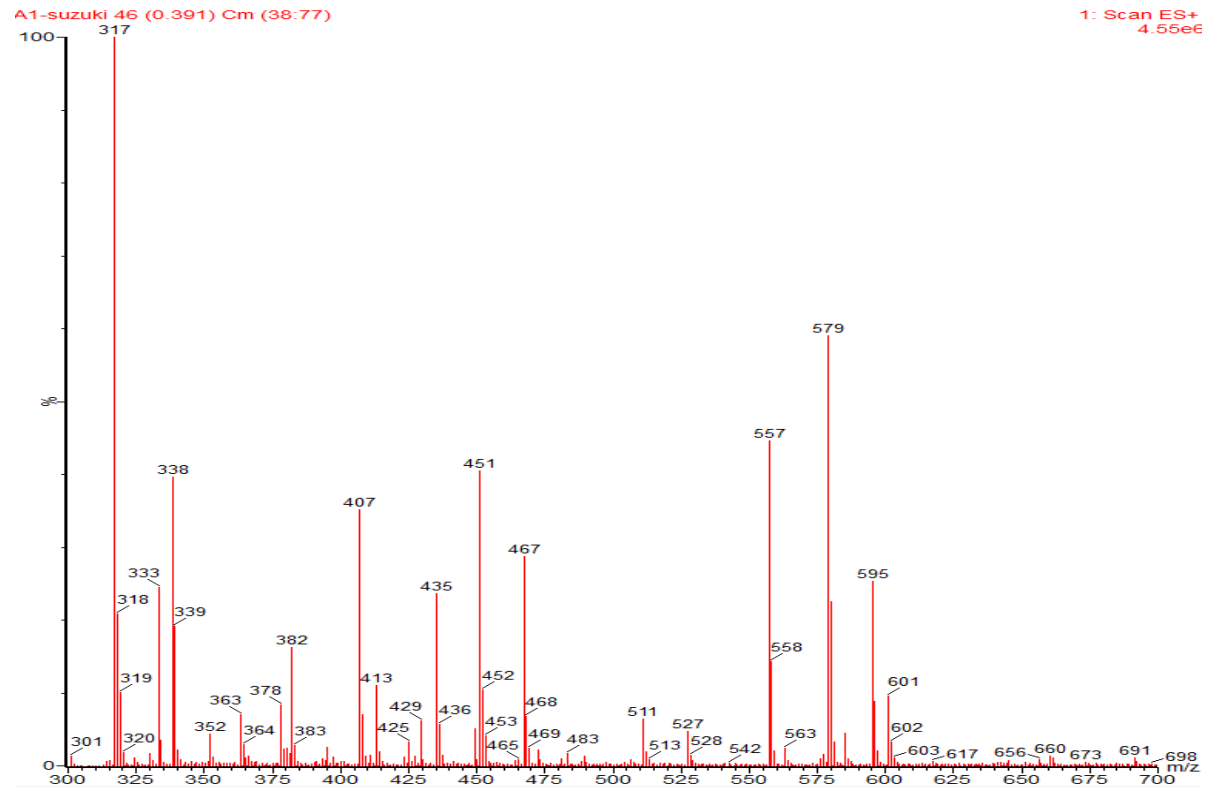


A1-suzuki
1: Scan ES+
TIC
8.53e7

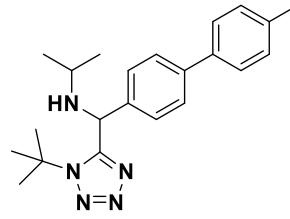


A1-suzuki 46 (0.391) Cm (38:77)

1: Scan ES+
4.55e8

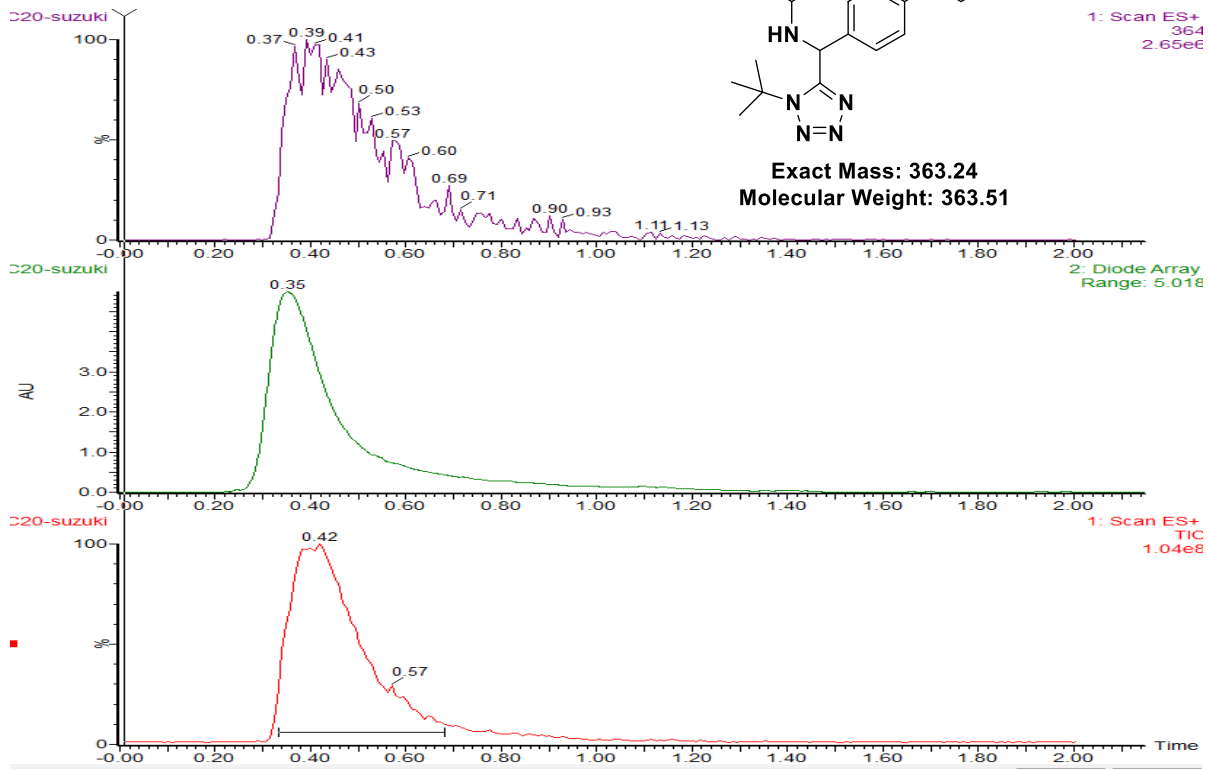


C20 (Yellow)

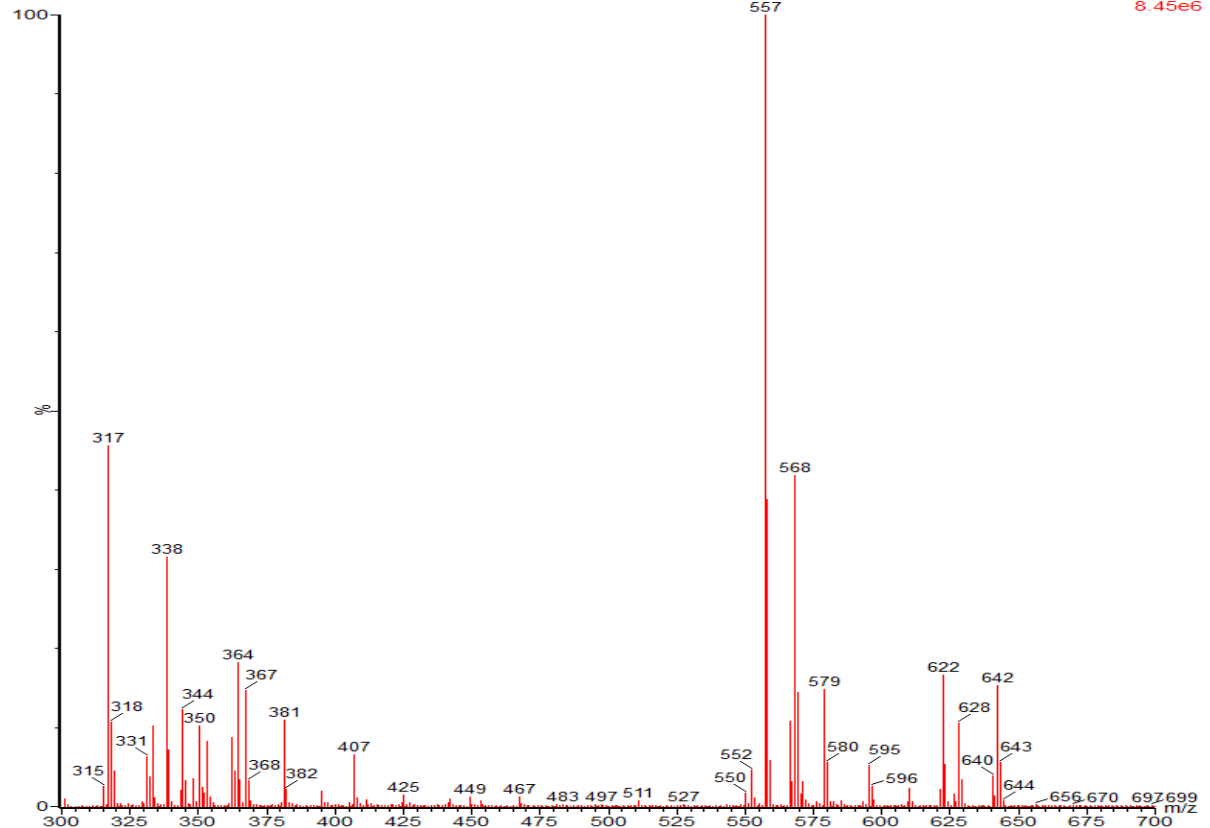


Exact Mass: 363.24
Molecular Weight: 363.51

1: Scan ES+
364
2.65e6

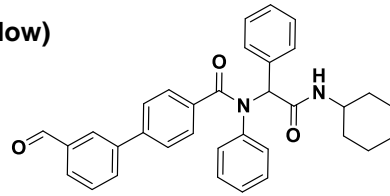


C20-suzuki 49 (0.417) Cm (39:79)



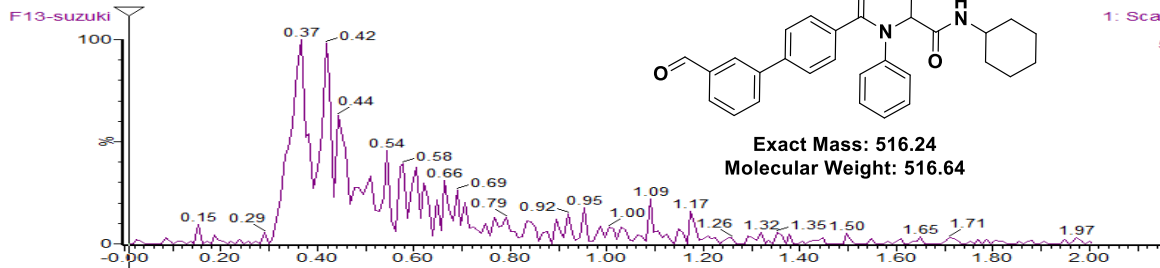
1: Scan ES+
8.45e6

F13 (Yellow)

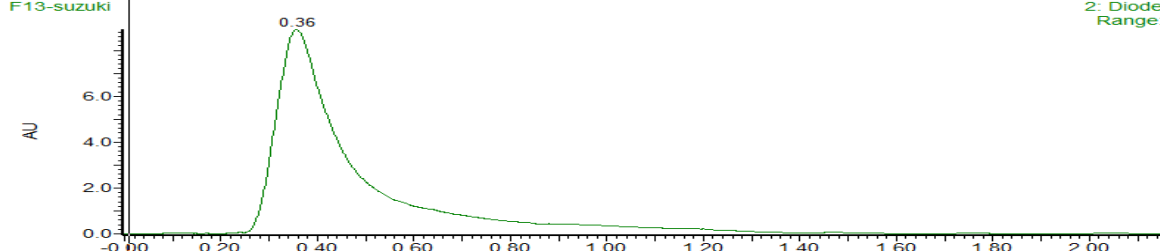


Exact Mass: 516.24
Molecular Weight: 516.64

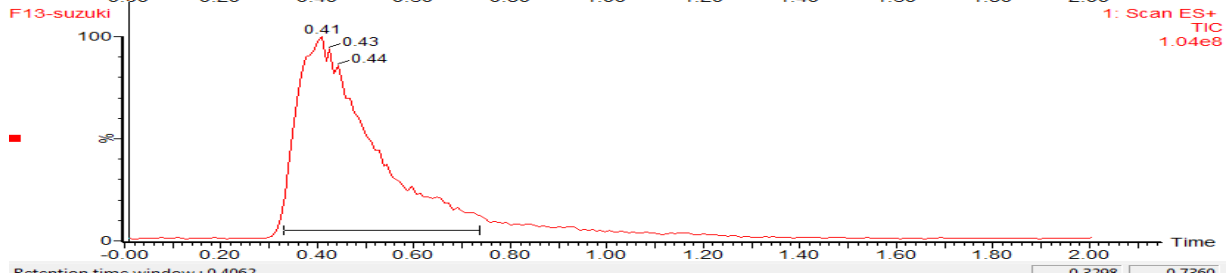
1: Scan ES+
517
5.14e5



2: Diode Array
Range: 8.924

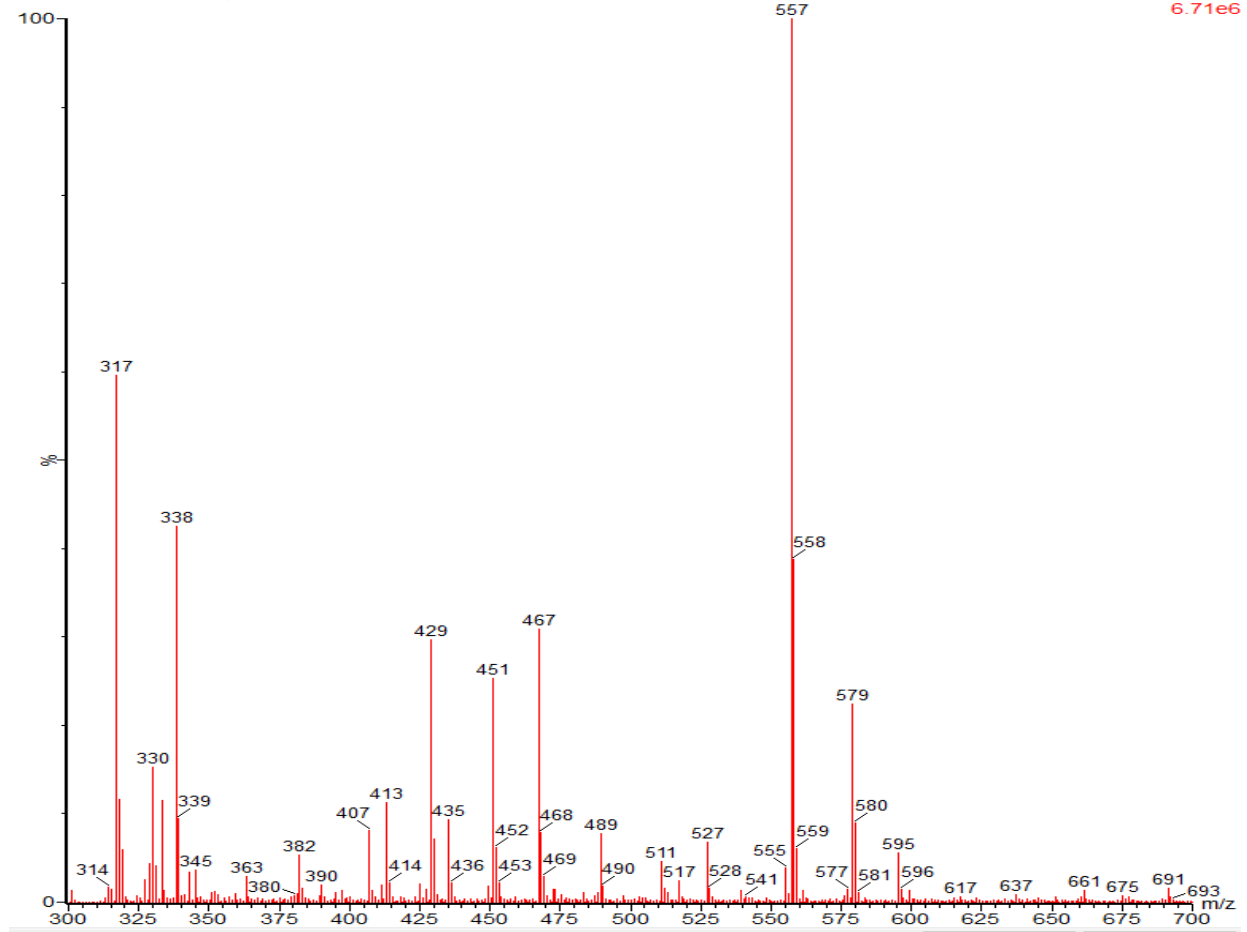


1: Scan ES+
TIC
1.04e8

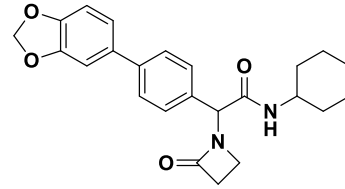


F13-suzuki 48 (0.408) Cm (40:90)

1: Scan ES+
6.71e6

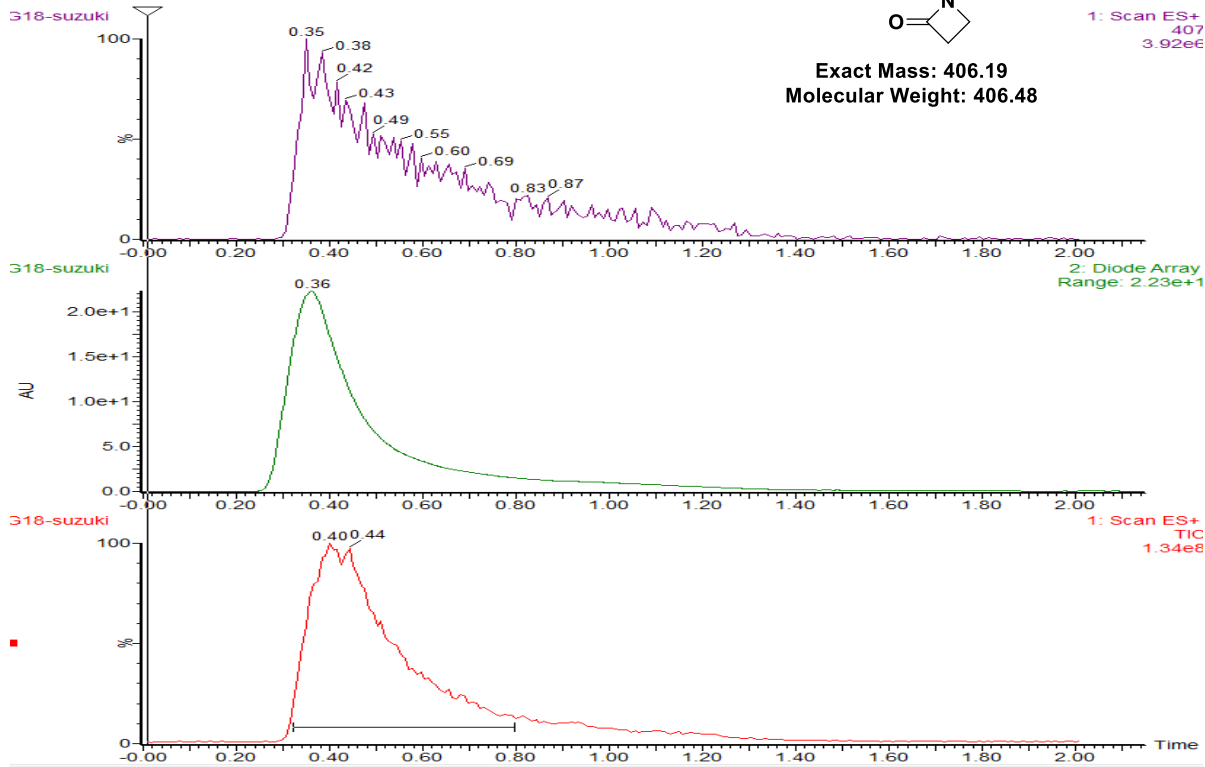


G18 (Yellow)



Exact Mass: 406.19
Molecular Weight: 406.48

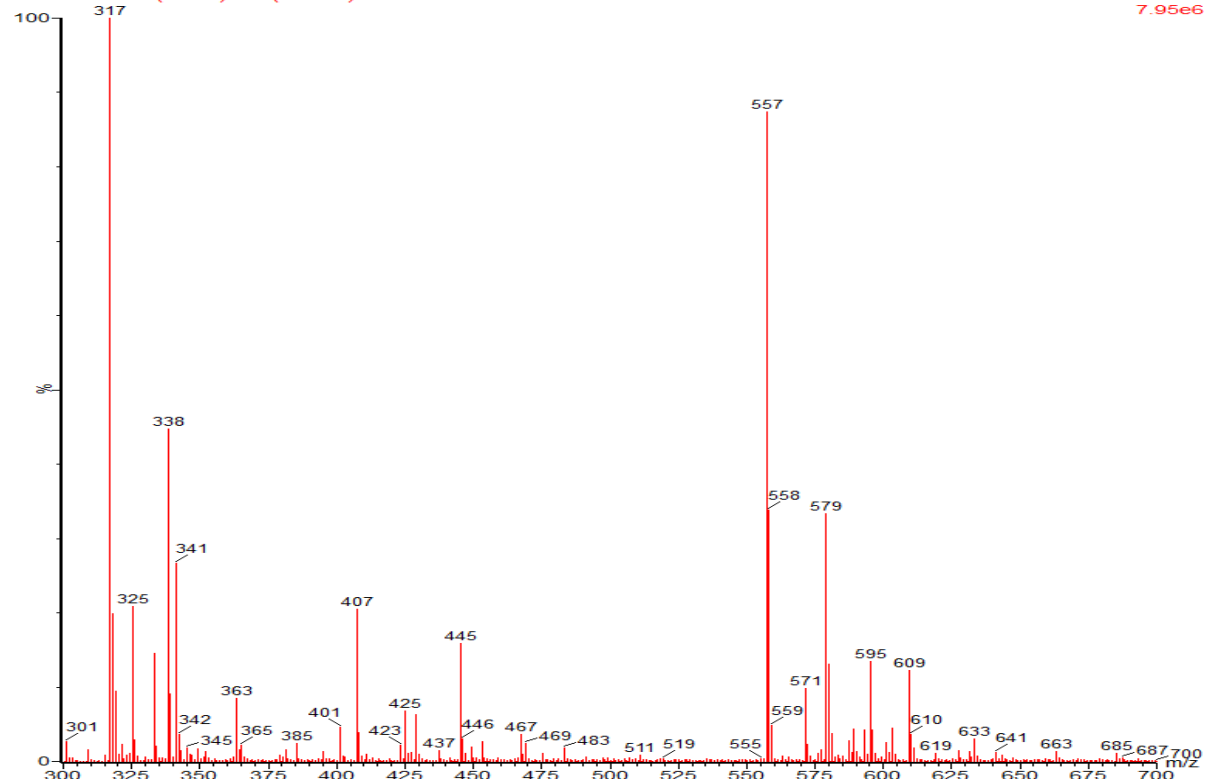
1: Scan ES+
407
3.92e6



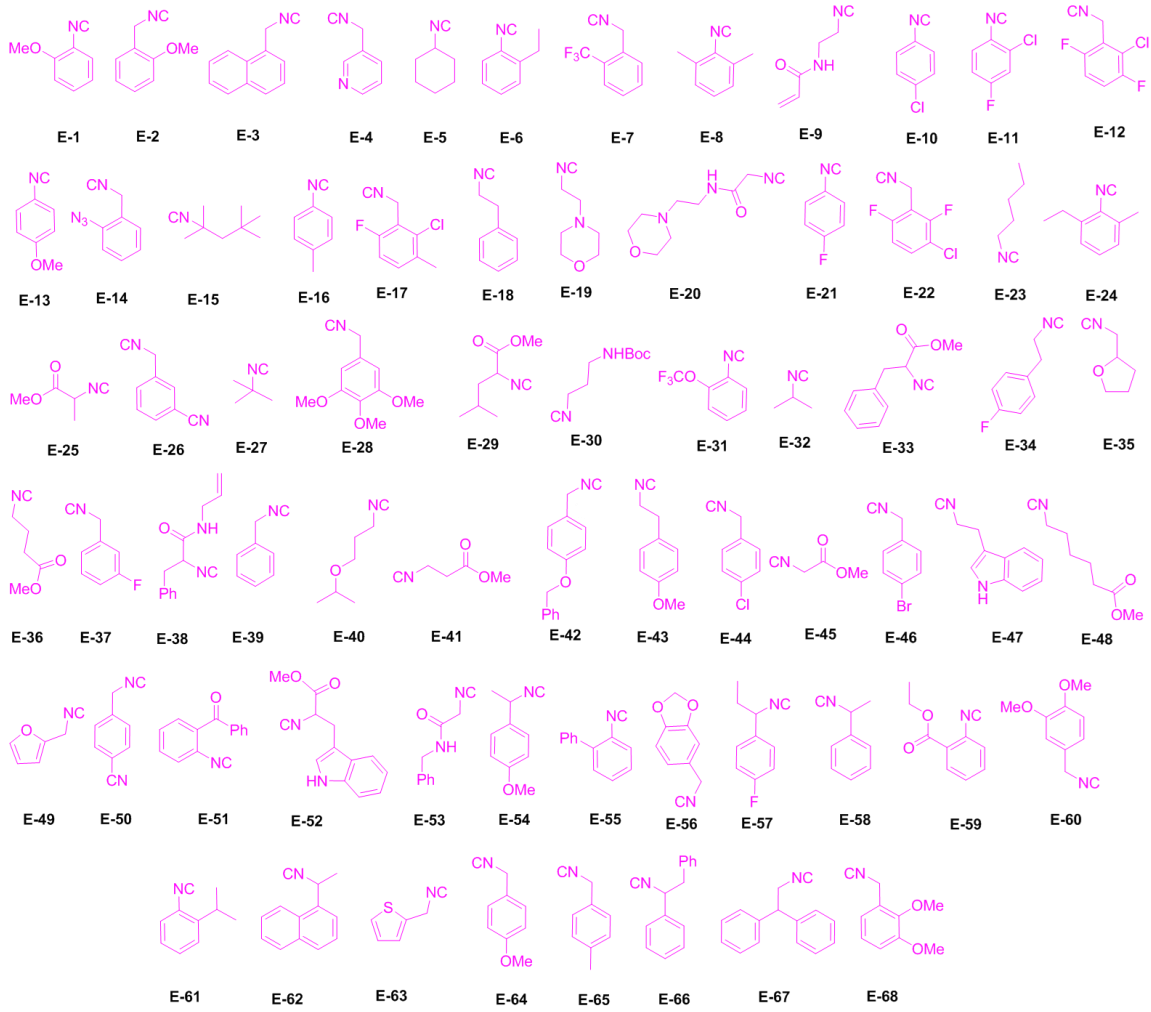
318-suzuki

G18-suzuki 47 (0.400) Cm (38:102)

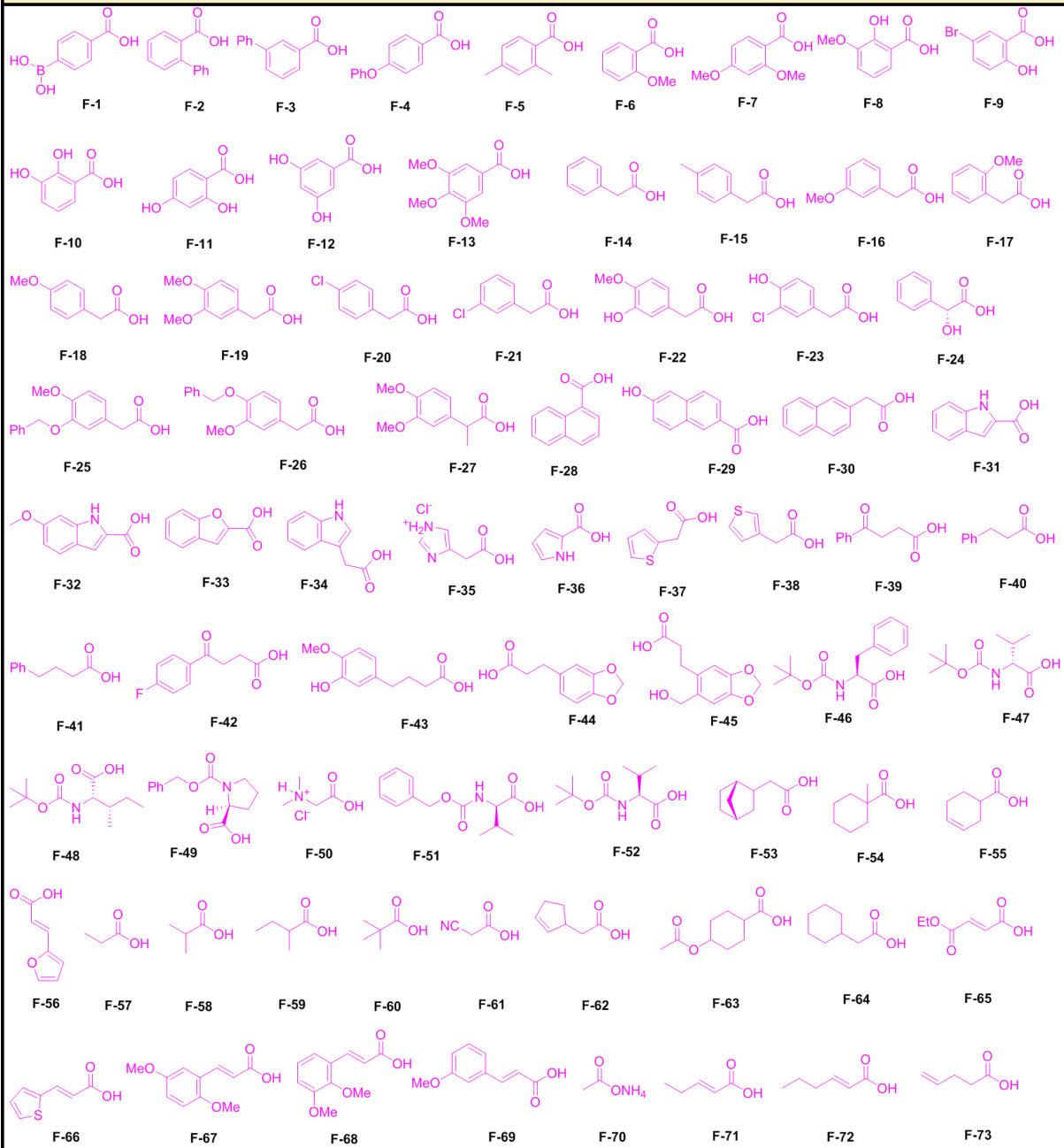
1: Scan ES+
7.95e6



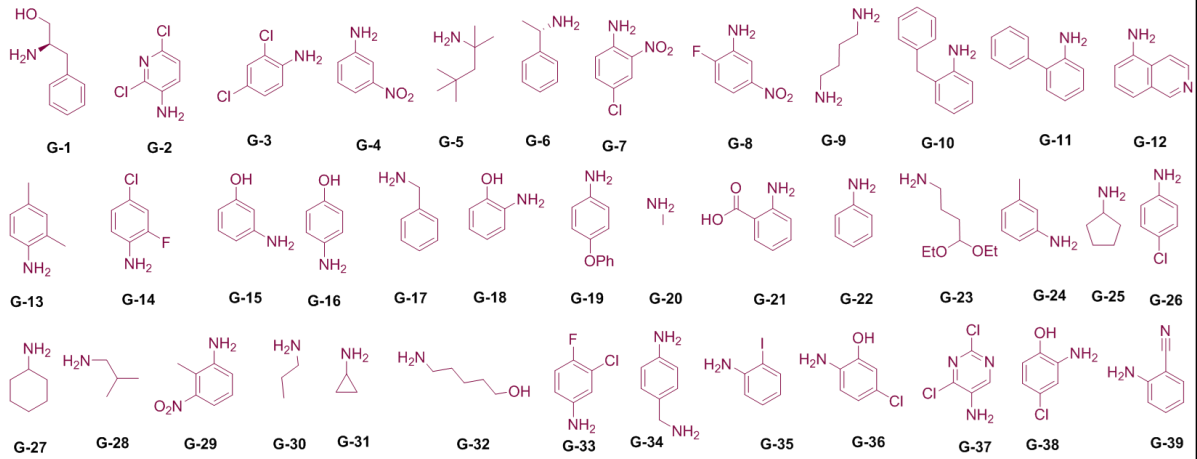
Isocyanides



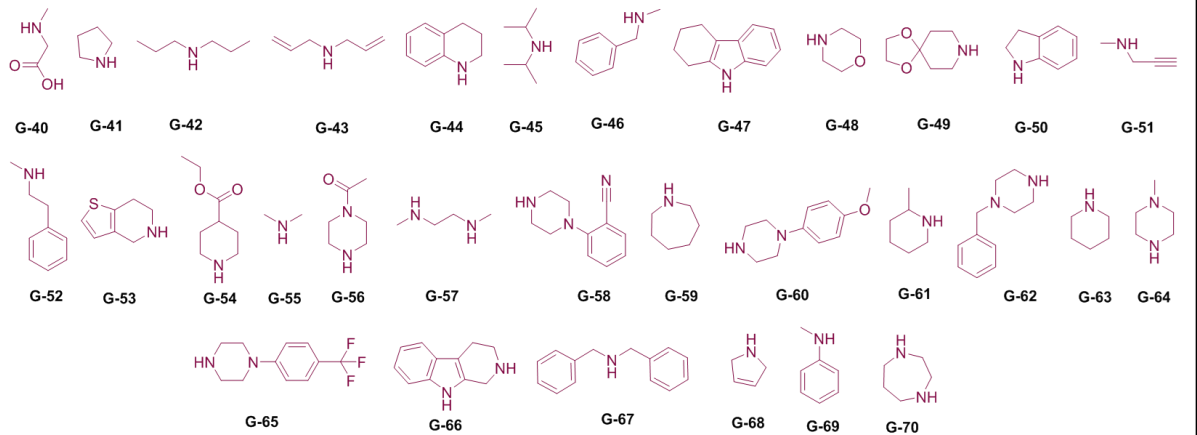
Carboxylic acids



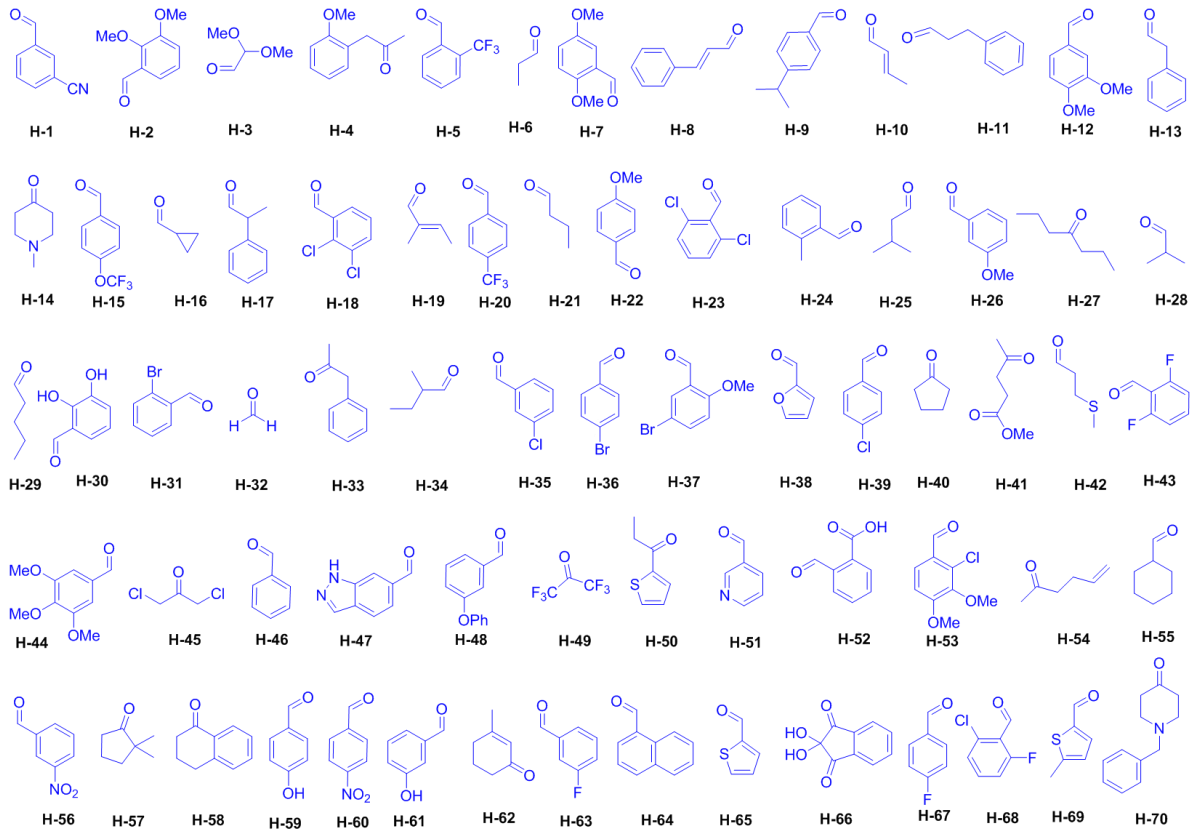
Primary amines



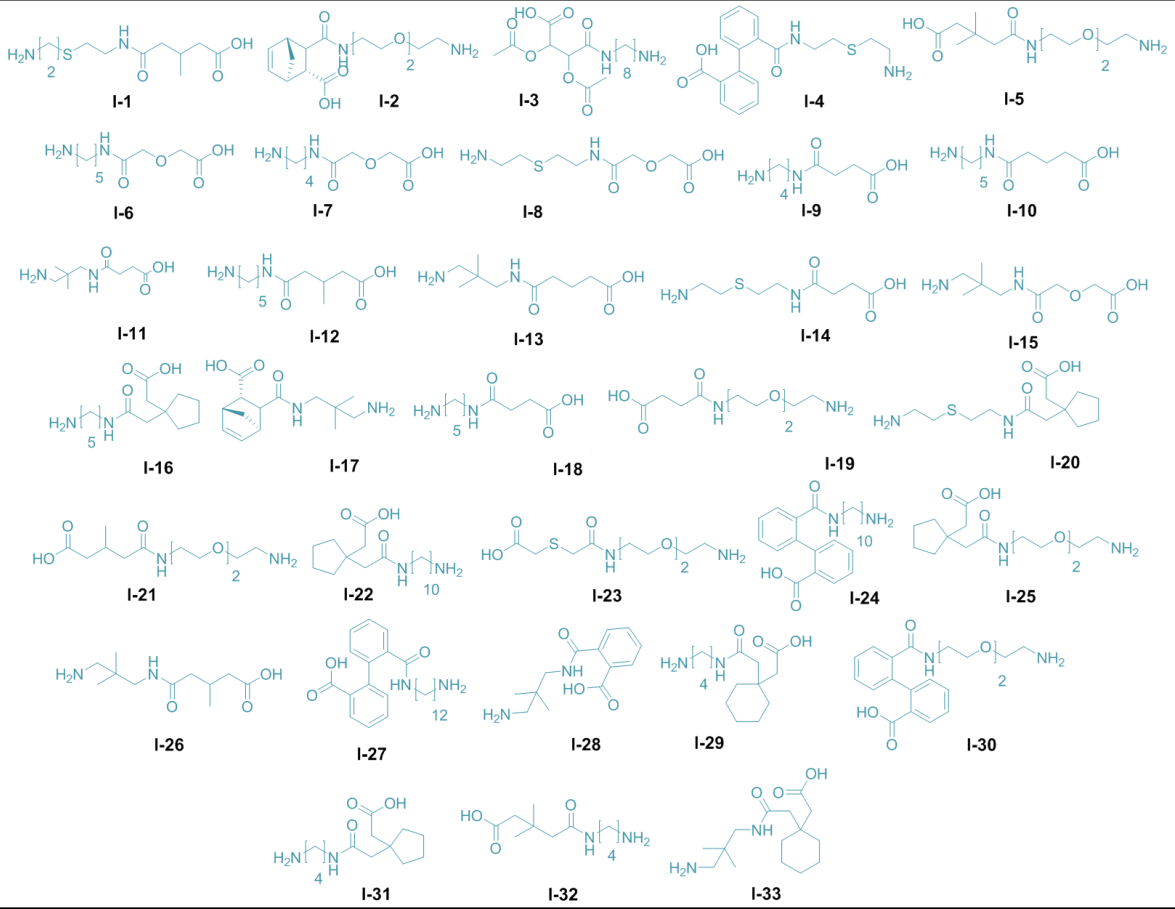
Secondary amines



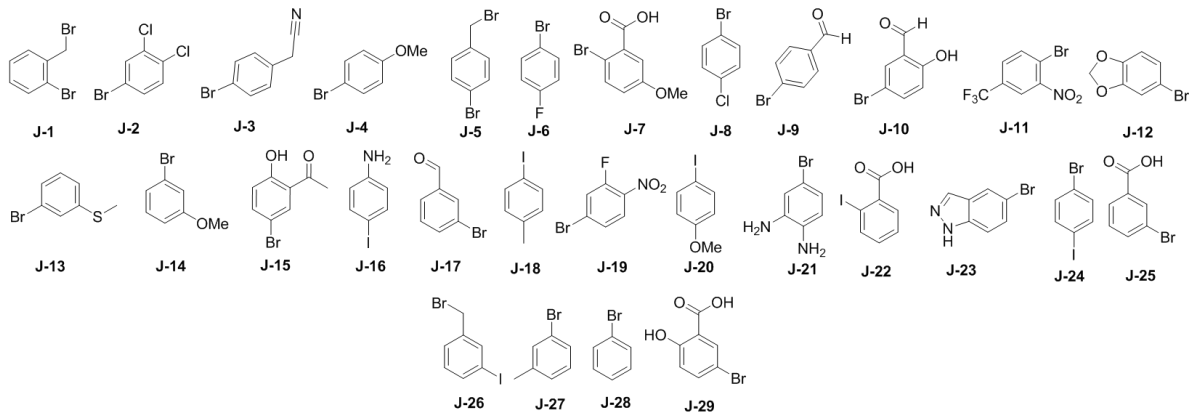
Oxo components



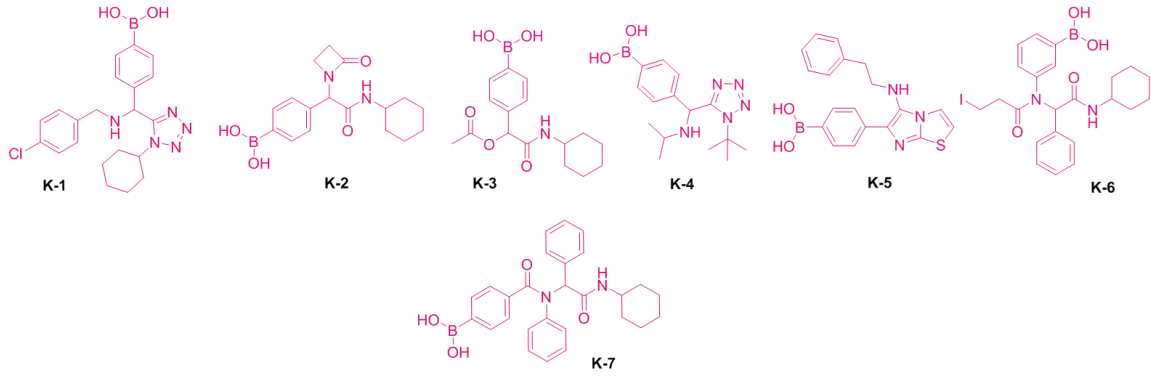
α,ω -Amino carboxylic acids



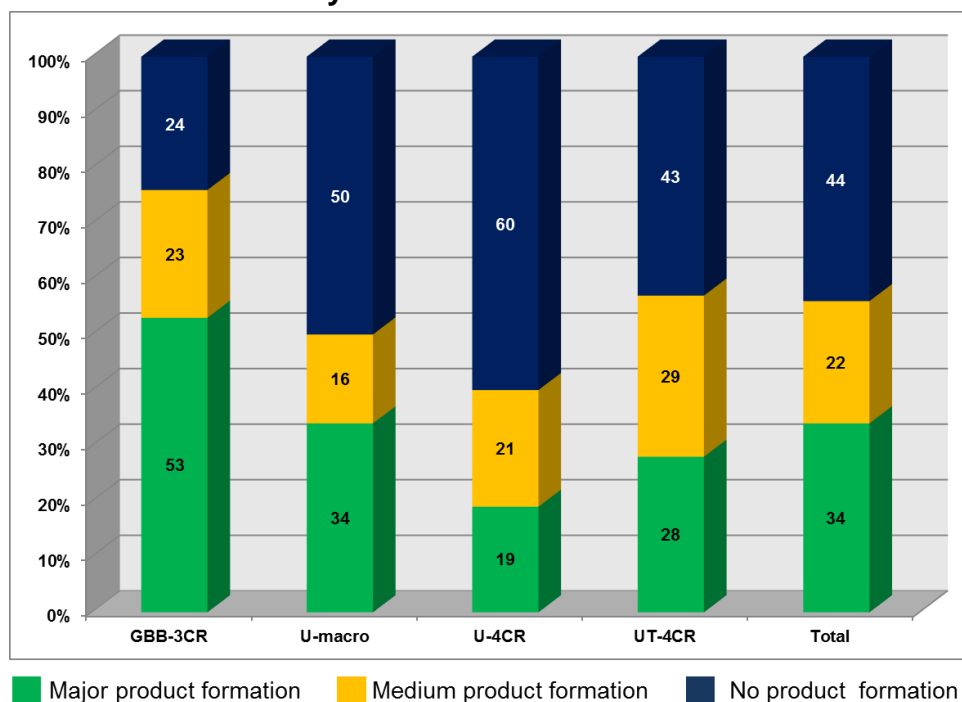
Aryl halides



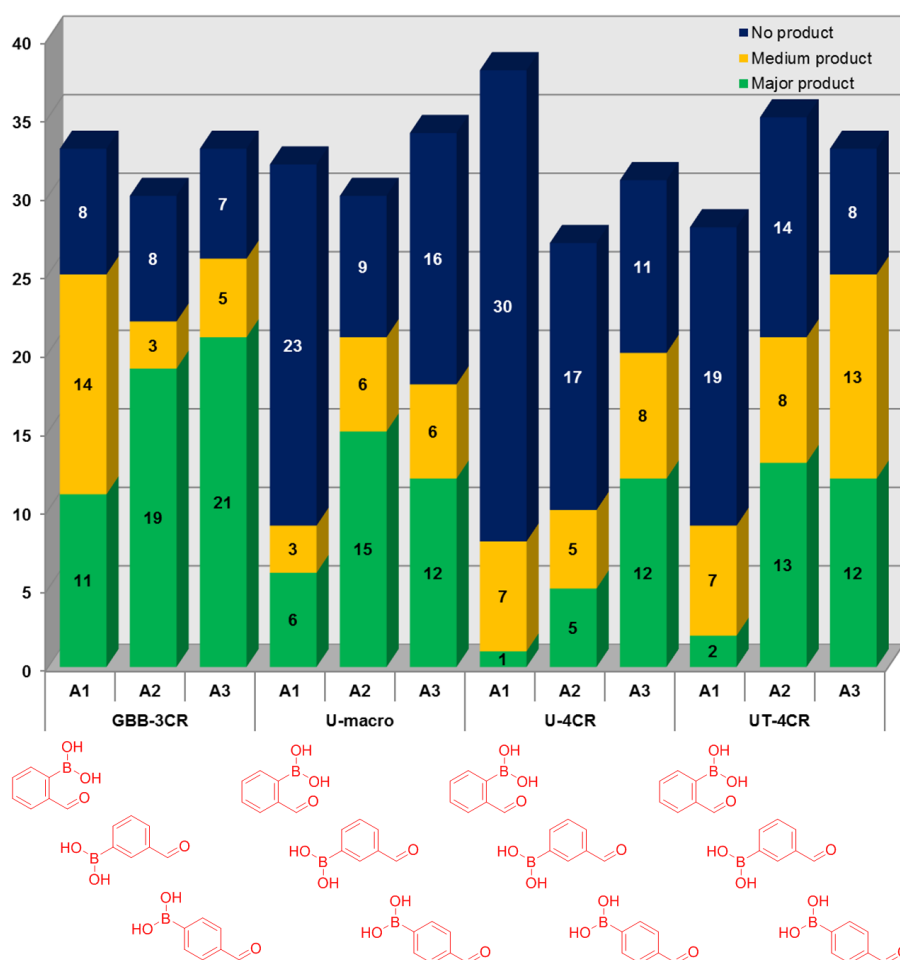
MCR boronic acid building blocks



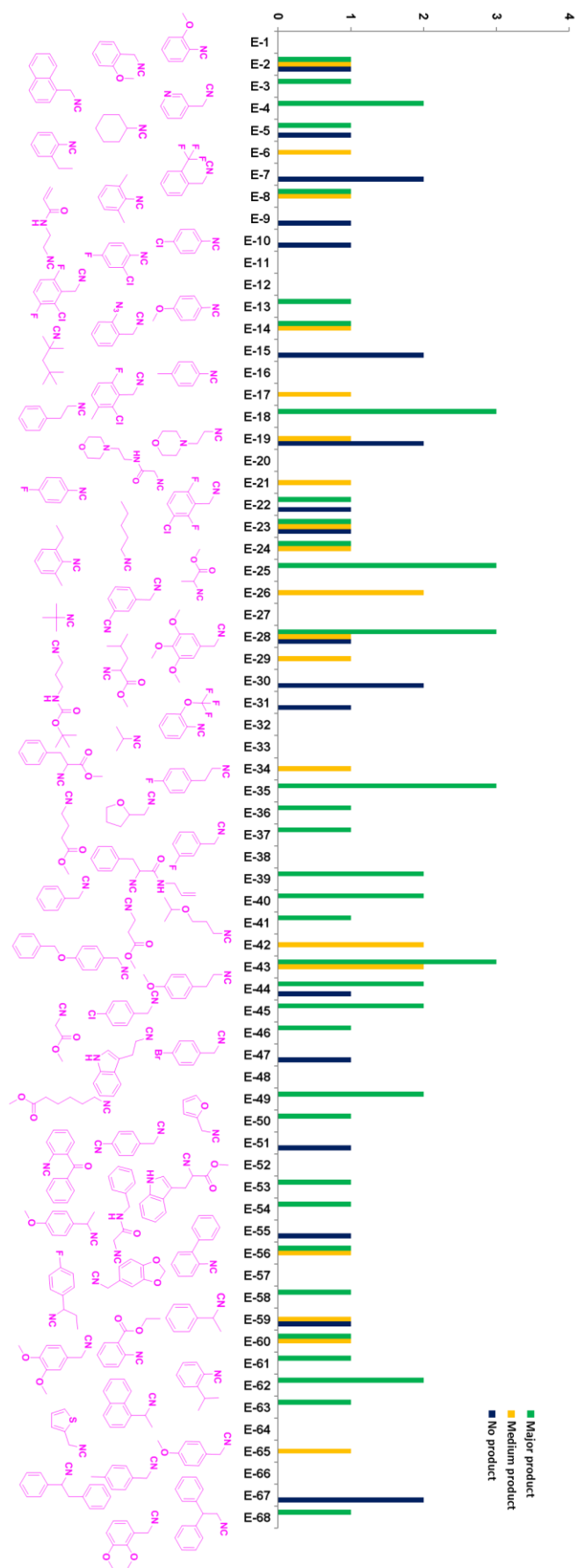
5. Statistical reaction analysis



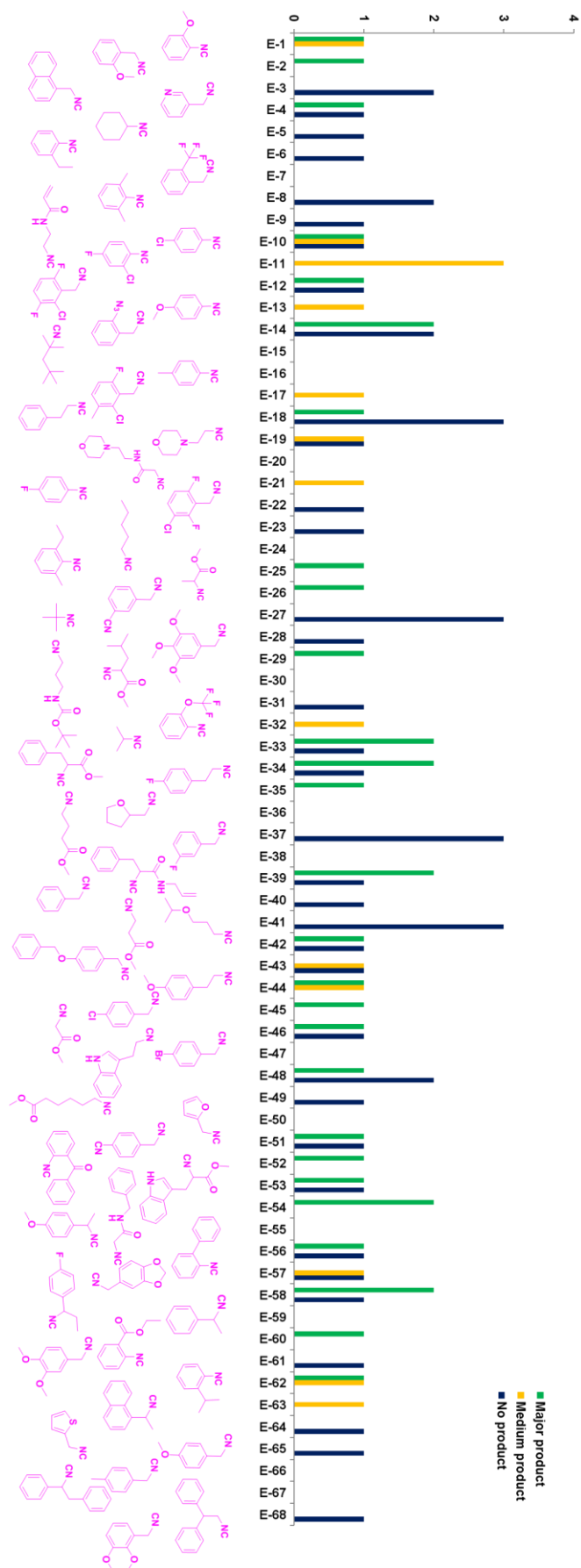
Scheme S1. Quality control results for destination plate I.



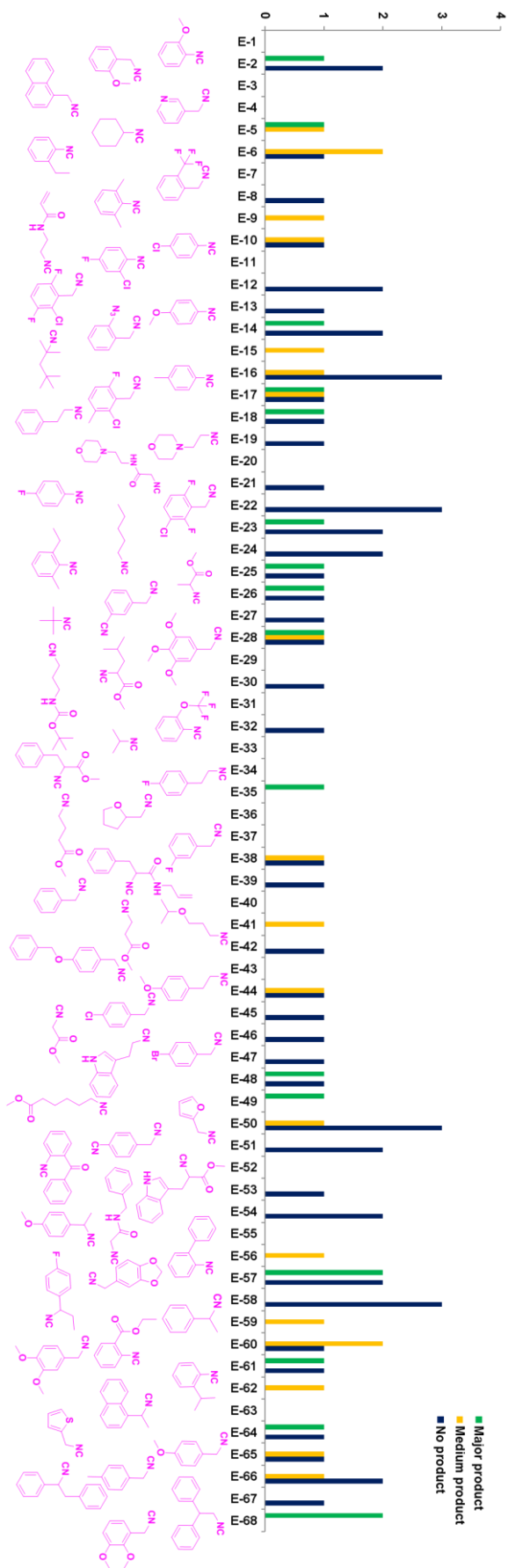
Scheme S2. Performance of formylphenyl boronic acids in destination plate I.



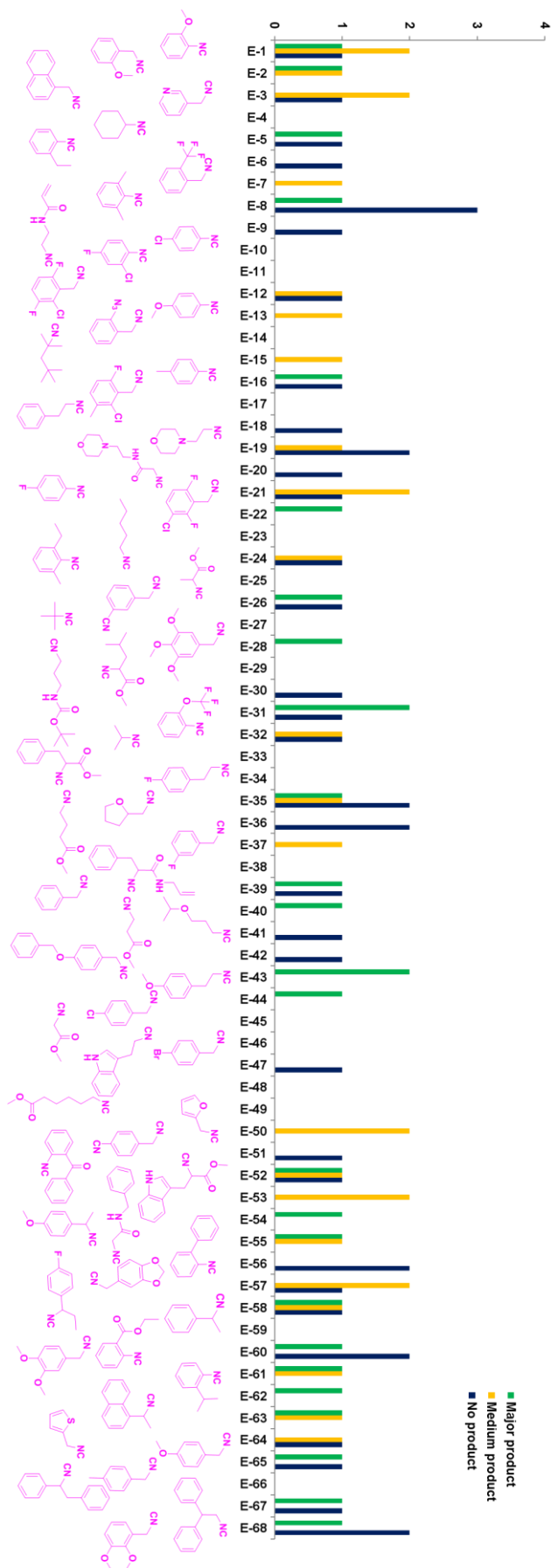
Scheme S3. Performance of isocyanides in GBB-3CR reaction in destination plate I.



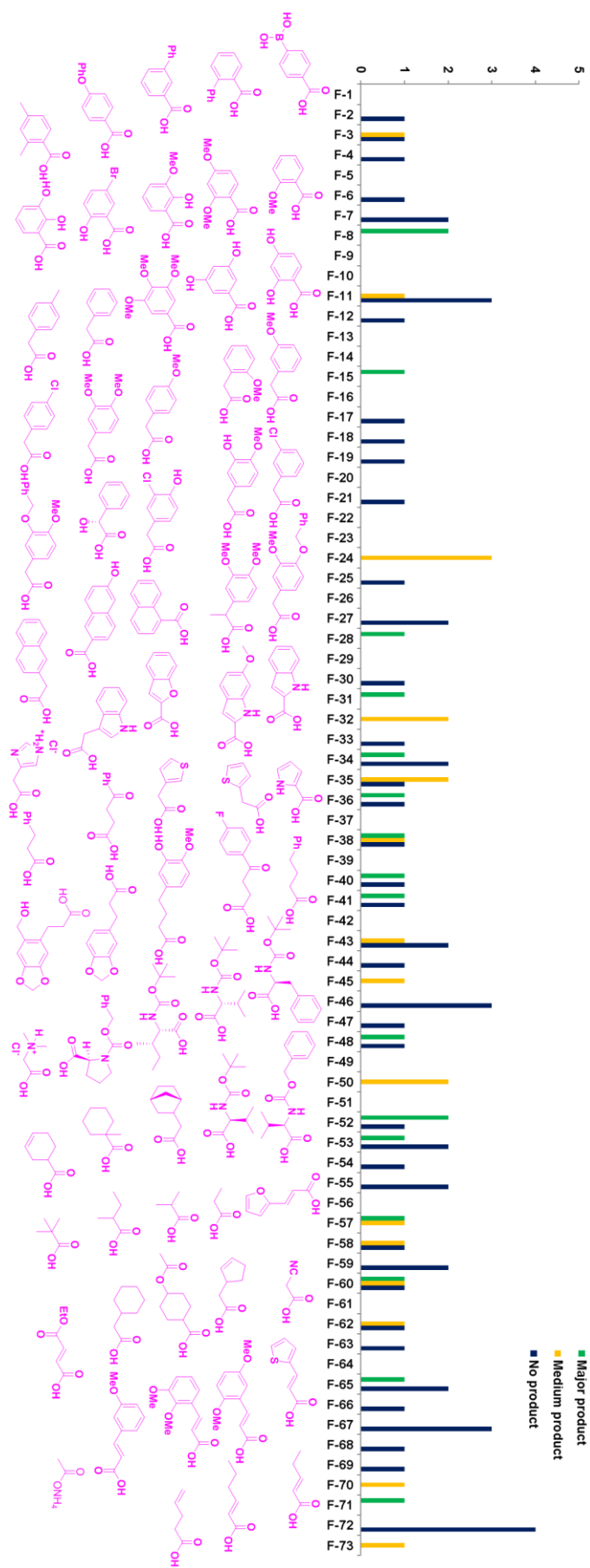
Scheme S4. Performance of isocyanides in Ugi-based macrocycles in destination plate I.



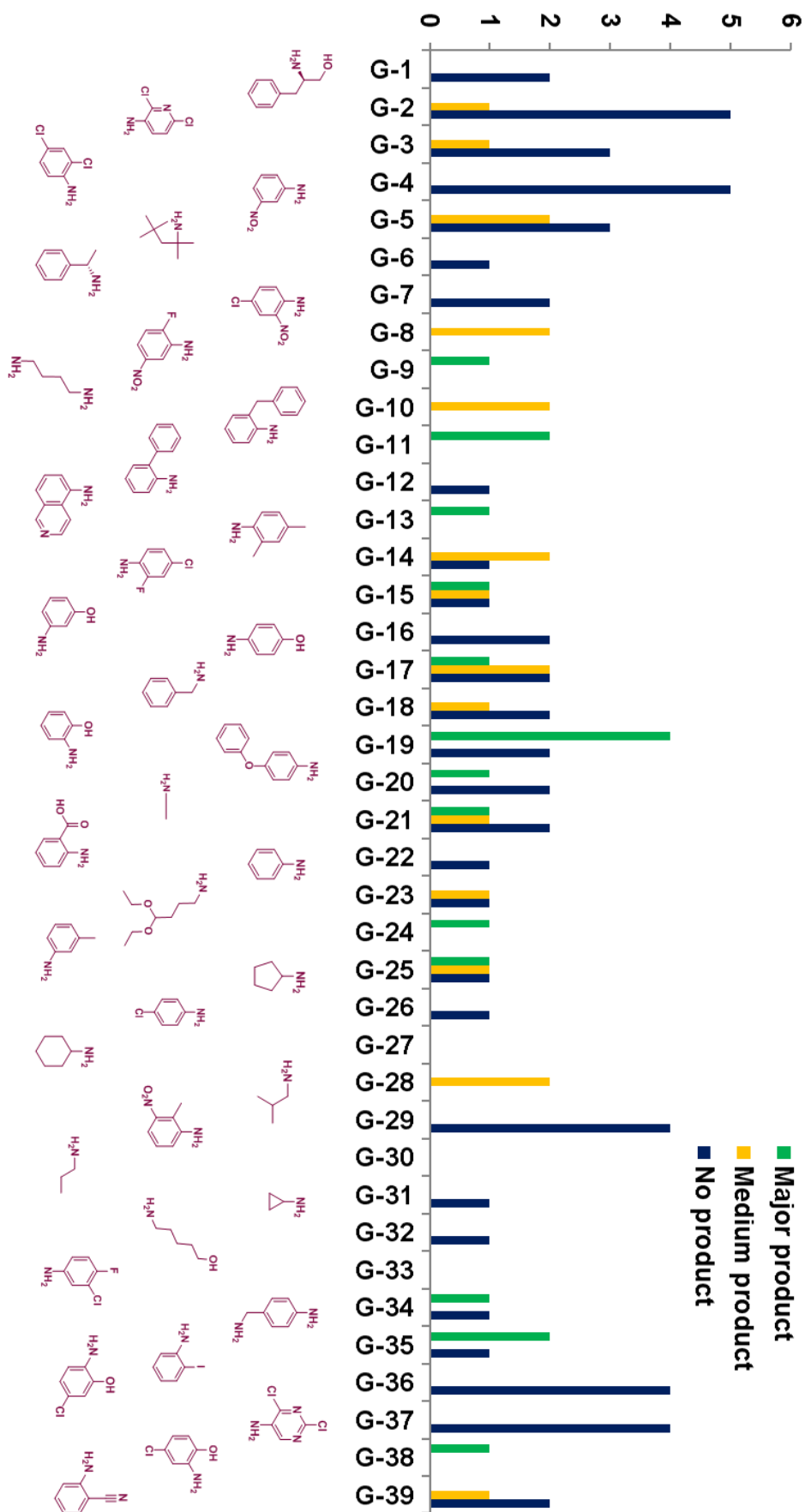
Scheme S5. Performance of isocyanides in U-4CR in destination plate I.



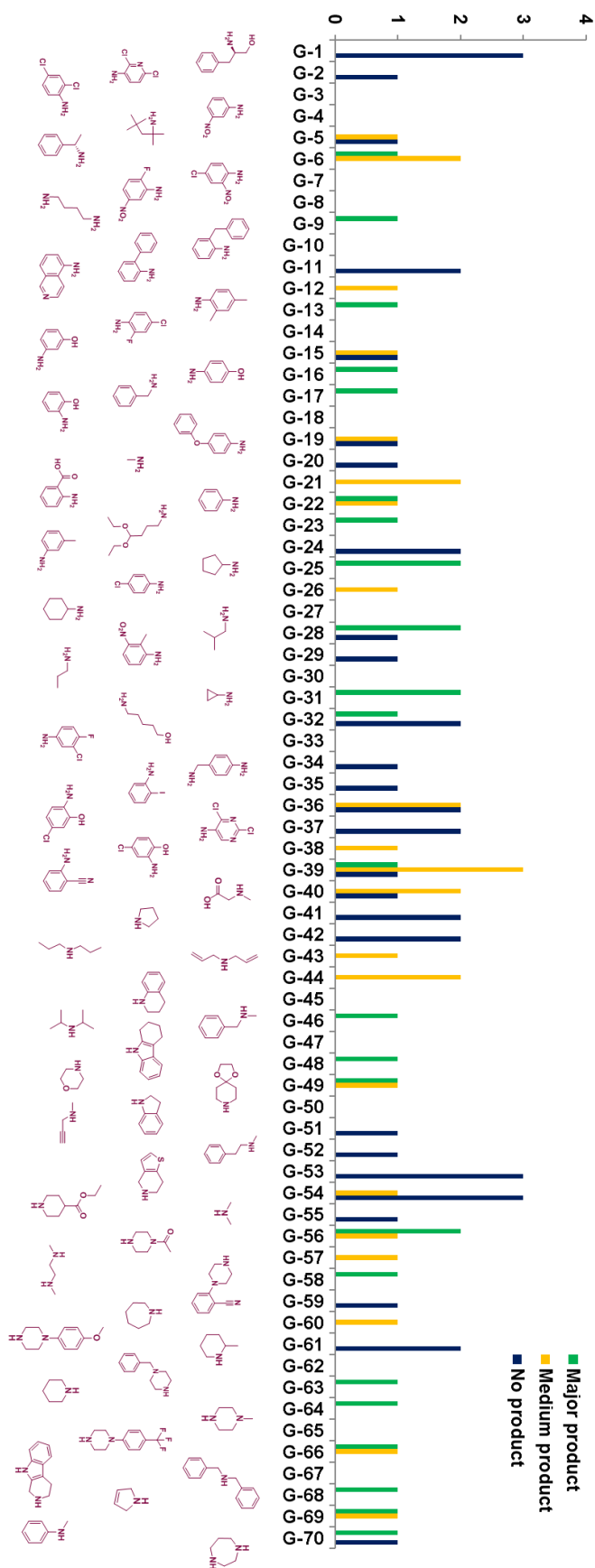
Scheme S6. Performance of isocyanides in UT-4CR in destination plate I.



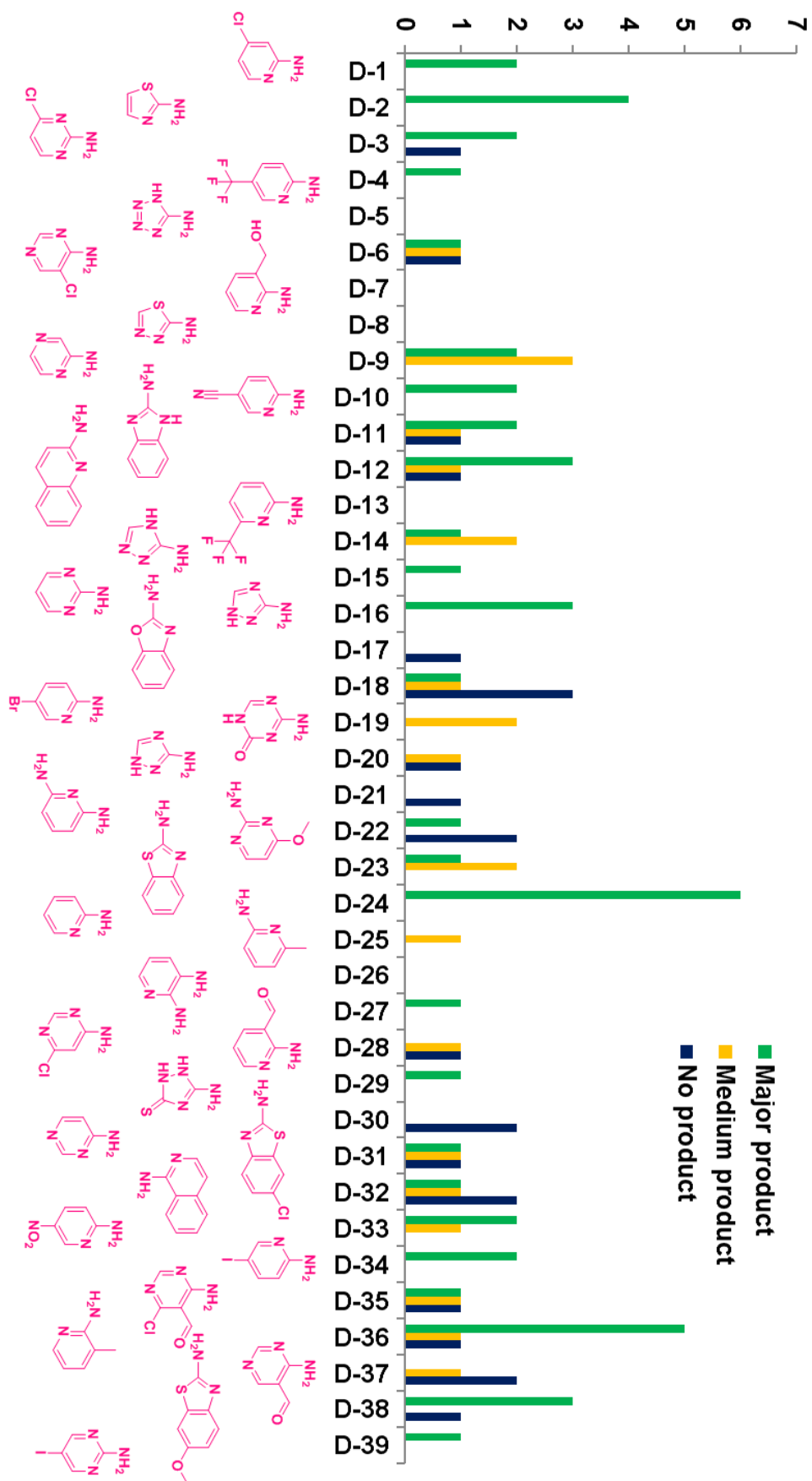
Scheme S7. Performance of carboxylic acids in U-4CR in destination plate I.



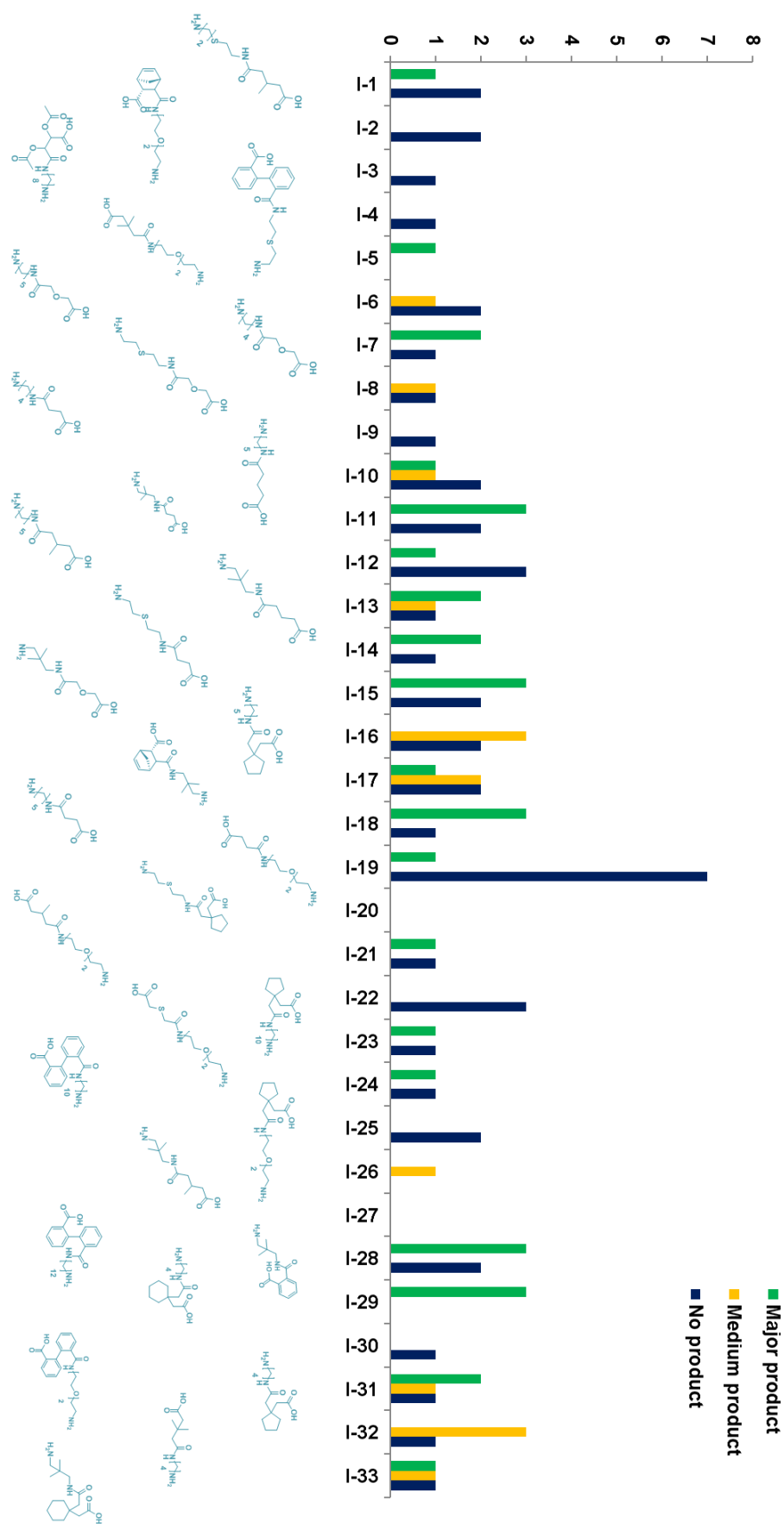
Scheme S8. Performance of amines in U-4CR in destination plate I.



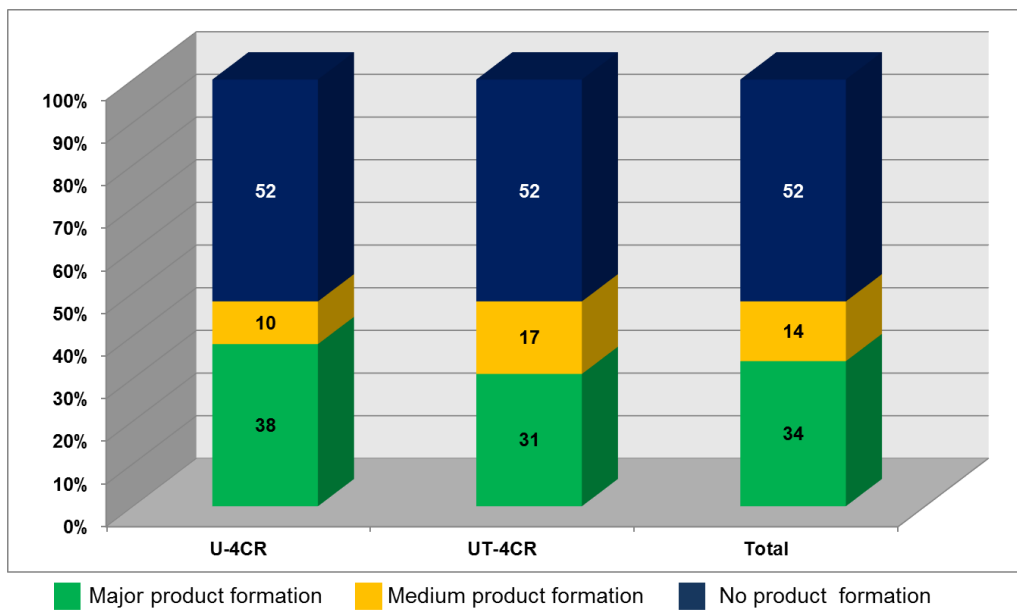
Scheme S9. Performance of amines in UT-4CR in destination plate I.



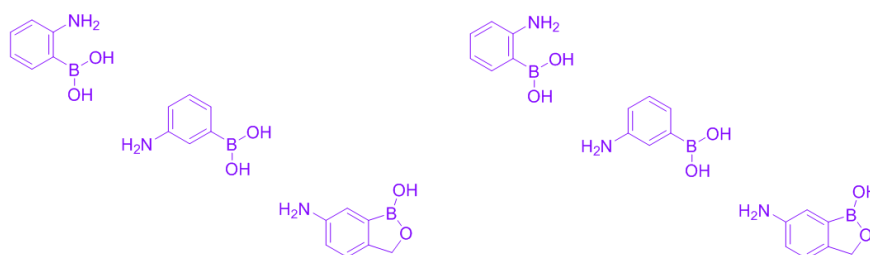
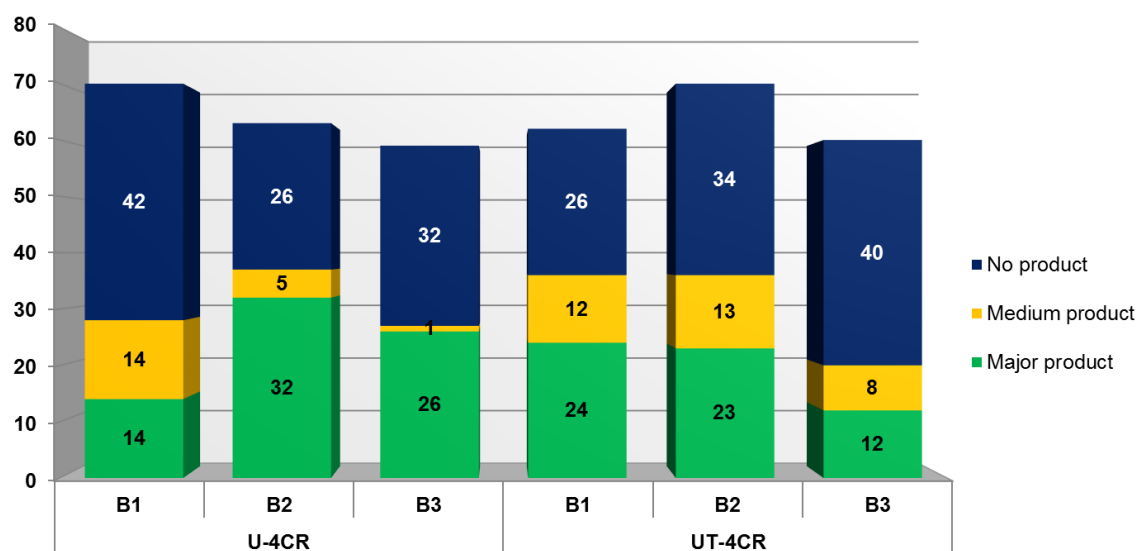
Scheme S10. Performance of amidines in GBB-3CR reaction in destination plate I.



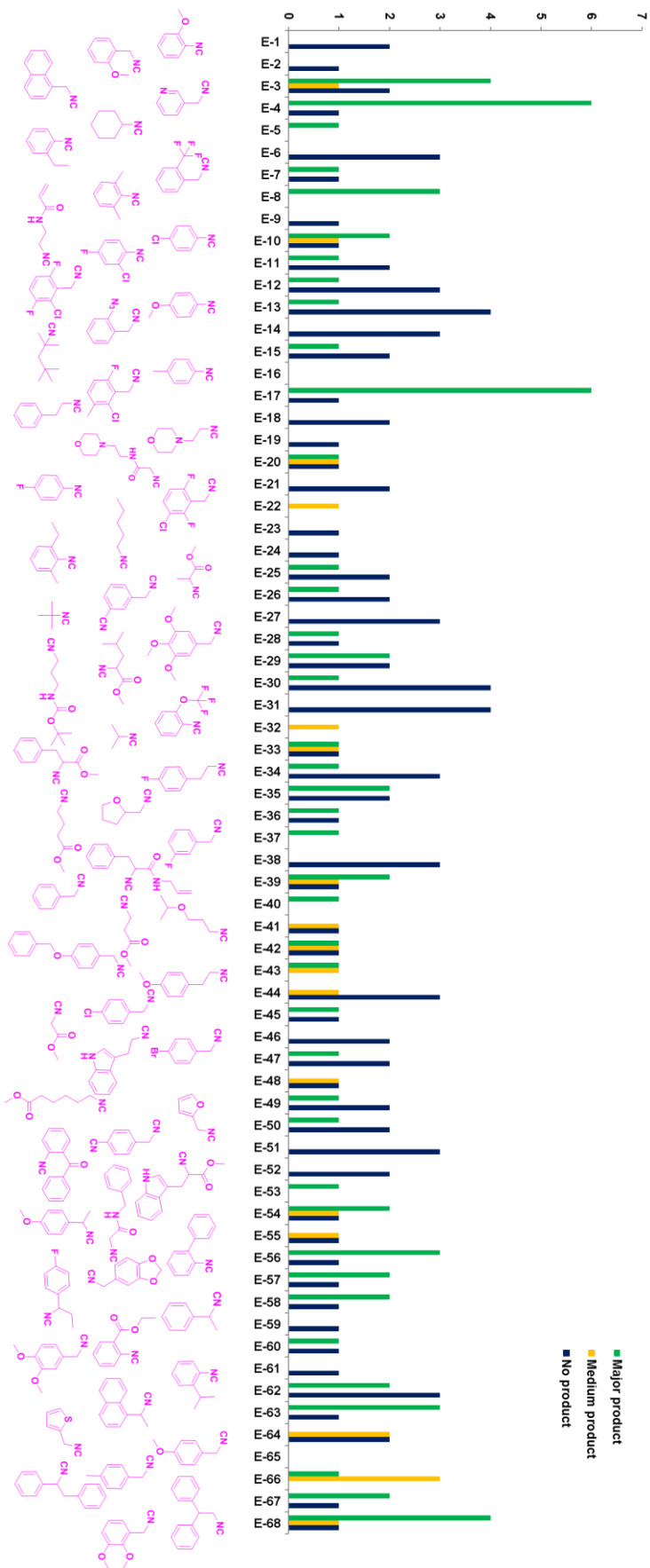
Scheme S11. Performance of α,ω -amino carboxylic acids in Ugi-based macrocycles in destination plate I.



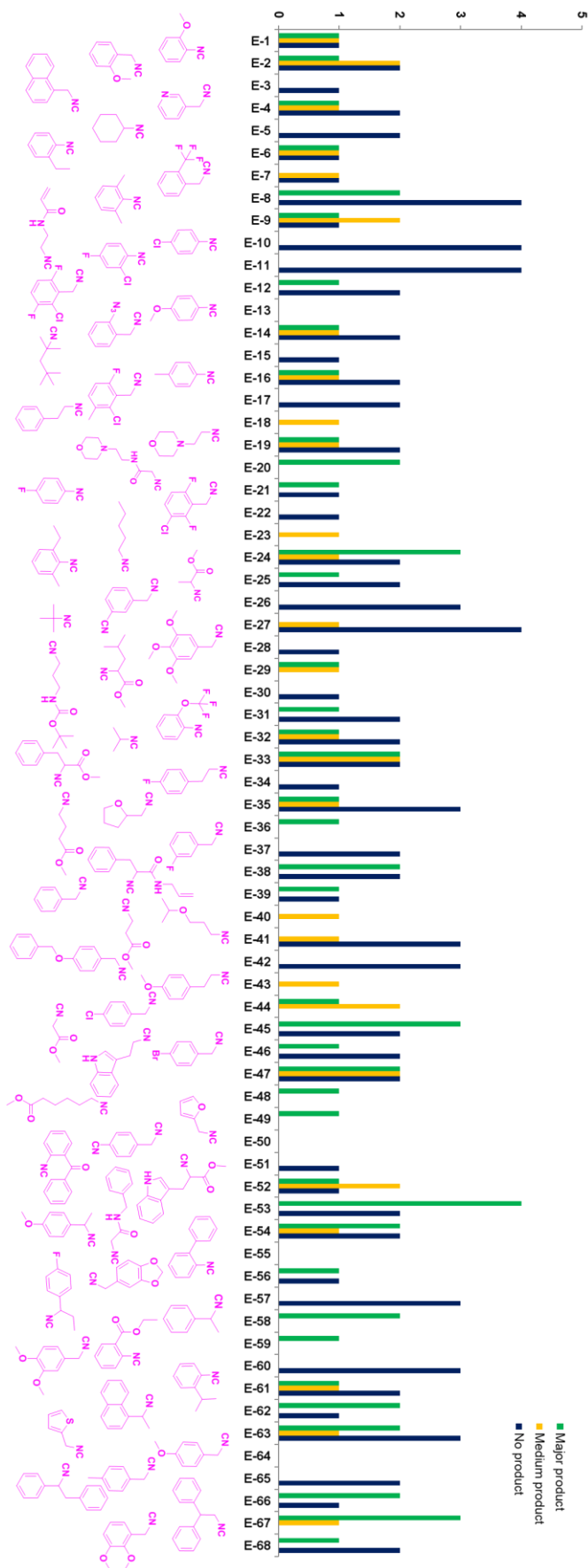
Scheme S12. Quality control results for destination plate II.



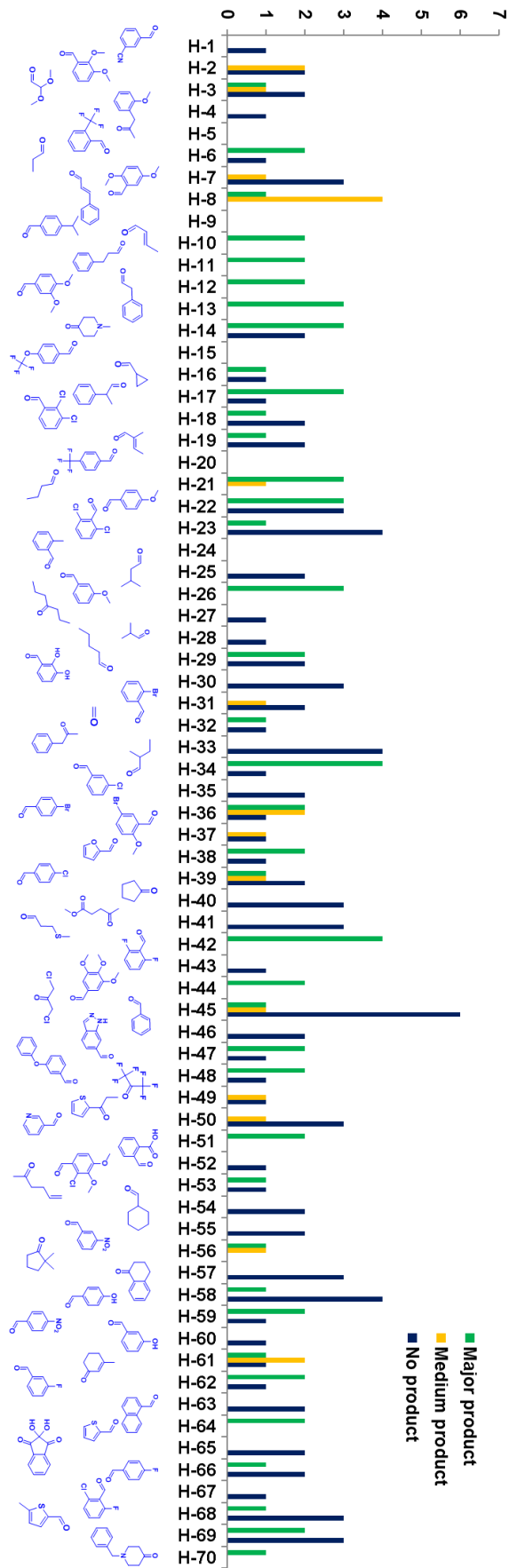
Scheme S13. Performance of aminophenyl boronic acids in destination plate II.



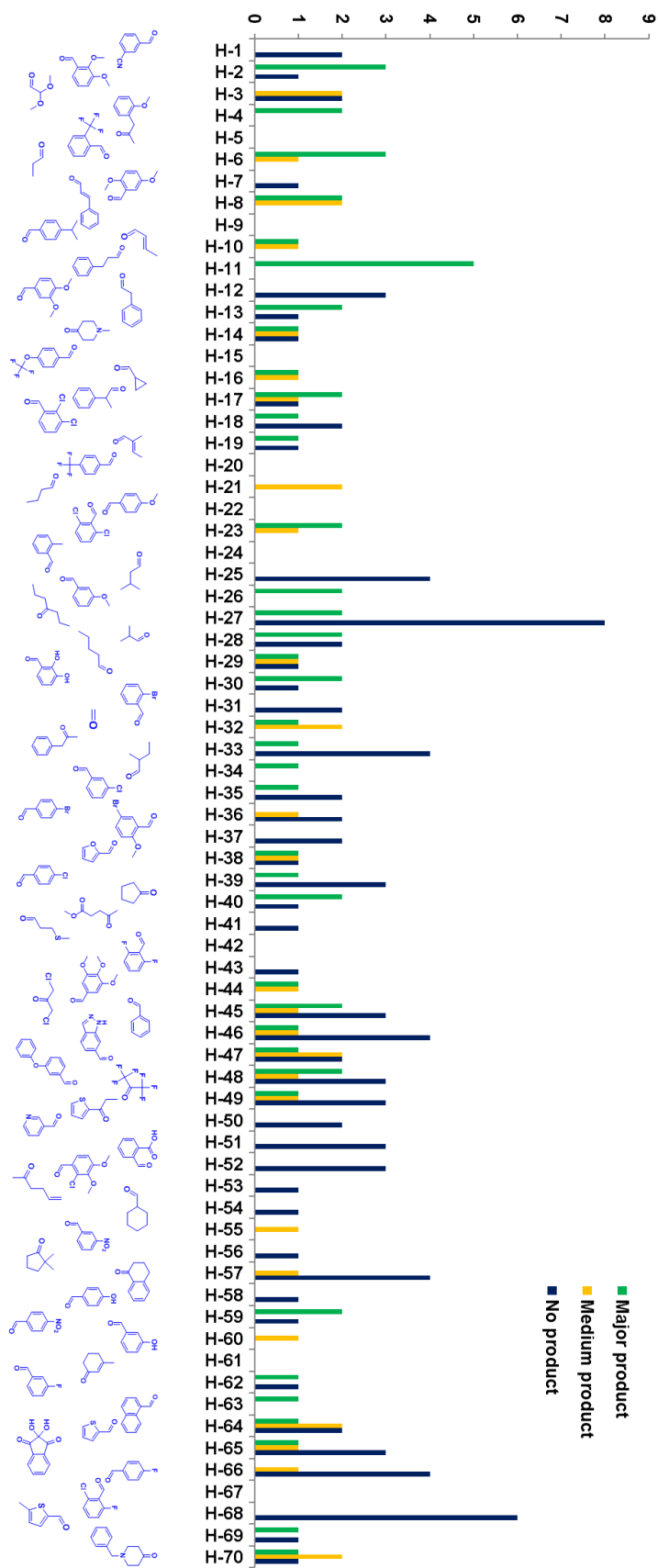
Scheme S14. Performance of isocyanides in U-4CR in destination plate II.



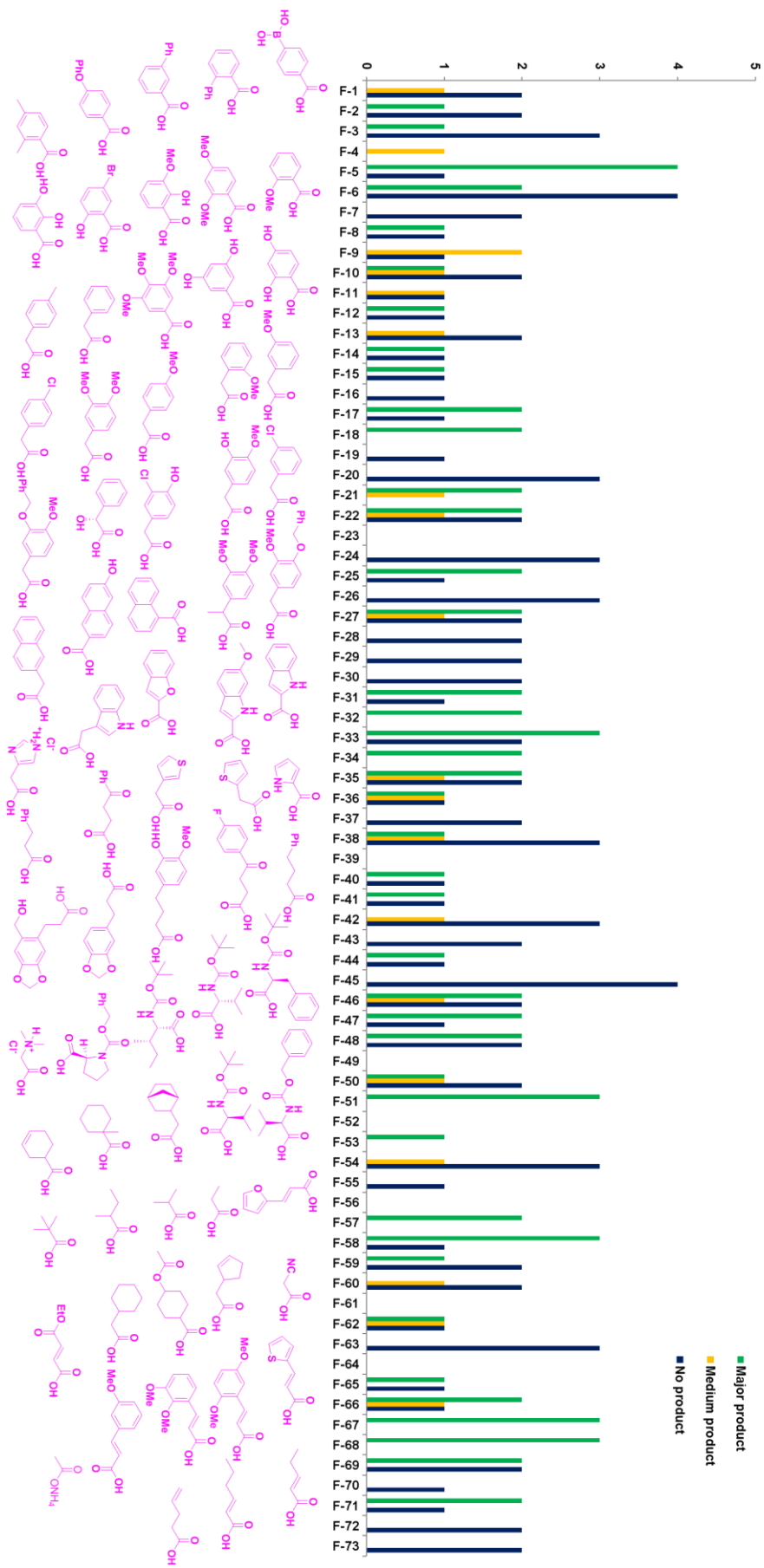
Scheme S15. Performance of isocyanides in UT-4CR in destination plate II.



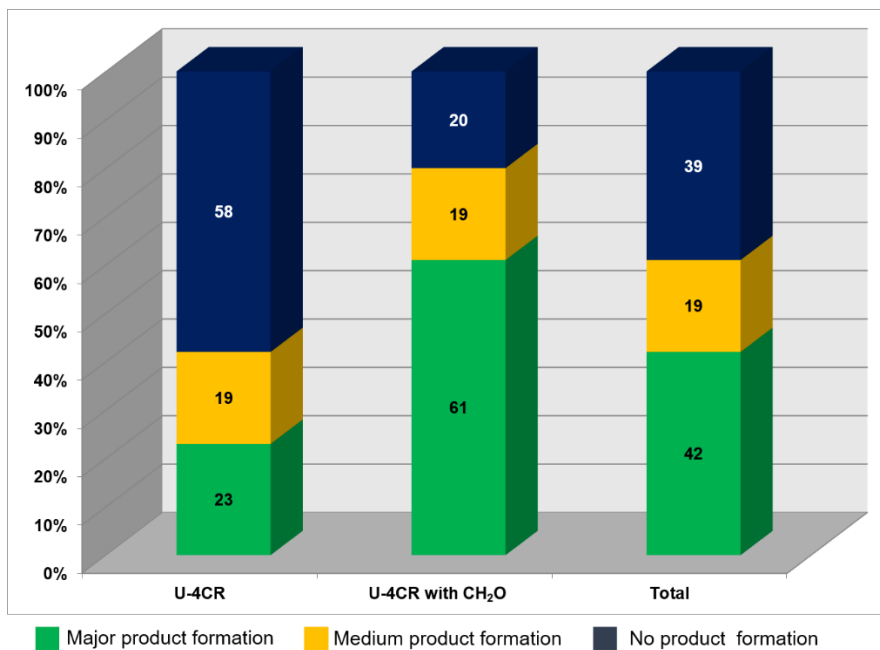
Scheme S16. Performance of oxo components in U-4CR in destination plate II.



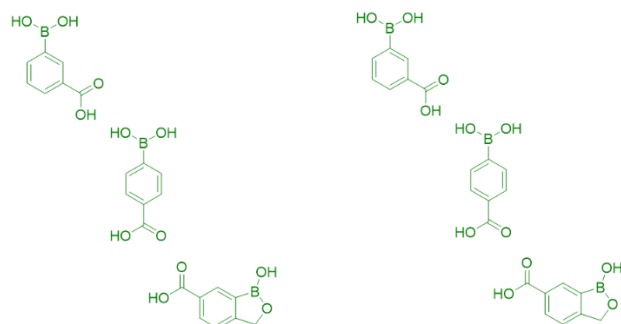
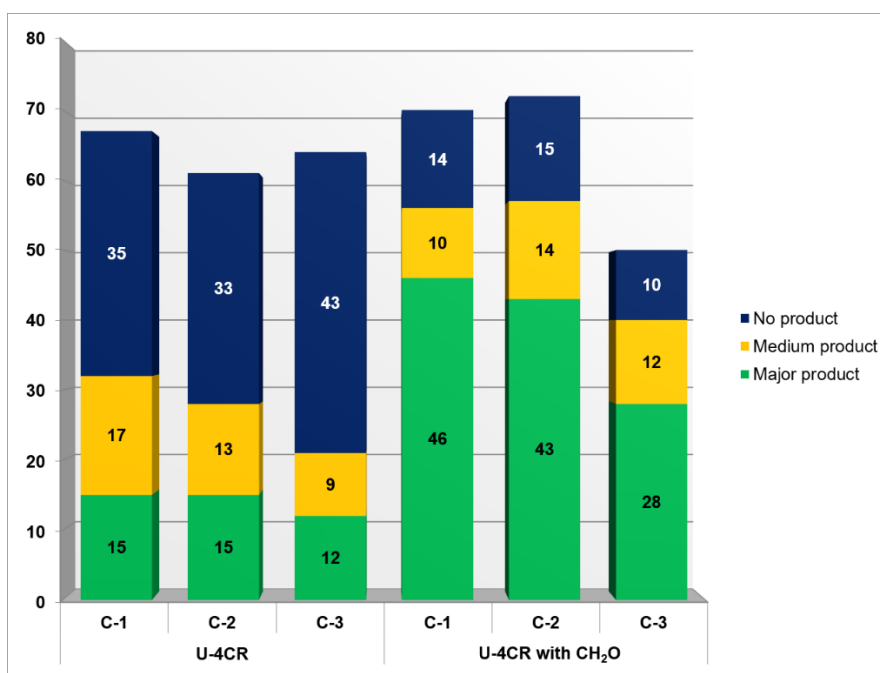
Scheme S17. Performance of oxo components in UT-4CR in destination plate II.



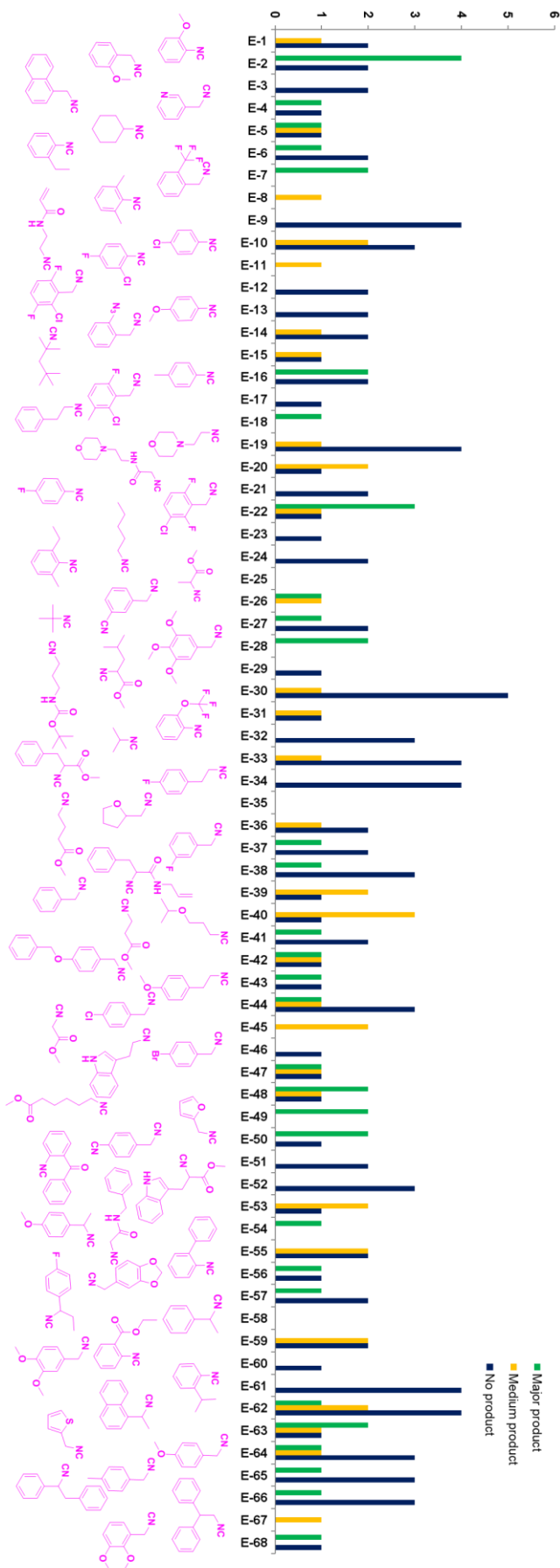
Scheme S18. Performance of carboxylic acids in U-4CR in destination plate II.



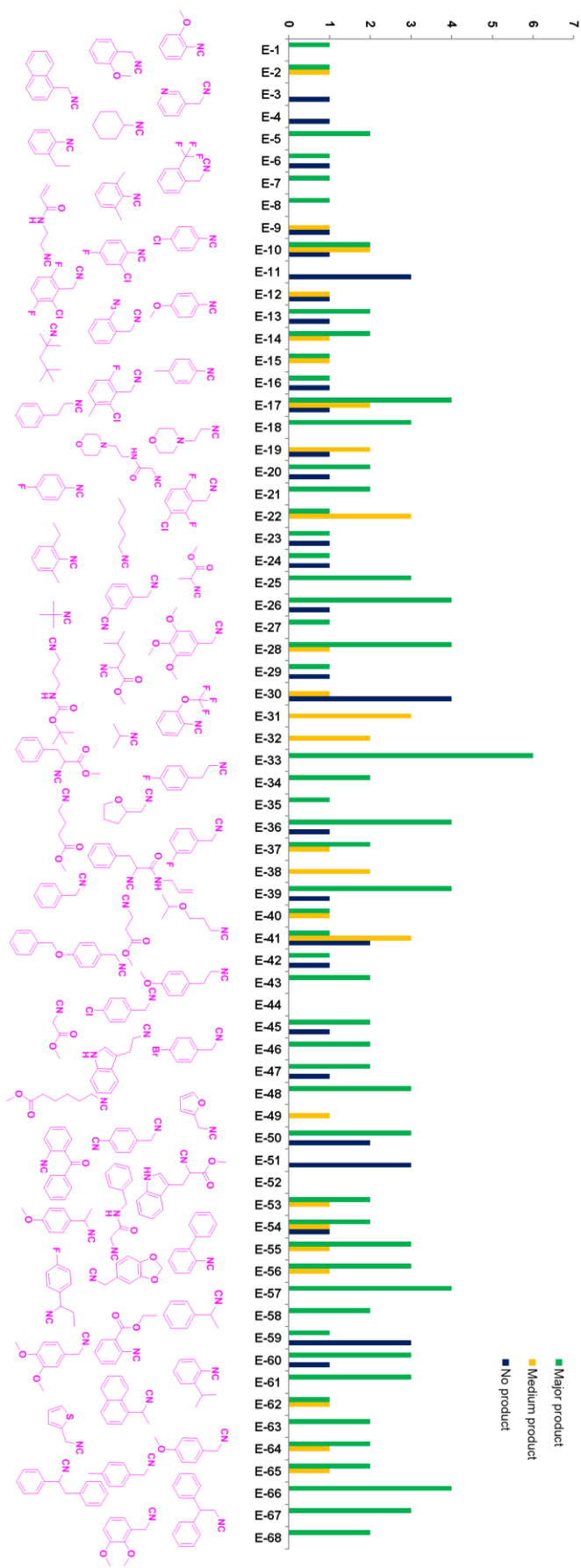
Scheme S19. Quality control results for destination plate III.



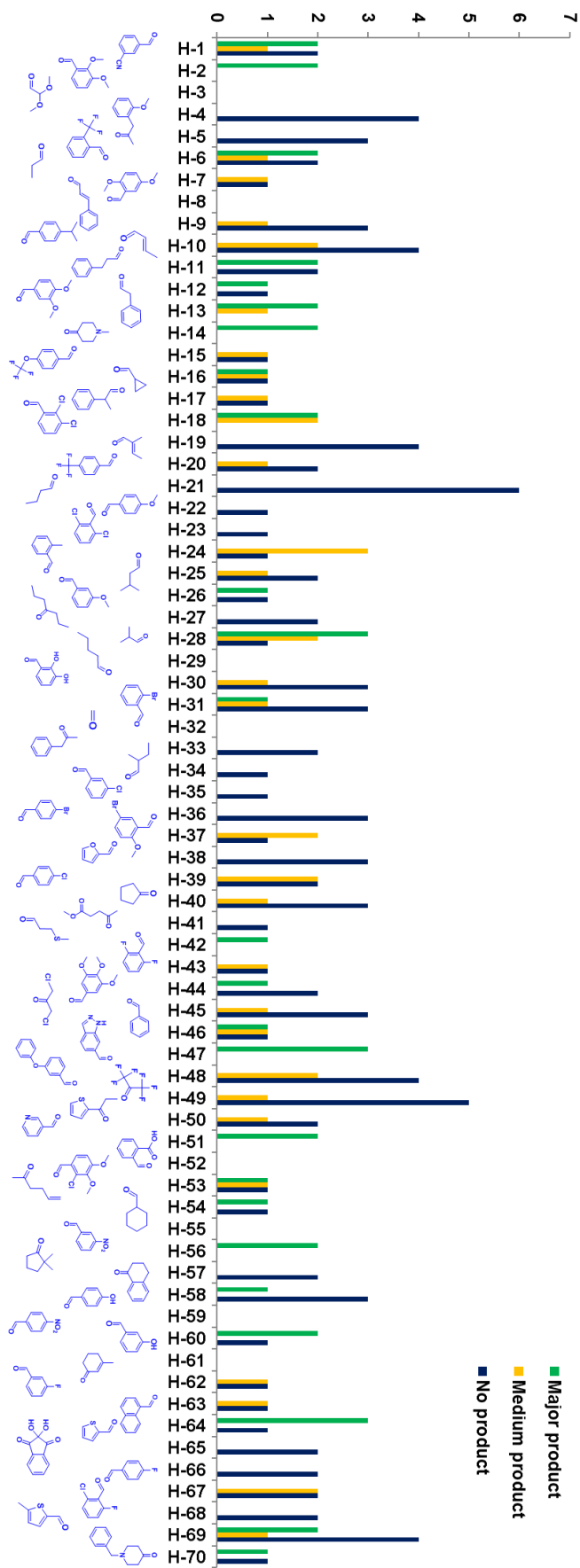
Scheme S20. Performance of carboxyphenyl boronic acids in destination plate III.



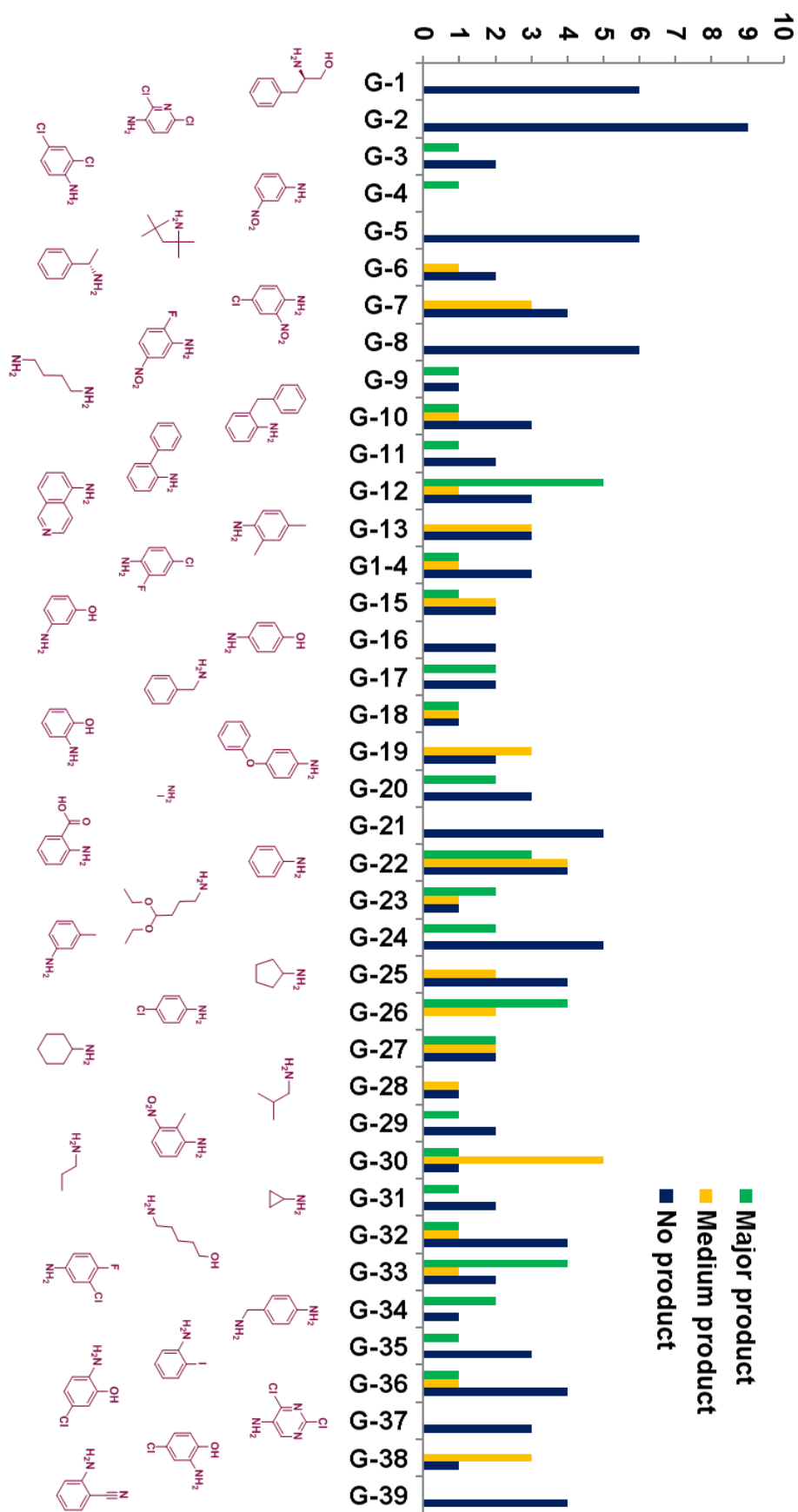
Scheme S21. Performance of isocyanides in U-4CR in destination plate III.



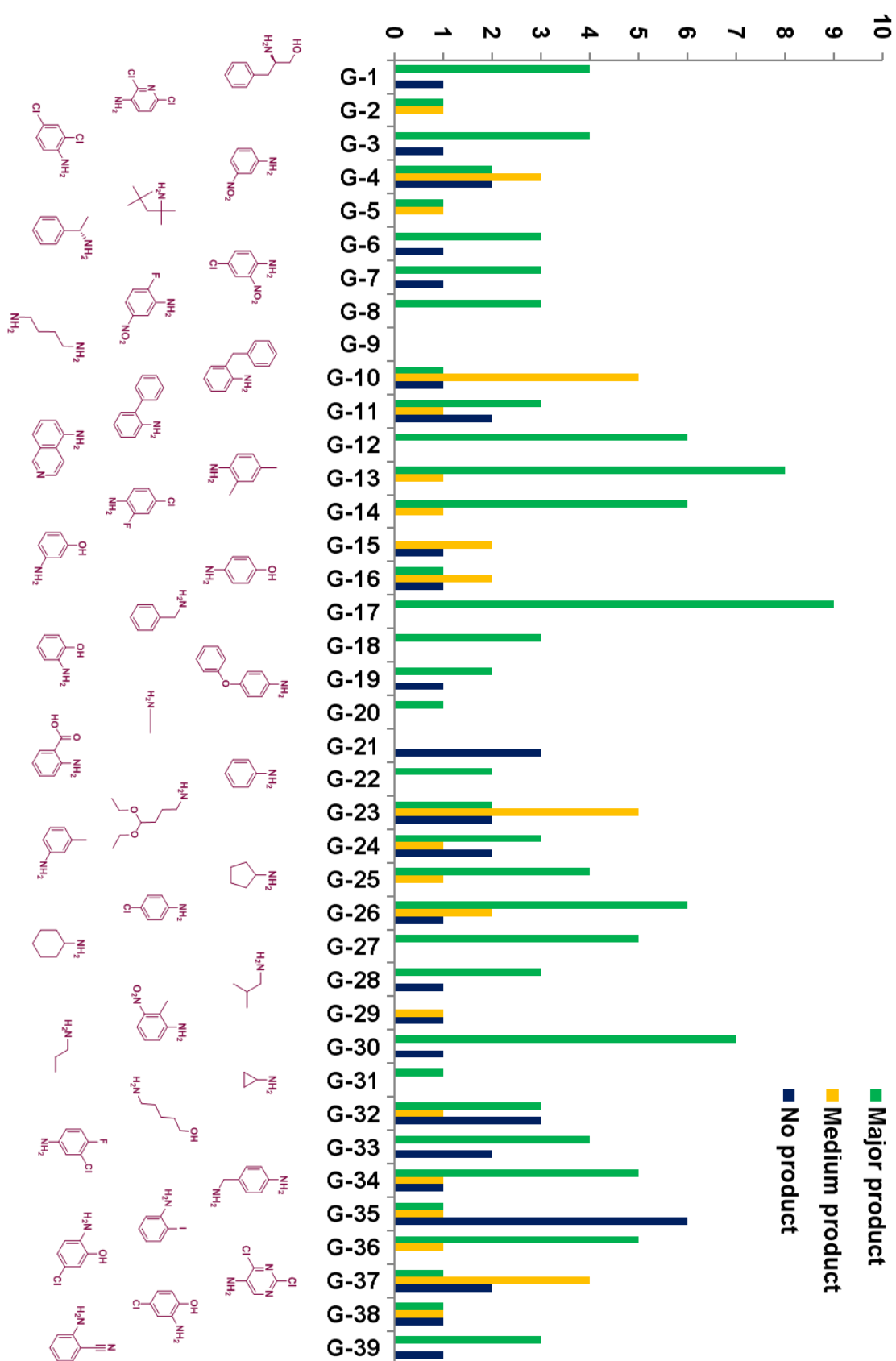
Scheme S22. Performance of isocyanides in U-4CR with CH₂O in destination plate III.



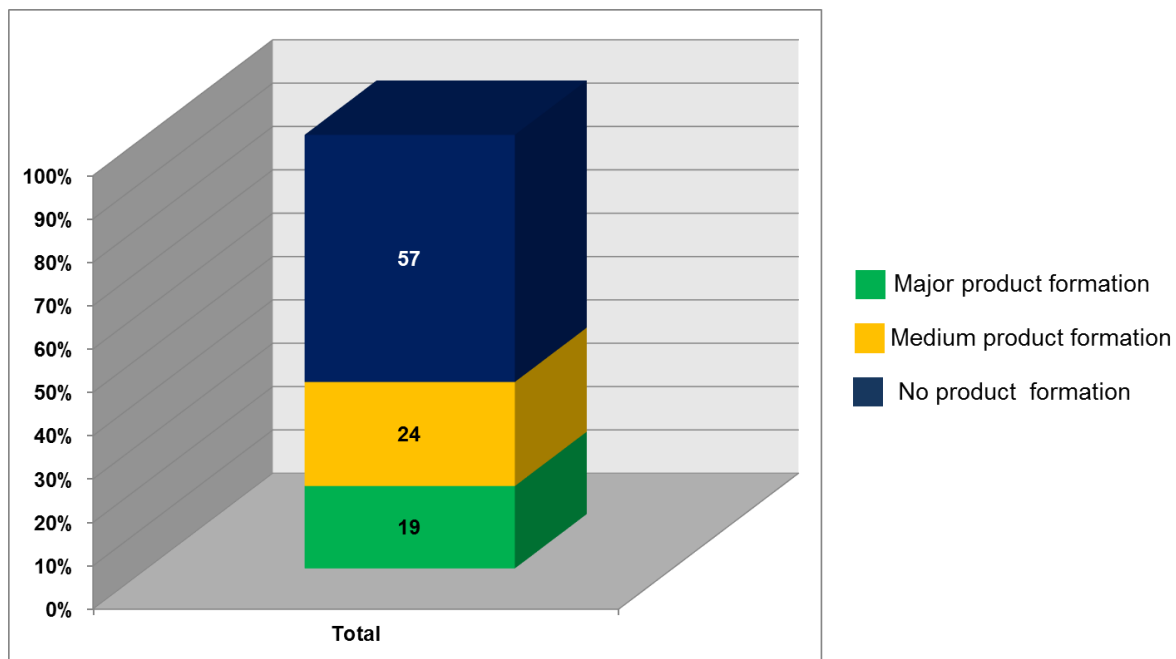
Scheme S23. Performance of oxo component in U-4CR in destination plate III.



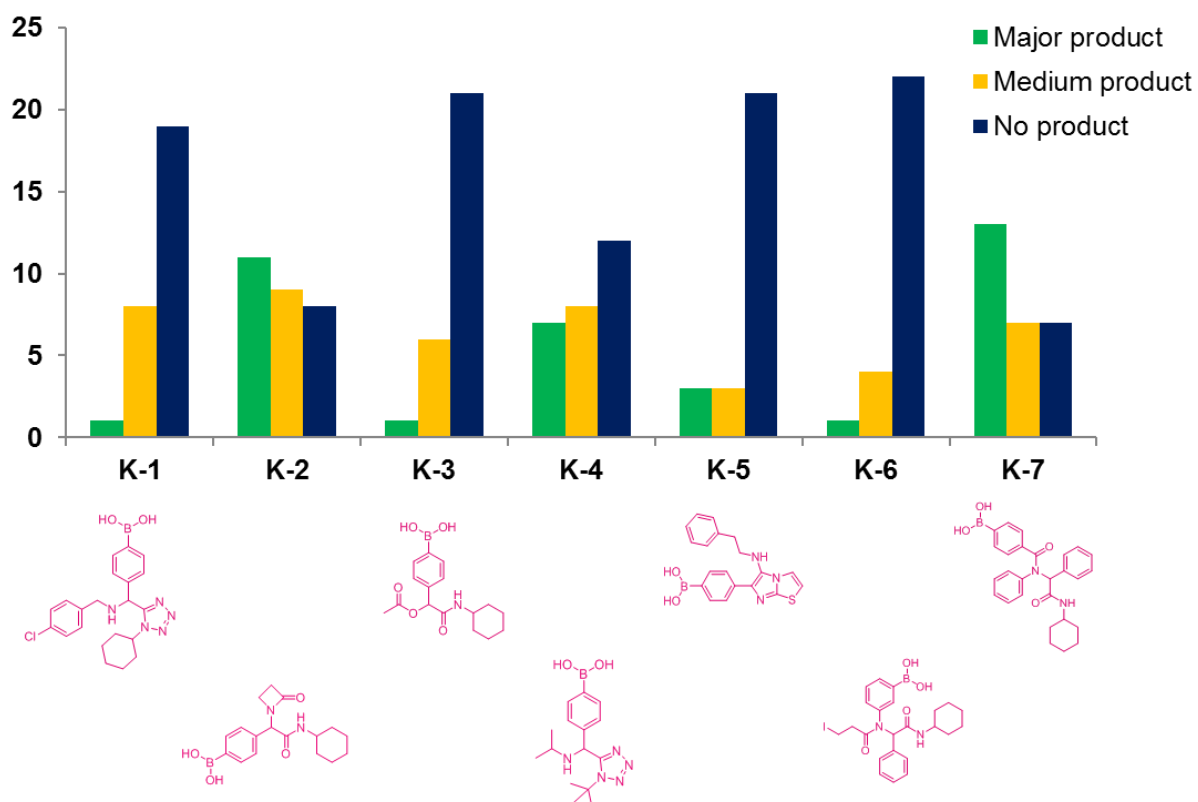
Scheme S24. Performance of amines in U-4CR in destination plate III.



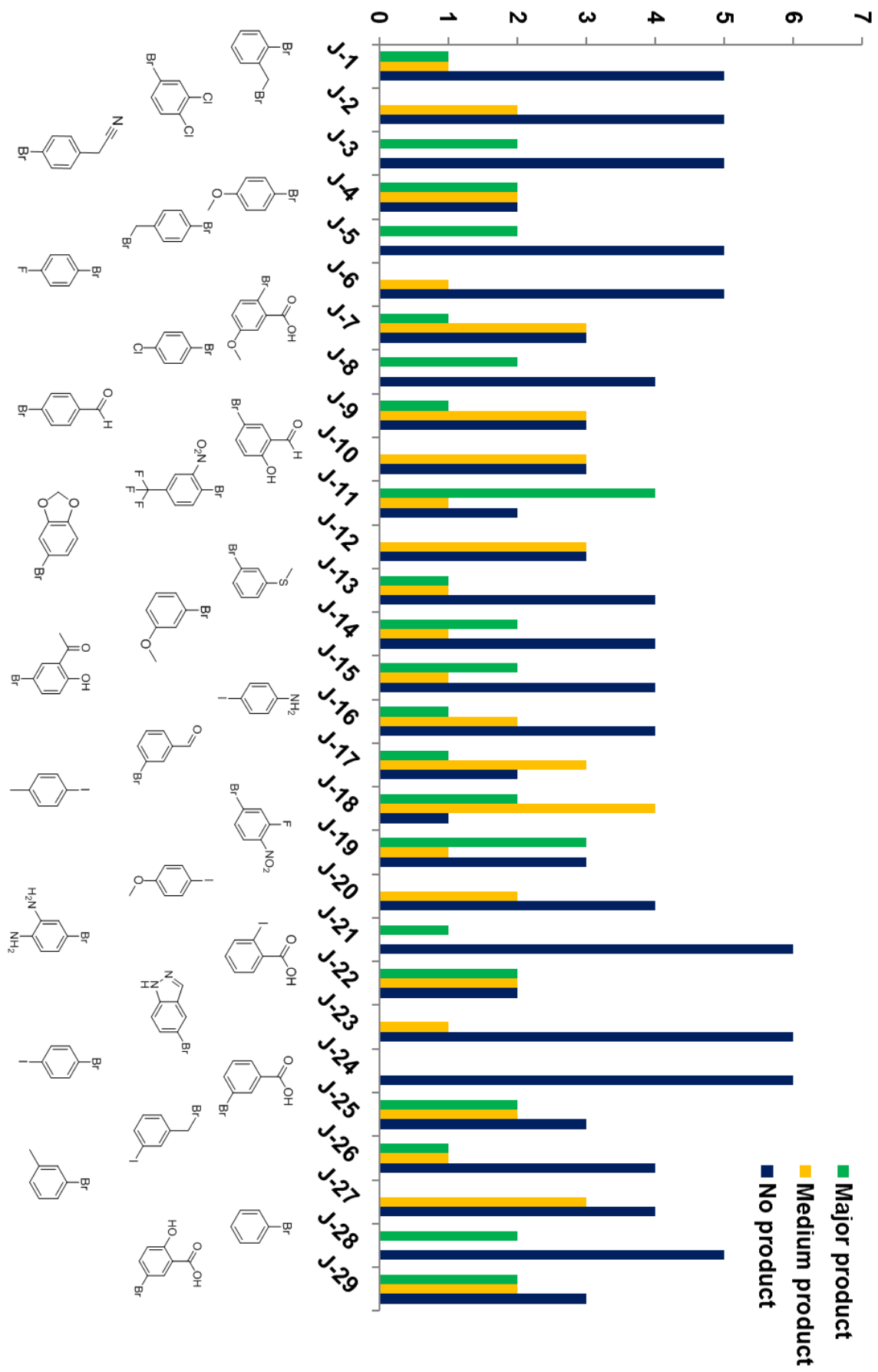
Scheme S25. Performance of amines in U-4CR with CH₂O in destination plate III.



Scheme S26. Quality control results for destination plate IV.



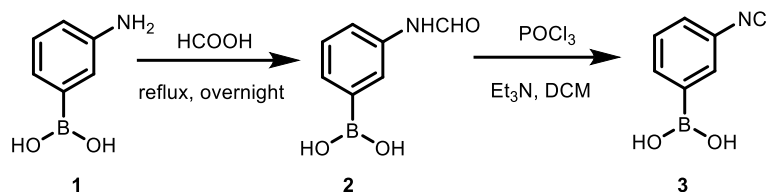
Scheme S27. Performance of MCR boronic acid building blocks in destination plate IV.



Scheme S28. Performance of aryl halides in destination plate IV.

6. Synthetic procedures and analytical data

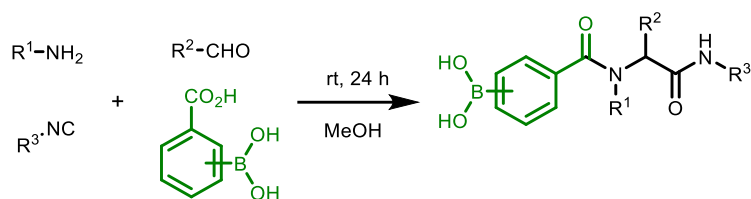
6.1. Procedure and analytical data of the formamide **2** and utilization of isocyanide **3**



A stirred solution of 3-aminophenylboronic acid (**1**) (5.0 mmol) in formic acid (15 mL) was refluxed overnight. Afterwards, the excess of formic acid was evaporated and the residue was washed by ether affording the targeted (3-formamidophenyl)boronic acid (**2**); White solid, 81% yield; mixture of *E* and *Z* isomers observed, major isomer reported; ¹H NMR (500 MHz, DMSO-*d*₆) δ 10.10 (d, *J* = 15.5 Hz, 1H), 8.26 (s, 1H), 8.07 (d, *J* = 24.0 Hz, 2H), 7.83 (s, 1H); ¹³C NMR (126 MHz, DMSO-*d*₆) δ 162.5, 159.6, 137.5, 129.5, 127.9, 125.1, 121.3. HRMS (ESI) *m/z* calculated for C₇H₈BNO₃ [M+H]⁺: 166.0670; found [M+H]⁺: 166.0669

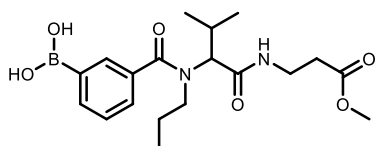
Next, the corresponding formamide (1.0 equiv) was dissolved in DCM and Et₃N (4.0 equiv) was added at 0 °C. After 10 min, POCl₃ (1.0 equiv) was added dropwise and the reaction mixture was stirred at rt for 4 h. Then, the mixture was added to a solution of NaHCO₃ in water with ice and extractions with DCM followed. The resulting oil was filtrated through silica and used as it was in the subsequent reactions.

6.2. Procedure and analytical data of U-4CR adducts 12-15



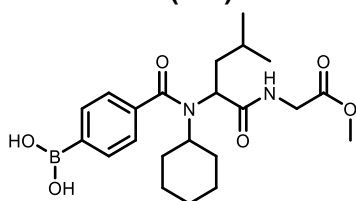
To a stirred solution of the corresponding 3- or 4- carboxyphenylboronic acid (1.0 mmol) in MeOH (1 mL), the amine (1.0 mmol), aldehyde (1.0 mmol) and isocyanide (1.0 mmol) were added. The reaction mixture was stirred at rt for 24 h. Afterwards, the solvent was evaporated and the crude product was purified with column chromatography on silica gel eluted with DCM-methanol (10:1) affording the targeted compounds.

(3-((1-((3-methoxy-3-oxopropyl)amino)-3-methyl-1-oxobutan-2-yl)(propyl)carbamoyl)phenyl)boronic acid (12a)



Pale white solid, 69% yield; $^1\text{H NMR}$ (500 MHz, methanol-*d*4) δ 7.91 (s, 1H), 7.85 (s, 1H), 7.42 (s, 2H), 3.71 (s, 3H), 3.65 (dd, $J = 13.5, 4.8$ Hz, 2H), 3.55 (s, 2H), 3.20 (t, $J = 7.6$ Hz, 2H), 2.59 (t, $J = 5.8$ Hz, 2H), 1.50 – 1.40 (m, 1H), 1.40 – 1.31 (m, 1H), 1.27 (s, 1H), 1.07 – 0.97 (m, 6H), 0.92–0.87 (m, 2H), 0.73 (br s, 1H), 0.57 (t, $J = 7.2$ Hz, 2H); $^{13}\text{C NMR}$ (126 MHz, CDCl_3) δ 174.2, 172.8, 171.6, 135.6, 132.2, 129.8, 128.6, 128.3, 127.8, 126.6, 68.3, 52.0, 51.2, 35.0, 34.0, 29.7, 26.5, 22.4, 20.0, 19.3, 11.6, 11.1. HRMS (ESI) m/z calculated for $\text{C}_{19}\text{H}_{29}\text{BN}_2\text{O}_6$ $[\text{M}+\text{H}]^+$: 393.21914; found $[\text{M}+\text{H}]^+$: 393.21902.

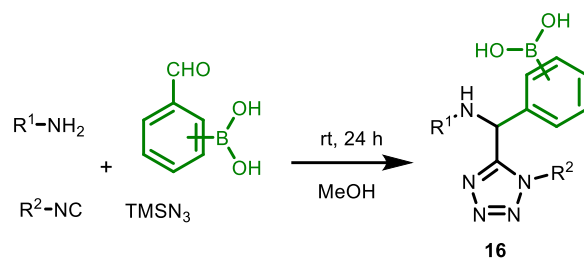
4-(cyclohexyl(1-((2-methoxy-2-oxoethyl)amino)-4-methyl-1-oxopentan-2-yl)carbamoyl)phenyl)boronic acid (12b)



White solid, 70% yield; $^1\text{H NMR}$ (500 MHz, methanol-*d*4) δ 7.80 (s, 2H), 7.38 (d, $J = 6.5$ Hz, 2H), 4.01–3.93 (m, 2H), 3.72 (s, 3H), 1.97 – 1.46 (m, 9H), 1.32 (d, $J = 4.5$ Hz, 1H), 1.00 (s, 7H), 0.66 (d, $J = 87.5$ Hz, 2H); $^{13}\text{C NMR}$ (126 MHz, methanol-*d*4) δ 175.2, 171.6, 139.6, 135.0, 126.0, 62.5, 60.0, 52.7, 52.6, 42.3, 42.0, 41.8, 40.6, 32.6, 26.8, 26.1, 22.9. HRMS (ESI) m/z calculated for $\text{C}_{22}\text{H}_{33}\text{BN}_2\text{O}_6$ $[\text{M}+\text{H}]^+$: 433.25044; found $[\text{M}+\text{H}]^+$: 433.25058.

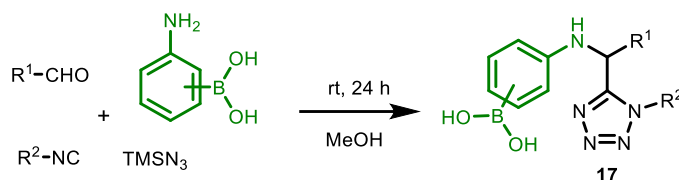
6.3. Procedure and analytical data of UT-4CR adducts 16-18

A.



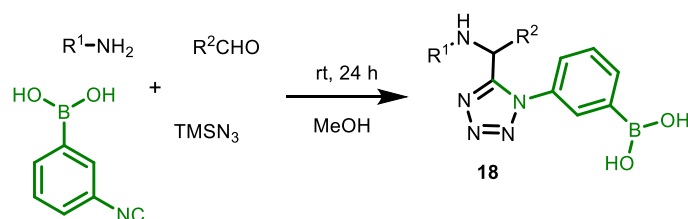
To a stirred solution of the corresponding 3- or 4-formylphenylboronic acid (1.0 mmol) in MeOH (1 mL), the amine (1.0 mmol), isocyanide (1.0 mmol) and TMS-azide (1.1 mmol) were added. The reaction mixture was stirred at rt for 24 h. Afterwards, the solvent was evaporated and the crude product was purified with column chromatography on silica gel eluted with DCM-methanol (10:1) affording the targeted compounds.

B.



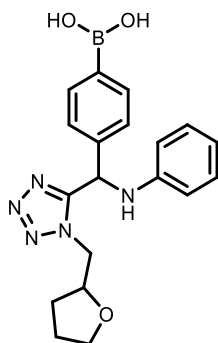
To a stirred solution of the corresponding 3- or 4-aminophenylboronic acid (1.0 mmol) in MeOH (1 mL), the aldehyde (1.0 mmol), isocyanide (1.0 mmol) and TMS-azide (1.1 mmol) were added. The reaction mixture was stirred at rt for 24 h. Afterwards, the solvent was evaporated and the crude product was purified with column chromatography on silica gel eluted with DCM-methanol (10:1) affording the targeted compounds.

C.



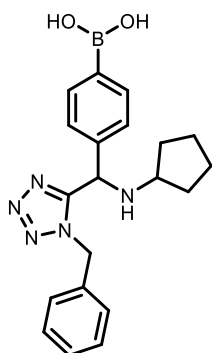
To a stirred solution of the the amine (1.0 mmol), aldehyde (1.0 mmol) in MeOH (1 mL), 3-isocyanophenyl boronic acid (1.0 mmol) and TMS-azide (1.1 mmol) were added. The reaction mixture was stirred at rt for 24 h. Afterwards, the solvent was evaporated and the crude product was purified with column chromatography on silica gel eluted with DCM-methanol (10:1) affording the targeted compounds.

(4-((phenylamino)(1-((tetrahydrofuran-2-yl)methyl)-1H-tetrazol-5-yl)methyl)phenyl)boronic acid (16a)



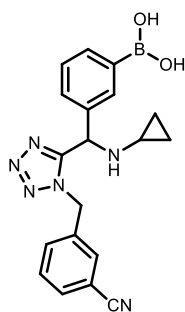
Yellow oil, 35% yield; ^1H NMR (500 MHz, CDCl_3) δ 8.16 (d, $J = 6.3$ Hz, 1H), 7.75 (dd, $J = 7.7, 2.9$ Hz, 1H), 7.52 (d, $J = 6.1$ Hz, 1H), 7.39 (t, $J = 6.8$ Hz, 1H), 7.16 (tt, $J = 7.8, 4.0$ Hz, 2H), 6.76 (dd, $J = 13.4, 6.5$ Hz, 1H), 6.68 (dt, $J = 15.1, 7.5$ Hz, 2H), 6.31 (t, $J = 34.8$ Hz, 1H), 5.30-5.24 (br s, 1H), 4.55 – 4.09 (m, 3H), 3.80 (dt, $J = 26.5, 7.0$ Hz, 2H), 2.15 – 2.06 (m, 1H), 1.89 (d, $J = 12.3$ Hz, 1H), 1.72 (br s, 4H); ^{13}C NMR (126 MHz, CDCl_3) δ 156.4, 146.1, 136.6, 134.9, 129.6, 127.1, 126.9, 119.1, 114.0, 68.9, 53.2, 51.3, 28.9, 28.6, 25.8. HRMS (ESI) m/z calculated for $\text{C}_{19}\text{H}_{22}\text{BN}_5\text{O}_3$ $[\text{M}+\text{H}]^+$: 380.18885; found $[\text{M}+\text{H}]^+$: 380.18875.

(4-((1-benzyl-1H-tetrazol-5-yl)(cyclopentylamino)methyl)phenyl)boronic acid (16b)



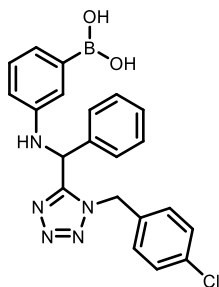
White solid, 55% yield; ^1H NMR (500 MHz, CDCl_3) δ 7.81 (d, $J = 8.1$ Hz, 2H), 7.33 – 7.31 (m, 2H), 7.21 (d, $J = 8.0$ Hz, 2H), 7.06 (dd, $J = 6.4, 3.0$ Hz, 2H), 6.43 (s, 2H), 5.50 (d, $J = 15.4$ Hz, 1H), 5.26 (d, $J = 15.4$ Hz, 1H), 5.07 (s, 1H), 2.82 (s, 1H), 2.59 (dt, $J = 3.7, 1.8$ Hz, 1H), 1.61-1.59 (m, 4H), 1.42 (br s, 2H), 1.30 – 1.13 (m, 3H); ^{13}C NMR (126 MHz, CDCl_3) δ 134.9, 129.0, 128.7, 127.4, 126.5, 56.9, 55.9, 50.9, 32.7, 32.6, 23.8. HRMS (ESI) m/z calculated for $\text{C}_{20}\text{H}_{24}\text{BN}_5\text{O}_2$ $[\text{M}+\text{H}]^+$: 378.20958; found $[\text{M}+\text{H}]^+$: 378.20999.

(3-((1-(3-cyanobenzyl)-1H-tetrazol-5-yl)(cyclopropylamino)methyl)phenyl)boronic acid (16c)



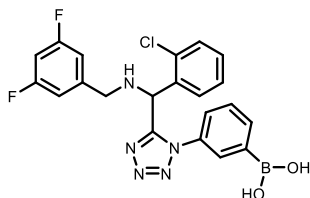
Yellow oil, 71% yield; ^1H NMR (500 MHz, methanol-*d*4) δ 7.64 – 7.51 (m, 3H), 7.37 – 7.31 (m, 2H), 7.27 – 7.19 (m, 2H), 7.13 (s, 1H), 5.67 (dd, J = 41.1, 15.9 Hz, 2H), 5.39 (s, 1H), 2.11 – 2.04 (m, 1H), 0.44 – 0.30 (m, 4H); ^{13}C NMR (126 MHz, methanol-*d*4) δ 194.7, 157.9, 137.8, 136.7, 135.0, 134.3, 133.1, 132.9, 132.0, 130.8, 130.6, 130.5, 129.3, 129.2, 119.0, 113.7, 58.6, 50.7, 29.8, 6.7. HRMS (ESI) m/z calculated for $\text{C}_{19}\text{H}_{19}\text{BN}_6\text{O}_2$ $[\text{M}+\text{H}]^+$: 375.17353; found $[\text{M}+\text{H}]^+$: 375.17355.

(3-(((1-(4-chlorobenzyl)-1H-tetrazol-5-yl)(phenyl)methyl)amino)phenyl)boronic acid (17a)



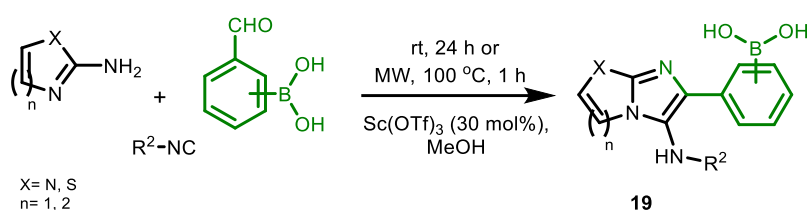
White solid, 45% yield; ^1H NMR (500 MHz, methanol-*d*4) δ 7.33 – 7.26 (m, 5H), 7.20 (d, J = 8.3 Hz, 2H), 7.06 (t, J = 7.7 Hz, 1H), 7.01 (d, J = 8.3 Hz, 2H), 6.89 (d, J = 7.2 Hz, 1H), 6.77 (s, 1H), 6.63 – 6.58 (m, 1H), 6.05 (s, 1H), 5.69 (d, J = 15.5 Hz, 1H), 5.60 (d, J = 15.5 Hz, 1H); ^{13}C NMR (126 MHz, methanol-*d*4) δ 148.1, 137.4, 129.1, 126.0, 124.4, 121.3, 120.5, 120.5, 120.1, 120.0, 119.9, 119.4, 115.1, 110.1, 106.8, 44.5, 42.0. HRMS (ESI) m/z calculated for $\text{C}_{21}\text{H}_{19}\text{BClN}_5\text{O}_2$ $[\text{M}+\text{H}]^+$: 420.13931; found $[\text{M}+\text{H}]^+$: 420.13931.

3-(5-((2-chlorophenyl)((3,5-difluorobenzyl)amino)methyl)-1H-tetrazol-1-yl)phenyl)boronic acid (18a)



Yellow oil, 87% yield; ^1H NMR (500 MHz, methanol-*d*4) δ 7.81 (s, 1H), 7.61 (d, J = 7.5 Hz, 1H), 7.49 (s, 1H), 7.44 (t, J = 7.2 Hz, 2H), 7.37 – 7.27 (m, 4H), 7.27 – 7.16 (m, 2H), 7.09 (d, J = 6.1 Hz, 1H), 7.06 – 7.00 (m, 1H), 6.84 – 6.72 (m, 4H), 5.50 (s, 1H), 3.73 (d, J = 3.1 Hz, 2H); ^{13}C NMR (126 MHz, methanol-*d*4) δ 165.4, 165.3, 163.5, 163.4, 157.3, 145.1, 136.9, 136.4, 134.8, 134.0, 131.4, 131.0, 130.8, 130.6, 129.7, 128.7, 112.9, 112.8, 112.7, 112.2, 112.1, 112.0, 112.0, 103.4, 103.2, 103.0, 53.4, 51.3, 43.6. HRMS (ESI) m/z calculated for $\text{C}_{21}\text{H}_{17}\text{BClF}_2\text{N}_5\text{O}_2$ $[\text{M}+\text{H}]^+$: 456.12047; found $[\text{M}+\text{H}]^+$: 456.12088.

6.4. Procedure and analytical data of GBB-3CR adducts 19

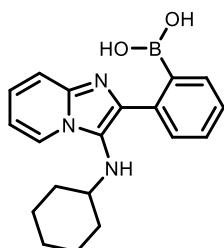


To a stirred solution of the corresponding formylphenylboronic acid (1.0 mmol) in MeOH (1 mL), the 2-aminopyridine or 2-aminothiazole (1.0 mmol), isocyanide (1.0 mmol) and catalytical amount of Sc(OTf)₃ (30 mol%) were added. The reaction mixture was stirred at rt for 24 h. Afterwards, the solvent was evaporated and the crude product was purified with column chromatography on silica gel eluted with DCM-methanol (10:1) affording the targeted compounds.

Alternatively

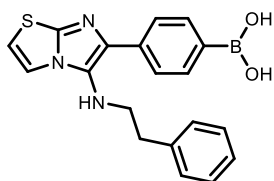
In a microwave vial, the corresponding formylphenylboronic acid (1.0 mmol), the 2-aminopyridine or 2-aminothiazole (1.0 mmol), isocyanide (1.0 mmol) and Sc(OTf)₃ (30 mol%) were dissolved in MeOH (1 mL). The reaction mixture was irradiated at 100 °C for 1 h.

(2-(3-(cyclohexylamino)imidazo[1,2-a]pyridin-2-yl)phenyl)boronic acid (19a)



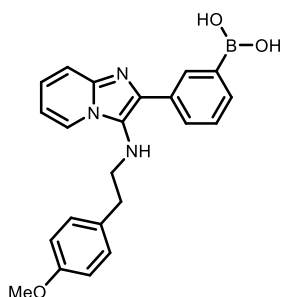
White solid, 69% yield; ¹H NMR (500 MHz, methanol-*d*₄) δ 8.49 (d, *J* = 6.4 Hz, 1H), 7.82 (d, *J* = 7.1 Hz, 1H), 7.76 (d, *J* = 8.9 Hz, 1H), 7.62 (br s, 1H), 7.54 (d, *J* = 6.6 Hz, 1H), 7.37 – 7.28 (m, 2H), 7.21 (br s, 1H), 3.08 (br s, 1H), 1.96 (d, *J* = 11.0 Hz, 2H), 1.76 (br s, 2H), 1.64 (br s, 1H), 1.42 (br s, 2H), 1.34 – 1.21 (m, 3H); ¹³C NMR (126 MHz, methanol-*d*₄) δ 128.9, 128.1, 126.4, 121.9, 121.3, 119.8, 119.1, 116.7, 114.0, 113.7, 106.0, 104.5, 48.9, 25.7, 17.4, 16.6. HRMS (ESI) *m/z* calculated for C₁₉H₂₂BN₃O₂ [M+H]⁺: 336.18051; found [M+H]⁺: 336.18187.

(4-(5-(phenethylamino)imidazo[2,1-b]thiazol-6-yl)phenyl)boronic acid (19b)



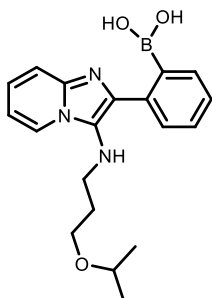
Yellow oil, 75% yield; ^1H NMR (500 MHz, methanol-*d*4) δ 7.76 (t, J = 7.1 Hz, 2H), 7.60 (d, J = 8.0 Hz, 2H), 7.38 (d, J = 4.5 Hz, 1H), 7.27 – 7.22 (m, 3H), 7.19-7.15 (m, 2H), 7.02 (d, J = 4.4 Hz, 1H), 3.31 – 3.26 (m, 2H), 2.82 (t, J = 6.8 Hz, 2H); ^{13}C NMR (126 MHz, methanol-*d*4) δ 131.5, 125.6, 125.4, 120.5, 120.0, 117.8, 116.9, 109.3, 104.0, 41.5, 28.3. HRMS (ESI) m/z calculated for $\text{C}_{19}\text{H}_{18}\text{BN}_3\text{O}_2\text{S}$ $[\text{M}+\text{H}]^+$: 364.12855; found $[\text{M}+\text{H}]^+$: 364.12866.

(3-(3-((4-methoxyphenethyl)amino)imidazo[1,2-a]pyridin-2-yl)phenyl)boronic acid (19c)



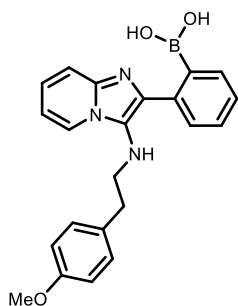
Yellow oil, 79% yield; ^1H NMR (500 MHz, methanol-*d*4) δ 8.17 (d, J = 6.8 Hz, 1H), 8.06 (s, 1H), 7.73 (d, J = 7.8 Hz, 2H), 7.63 (dd, J = 8.2, 7.7 Hz, 1H), 7.56 (d, J = 8.9 Hz, 1H), 7.40 (t, J = 7.6 Hz, 1H), 7.16 (t, J = 6.8 Hz, 1H), 6.84 (d, J = 8.5 Hz, 2H), 6.58 (d, J = 8.5 Hz, 2H), 3.60 (s, 3H), 3.16 (t, J = 6.8 Hz, 2H), 2.63 (t, J = 6.8 Hz, 2H); ^{13}C NMR (126 MHz, methanol-*d*4) δ 150.0, 129.1, 126.2, 124.3, 123.1, 122.8, 121.0, 120.4, 119.9, 119.4, 119.0, 118.4, 116.2, 107.4, 105.1, 103.8, 46.1, 40.4, 40.0, 27.3. HRMS (ESI) m/z calculated for $\text{C}_{22}\text{H}_{22}\text{BN}_3\text{O}_3$ $[\text{M}+\text{H}]^+$: 388.1827; found $[\text{M}+\text{H}]^+$: 388.18301.

(2-(3-((3-isopropoxypropyl)amino)imidazo[1,2-a]pyridin-2-yl)phenyl)boronic acid (19d)



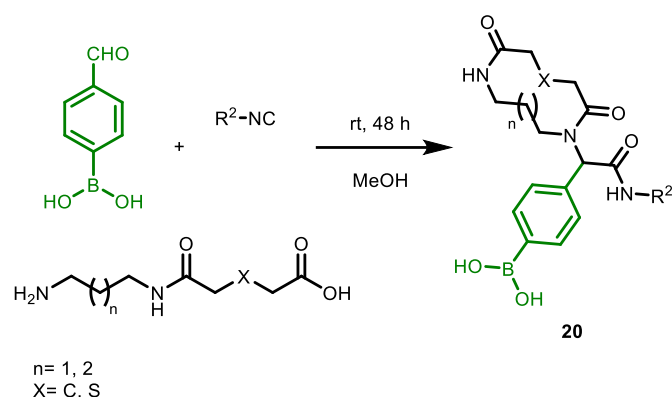
Yellow oil, 67% yield; ^1H NMR (500 MHz, methanol-*d*4) δ 8.50 (d, J = 6.8 Hz, 1H), 7.85 – 7.80 (m, 1H), 7.77 – 7.73 (m, 1H), 7.62 (q, J = 7.8 Hz, 1H), 7.55 – 7.50 (m, 1H), 7.35 – 7.28 (m, 2H), 7.20 (q, J = 6.7 Hz, 1H), 3.62 – 3.59 (m, 2H), 3.28 – 3.23 (m, 2H), 1.92 – 1.86 (m, 2H), 1.14 – 1.09 (m, 6H); ^{13}C NMR (126 MHz, methanol-*d*4) δ 129.8, 128.9, 128.8, 128.6, 126.6, 124.5, 124.5, 117.2, 113.6, 73.1, 67.3, 46.3, 31.9, 22.6. HRMS (ESI) m/z calculated for $\text{C}_{19}\text{H}_{24}\text{BN}_3\text{O}_3$ $[\text{M}+\text{H}]^+$: 354.19835; found $[\text{M}+\text{H}]^+$: 354.1987.

(2-(3-((4-methoxyphenethyl)amino)imidazo[1,2-a]pyridin-2-yl)phenyl)boronic acid (19e)



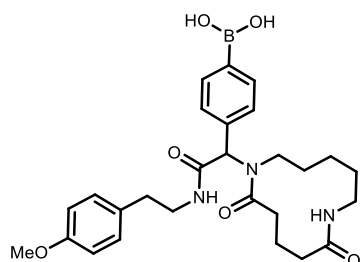
Yellow oil, 66% yield; ^1H NMR (500 MHz, methanol-*d*₄) δ 8.15 (dd, $J = 6.9, 0.8$ Hz, 1H), 7.71 – 7.66 (m, 1H), 7.57 – 7.52 (m, 2H), 7.49-7.48 (m, 1H), 7.25-7.24 (m, 2H), 7.10 (d, $J = 8.4$ Hz, 2H), 7.06 (t, $J = 6.9$ Hz, 1H), 6.77 (d, $J = 8.5$ Hz, 2H), 3.72 (s, 3H), 3.40 (t, $J = 6.9$ Hz, 2H), 2.86 (t, $J = 6.9$ Hz, 2H); ^{13}C NMR (126 MHz, methanol-*d*₄) δ 159.8, 138.2, 135.7, 132.7, 131.4, 130.9, 130.7, 129.3, 128.6, 125.9, 124.5, 123.1, 115.3, 114.9, 113.9, 55.7, 50.9, 37.2. HRMS (ESI) m/z calculated for $\text{C}_{22}\text{H}_{22}\text{BN}_3\text{O}_3$ $[\text{M}+\text{H}]^+$: 388.17542; found $[\text{M}+\text{H}]^+$: 388.17520.

6.5. Procedure and analytical data of Ugi-based macrocycles **20**



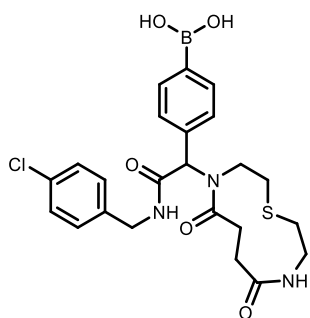
To a stirred solution of the 4-formylphenylboronic acid (1.0 mmol) in MeOH (10 mL), the corresponding aminoacid (1.0 mmol) was added (**51**). After stirring for 30 min, more MeOH (90 mL) was added and then the isocyanide (1.0 mmol). The reaction mixture was stirred at rt for 48 h. Afterwards, the solvent was evaporated and the crude product was purified with column chromatography on silica gel eluted with DCM-methanol (10:1) affording the targeted compounds.

(4-(1-(2,6-dioxo-1,7-diazacyclododecan-1-yl)-2-((4-methoxyphenethyl)amino)-2-oxoethyl)phenyl)boronic acid (**20a**)



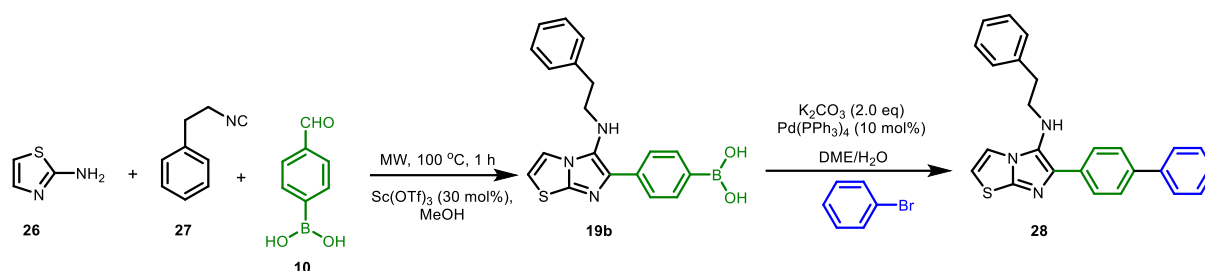
Yellow oil, 31% yield; $^1\text{H NMR}$ (500 MHz, methanol-*d*4) δ 7.73 (s, 1H), 7.23 (d, $J = 7.3$ Hz, 2H), 7.06 (d, $J = 7.9$ Hz, 2H), 6.79 (d, $J = 8.3$ Hz, 2H), 5.82 (s, 1H), 4.28 (d, $J = 10.9$ Hz, 1H), 4.08 (dd, $J = 19.0, 12.0$ Hz, 1H), 3.90 (d, $J = 13.2$ Hz, 1H), 3.77 (s, 3H), 3.43 (dd, $J = 23.5, 6.8$ Hz, 2H), 2.72 (s, 2H), 1.62 – 1.35 (m, 3H), 1.35 – 1.22 (m, 1H), 1.22 – 1.12 (m, 1H), 1.04 (s, 1H); $^{13}\text{C NMR}$ (126 MHz, methanol-*d*4) δ 171.9, 171.5, 159.8, 135.5, 132.6, 132.5, 131.0, 130.2, 115.1, 72.9, 69.5, 64.5, 55.8, 47.5, 42.3, 41.2, 35.5, 30.4, 27.1, 25.2. HRMS (ESI) m/z calculated for $\text{C}_{27}\text{H}_{36}\text{BN}_3\text{O}_6$ $[\text{M}+2\text{H}]^+$: 512.26972; found $[\text{M}+2\text{H}]^+$: 512.25641.

(4-(2-((4-chlorobenzyl)amino)-1-(5,8-dioxo-1-thia-4,9-diazacycloundecan-4-yl)-2-oxoethyl)phenyl)boronic acid (20b)



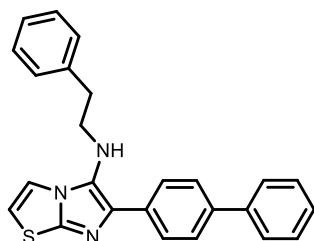
Yellow oil, 30% yield; ^1H NMR (500 MHz, methanol- d_4) δ 7.76 (br s, 1H), 7.46 – 7.36 (m, 1H), 7.27-7.21 (m, 2H), 7.17 (t, J = 9.5 Hz, 1H), 5.48 (s, 1H), 4.35 (s, 1H), 3.73 – 3.59 (m, 1H), 3.59 – 3.49 (m, 1H), 3.43 – 3.36 (m, 1H), 3.33 – 3.30 (m, 1H), 3.15 – 2.92 (m, 1H), 2.82 – 2.64 (m, 2H), 2.57 (d, J = 8.7 Hz, 1H), 2.48 – 2.34 (m, 1H); ^{13}C NMR (126 MHz, methanol- d_4) δ 176.7, 176.6, 175.6, 174.6, 172.8, 172.3, 138.9, 138.6, 135.4, 134.2, 133.9, 131.2, 131.0, 130.5, 130.4, 130.1, 129.8, 129.6, 129.5, 127.7, 127.2, 68.1, 66.4, 49.2, 46.5, 45.7, 43.8, 43.6, 43.1, 41.3, 35.8, 35.7, 35.0, 34.4, 34.0, 33.7, 33.4, 32.4, 31.3, 26.7, 26.1. HRMS (ESI) m/z calculated for $\text{C}_{23}\text{H}_{27}\text{BClN}_3\text{O}_5\text{S}$ $[\text{M}+\text{H}]^+$: 504.15258; found $[\text{M}+\text{H}]^+$: 504.15283.

6.6. Procedure and analytical data of the Suzuki adduct 28



In a microwave vial, 4-formylphenylboronic acid (1.0 mmol), 2-aminothiazole (1.0 mmol), phenyl ethyl isocyanide (1.0 mmol) and Sc(OTf)₃ (30 mol%) were dissolved in MeOH (1 mL). The reaction mixture was irradiated at 100 °C for 1 h. After cooling down, extractions with dichloromethane (3x30 mL) followed. The organic layer was separated, washed with water, dried with magnesium sulfate, filtered and concentrated *in vacuo*. Then, the residue was dissolved in DME (5 mL) and H₂O (2 mL). Bromobenzene (1.0 mmol), K₂CO₃ (1.5 mmol) and Pd(PPh₃)₄ (10 mol%) as catalyst were added to the reaction mixture. The solution was refluxed overnight under N₂ atmosphere. Afterwards, the solvents were removed and the organic layer was separated, washed with water, dried with magnesium sulfate, filtered and concentrated *in vacuo*. The crude product was purified with column chromatography on silica gel eluted with petroleum ether-ethyl acetate (5:1) affording compound 28.

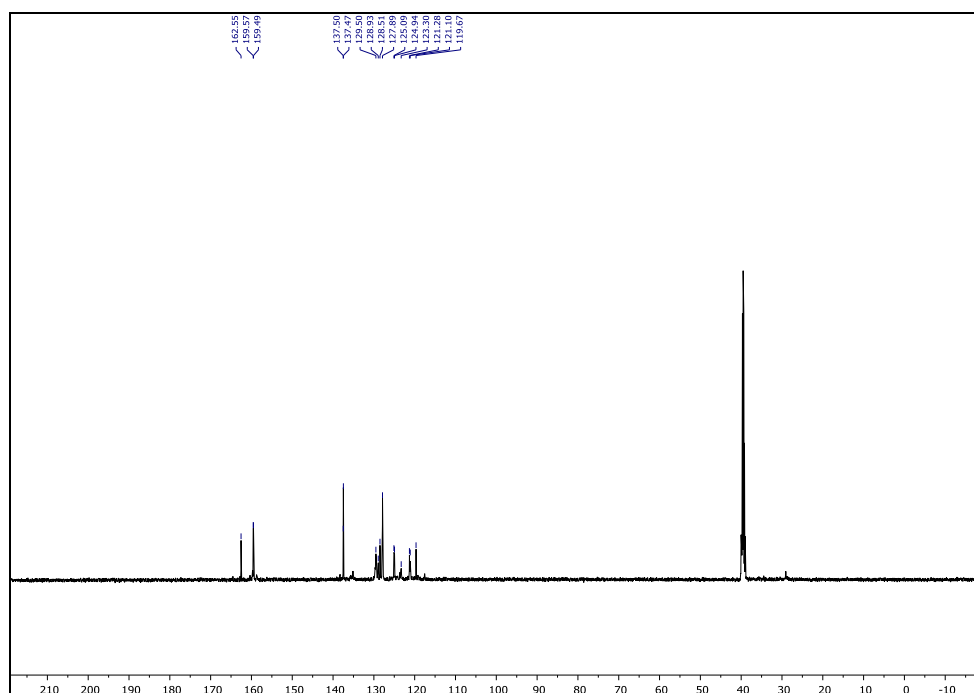
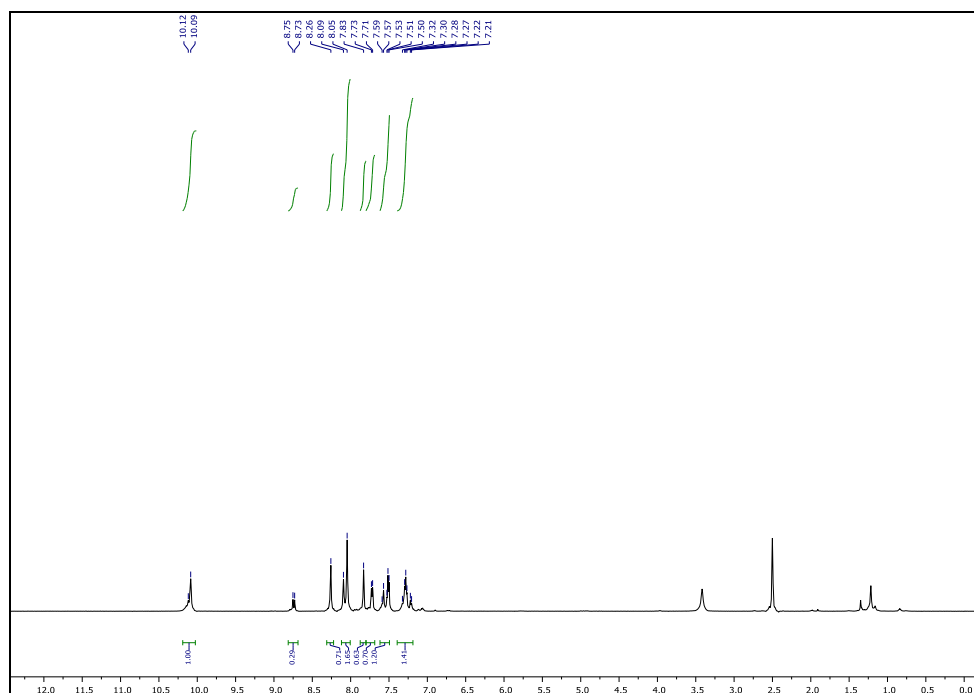
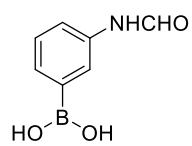
6-([1,1'-biphenyl]-4-yl)-N-phenethylimidazo[2,1-b]thiazol-5-amine (28)

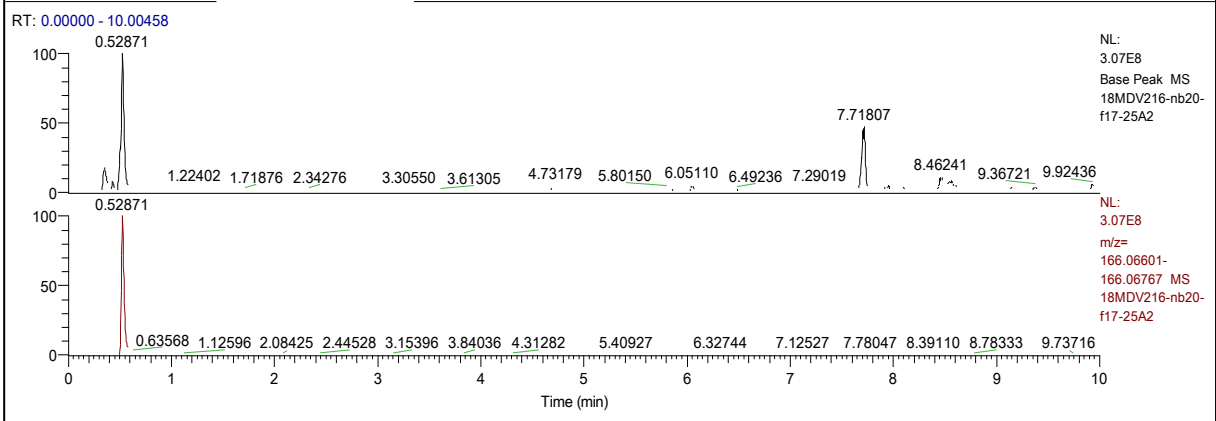


White solid, 45% yield (2 steps); ¹H NMR (500 MHz, CDCl₃) δ: 7.81 (d, *J* = 8.3 Hz, 2H), 7.64 – 7.60 (m, 2H), 7.56 (d, *J* = 8.3 Hz, 2H), 7.43 (d, *J* = 7.8 Hz, 2H), 7.36 – 7.29 (m, 4H), 7.26 (d, *J* = 7.3 Hz, 1H), 7.21 (d, *J* = 7.1 Hz, 2H), 6.99 (d, *J* = 4.5 Hz, 1H), 6.64 (d, *J* = 4.5 Hz, 1H), 3.33 (q, *J* = 6.5 Hz, 2H), 3.14 (t, *J* = 6.2 Hz, 1H), 2.88 (t, *J* = 6.6 Hz, 2H). ¹³C NMR (126 MHz, CDCl₃) δ 144.9, 140.8, 139.0, 135.8, 133.5, 128.9, 128.7, 128.7, 128.5, 128.3, 127.2, 127.1, 126.9, 126.6, 126.2, 125.9, 116.6, 111.8, 50.0, 36.6. HRMS (ESI) *m/z* calculated for C₂₅H₂₁N₃S [M+H]⁺: 396.14562; found [M+H]⁺: 396.14570.

Exemplary copies of NMR and MS data of novel compounds

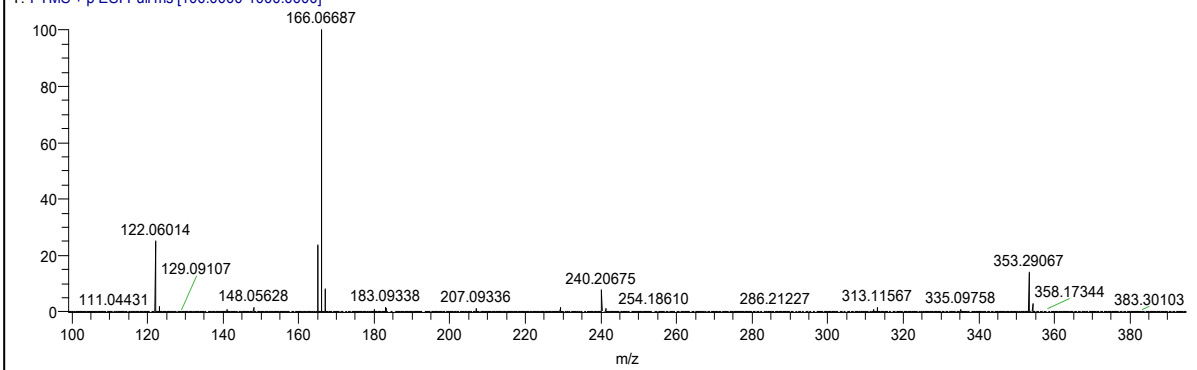
(3-formamidophenyl)boronic acid (2)





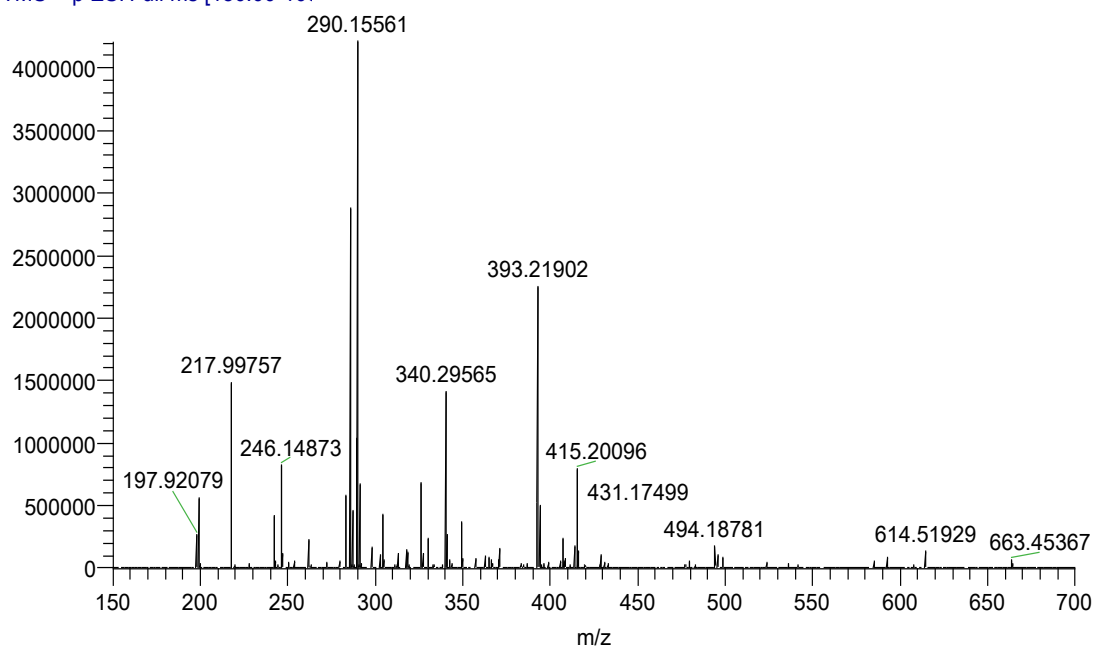
18MDV216-nb20-f17-25A2 #119 RT: 0.52871 AV: 1 SB: 2 0.47522, 1.12150 NL: 2.83E8

T: FTMS + p ESI Full ms [100.0000-1000.0000]

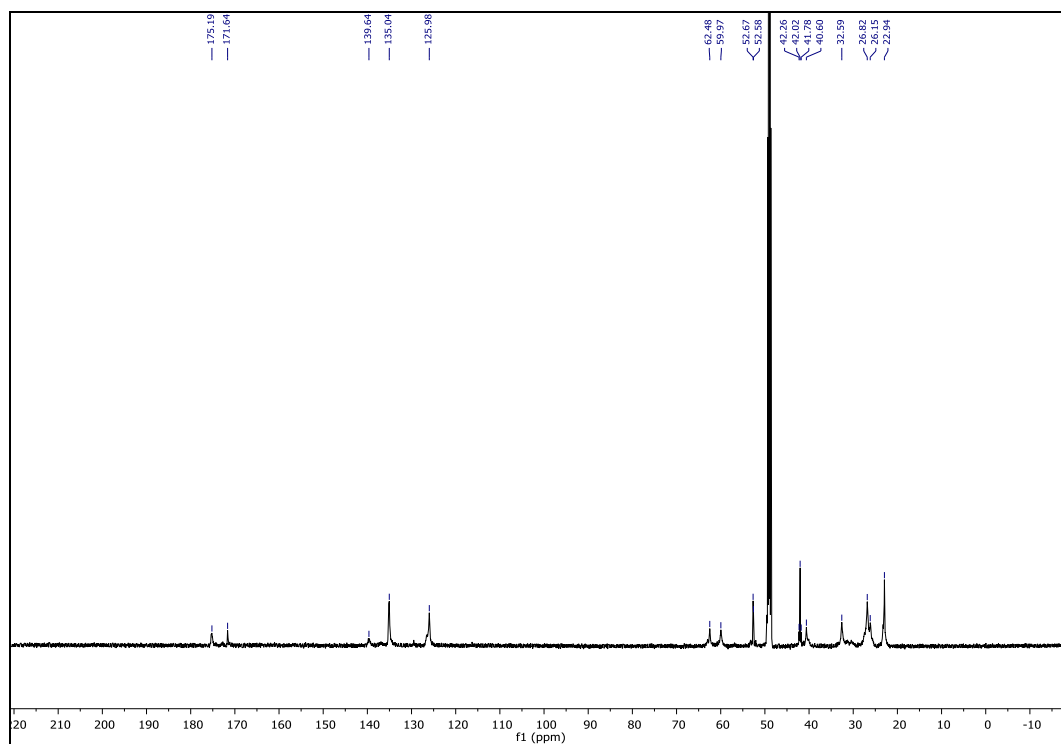
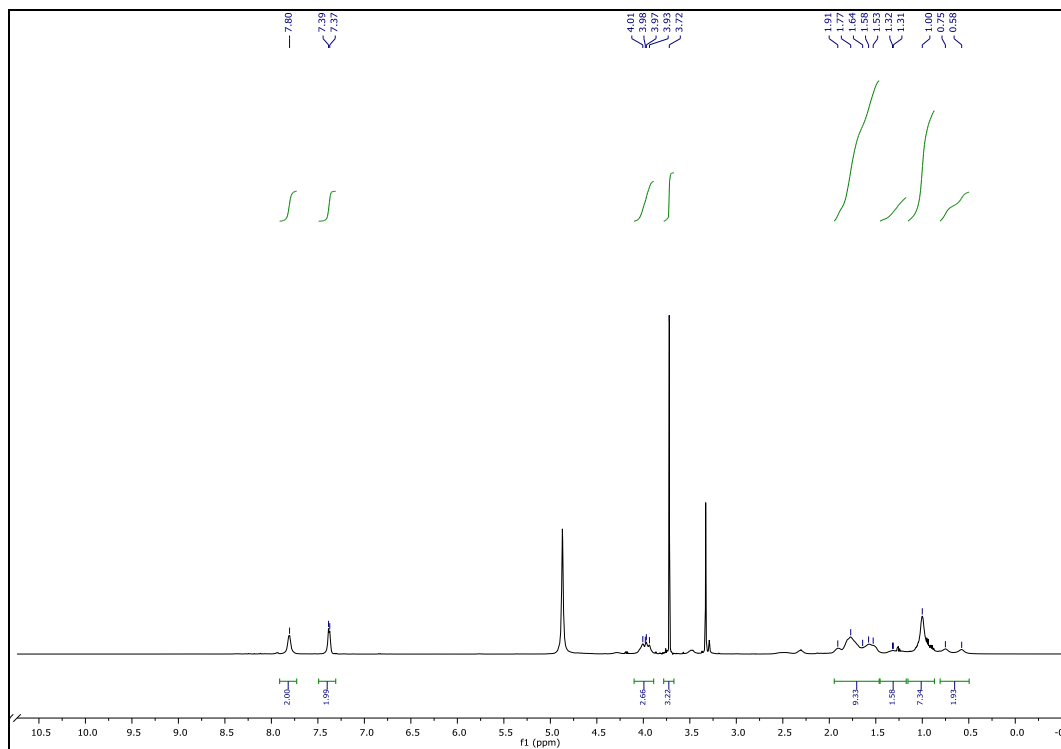
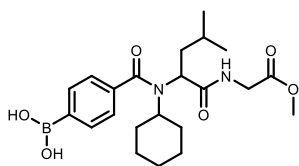


18MDV090-34_180314183649 #14
T: FTMS + p ESI Full ms [150.00-1000.00]

V: 1 NL: 4.21E6

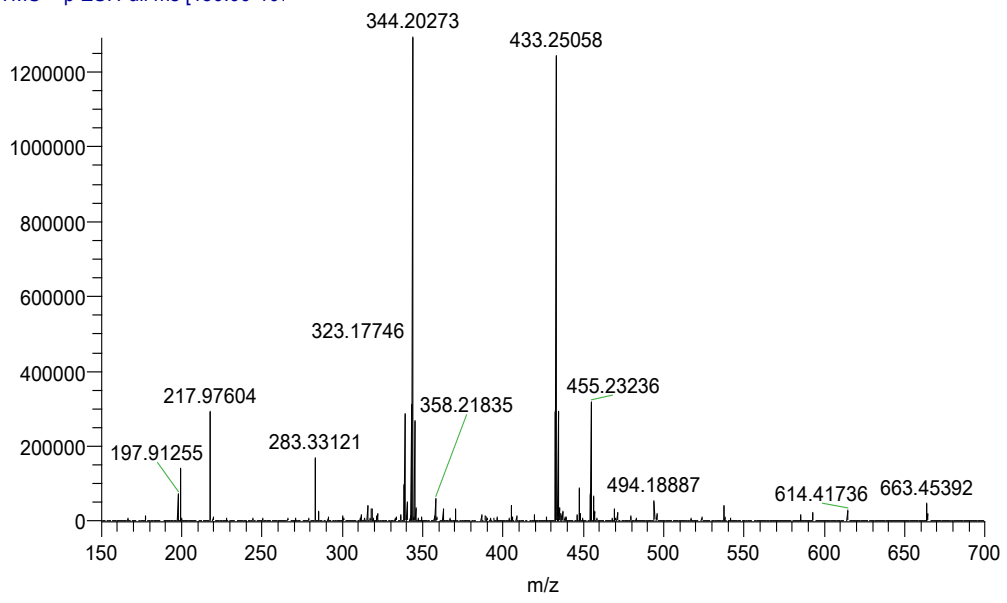


4-(cyclohexyl(1-((2-methoxy-2-oxoethyl)amino)-4-methyl-1-oxopentan-2-yl)carbamoyl)phenyl)boronic acid (12b)

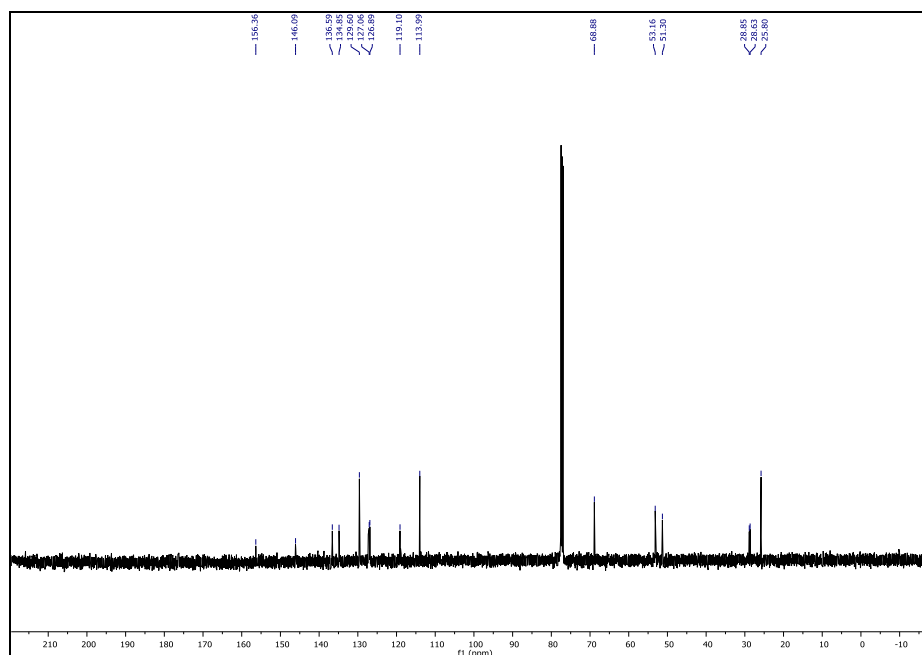
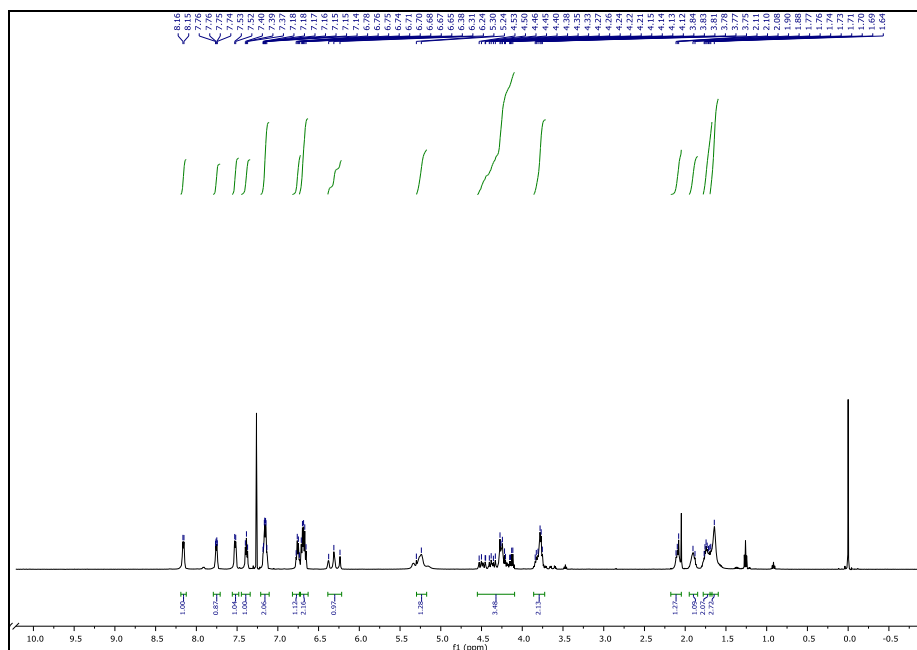
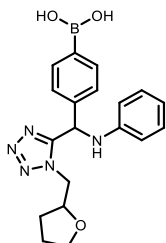


18MDV090-33_180314183404 #17
T: FTMS + p ESI Full ms [150.00-1000.00]

(V: 1 NL: 1.29E6)



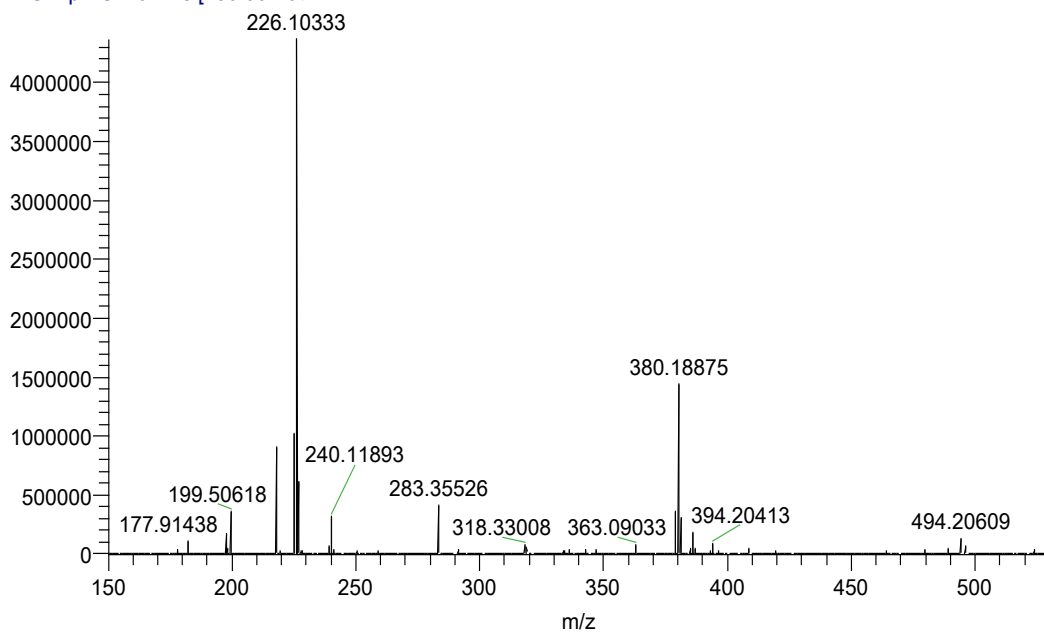
(4-((phenylamino)(1-((tetrahydrofuran-2-yl)methyl)-1H-tetrazol-5-yl)methyl)phenyl) boronic acid (16a)



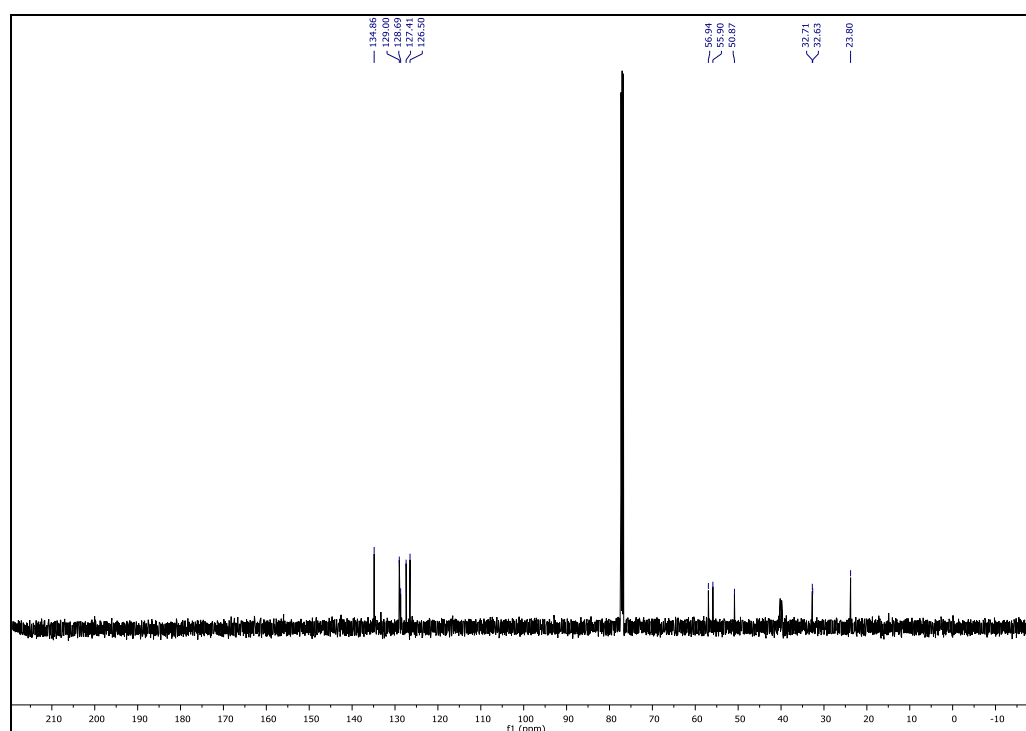
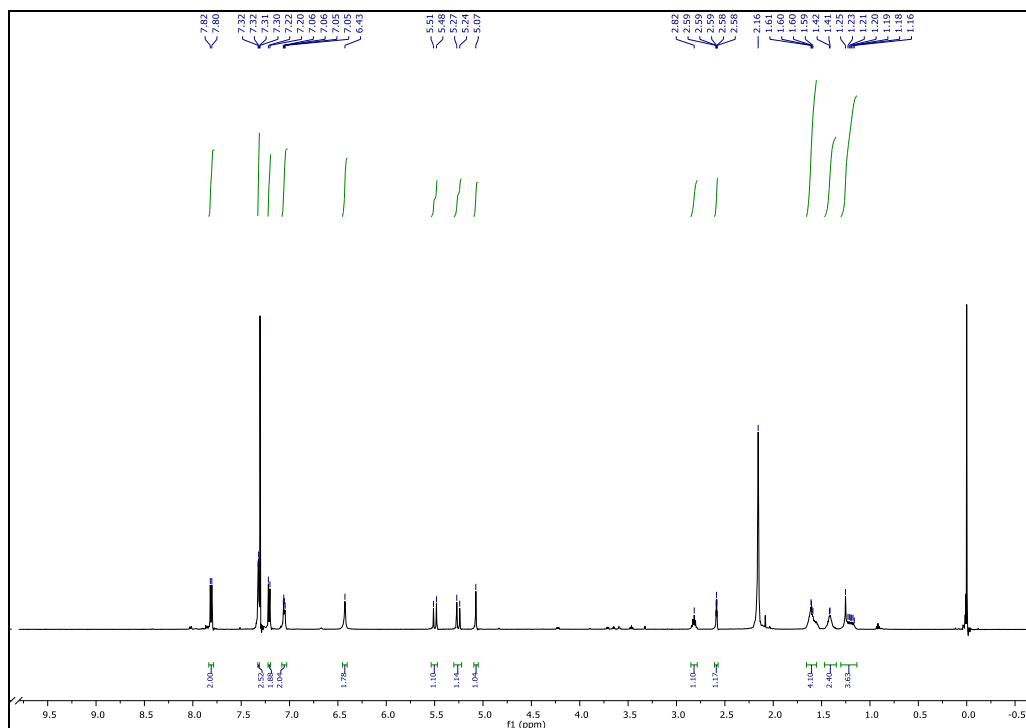
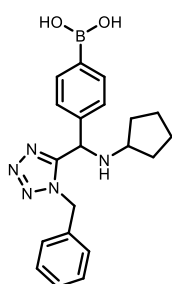
18MDV090-04_180314171438 #15

V: 1 NL: 4.37E6

T: FTMS + p ESI Full ms [150.00-100

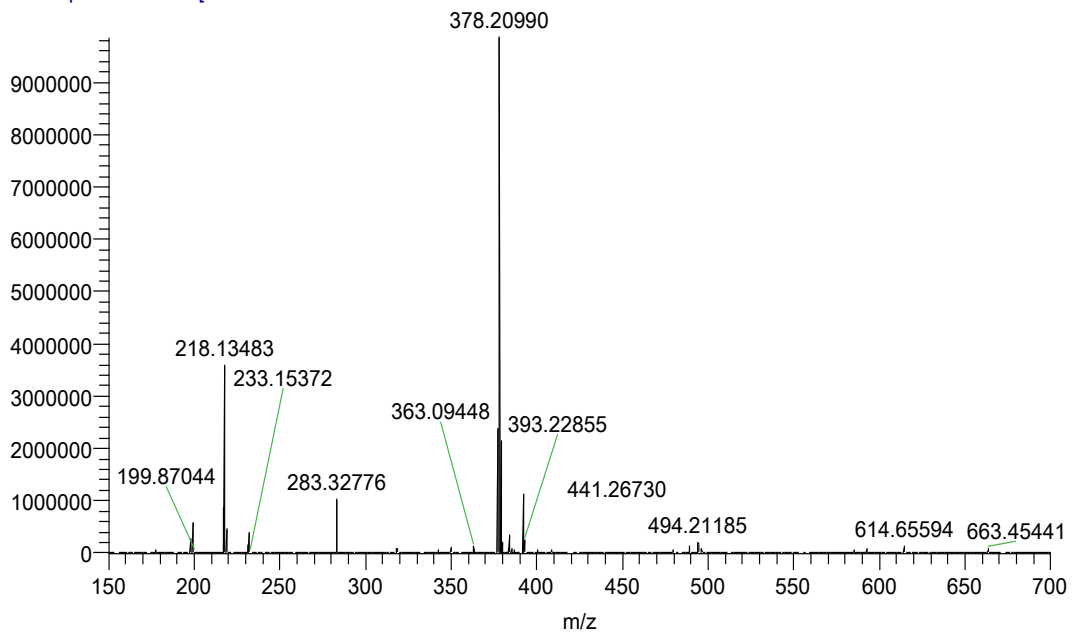


(4-((1-benzyl-1H-tetrazol-5-yl)(cyclopentylamino)methyl)phenyl)boronic acid (16b)

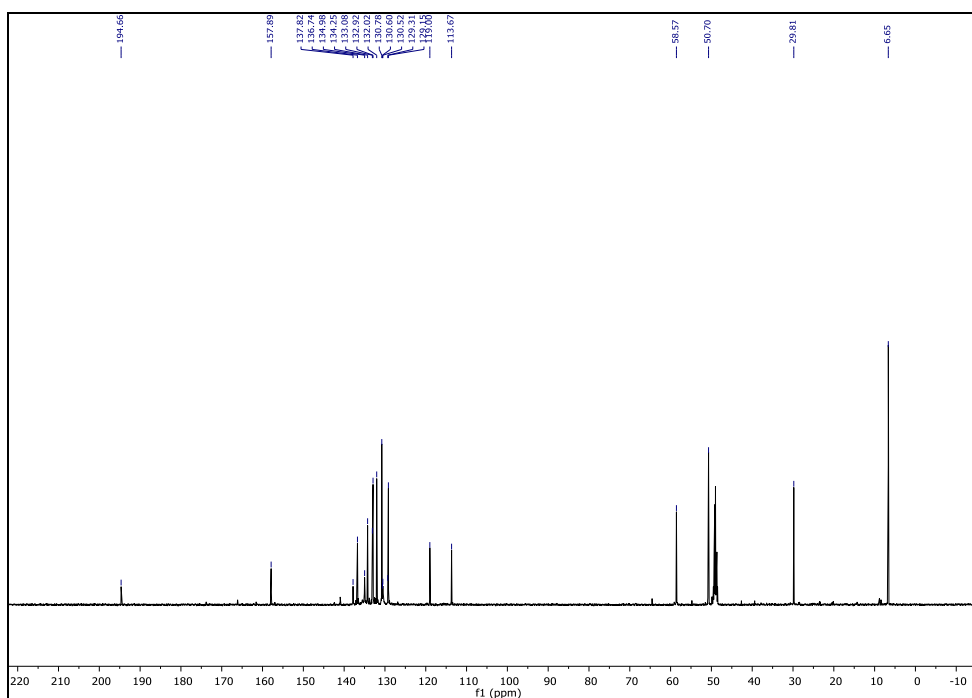
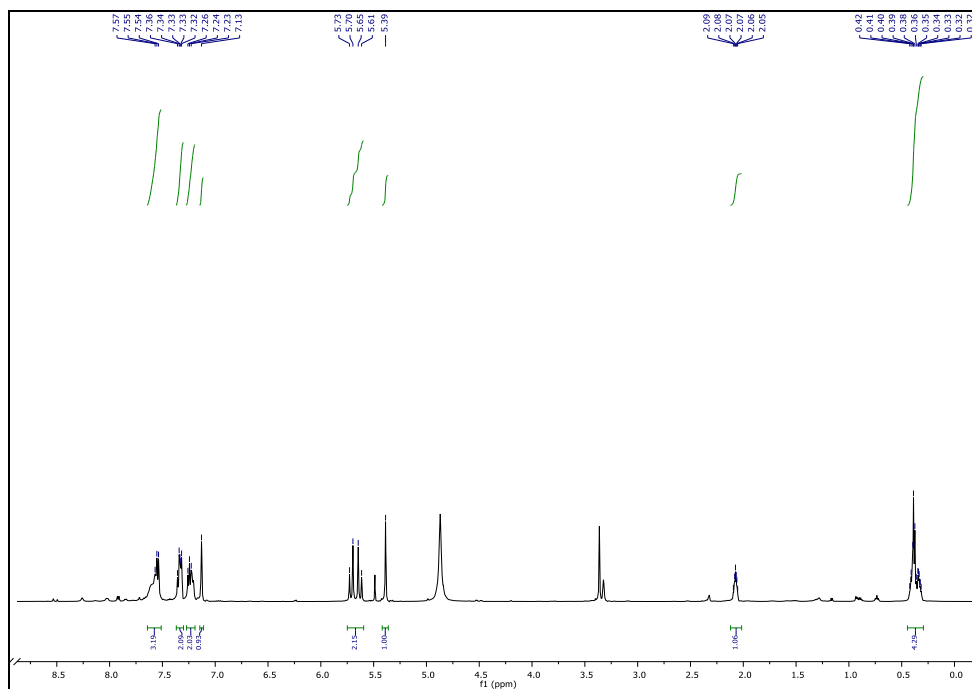
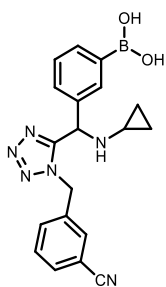


18MDV090-05_180314171723 #13
T: FTMS + p ESI Full ms [150.00-100

v: 1 NL: 9.86E6

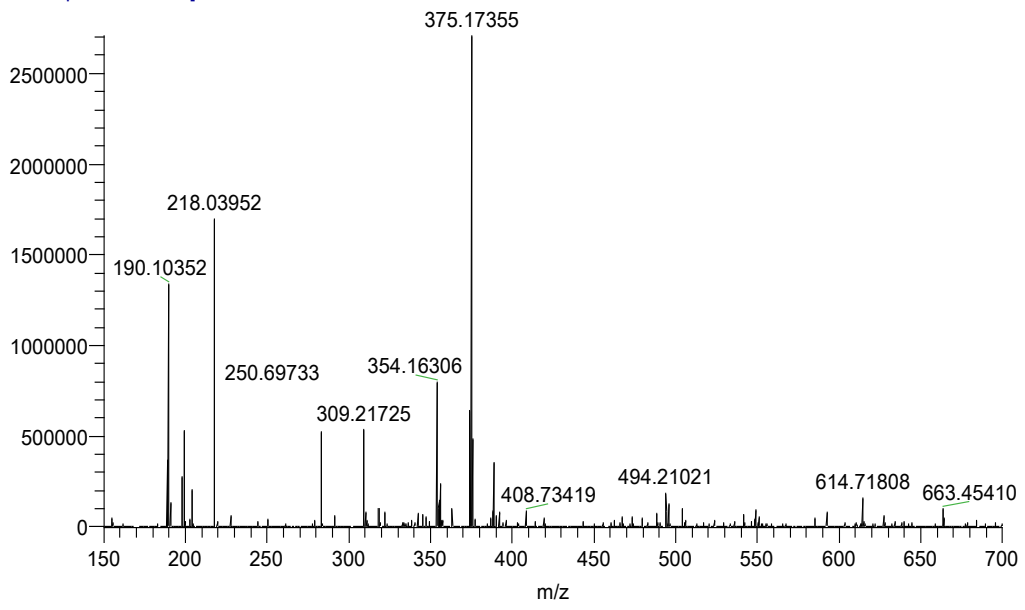


(3-((1-(3-cyanobenzyl)-1H-tetrazol-5-yl)(cyclopropylamino)methyl)phenyl)boronic acid (16c)

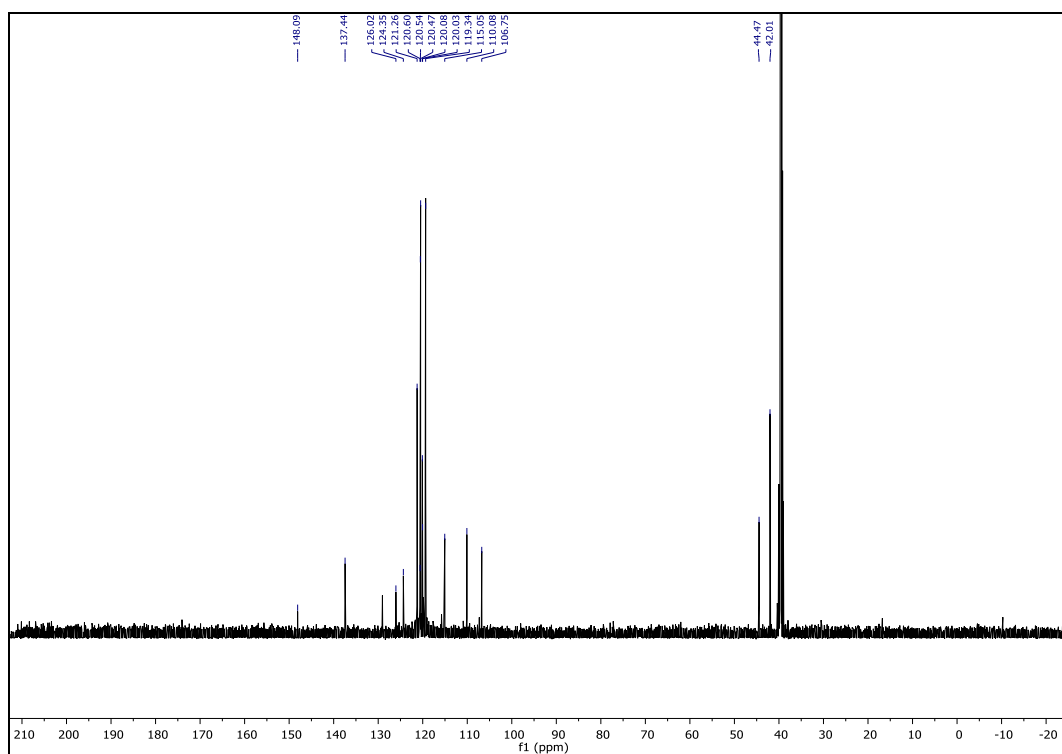
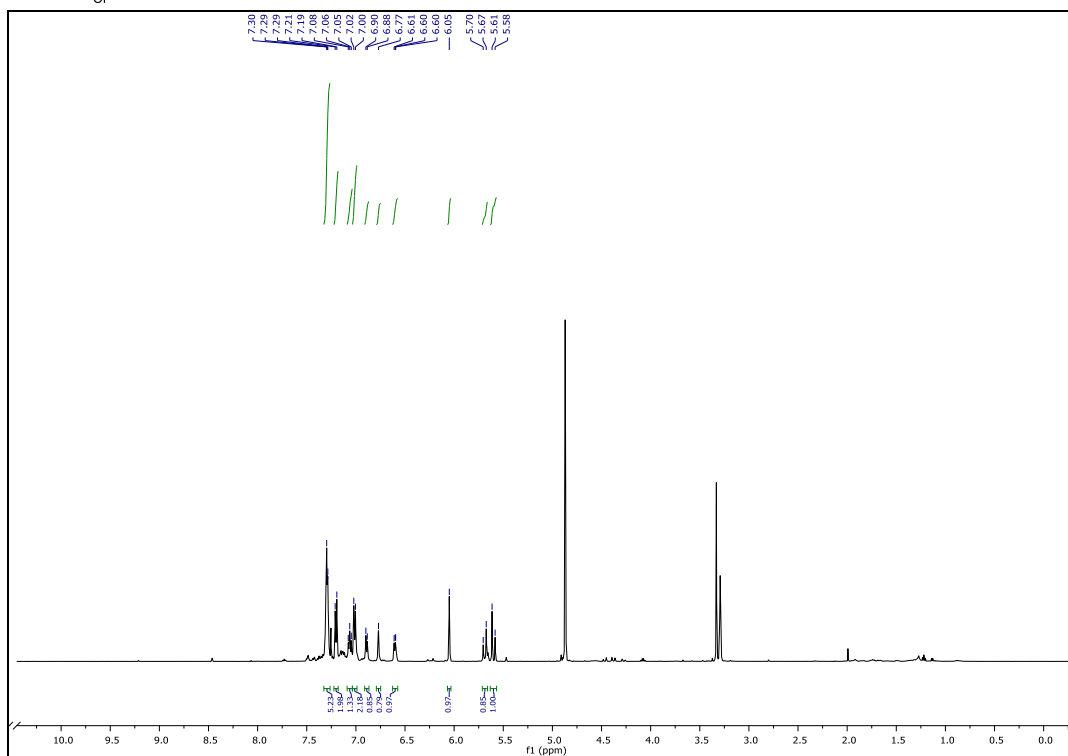
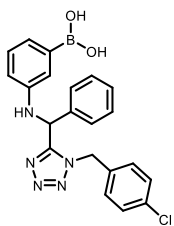


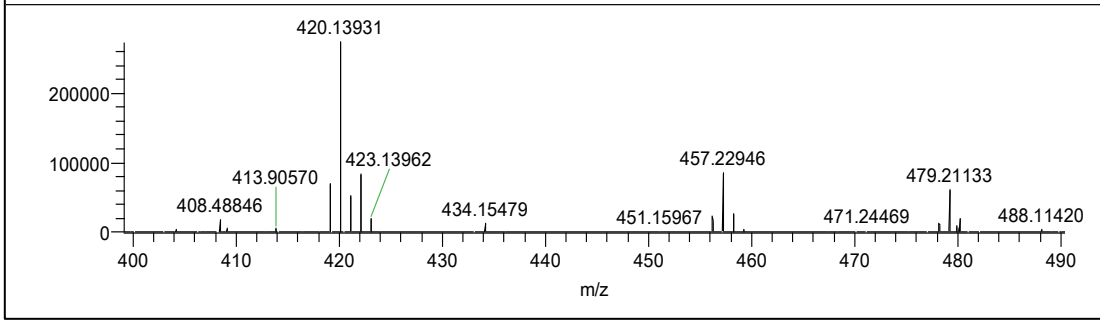
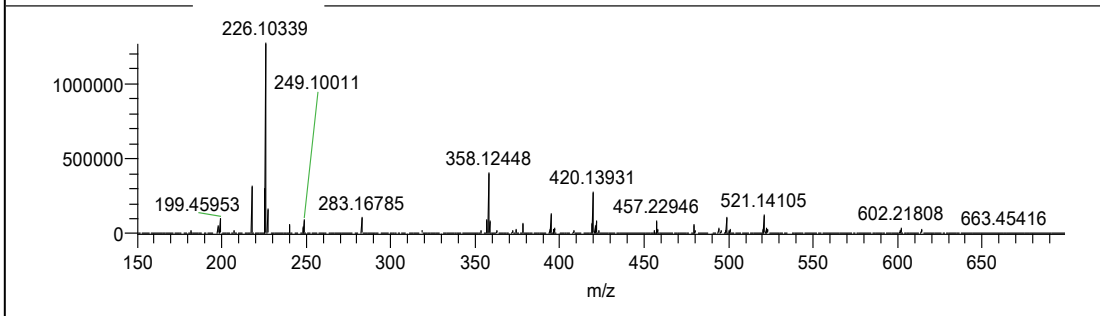
18MDV090-10_180314173107 #14
T: FTMS + p ESI Full ms [150.00-1000.00]

V: 1 NL: 2.71E6

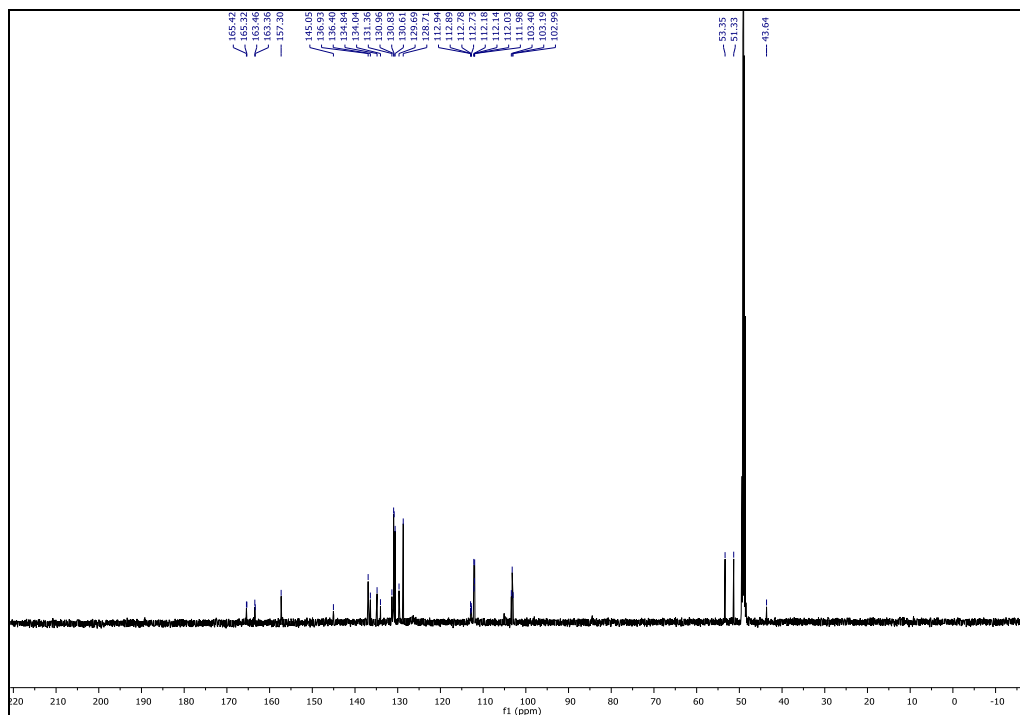
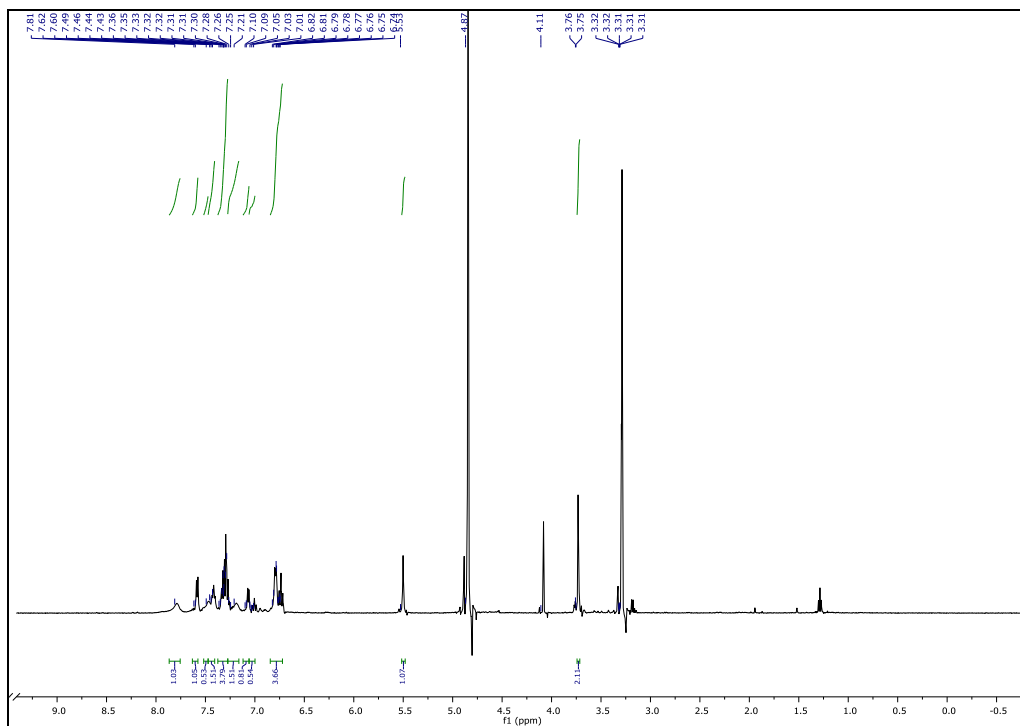
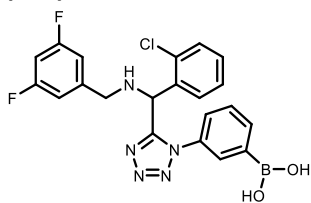


(3-(((1-(4-chlorobenzyl)-1H-tetrazol-5-yl)(phenyl)methyl)amino)phenyl)boronic acid (17a)



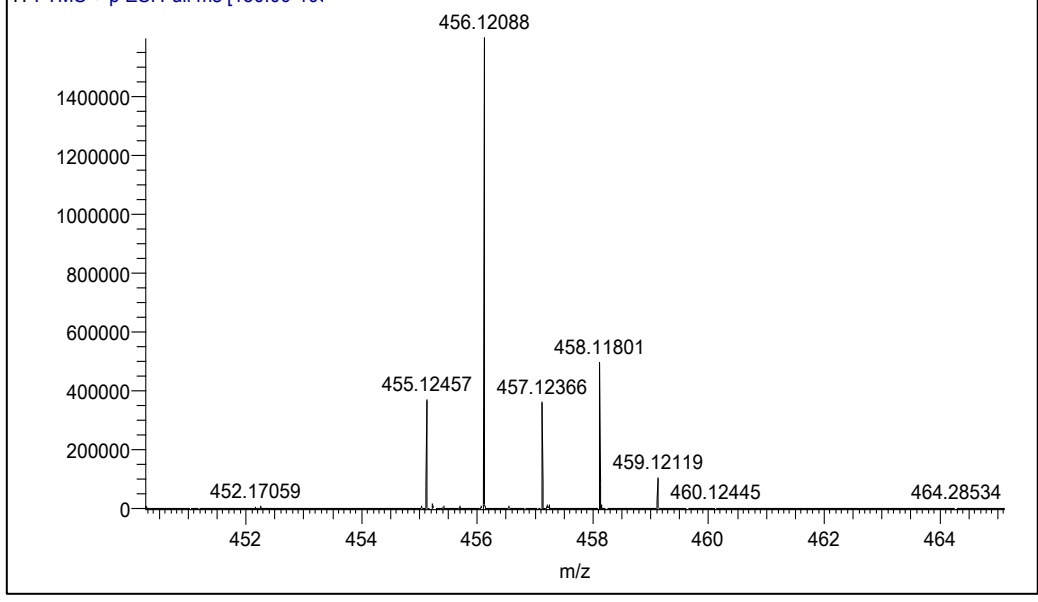


3-(5-((2-chlorophenyl)((3,5-difluorobenzyl)amino)methyl)-1H-tetrazol-1-yl)phenylboronic acid (18a)

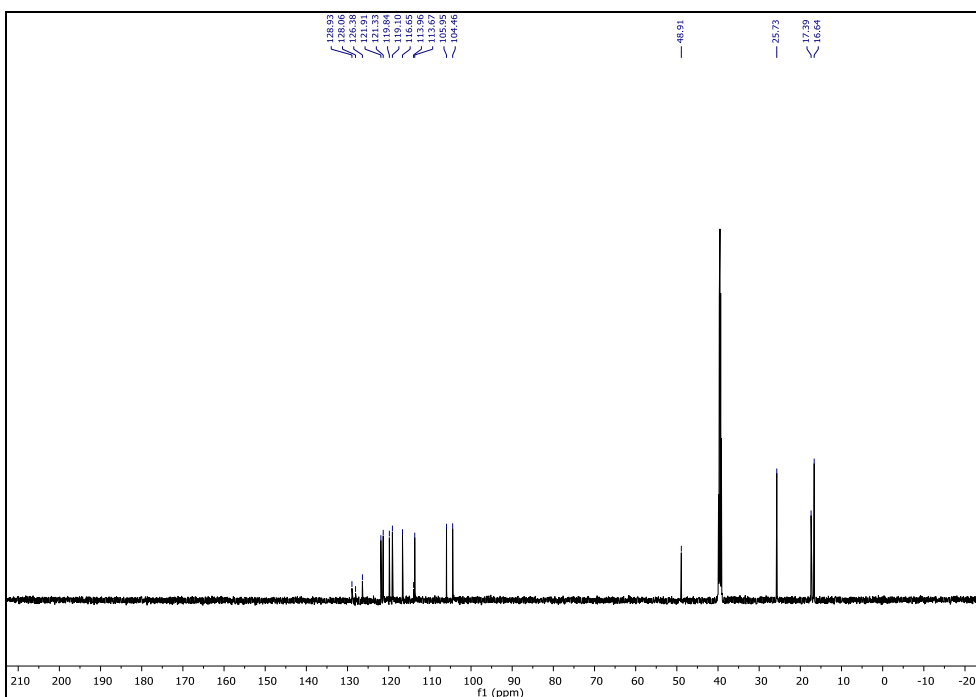
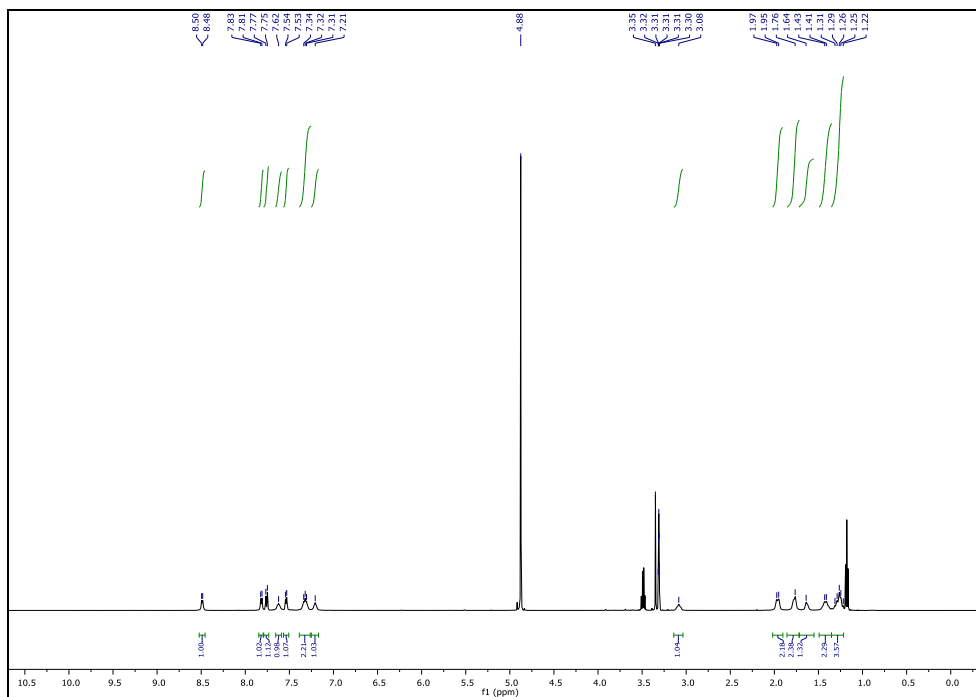
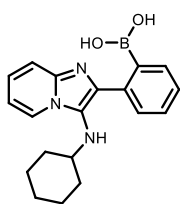


18MDV090-26_180314181453 #13
T: FTMS + p ESI Full ms [150.00-100

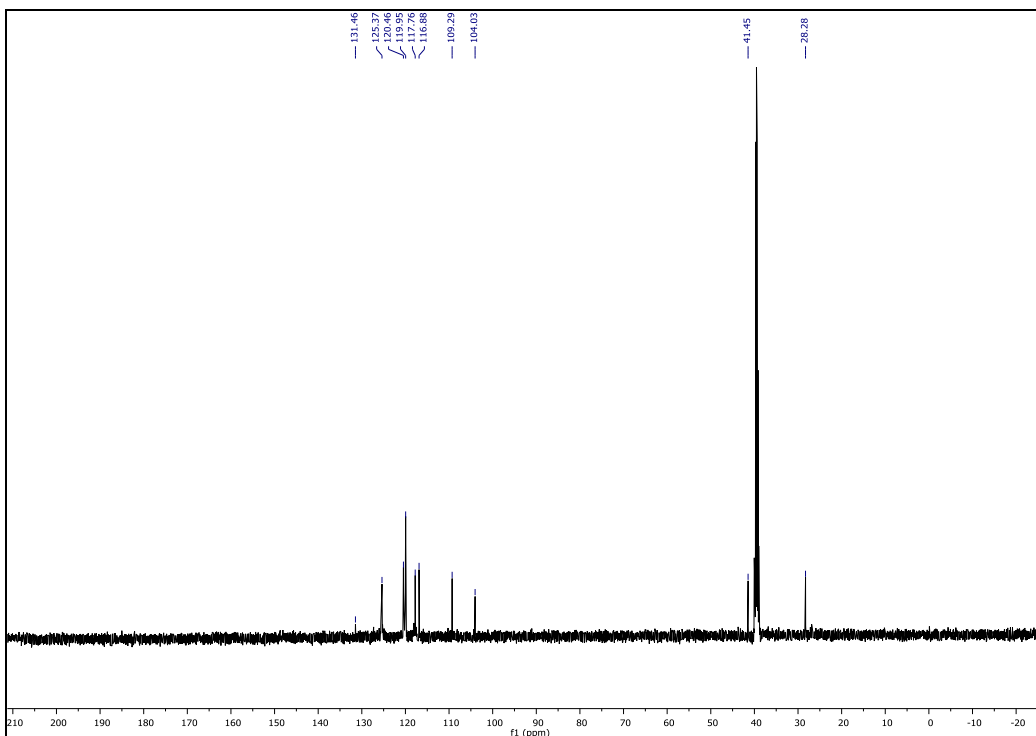
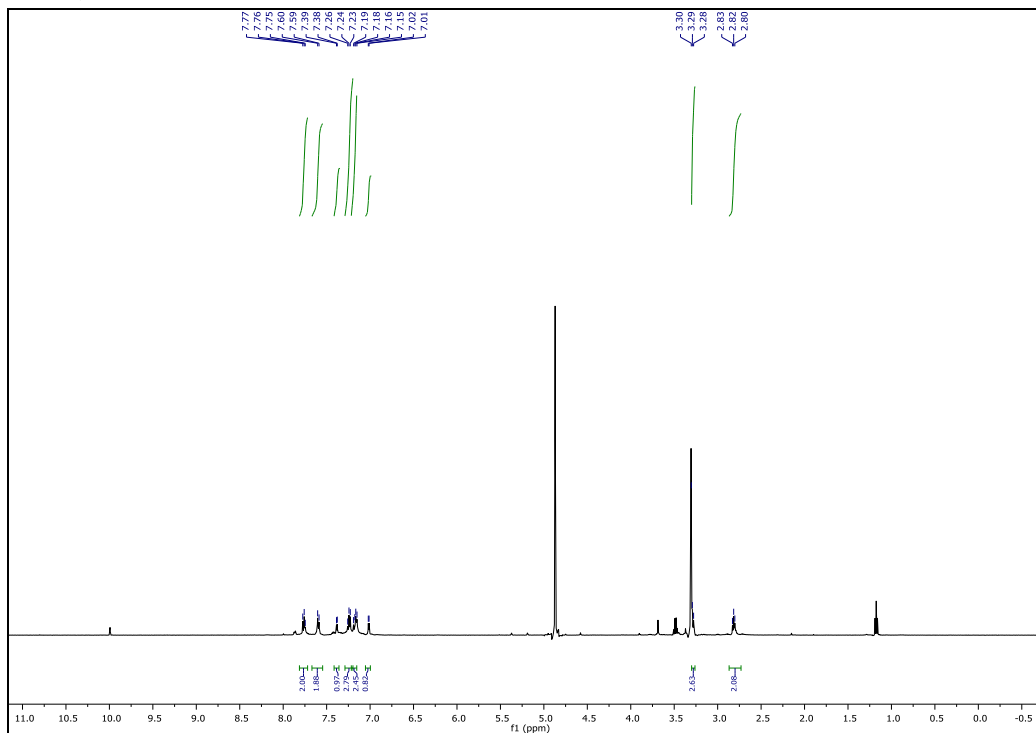
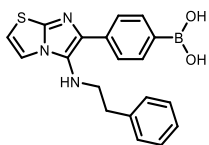
(V: 1 NL: 1.60E6



(2-(3-(cyclohexylamino)imidazo[1,2-a]pyridin-2-yl)phenyl)boronic acid (19a)

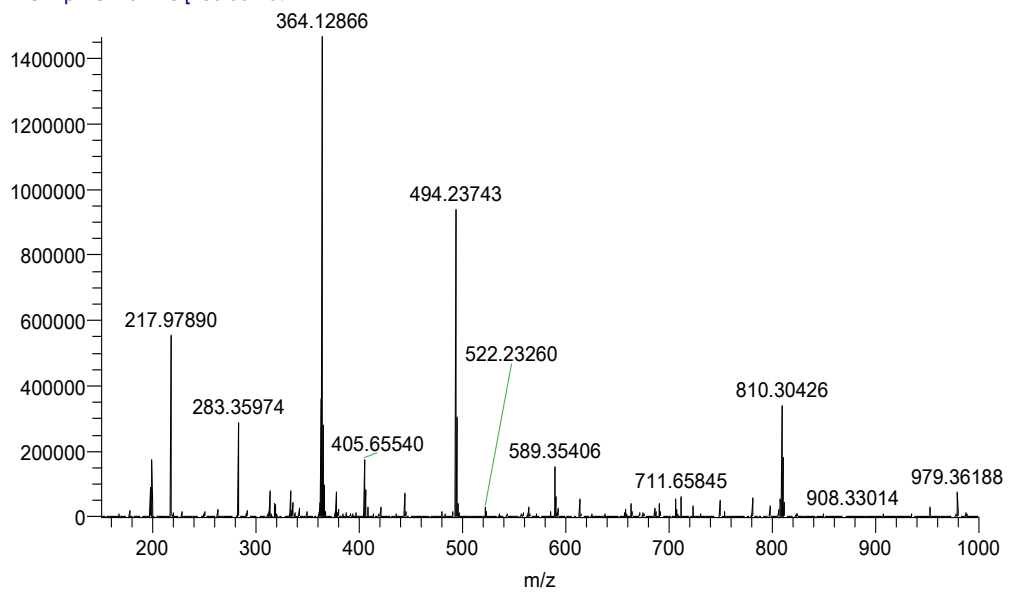


(4-(5-(phenethylamino)imidazo[2,1-b]thiazol-6-yl)phenyl)boronic acid (19b)

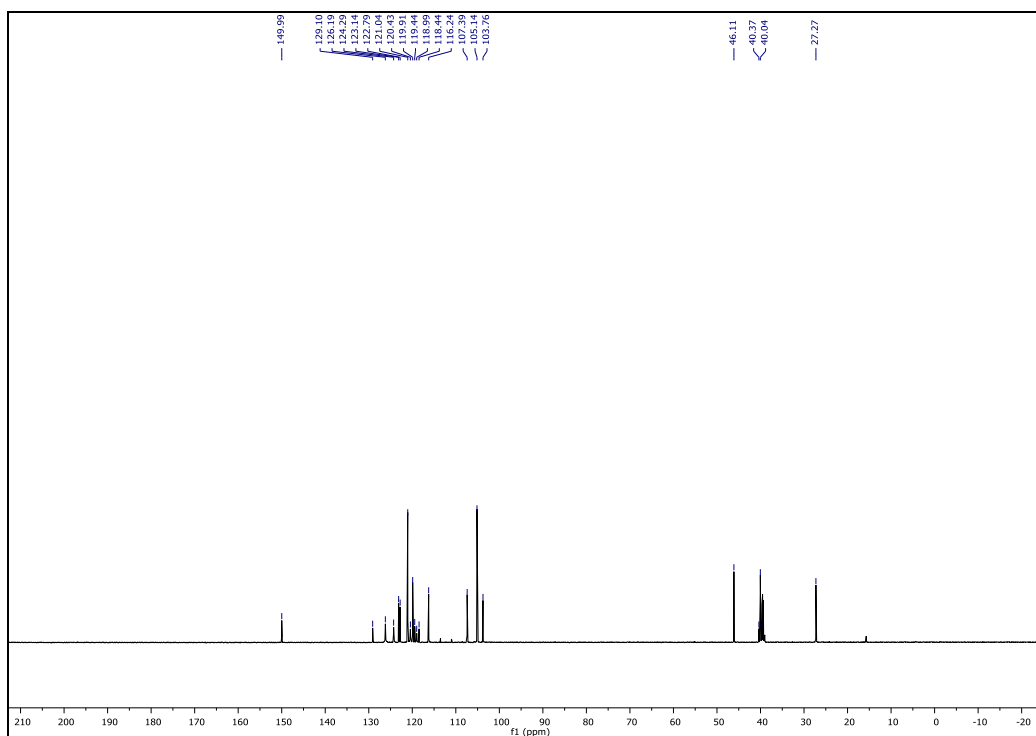
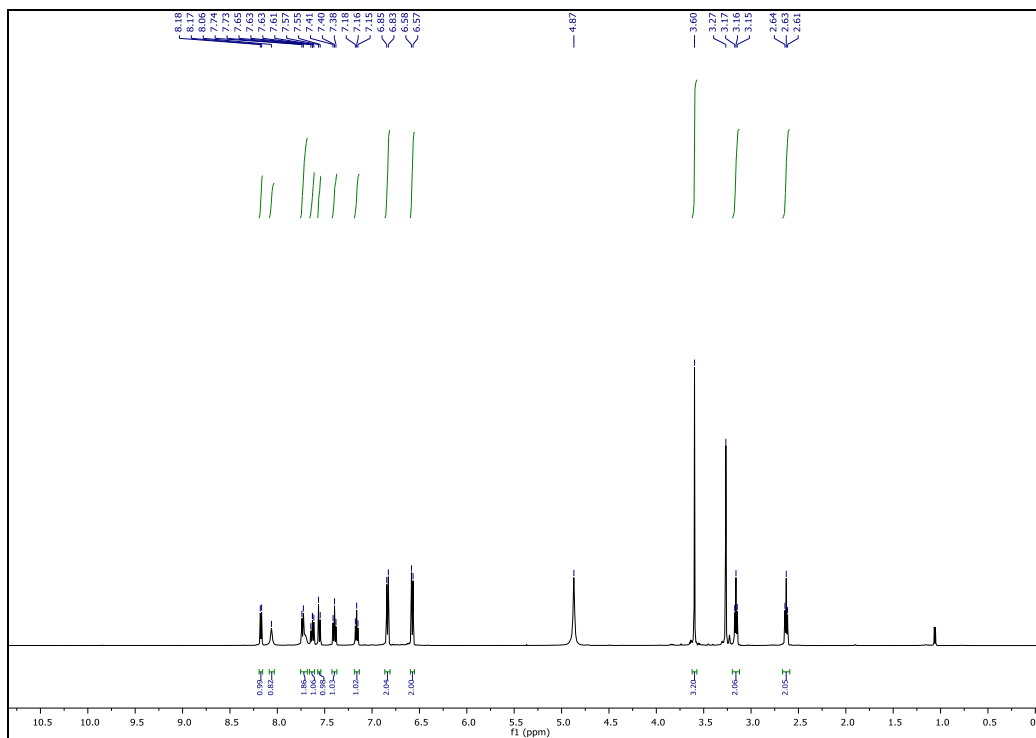
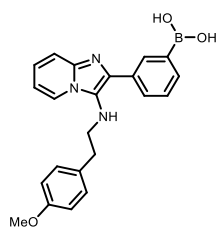


18MDV090-20_180314175835 #17
T: FTMS + p ESI Full ms [150.00-1000.00]

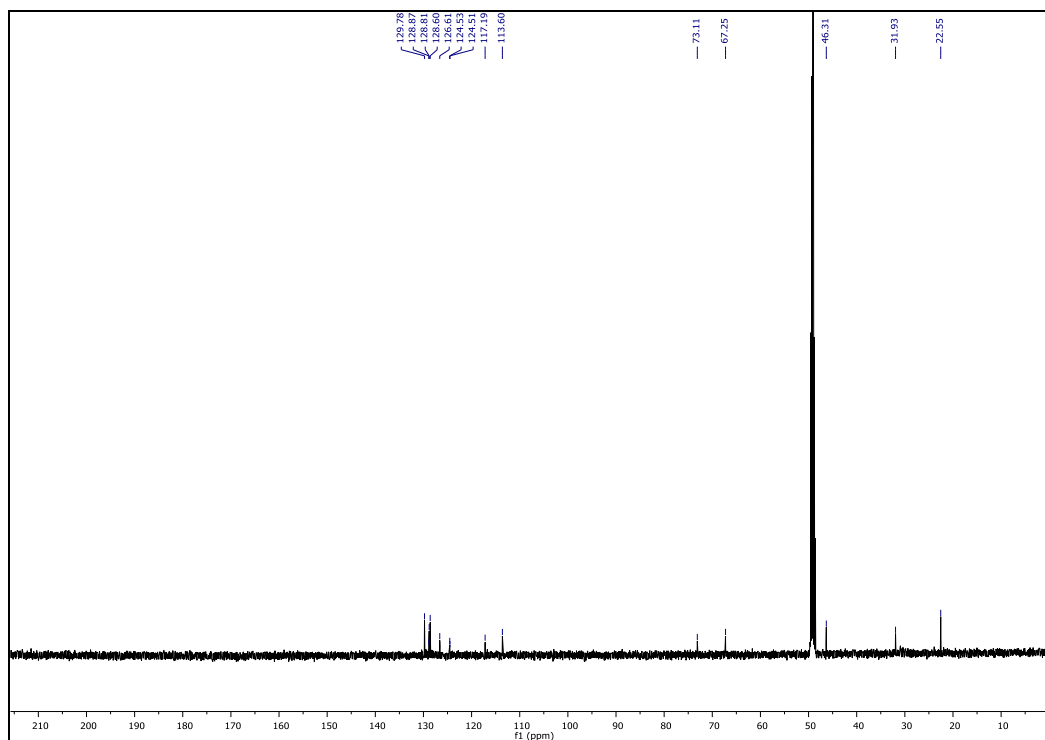
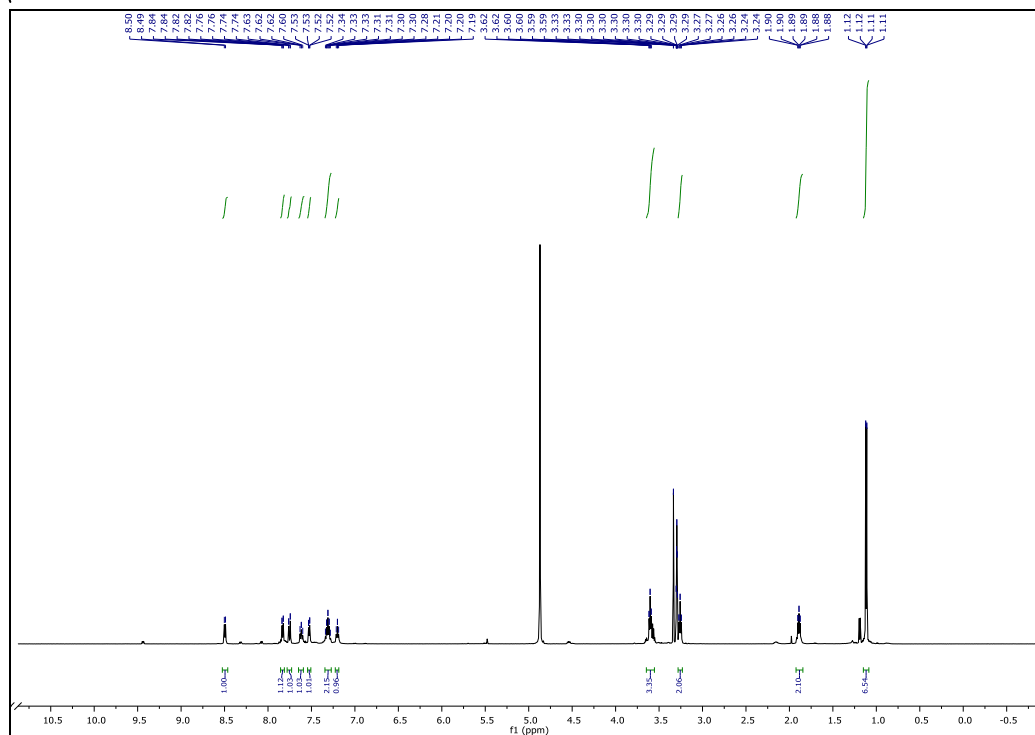
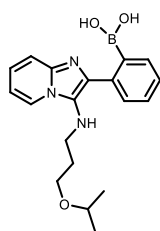
(V: 1 NL: 1.47E6)



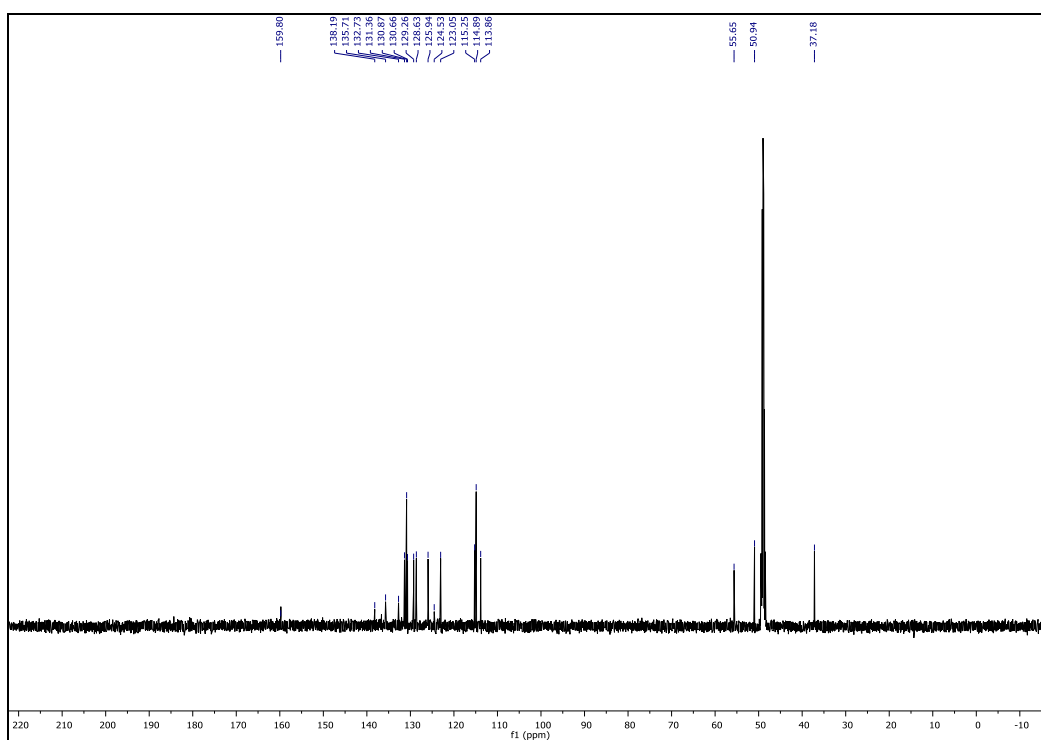
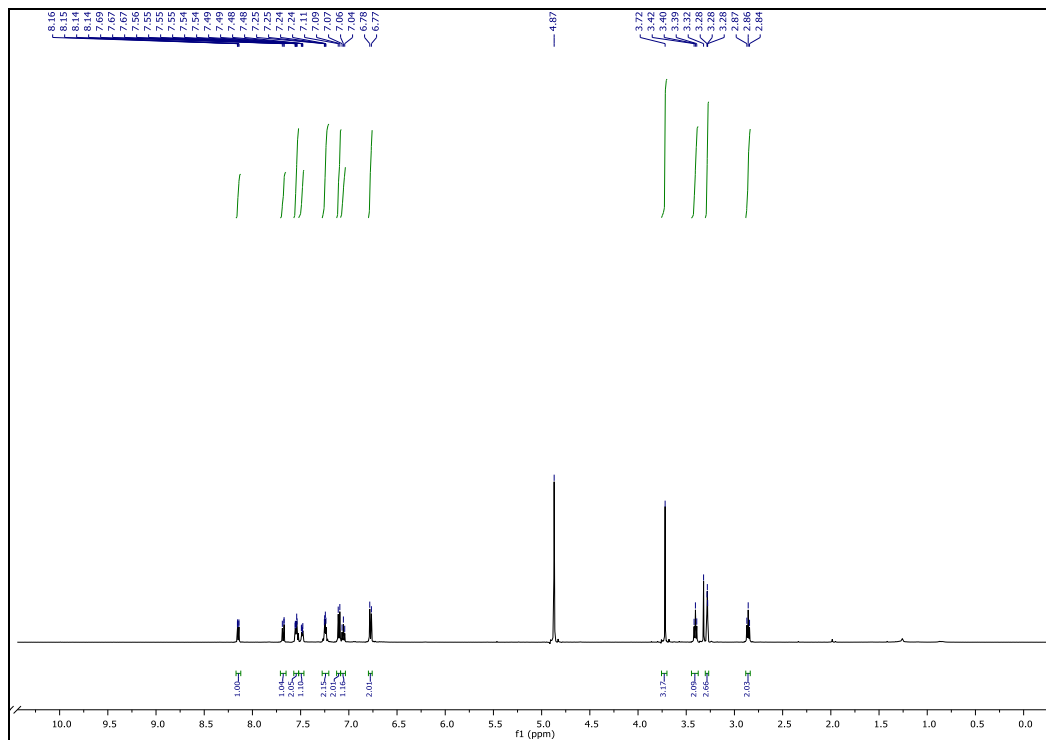
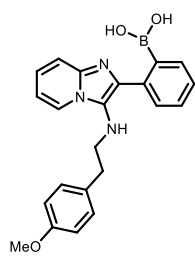
(3-(3-((4-methoxyphenethyl)amino)imidazo[1,2-a]pyridin-2-yl)phenyl)boronic acid (19c)



(2-(3-((3-isopropoxypropyl)amino)imidazo[1,2-a]pyridin-2-yl)phenyl)boronic acid (19d)

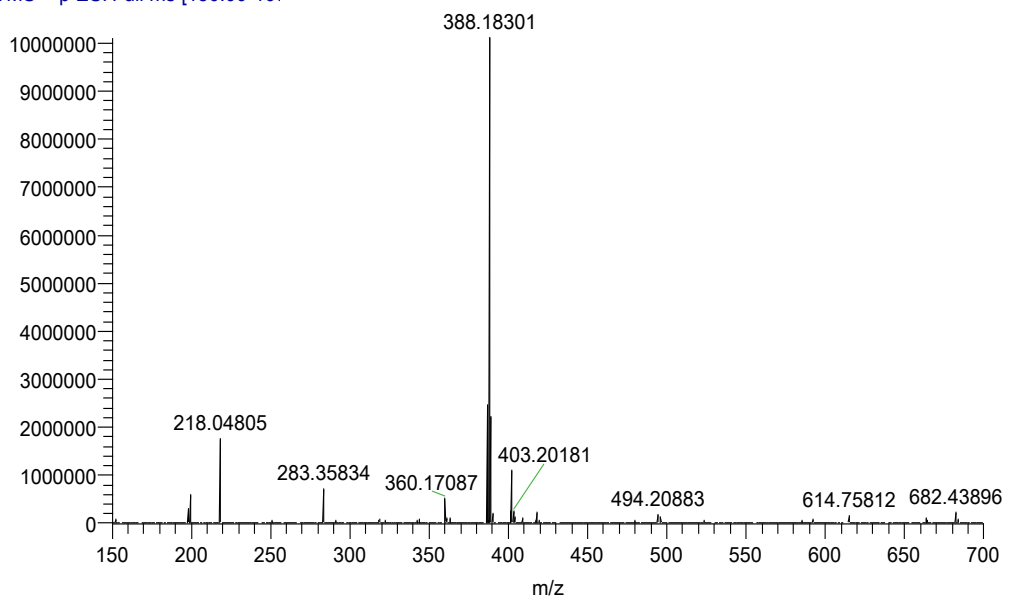


(2-(3-((4-methoxyphenethyl)amino)imidazo[1,2-a]pyridin-2-yl)phenyl)boronic acid (19e)

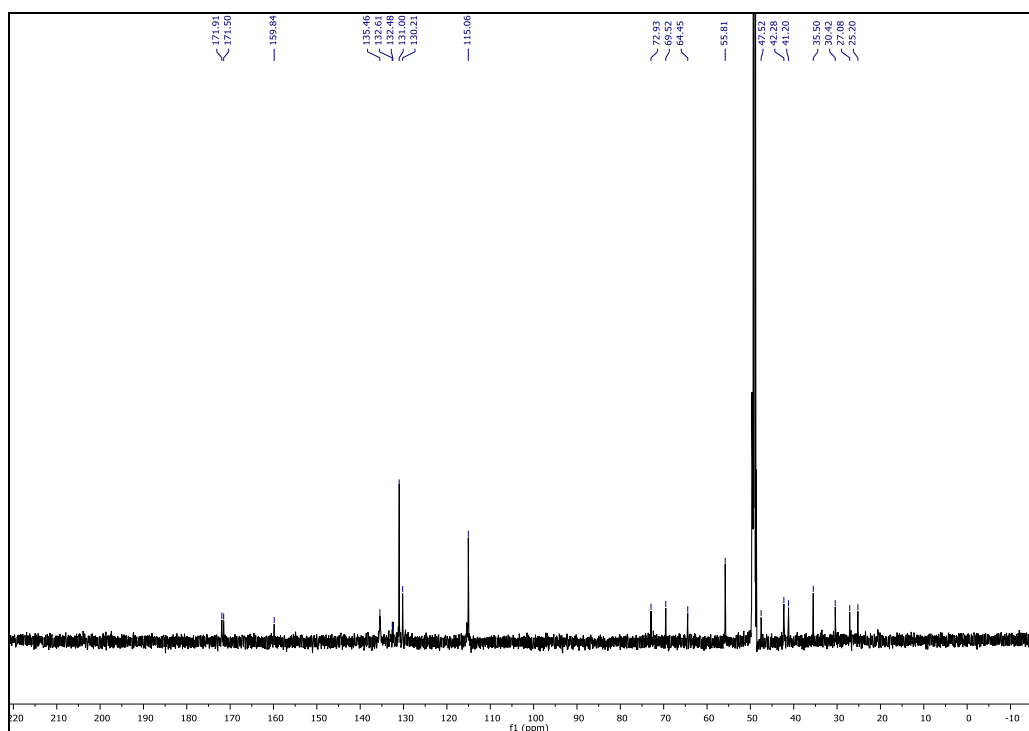
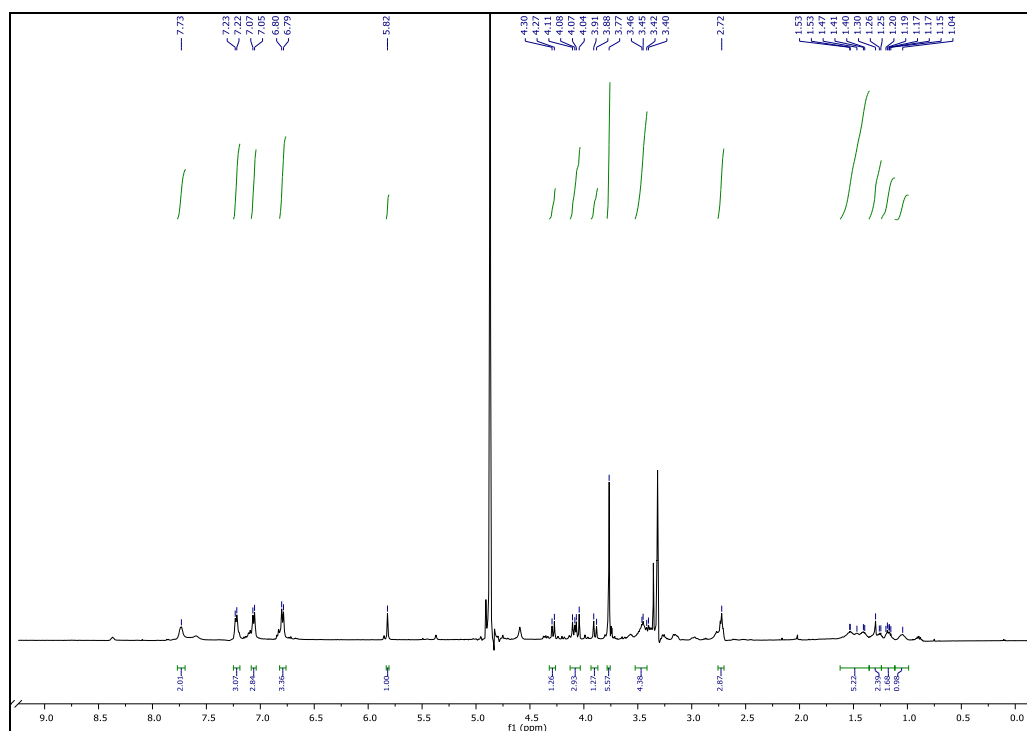
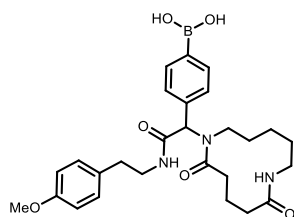


18MDV090-11_180314173351 #14
T: FTMS + p ESI Full ms [150.00-1000.00]

(V: 1 NL: 1.01E7

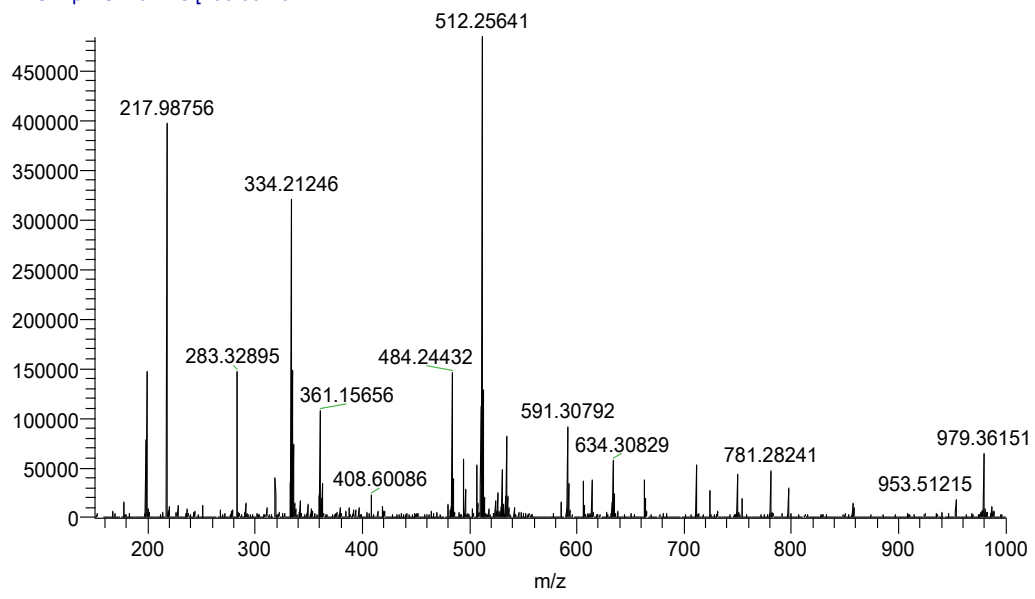


(4-(1-(2,6-dioxo-1,7-diazacyclododecan-1-yl)-2-((4-methoxyphenethyl)amino)-2-oxoethyl)phenyl)boronic acid (20a)

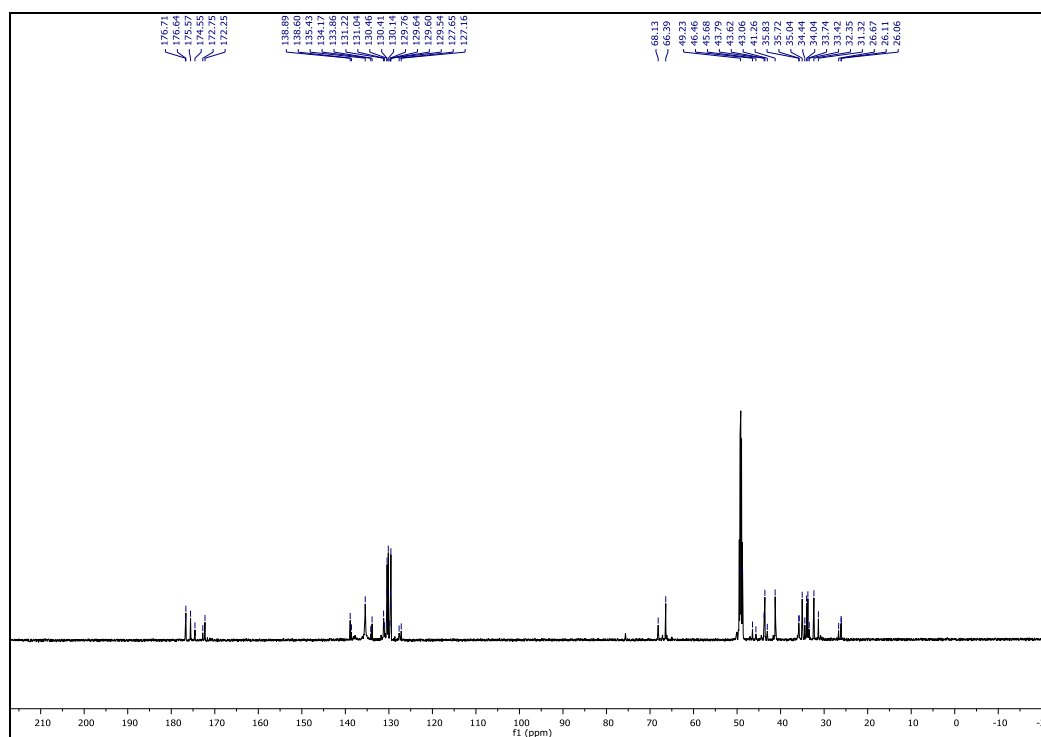
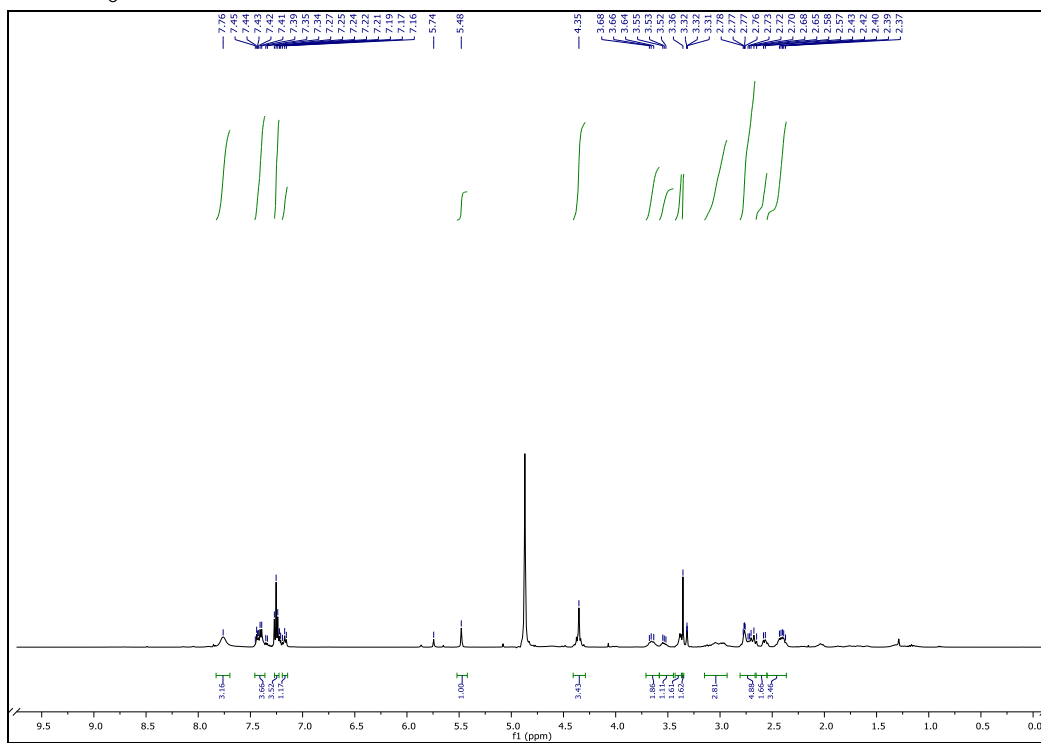
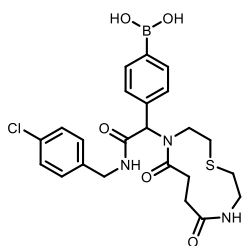


18MDV090-22_180314180401 #19
T: FTMS + p ESI Full ms [150.00-1000.00]

V: 1 NL: 4.84E5

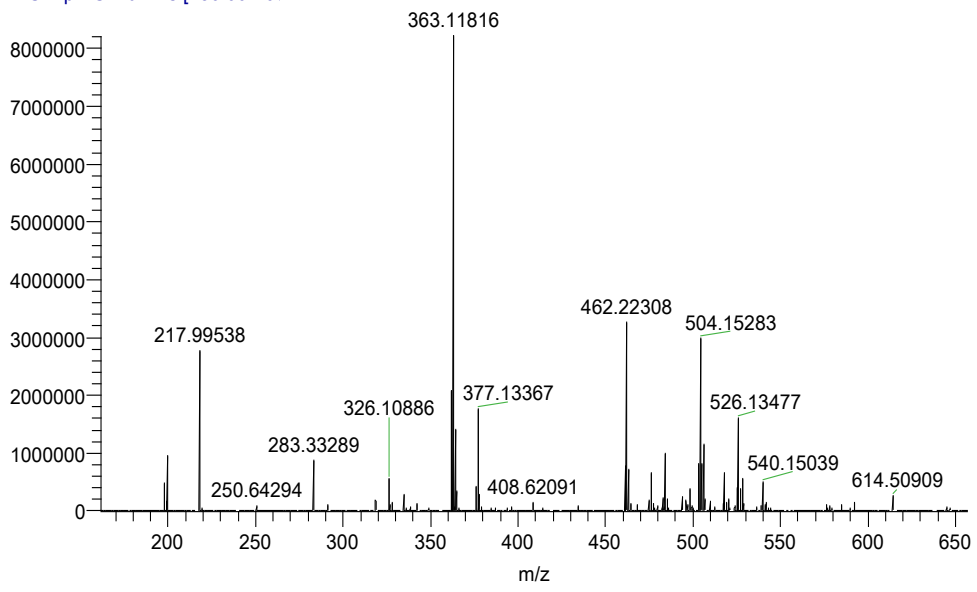


(4-(2-((4-chlorobenzyl)amino)-1-(5,8-dioxo-1-thia-4,9-diazacycloundecan-4-yl)-2-oxoethyl)phenyl)boronic acid (20b)

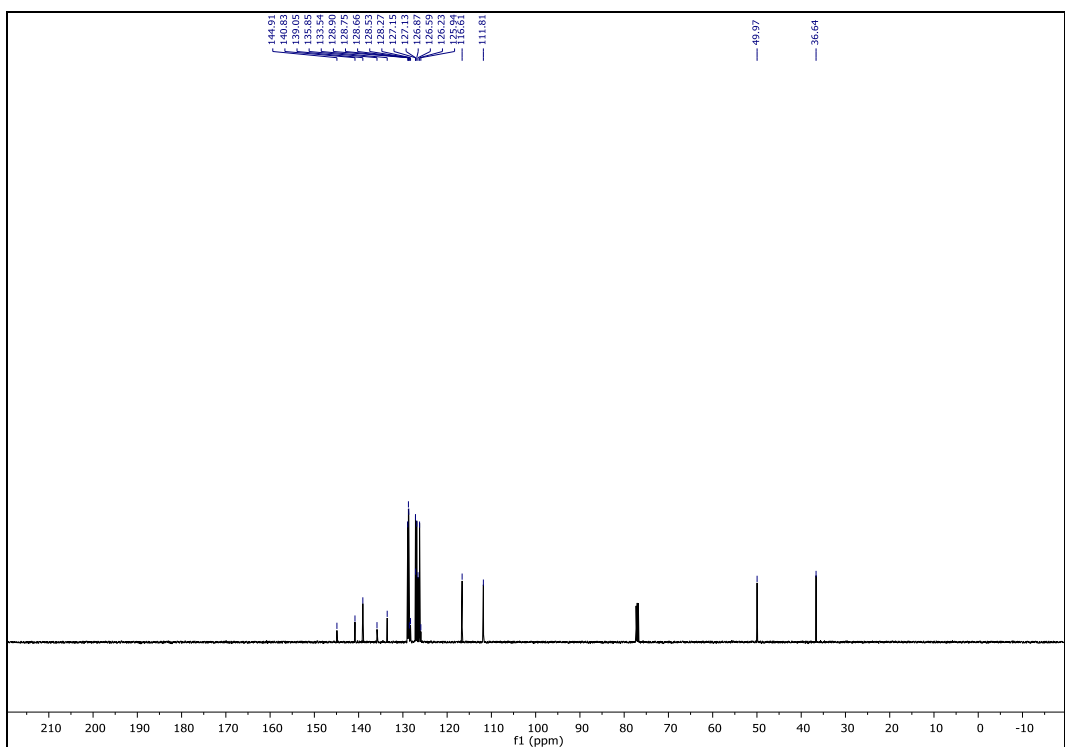
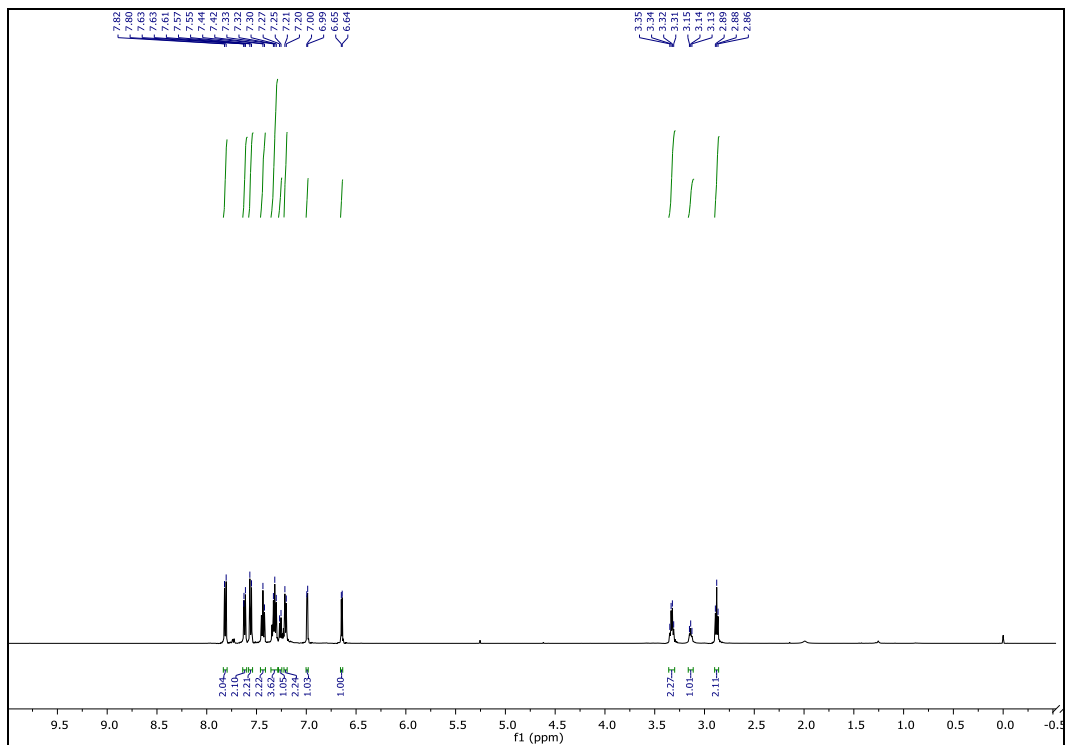
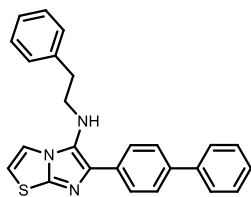


18MDV090-23_180314180642 #11
T: FTMS + p ESI Full ms [150.00-100

(V: 1 NL: 8.21E6



6-([1,1'-biphenyl]-4-yl)-N-phenethylimidazo[2,1-b]thiazol-5-amine (28)



7. Protein expression and purification

E. Coli Rosetta 2 (DE3) pLysS (Novagen) were transformed with the pETM-11 vector bearing the *PtpB* gene for recombinant protein production. The cells were grown in Terrific Broth (TB) media supplemented with 50 µg/ml kanamycin and 35 µg/ml chloramphenicol. An overnight pre-culture grown at 310 K was used to inoculate the main production culture (supplemented by 0.5 % glucose to prevent leaky expression containing), which was grown at 310 K until an OD₆₀₀ interval of 0.6 – 0.8. Subsequently, the enzyme expression was induced with 1 mM isopropyl β-D-1-thiogalactopyranoside (IPTG), and the bacterial cultures were incubated for 16 -18 hours at 310 K. The cells were harvested by centrifugation at 5000 rpm for 20 minutes at 257.59 K and resuspended in lysis buffer (50 mM Tris-HCl, 100 mM NaCl, 30 mM Imidazole, pH 7.5) protease inhibitors (Complete Mini EDTA-free, Roche Applied Science) and a spatula tip of lysozyme. After sonication on ice, the lysate was centrifuged for 45 minutes at 18000 rpm and 257.59 K. Subsequently, the supernatant was passed through a 0.45 µm filter (Whatman) to remove traces of unlysed cells and aggregates. For purification, the clarified cell lysate was purified by immobilized metal ion affinity chromatography (IMAC) with buffer A (50 mM Tris-HCl, 100 mM NaCl, pH 7.5) and buffer B (50 mM Tris-HCl pH 7.5, 100 mM NaCl, 500 mM imidazole) in a 5 mL His-Trap HP (GE Healthcare). Bound protein eluted from the column between 125-150 mM imidazole by step gradient elution. The sample obtained after Ni-NTA purification was diluted 6-fold with 50 mM Tris-HCl pH 7.5 and loaded on a 5 ml Anion Exchange column (GE Healthcare). The protein was eluted from the column by a linear gradient ranging from 50 mM to 1 M of NaCl. Next, the sample was injected onto a HiLoad 16/60 Superdex 75 column (GE Healthcare), previously equilibrated in buffer C (20 mM Tris-HCl pH 7.5 and 50 mM NaCl). The final yield of pure protein from 1 L culture was typically between 6 and 10 mg/mL.

8. Activity assay

The phosphatase activity was performed in 96-well plates (Sigma-Aldrich, Greiner CELLSTAR®) containing 50 µM compounds and 100 nM recombinant MtpB (protein and compounds ratio 1:500) in total volume 50 µl of assay buffer (50 mM Tris- HCl, 100 mM NaCl, 10 % glycerol and 5 mM BME, pH 7.5). The plates were centrifuged for 1 minute at 1000 rpm and incubated for 10 minutes at 37 °C. The measurements were led in triplicates by using spectrophotometer reader (BMG Labtech) at 410 nm. The IC₅₀ value was determined by compound concentrations ranging from 1 mM to 500 nM (1.9fold dilution factor) at 250 nM of MtpB to linearly correlate the time and the enzymatic activity. The reaction was started by the addition of the p-nitrophenyl phosphate (pNPP) in order to assess the dephosphorylation activity at a final concentration of 20 mM. The results were analyzed with GraphPad Prism 5.0 and Origin.

9. Differential scanning fluorimetry (DSF)

Thermal-shift assay (Thermofluor), also called differential scanning fluorimetry (DSF), is a technique to screen compounds that can bind the protein previously labelled with a fluorescent dye (52).

Furthermore it is employed to optimize the buffer conditions such as pH, salts concentrations and disulfide bonds reducing agents (53) (e.g. 2-mercaptoethanol and dithiothreitol). As a result of protein denaturation under a thermal gradient, the compounds can stabilize (positive shift) or destabilize the complex (negative shift); such effect can be quantified as melting point temperature at which the denaturation occurs. In this study case, each reaction is composed of 1 µl compound at 1 mM concentration (50 mM stock in 100% DMSO), 49 µl master mix (10x Sypro Orange (Invitrogen), 5 µM protein in 50 mM Tris- HCl, 100 mM NaCl, 10 % glycerol and 5 mM BME, pH 7.5. The final DMSO concentration is 2% (v/v) and the control was treated with the same percentage of DMSO. The DSF study demonstrated that the protein could tolerate DMSO up to 7% (v/v) (data are not shown). The

melting curves and the melting temperature were examined using BioRad CSX 96 control software (fig. S8).

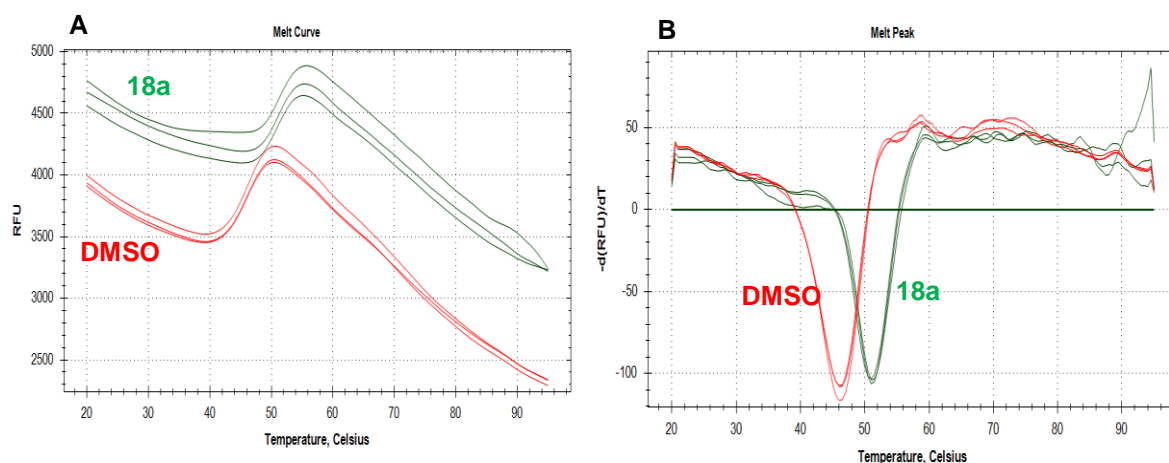


Fig. S8. Stabilization effect of 18a as proof of interaction with MptpB as assessed by DSF. Melting curves (A) and peaks (B) obtained in the presence of 1 mM of **18a** (highlighted in green) and DMSO as a control (highlighted in red). The experiments were run in triplicate. The difference of the melting temperature ($\Delta T_m = 5.5$) indicates a strong stabilization of the ligand – protein complex as a consequence of compound binding.

10. Microscale thermophoresis (MST)

The dissociation constant (K_d) was measured using Nanotemper Monolith NT.115 (Nanotemper Technologies GmbH). The targeted protein was labelled with Monolith His-Tag Labeling Kit RED-tris-NTA according to manufacturer's protocol in standard capillaries (Nanotemper Technologies GmbH) containing MST buffer (20 mM Tris-base pH 8.0, 50 mM NaCl) supplemented by 0.05% (v/v) Tween 20 to prevent protein aggregation. Before loading the samples, the mixture of protein (100 nM) and compound (1 mM) was previously incubated for 30 minutes, followed by centrifugation at 14000 rpm for 5 minutes. As a result, a K_d of 8.07 μ M was detected in single point measure with response amplitude and signal to noise of 5.4 and 6.4 respectively (fig. S9).

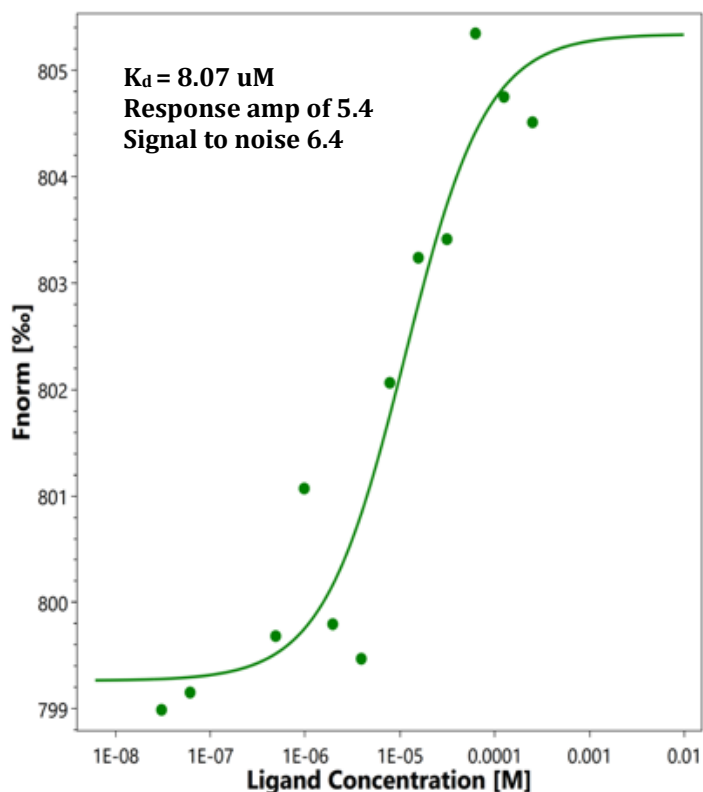


Fig. S9. Binding curve of 18a to the fluorescently labeled MptpB sample as assessed by MST.

11. Molecular modeling

Prior to proceed to dock compound **18a** we visually inspected for possible candidates that can form a covalent bond with the boronic acid, for example the threonines and the serines (fig. S10). We excluded the solvent exposed residues and kept the Ser – 57 and Thr – 223 as they were the only exposed to the phospho tyrosine binding site.

The boronic acid inhibitor **18a** was prepared with LigPrep by assigning the ionization state with Epik (54) at pH 8.0. The protein phosphatase B in complex with the previously described inhibitor OMTS (55) was imported with Protein Preparation Wizard (56) which allows to assign hydrogens and partial charges to heteroatoms. In addition, the final refinement (hydrogen bond assignment and restrained minimization) was performed with standard parameters.

The ligand was then docked with CovDock (57), an all-in-one workflow to predict the poses and the score of compounds which covalently binds nucleophilic side chain residues. For the formation of the boronic acid addition product with Cys – 160 and Ser - 57, proximal OMTS-A atomic coordinates were used to generate the grid box within which the compounds were docked in a box length size of 20 Å. Distal OMTS – B atomic coordinates were then used as they were closer to the nucleophile partner for docking the compound in the cavity. The final poses were visually inspected and the network of molecular interactions was generated with Scorpion (57). The prediction of the docking score derives from the genetic algorithm parametrization of both the interaction network and the specific type of contacts. The final scores are summarized in Table S1 while the proposed docking models for Cys – 160 (fig. S11), Ser -57 (fig. S12) and Thr – 223 (fig. S13) were rendered with Pymol. In the highest-ranking interaction with Cys-160 the boronic acid hydroxyls are nicely stabilized by a hydrogen bonding network towards Ala-162 and Arg-166.

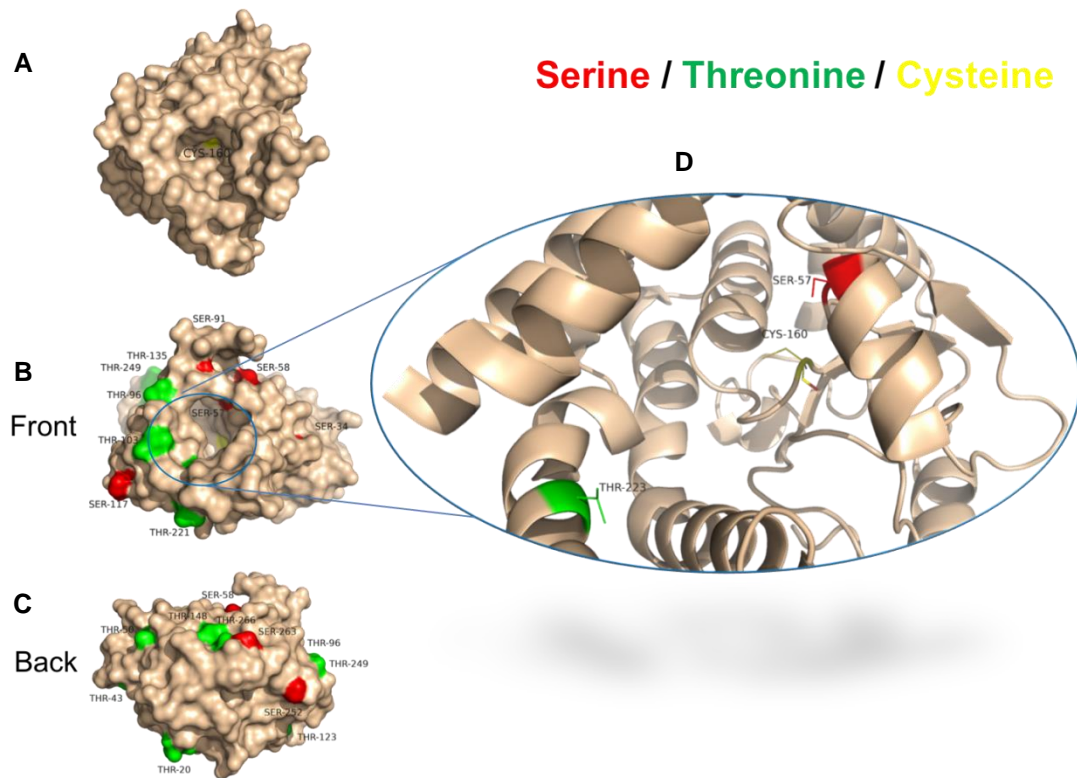


Fig. S10. Three-dimensional structure of the target phosphatase (A) Surface representation of MptpB (PDB: 2OZ5) showing both the position of the reactive cysteine (yellow) and (B,C) the distribution of the serines (red) and threonine (green) that can react with the boronic acid, thus forming a covalent bond. (D) Magnification of the phosphotyrosine binding site reveals that Ser57 and Thr223 are exposed, thus they were selected among the other residues for the docking studies. The pictures were rendered with Pymol.

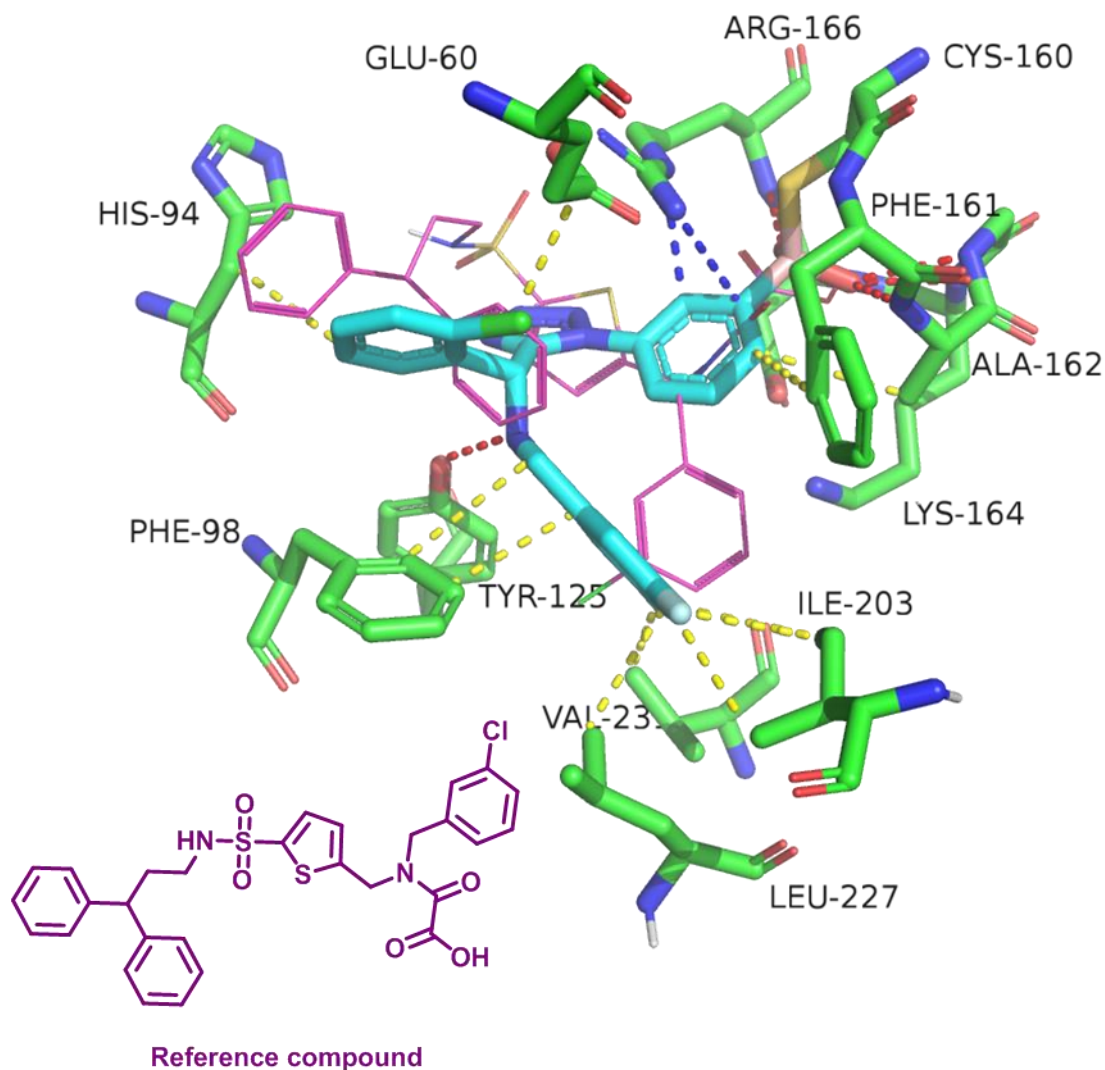


Fig. S11. Proposed docking model for 18a covalently bound to Cys¹⁶⁰ (PDB ID: 2OZ5). This complex is further stabilized by polar interactions such as confocal hydrogen bonds between the amidic hydrogens and hydroxyl group of boronic acid moiety (red) and cation – pi between the Arg – 166 positively charged side chain and the benzene (blue); moreover van der Waals interactions (yellow) with hydrophobic side chains between the Val231, Leu227, ILE203, Phe98 and the 1,3-difluorophenyl moiety extends the contact surface with the receptor cavity. The reference cocrystallized compound is depicted in magenta lines.

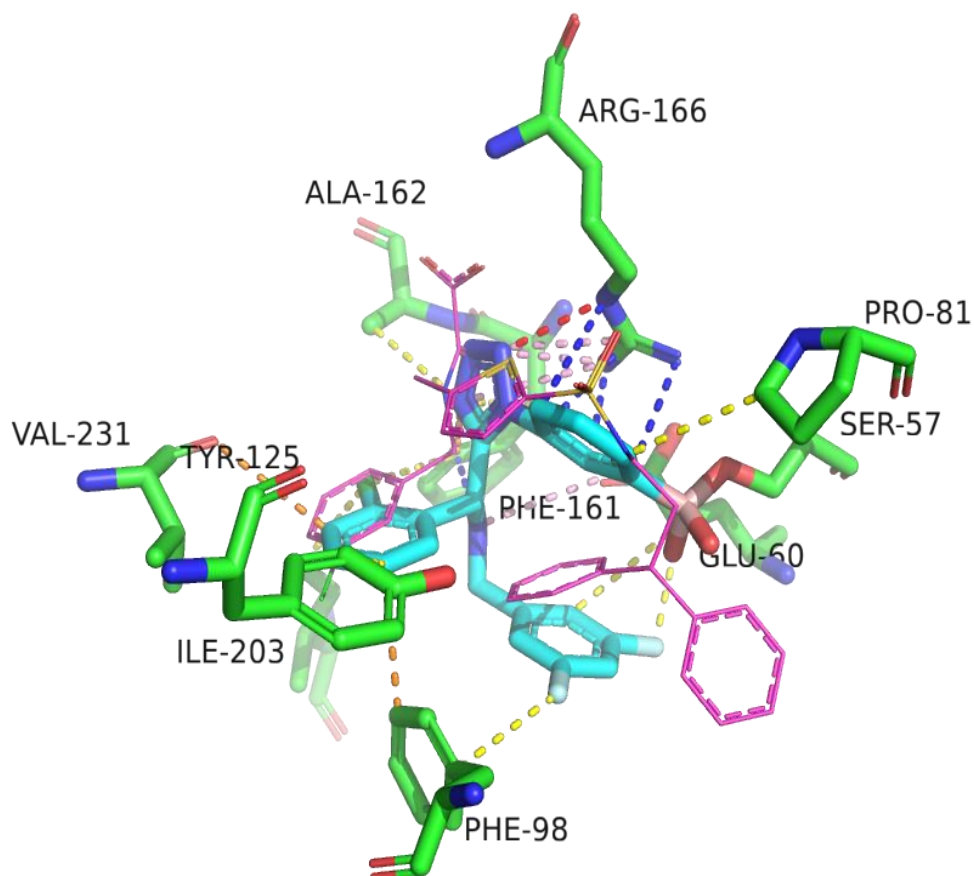


Fig. S12. Proposed docking model for 18a covalently bound to Ser⁵⁷ (PDB ID: 2OZ5). Polar contacts between the positively charged side chain of Arg166 and the benzene (blue) are maintained as well as the van der Waals interactions (yellow) between hydrophobic side chain of Phe98 and the 1,3-difluorophenyl group. Additionally, new ionic contacts are formed between the Arg166 guanidine and the tetrazole (purple dash lines) as well as one extra pi-pi interaction with Phe98 and the chlorophenyl group.

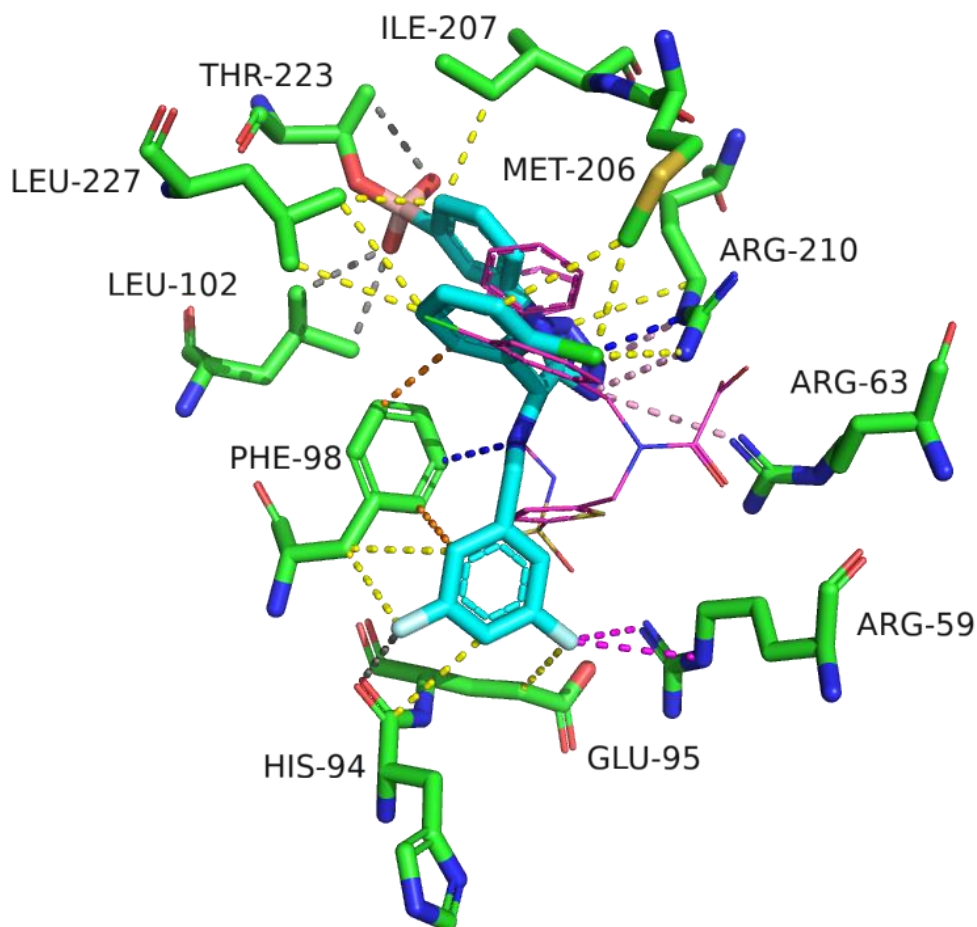


Fig. S13. Proposed docking model for 18a covalently bound to Thr²²³ (PDB ID: 2OZ5). In addition to the van der Waals interactions (yellow) between Phe – 98 and the compound, new contacts are formed such as pi-pi interactions (orange) and cation – dipole (magenta). Unfavorable interactions due to steric collision (gray) were also found around the aromatic ring immediately attached to the boronic acid moiety.

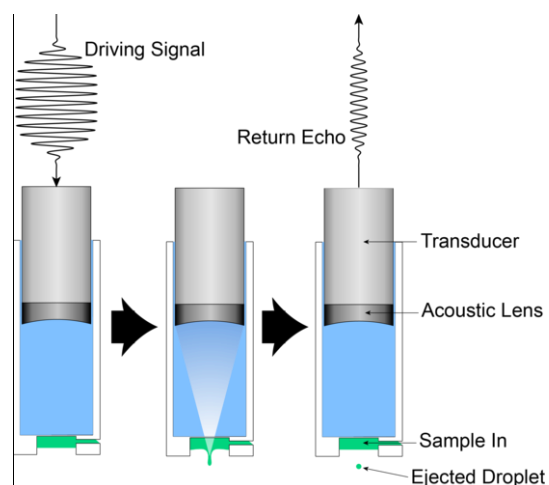
Table S1. Summary table of the docking scores for Covdock and Scorpion.

Pose number	Covdock affinity	Scorpion score	Reference compound Scorpion score
Cys - 160	-8.285	10.7	18.1
Ser - 57	-6.795	11.1	18.1
Thr - 223	-5.600	8.5	11.5

12. Acoustic droplet ejection technology description and workflow

In the figure below we describe the principles of ADE technology as reported by Fuller, F. *et al.* Protocol Exchange (2017) (doi:10.1038/protex.2017.01). A driving pulse is sent to the transducer and the resulting acoustic wave (center) is focused on the sample-air interface creating a column of sample. A droplet of sample is ejected in the final step (right) and an echo of the driving pulse is returned to the transducer. The sample is connected to the transducer via a column of coupling water (that is isolated from the sample) (58). In addition we describe its incorporation in our workflow.

A.



B.

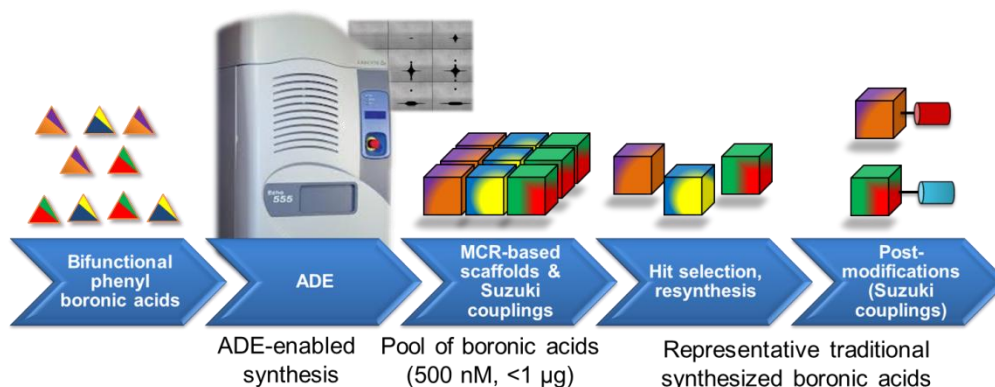


Fig. S14. ADE technology. (A) Description of the principles (licence under Attribution 4.0 International (CC BY 4.0)). (B) The workflow of our current approach towards the synthesis of complex boronic acids